

The Morphological Representation of Channel-Forming Flow in Arroyos

Lucy A. Ellis



Thesis submitted to the University of Nottingham
for the degree of Doctor of Philosophy, May 2004

Table of Contents

List of Figures	v
List of Tables	xiv
Abstract.....	xv
Acknowledgements.....	xvi
Chapter 1 Introduction.....	1
1.1 Definition of an Arroyo.....	1
1.2 Project Aims and Rationale.....	3
1.3 Methods of Study	5
1.4 Study Areas	8
Rio Puerco	10
Santa Cruz River.....	11
San Simon River	12
Chapter 2 Channel-Forming Flow and Fluvial System Behaviour	15
2.1 Introduction.....	15
2.2 Theories of Channel-Forming Flow	16
2.2.1 Effective and Channel-Forming Discharge	16
2.2.2 Equilibrium and Threshold Concepts	19
2.2.3 Non-Linear Dynamical Systems Theory	24
2.2.4 Catastrophe Theory	26
2.2.5 Models of Channel Evolution	28
2.3 Channel-Forming Flow in Ephemeral Streams.....	31
2.3.1 Flow Variability and Ephemeral Channel Form.....	32
2.3.2 Applicability of Channel-Forming Flow Theories	34
2.4 Models of Arroyo Evolution.....	36
Chapter 3 Arroyo Initiation	44
3.1 Arroyo Initiation Theories.....	44
3.1.1 Human Land-Use Change	45
3.1.2 Climatic Change.....	50
3.1.3 Random Frequency-Magnitude Variations.....	52

3.2	Arroyo Initiation in Study Areas	56
	Rio Puerco	56
	Santa Cruz River.....	62
	San Simon River	69
3.3	Comparison of Initiation Processes.....	71
Chapter 4 Flow and Sediment Discharge Variability		73
4.1	Factors Controlling Storm Events in Study Areas	73
4.2	Discharge Trends	79
4.2.1	Seasonality of Flow	79
4.2.2	Annual Discharge Trends.....	82
4.2.3	Peak Discharge Trends.....	84
4.2.4	Effects of Infiltration	88
	Infiltration Rates.....	88
	Infiltration During Flow Events	89
	Infiltration Trends.....	93
4.3	Sediment Trends.....	93
4.3.1	Nature of the Sediment Load	93
4.3.2	Sediment Size.....	94
4.3.3	Sediment Discharge	97
4.3.4	Hysteresis	106
4.4	Comparison of Flow Variability in Study Areas	109
Chapter 5 Evolution of Study Arroyos		111
5.1	Geological Evolution of Study Areas	111
	Rio Puerco	111
	Santa Cruz River and San Simon River.....	117
5.2	Recent Arroyo Evolution.....	123
	Rio Puerco	123
	Factors Affecting Evolution	123
	Arroyo Evolution	127
	Santa Cruz River.....	149
	Factors Affecting Evolution	149
	Arroyo Evolution	157
	San Simon River	165
	Factors Affecting Evolution	165
	Arroyo Evolution	168
5.3	Comparison of Evolution in Arroyos Studied	176

Chapter 6 Contemporary Arroyo Morphology.....	182
6.1 Contemporary Processes.....	182
6.1.1 Modification During Periods without Flow	182
6.1.2 Flood Modification.....	187
6.1.3 Flood Modification along Channelised Reaches.....	191
6.2 Arroyo Morphology	192
Rio Puerco	193
General Observations	193
Upper Reach 1 – above Arroyo Chijuilla	193
Upper Reach 2 – between Arroyo Chijuilla and Ventana artificial channel	194
Upper Reach 3 – between Ventana and Arroyo Chico	196
Middle Reach – between Arroyo Chico and Benavidez Ranch Reach.....	197
Lower Reach – downstream of Benavidez Ranch Reach.....	200
Santa Cruz River.....	203
General Observations	203
Pleistocene Reach.....	205
2000 Survey.....	205
Morphological Change due to 2000 Flood.....	208
Holocene Reach.....	211
2000 Survey.....	211
Morphological Change due to 2000 Flood.....	215
San Simon River	217
General Observations	217
Upstream Reach – coarse sediments	220
Upstream Reach – fine sediments	222
Lower Reach	223
6.3 Comparison of Morphology in Arroyos Studied	226
6.4 Flood-Scale Arroyo Modification Model	231
Chapter 7 Effective Discharge	234
7.1 Effective Discharge Calculations.....	234
Methodology	234
Rio Puerco Effective Discharge Results	239
Bernardo Gauge	239
Rio Puerco Gauge	241
Rio Puerco above Arroyo Chico Gauge	242
Arroyo Chico Gauge	243

Santa Cruz River Effective Discharge Results.....	243
Tucson Gauge	243
Continental Gauge	245
San Simon River Effective Discharge Results	247
Conclusion	248
7.2 Slope-Area Calculations.....	249
Methodology	249
Rio Puerco Slope-Area Results	250
Santa Cruz River Slope-Area Results.....	252
San Simon River Slope-Area Results	253
Conclusion	254
7.3 Morphological Representation of Effective and Bankfull Discharges	254
Rio Puerco	254
Santa Cruz River.....	255
San Simon River	256
7.4 Interpretation	256
Chapter 8 Discussion and Conclusions	259
8.1 Discussion	259
8.1.1 Arroyo Evolution and Contemporary Morphology.....	259
8.1.2 General Conceptual Model of Arroyo Evolution.....	262
8.1.3 Channel-Forming Flow in Arroyos	267
8.2 Conclusions	272
8.3 Future research and Management Issues.....	276
References	279
Appendix 1 Data Collection and Collation.....	A1-1
A1.1 Daily Average Discharge Data.....	A1-2
A1.2 15 Minute Discharge Data	A1-2
A1.3 Sediment Discharge Data	A1-6
A1.4 Effective Discharge Calculation	A1-8
A1.5 Cross-Section Surveys.....	A1-10
Appendix 2 Location of Cross-Sections.....	A2-1
Appendix 3 Data Summary	A3-1

List of Figures

Figure 1.1	Geomorphological features of arroyo systems	2
Figure 1.2	Location of study areas	8
Figure 1.3	Major landforms, settlements and gauging stations of the Rio Puerco Basin.....	10
Figure 1.4	Major landforms, settlements and gauging stations of the Tucson Basin.....	12
Figure 1.5	Major landforms, settlements and gauging stations of the San Simon Basin	13
Figure 2.1	Schematic representation of effective discharge (after Thorne <i>et al.</i> , 1998).....	16
Figure 2.2	Types of equilibrium (after Chorley <i>et al.</i> , 1984; Renwick, 1992).	20
Figure 2.3	Diagrammatic representation of cusp catastrophe and different system behaviour according to initial proximity to cusp (after Graf, 1979a).....	28
Figure 2.4	Composite incised channel evolution model (after Schumm <i>et al.</i> , 1984; Harvey and Watson, 1986; Simon and Hupp, 1991; Thorne, 1999).	30
Figure 2.5	Hypothetical sequence of geomorphological evolution of large-scale arroyos (after Elliott, 1979; Elliott <i>et al.</i> , 1999).....	38
Figure 2.6	Model of arroyo development showing influence of sediment load and grain size on stability (after Meyer, 1989)	42
Figure 3.1	Summary of environmental changes responsible for arroyo initiation (after Cooke and Reeves, 1976).....	46
Figure 3.2	Palaeoarroyos exposed in the outer bank of XS-17, Rio Puerco (courtesy John Elliott).....	48
Figure 3.3	Location of historic sites of the Rio Puerco Basin (after Widdison, 1959)	57
Figure 3.4	1884 photograph of the unincised Rio Puerco at Cabezon, looking south towards Cabezon Peak (EA Bass, courtesy of the Library of Congress Prints and Photographs Division Lot No. 3286).....	59

Figure 3.5	Location of historic sites of Santa Cruz River in the San Xavier and Tucson reaches (after Betancourt, 1987; 1990)	63
Figure 3.6	1885 photograph of Silver Lake Reservoir (courtesy of Arizona Historical Society, Tucson, AHS #18,335)	65
Figure 3.7	Unincised channel at the Punta de Agua on the west barranca of the Santa Cruz River, 1912 (Photographer unknown)	67
Figure 4.1	Southern Oscillation Index (Tahiti – Darwin), five month running mean for 1914 to present (after Dahm and Moore, 2003).....	76
Figure 4.2	Time series of total annual precipitation (Rio Puerco data and NOAA climatic division data after Molnar (2001))	77
Figure 4.3	Variation in monthly rainfall data. a) Rio Puerco basin between 1952 and 1986 (after Molnár, 2001). b) University of Arizona, Tucson, between 1868 and 1996, and San Simon, between 1882 and 1997, showing percentage change before and after 1960.....	78
Figure 4.4	Percentage of a. average annual precipitation and b. average annual streamflow occurring each month, over entire period of record.....	79
Figure 4.5	Average daily flow over entire period of record.....	81
Figure 4.6	Comparison of daily average and 15 minute instantaneous discharge data, Rio Puerco at Bernardo and Santa Cruz River at Tucson.....	82
Figure 4.7	Total annual flow and annual flashiness index at all gauges along the Rio Puerco, Santa Cruz and San Simon Rivers for available period of record	83
Figure 4.8	Peak annual flows at all gauges along Rio Puerco, Santa Cruz River and San Simon River for available period of record	85
Figure 4.9	Time series showing percentage of year with zero flows for available gauges on Rio Puerco, San Simon River and Santa Cruz River Rivers.....	87
Figure 4.10	a) Difference in flow volumes between gauges along the Rio Puerco and Santa Cruz River. b) Volume of flow at lower gauge expressed as a percentage of volume of flow at upper gauge	90

Figure 4.11	Time series showing consistency of infiltration.....	93
Figure 4.12	Relationship between instantaneous discharge and sediment loads, Rio Puerco at Bernardo Gauge and Santa Cruz River at Tucson Gauge	98
Figure 4.13	Relationship between daily average discharge and sediment loads, Rio Puerco at Bernardo and above Arroyo Chico Gauges, Arroyo Chico Gauge and San Simon at Solomon Gauge	98
Figure 4.14	Comparison between instantaneous and daily average discharge and sediment load relationship, Rio Puerco at Bernardo	99
Figure 4.15	a) Variability in monthly sediment concentration and b) Seasonal variability in relationship between discharge and sediment load, from instantaneous measurements between 1948 and 2000, Rio Puerco at Bernardo.....	102
Figure 4.16	Average monthly discharge and sediment load over period of record, Rio Puerco at Bernardo (1955 – 2000), Arroyo Chico (1978 – 1986) and above Arroyo Chico (1994 – 1999)....	102
Figure 4.17	Average monthly discharge and sediment load between 1982 and 1995, San Simon River at BLM Gauge at Barrier Dam.....	103
Figure 4.18	Trend in average annual sediment discharge (tonnes/day), Rio Puerco at a. Bernardo, b. above Arroyo Chico, c. Arroyo Chico and d. San Simon River at Barrier Dam.....	104
Figure 4.19	Examples of different hysteresis types from instantaneous data at Bernardo, Rio Puerco.....	107
Figure 4.19	Continued.....	108
Figure 4.20	Hysteresis types, Rio Puerco at Bernardo.....	109
Figure 5.1	Generalised geology of Rio Puerco Basin (after Love, 1986; Gorbach, 1996)	112
Figure 5.2	Schematic diagram showing erosional levels preserved by successive basalt flows in the Cabezon area of the Rio Puerco Basin (after Slavin, 1991)	114
Figure 5.3	Surficial geology of the Tucson Basin (after Parker, 1996).....	120
Figure 5.4	Artificial cut-off at Ventana, 1968 (photographer unknown).....	126

Figure 5.5	Pre- and post-avulsion channels, 1935 aerial photograph	128
Figure 5.6	1935 aerial photographs showing the difference in morphology due to different over-flight dates	131
Figure 5.7	Change in morphology at the confluence with Arroyo Chico, 1935 aerial photograph.....	133
Figure 5.8	Arroyo evolution between 1935 and 1996, Lower Reach	135
Figure 5.9	Morphological change due to the construction of artificially straightened reach at Ventana.....	138
Figure 5.10	Longitudinal profiles across the neck of Horsefly meander before and after its cut-off in 1989 (after Love, 1992).....	141
Figure 5.11	Anomalous morphology of Guadalupe sub-reach and point of geomorphological change at confluence with Arroyo Chico	143
Figure 5.12	Geomorphological change at the Benavidez Ranch reach, arrow indicating point of change.....	145
Figure 5.13	View downstream from Highway 6 bridge, Rio Puerco at Rio Puerco, showing morphological change. (1936 photograph courtesy H. Yeo, Ms 94 Box 16/76, Rio Grande Historical Collections, New Mexico State University Library; 1996 photograph courtesy J. Wall, BLM).....	146
Figure 5.14	Development of hooked meanders downstream of the Benavidez Ranch reach	147
Figure 5.15	Lateral erosion of meander bends causing breakthrough of the Rio San Jose to the Rio Puerco, 1996	148
Figure 5.16	Aerial photograph showing compression of meanders against Martinez Hill and subsequent straightening during series of large floods	150
Figure 5.17	Aerial photograph showing collapse of I19 during 1983 flood	153
Figure 5.18	Aerial photograph of mid-San Xavier reach showing sediment extraction for construction of I19, 1967	155
Figure 5.19	Artificial channel between east- and west- branches of Santa Cruz River, 1936 and 1972.....	158
Figure 5.20	Aerial photographs showing narrowing and inner channel stabilisation of the Santa Cruz River between 1960 and 1974 at Valencia Road.....	160

Figure 5.21	Aerial photographs showing geomorphological changes of the Santa Cruz River at Pima Mine Road due to high-magnitude flooding in October 1977 and December 1978	161
Figure 5.22	View upstream from St. Mary's Road before and during 1983 flood (courtesy P. Kresan).....	162
Figure 5.23	Trench-full flow at Pima Mine Road and significantly lower flood stage at Valencia Road, January 1993. Photograph taken during recession of flood, just after peak (courtesy J. Parker)	163
Figure 5.24	View from Pima Mine Road bridge after 1983, 1993 and 2000 floods (1983 photograph courtesy J. Parker)	164
Figure 5.25	Headcutting tributary gullies, 1963 (courtesy of Safford BLM)	165
Figure 5.26	Goat Well Detention Dam a) looking upstream at aggraded channel, b) looking down drop structure into Slick Rock Wash arroyo.....	166
Figure 5.27	Arroyo evolution between Gold Gulch and Timber Draw, 1935 – 1992.....	169
Figure 5.28	Straightened arroyo trench along Yellowhammer reach, 1941	169
Figure 5.29	Arroyo evolution between 1935 and 1996, Goat Well Sub-Reach, Lower San Simon.....	171
Figure 5.30	Morphological change caused by the Fan Dam.....	174
Figure 6.1	Model of arroyo behaviour during flow events, developed for the Santa Cruz River (after Ellis, 1993)	183
Figure 6.2	Desiccation and exfoliation flakes along the arroyo walls, Goat Well Sub-Reach, San Simon River	185
Figure 6.3	Sink holes along western valley floor of San Xavier Sub-Reach of the Santa Cruz River.....	186
Figure 6.4	Large pipe and pipe outlet, Guadalupe Sub-Reach, Rio Puerco	187
Figure 6.5	Seepage notches along the Santa Cruz River, upper level representing 1993 flood, lower level representing 2000 flood	189

Figure 6.6	Parallel laminated sediments deposited in the San Xavier Reach of the Santa Cruz River during the October 2000 flood	190
Figure 6.7	Active channel and stabilised inner floodplain at Elliott's XS-1, Upper Reach 1, 1996 (courtesy J. Elliott).....	194
Figure 6.8	Broad, braided low-flow channel of XS-9, Upper Reach 2, 1997 (courtesy J. Elliott).....	195
Figure 6.9	Broad, shallow active channel of Upper Reach 3, 1997 (courtesy J. Elliott).....	196
Figure 6.10	Upstream limit of Middle Reach, showing broad, straight Guadalupe Sub-Reach and more representative sinuous planform, 1997	198
Figure 6.11	Guadalupe Sub-Reach, Middle Reach, 1999.....	198
Figure 6.12	Arroyo wall dissected by piping, behind stabilised berm, Guadalupe sub-reach, 1999.....	199
Figure 6.13	Difference in active channel morphology within Lower Reach a) Trapezoidal channel at XS-15, situated in a low-sinuosity sub-reach, 1997 (courtesy J. Elliott). b) Asymmetric channel at XS-17, located in a sinuous sub-reach, 1999	200
Figure 6.14	Large meander at XS-17, showing increase in age of vegetation with distance from active channel	202
Figure 6.15	Preferential erosion of different sedimentary layers in flutes, Valencia Road Sub-Reach.....	204
Figure 6.16	Erosional terrace, XS-3, North Pima Mine Road Sub-Reach, pre-and post-October 2000 flood	206
Figure 6.17	Point bar armoured with cobbles close to widening of Pima Mine Road Sub-Reach, during 2000 flood	209
Figure 6.18	XS-1, North Pima Mine Road Sub-Reach, showing collapse of narrow wall of sediment separating tributary from main Santa Cruz River during 2000 flood	210
Figure 6.19	Arch formed due to tree roots binding sediments of upper layer, close to cross-section at Martinez Hill.....	212
Figure 6.20	Braid bar deposited downstream of mid-stream pylon during 2000 flood, Valencia Road Sub-Reach.....	215

Figure 6.21	View upstream into Timber Draw emphasising the difference in bed elevation between the tributary and main channel of the San Simon River	218
Figure 6.22	View upstream into Gold Gulch and San Simon River	218
Figure 6.23	Felled Tamarisk sediment traps in the main channel of the San Simon River, downstream of Gold Gulch.....	219
Figure 6.24	Headwards progression of tributary arroyo network due to sheetwash concentration into rills, then abrupt, deep headcut	220
Figure 6.25	Morphological features of the San Simon Sub-Reach.....	221
Figure 6.26	Sheetwash causing large blocks to become situated on pedestals, close to San Simon Sub-Reach	221
Figure 6.27	Vegetated, stepped floodplain of Yellowhammer Sub-Reach.....	222
Figure 6.28	Bed cambering along Yellowhammer Sub-Reach, showing difference between bed and bank sediments of active channel.....	223
Figure 6.29	Trapezoidal active channel in a) Bailey Well Sub-Reach and b) Tanque Sub-Reach, Lower Reach.....	224
Figure 6.30	Morphological characteristics of Goat Well Sub-Reach, Lower Reach	226
Figure 6.31	Trapezoidal active channel in Goat Well Sub-Reach, Lower Reach.....	226
Figure 7.1	Effective discharge for Bernardo Gauge using a. 15 minute/instantaneous and b. Daily average flow and sediment discharge data, 1949 – 2000.....	239
Figure 7.2	Effective discharge for Bernardo Gauge using a. 15 minute/instantaneous and b. Daily average flow and sediment discharge data, 1975 – 2000.....	239
Figure 7.3	Effective discharge for Bernardo Gauge using a. 15 minute/instantaneous and b. Daily average flow and sediment discharge data, 1997 – 2000.....	239
Figure 7.4	Effective discharge for Rio Puerco Gauge using daily average flow data, 1934 – 1976	241
Figure 7.5	Effective discharge for Rio Puerco Gauge using daily average flow data, 1960 – 1976	241

Figure 7.6	Effective discharge for Rio Puerco above Arroyo Chico Gauge using daily average flow data, 1951 – 2000.....	242
Figure 7.7	Effective discharge for Rio Puerco above Arroyo Chico Gauge using daily average flow data, 1990 – 2000.....	242
Figure 7.8	Effective discharge for Arroyo Chico Gauge using daily average flow data, 1943 – 1986	243
Figure 7.9	Effective discharge for Tucson Gauge using daily average flow data, 1905 – 2002.....	244
Figure 7.10	Effective discharge for Tucson Gauge using daily average flow data, 1960 – 2002.....	244
Figure 7.11	Effective discharge for Tucson Gauge using a. 15 minute/instantaneous and b. Daily average flow and sediment data, 1998 – 2000.....	245
Figure 7.12	Effective discharge for Continental Gauge using daily average flow data, 1940 – 2002.....	246
Figure 7.13	Effective discharge for Continental Gauge using daily average flow data, 1960 – 2002	246
Figure 7.14	Effective discharge for Continental Gauge using a. 15 minute/instantaneous and b. Daily average flow and sediment data, 1987 – 2000.....	247
Figure 7.15	Effective discharge for Solomon and Barrier Dam Gauges combined, using daily average flow and sediment data, 1931 – 2000.....	248
Figure 7.16	Effective discharge for Solomon and Barrier Dam Gauges combined using daily average flow and sediment data, 1960 – 2000.....	248
Figure 7.17	Comparison between actual values at the Bernardo Gauge and calculated bankfull values in the Lower Reach of the Rio Puerco, showing relationship between discharge and a) area and b) flow velocity	252
Figure 8.1	General conceptual model of arroyo evolution	264
Figure 8.2	Simplified schematic representation of a) arroyo equilibrium and b) variation in flow and sediment discharge with time, in response to driving variables.....	268
Figure A1.1	Input form for CSU effective discharge program.....	A1-10
Figure A2.1	Location of Rio Puerco cross-sections	A2-2

Figure A2.2 Upper Reach 1, Elliott's XS-1, 2 and 3, Rio Puerco	A2-3
Figure A2.3 Upper Reach 2, Elliott's XS-4 to 10, Rio Puerco	A2-4
Figure A2.4 Middle Reach, Elliott's XS-13 and 14, Rio Puerco	A2-5
Figure A2.5 Lower Reach, Elliott's XS-15 and 16, Rio Puerco	A2-6
Figure A2.6 Lower Reach, Elliott's XS-17 and 31, Rio Puerco.....	A2-7
Figure A2.7 Lower Reach, Elliott's XS-18 and 19, Rio Puerco.....	A2-8
Figure A2.8 Lower Reach, Elliott's XS-20 to 29, Rio Puerco	A2-9
Figure A2.9 Lower Reach, XS-32 at Bernardo Cableway, Rio Puerco....	A2-10
Figure A2.10 Location of Santa Cruz River cross-sections	A2-11
Figure A2.11 South Pima Mine Road Sub-Reach, Pleistocene Reach, Santa Cruz River	A2-12
Figure A2.12 North Pima Mine Road Sub-Reach, Pleistocene Reach, Santa Cruz River	A2-13
Figure A2.13 Big Bend Sub-Reach, Holocene Reach, Santa Cruz River .	A2-14
Figure A2.14 South of Straight Sub-Reach, Holocene Reach, Santa Cruz River	A2-15
Figure A2.15 Martinez Hill Sub-Reach, Holocene Reach, Santa Cruz River	A2-16
Figure A2.16 Valencia Road Sub-Reach, Holocene Reach, Santa Cruz River	A2-17
Figure A2.17 Location of San Simon River cross-sections	A2-18
Figure A2.18 San Simon Sub-Reach, 2000 Survey, Upper Reach, San Simon River.....	A2-19
Figure A2.19 Yellowhammer Sub-Reach, XS-1 and 2, 2000 Survey; XS 3 and 4, 2001 Survey, Upper Reach, San Simon River	A2-20
Figure A2.20 Bailey Well Sub-Reach, 2001 Survey, Lower Reach, San Simon River.....	A2-21
Figure A2.21 Tanque Sub-Reach, 2001 survey, Lower Reach, San Simon River	A2-22
Figure A2.22 Corral Sub-Reach, Lower Reach, 2001 survey, San Simon River	A2-23

Figure A2.23 Goat Well Sub-Reach, 2001 survey, Lower Reach, San Simon River.....	A2-24
--	-------

List of Tables

Table 4.1 Variability in infiltration rates between gauges on the Rio Puerco, Santa Cruz River and San Simon River	92
Table 4.2 Classification of the total sediment load (after Thorne <i>et al.</i> , 1998; Soar, 2001)	93
Table 5.1 Morphological difference between Elliott's Type 1 and Type 2 reaches	140
Table 6.1 Comparison of bankfull geometry of trapezoidal channels.....	230
Table 7.1 Sediment rating curve variables	236
Table 7.2 Summary of effective discharge calculations for Bernardo Gauge for different time periods and data types	240
Table A3.1 1970s cross-section geometry, Rio Puerco	A3-2
Table A3.2 1990s cross-section geometry, Rio Puerco	A3-3
Table A3.3 Difference between 1970s and 1990s geometry, Rio Puerco	A3-4
Table A3.4 Geometry of Pleistocene Reaches, Santa Cruz River	A3-5
Table A3.5 Geometry of Holocene Reaches of Santa Cruz River.....	A3-6
Table A3.6 Difference in geometry of Santa Cruz River cross-sections due to October 2000 flood	A3-7
Table A3.7 Geometry of San Simon cross-sections, 2000 or 2001	A3-8
Table A3.8 Summary of flow, sediment and discharge data.....	A3-9

Abstract

This thesis presents a study of three similar, yet contrasting, arroyos: the Rio Puerco, New Mexico and the Santa Cruz and San Simon Rivers in Arizona. Arroyo systems have been subject to several periods of cut and fill within recent geologic time. The most recent incision phase occurred during the mid- to late-19th Century, enabling subsequent morphological changes to be observed. Observations indicate that these systems have developed distinct geomorphological reaches, which evolve at different rates within the constraints of the specific controlling variables, most importantly discharge, sediment load and artificial alteration. Thus, location-for-time substitution cannot be assumed. Within the continuum of morphological change, six stages were identified, enabling a general model of arroyo evolution to be developed.

Precipitation has increased in the south-western USA. However, within the arroyos studied, some gauges have seen a concurrent increase in discharge, whereas others have experienced a decline. It was discovered that the different responses were explained by the interaction between discharge and morphology at different stages of evolution.

The first four stages of arroyo evolution differ little from those proposed previously. However, this study has emphasised the necessity of recognising the event-driven nature of morphological change within the system during these stages. Since some change occurs during each flood, the arroyo morphology is controlled by a combination of the flow variability and channel-deforming events.

As aggradation predominates, the arroyo develops a quasi-stable form, creating a feedback between discharge and morphology. High-magnitude flows are suppressed and aggradation is promoted, permitting continued stabilisation until a quasi-equilibrium form is attained, typified by a trapezoidal active channel and densely vegetated inner floodplain. These morphological changes alter the discharge regime sufficiently that lower-magnitude flows assume greater relative effectiveness. It is not until a quasi-equilibrium morphology is achieved that the bankfull discharge becomes adjusted to the effective discharge, at which point the effective discharge becomes a truly channel-forming and maintaining flow.

Acknowledgements

This PhD would not have been possible without the help of a vast multitude of people, both in the UK and the USA. Since my research was mainly self-funded, I have had to rely on the kindness and generosity of friends, family and colleagues. Many apologies to those who I have inadvertently not included.

My parents, Rod and Ann Ellis, provided most of the financial (and emotional) support and without them I would not have been able to even contemplate thus study. I'm sure that if they had known what they were letting themselves in for at the start, they'd have had second thoughts. Financial help from Sue Eades and Austin Ellis enabled me to purchase vital equipment.

My supervisor, Professor Colin Thorne has given me encouragement, guidance and inspiration, as well as a considerable amount of financial help for fieldwork trips. My former co-supervisor, Dr Pete Downs, was invaluable before decamping to the USA.

Matt Birch got roped in to helping with fieldwork and surveying which went way beyond the call of duty. When he went on strike, Nick Wallerstein took over the unenviable task. Without them much of my research would have been impossible. Vince Smedley and Michael Neuser helped me fathom how to work with the huge datasets.

At the University of Nottingham, Professor Paul Mather provided financial assistance for fieldwork. Professor Nick Clifford, Dr Michèle Clarke, Dr Bob Dugdale and Professor Sarah O'Hara and Dr Phil Soar offered helpful advice.

Allen Gellis, John Elliott and John Parker have shared data, knowledge and experience which was invaluable. David Love, Ray Watts, Chris Gorbach, Jonathan Friedman, Kirk Vincent, Doug Lantz, Victor Baker, Zbig Osmolsky, Fazil Karim, John Sorrell, Richard Hereford, Eric Holler, Scott Miller and Tetratech, Tucson also provided information and discussion.

The US Geological Survey in Albuquerque allowed me to become a volunteer in order to carry out data collation. Linda Beal, Kathy Lange, Dan Winkless and Mark Shewmake were particularly helpful and tolerant. The BLM in Safford provided data, resources and equipment. Delbert Molitor allowed me to use data and information which he had collected and showed me the San Simon River. Christina Ramirez gave up her time to scan in BLM photographs and help unearth relevant facts. The San Xavier District were extremely kind in allowing me permission to carry out reconnaissance and surveying on their land and also provided funding for a monitor, for which I am extremely grateful. Scott Rogers shared information and took me out onto the reservation for reconnaissance. Marsha organised monitors. Much thanks must also go to the monitors themselves: Wayne Norris, Lawrence Capone, Alejandro Garcia, Natana Parra, Rosaria Burrell, Gregory Campos and Marlon Felix. On an initial reconnaissance trip, the Desert Research Institute in Las Vegas, especially Richard French, provided resources and information, and included me on a highly interesting trip to the Nevada Test Site. Pat Glancy also imparted useful information.

In Tucson, the surveying could not have been carried out without the incredible kindness and trust of Ron, Dan and Jerry at the Surveying and Optical Instrument Co., who allowed me to borrow an expensive total station for many weeks. Wesley Bilodeau at the University of Arizona also allowed me to borrow surveying equipment. John Hughes, against his better judgement, flew "low and slow" over the Santa Cruz River to allow me to see it from above.

Eric and Elissa Fazio-Rhieard have been my lifeline in Tucson, helping with accommodation, transport and all sorts of miscellaneous matters. Thanks also to Dwight and Sue White; Chris and Joanna Eckstein; John and Jane Hughes; Ned and Naomi Guy-Harris; Lance and Alissa Hadfield; Timy Fairfield, Mia Axon, Simon Dale and Tina Holt.

CHAPTER 1

Introduction

1.1 DEFINITION OF AN ARROYO

Arroyos are unique geomorphological features found specifically in the semi-arid south-western USA (Bryan, 1925; Antevs, 1952; Bull, 1997). For the purposes of this study, the stringent definition proposed by Graf (1983b) was applied:

“a trench with a roughly rectangular cross-section excavated in valley bottom alluvium with a major stream channel on the floor of the trench” (p280).

A further specification was that flow in an entrenched system must be ephemeral (Antevs, 1952; Schumm *et al.*, 1984).

Figure 1.1 shows the major geomorphological features of contemporary arroyo systems. The arroyo trench is incised into the alluvial valley floor, which represents the pre-incision floodplain and which is, therefore, no longer active within the contemporary regime. The trench can, in places, reach dimensions in excess of 15 metres deep and 600 metres wide. Runoff entering the trench over the arroyo walls causes them to become dissected by gully networks, which may be extensive.

Within the arroyo trench, a new channel system develops, which is, geomorphologically, entirely separate from the former valley. Flows are contained within the entrenched system and never overtop the trench walls. The inner system behaves in a similar way to a normal, unincised channel. Lateral point bars, berms and levees are deposited and may be stabilised by vegetation. The active channel is large enough to accommodate all but the high-magnitude flows. These flows overtop the banks of the active channel, inundating the floodplain that develops within the trench.

It should be noted that, although aggradation of the arroyo floor forms terraces which are commonly termed "floodplains", Schumm (1973) has observed that this is technically incorrect terminology, since these features



Figure 1.1 Geomorphological features of arroyo systems.

Key:	A	Active channel
	F	Inner floodplain, including point bars, berms and levees
	M	Abandoned meander terrace
	C	Meander core left by retreating active channel
	V	Valley floor (pre-incision floodplain)
	G	Gully networks
	T	Arroyo trench, base of which is termed arroyo floor
	W	Arroyo walls

were not formed in the same way as conventional floodplains. However, the use of this terminology is so widespread in arroyo literature that its suitability is no longer questioned. For the purposes of this study, the inner floodplain is defined as the depositional terrace within the arroyo trench.

As Figure 1.1 demonstrates, the planform of the active channel may be significantly different to that of the arroyo trench, both in geometry and pattern. Lateral erosion where the active channel impinges against the

arroyo walls causes the trench to become distorted and irregular in appearance. This is particularly prevalent in sinuous reaches, where outer bank erosion at the apices of large meander bends causes the active channel to punch laterally into the valley floor sediments. In time, the channel may cut-off or retreat, leaving an abandoned meander terrace, occasionally with an unincised remnant at the core, if cut-off was rapid.

The planform of the active channel in arroyos is often described as braided (for example, Elliott, 1979; Love, 1979; 1989; Guber, 1988; Meyer, 1979; Elliott *et al.*, 1999; Gellis and Elliott, 2001). However, this braiding is stage-dependent. At low-magnitude flows, the large volume of easily mobilised sediment on the floor of the arroyo trench always results in a braided planform. Increases in stage rapidly cause the temporary braid bars within the channel to be drowned out and the sediment stored within them to be mobilised. The stage at which the channel becomes single-thread is dependent on its width.

1.2 PROJECT AIMS AND RATIONALE

The principal aim of this project was to derive a general explanation of the relationship between the morphology of an arroyo, discharge variability and the antecedent sequence of events within the system. Within the context of this aim, the changing relationship between discharge and morphology, both temporally and spatially, was analysed using a combination of field observation; examination of aerial and ground-level photographs; and a review of existing literature. It is generally considered that channel-forming discharge theories related to a particular discharge have limited applicability in arroyos. The secondary aim of this project was to use the investigation of the relationship between discharge and morphology to test this hypothesis. The findings of the two strands of research were then combined to develop a general conceptual model of arroyo evolution, which both updated those proposed previously and incorporated the interaction between discharge and morphology.

It should be noted that, for the purposes of this thesis, the term “channel-forming flow” has been used in two senses. Firstly, and most importantly, this term has been used to describe the relationship and interaction between discharge and morphology, in particular, the extent to which the morphology of the arroyo trench has been controlled by the flow regime. Secondly, this term has been used in the traditional sense of dominant discharge. Channel-forming, or dominant discharge concepts, are based on the hypothesis that, over a period of time, the largest flows which occur within a channel are not the most geomorphologically effective, since they occur so rarely. Instead, it is the more frequent, lower-magnitude flows which, over time, transport the greatest amount of sediment (Wolman and Miller, 1960). Channel morphology is a product of the range of flows transporting sediment and the order in which these flows occur. It is argued that if, over a period of time, no significant change in either flow or sediment regime occur, the bankfull discharge becomes adjusted to the effective discharge. The channel-forming flow is, therefore, defined as the discharge equal to the steady flow which produces the same channel dimensions as the naturally occurring sequence of events (Wolman and Miller, 1960). These concepts are reviewed in Chapter 2.

The application of channel-forming flow concepts to arroyo systems is pertinent, since much of the literature concerning arroyo geomorphology has focused on their initiation and subsequent evolution. Arroyo trenches began downcutting semi-synchronously during the mid- to late-19th Century, at a time when interest in geomorphology was burgeoning. The dramatic headcutting of these incised channels provoked a significant amount of interest into the cause of this incision. There is, therefore, a vast literature database proposing different causal mechanisms and a variety of subsequent evolution and modification processes, which then operate to produce similar landforms; a concept known as equifinality (Cooke and Reeves, 1976; Graf 1979b, 1983b; Whittow, 1984; Bull, 1997). Theories regarding arroyo initiation mechanisms are discussed in Chapter 3.

Over a century of evolution has occurred since arroyo initiation in the south-western USA, enabling geomorphologists to observe patterns of development. Models of evolution based on these observations have been proposed. However, there have been few attempts to directly link this morphological progression to the flow and sediment regime. Added to this, those studies which have linked the two have used examples of other types of incised, ephemeral channels which do not fit the stringent definition described above (for example, Meyer, 1989; Graf *et al.*, 1991); have not attempted to relate the calculated effective discharge to the contemporary morphology (for example, Nash, 1993); have not used cross-sections representative of the entire range of morphologies (for example, Popp *et al.*, 1988) or have not used a quantitative analysis of effective discharge (for example, Guber, 1988). It should be noted that in some of the cases cited, the intention was not to explain the relationship between flow regime and arroyo morphology. It is, therefore, not altogether surprising that satisfactory conclusions have not been reached to date. This project has attempted to redress this imbalance by ensuring that all the above research issues were taken into consideration, particularly when developing the final geomorphological model of arroyo evolution.

1.3 METHODS OF STUDY

An essential objective of this study was to explain how the morphology of arroyos has evolved and to determine the controls on contemporary arroyo morphology forms and processes. Ephemeral arroyo systems are event-driven, with the vast majority of geomorphological change occurring during the temporally separate flow events. A thorough examination of the driving variables of these systems must, by necessity, place emphasis on the relationship between the flow regime and the morphological characteristics of the arroyo systems.

The flow and sediment regimes of each of the three selected arroyos were analysed to determine whether trends in the data could be observed. This was in order to ensure that the contemporary regime was used for effective

discharge analysis. Precipitation data was also analysed to examine whether changes in the flow regime were caused by changes in the amount or characteristics of precipitation, or morphological change within the arroyo. Chapter 4 presents a detailed analysis of the precipitation, flow and sediment data.

Within the context of the flow regime examined in Chapter 4, the morphological evolution of each arroyo was determined from past studies, combined with observations from aerial photos dating back to 1936 and ground-level photographs dating back to the late 1800s. This enabled examination of the interactions between the driving variables and the resultant process-form relationships, as each arroyo system evolved. The presence and effect of other potential controlling variables, such as the geology of the drainage basin, was also investigated. These findings are presented in Chapter 5, enabling a clearer understanding of the evolutionary steps which have resulted in the contemporary morphology.

A fundamental element of this study was to establish the characteristics of the contemporary morphology of each arroyo. Field reconnaissance of the arroyos in Arizona enabled distinct geomorphological reaches to be identified. More detailed surveys of these selected representative reaches were carried out. Along the Rio Puerco, cross-sections had been surveyed by John Elliott during the 1970s (Elliott, 1979). Allen Gellis and John Elliott had then repeated these surveys during the 1990s. These cross-sections are used in this project with their kind permission. Reconnaissance of the Rio Puerco was also carried out in order that geomorphologically distinct reaches were identified within the scope of this project, rather than relying on the observations of other researchers. Chapter 6 examines the processes-form relationships within modern arroyo systems and presents the contemporary geomorphological characteristics of each arroyo studied, providing a comparison of the different systems and reaches within these systems.

In order to determine whether the contemporary arroyo morphology is controlled by a definable channel-forming flow, the effective discharge for each gauging station along the arroyos studied was calculated. This was accomplished using a magnitude-frequency approach, combining the discharge and sediment load to determine which flows, over an extended period of time, transported the most sediment. A computer program was used to carry out these calculations. This was developed at Colorado State University by David Raff, using a methodology outlined by Holmquist-Johnson (2002). To determine whether the arroyo morphology was adjusted to the effective discharge, a comparison of the bankfull and effective discharges was made. The underlying assumption was that, if channel-forming discharge theories are applicable in arroyo systems, the bankfull and effective discharges will be very similar. Bankfull discharges were calculated from the surveyed cross-sections. Chapter 7 presents the results of the effective discharge and bankfull discharge calculations, examining the relationship between the discharge regime and the contemporary morphology.

The above research methods were used to achieve the project aims set out in Section 1.2. Examination of process/form relationships, both during arroyo evolution (discussed in Chapters 3 and 5) and within the contemporary arroyos (discussed in Chapter 6), was combined with analysis of hydrologic and sediment transport regimes (discussed in Chapter 4), including investigation of the applicability of effective discharge techniques (discussed in Chapter 7). Amalgamation of these two strands of research enabled a generalised conceptual model of arroyo evolution to be produced, which developed the ideas proposed in the earlier channel-evolution models (discussed in Chapter 2). The use of observations of contemporary arroyo morphology and contrasting study areas enabled a better understanding of the changing nature of process-form relationships to be gained, necessitating significant revisions to the previous evolution models. Chapter 8 presents a revised conceptual model of arroyo evolution. Emphasis is particularly placed on the importance of examining the changing nature of the

relationship and interaction between discharge (both flow and sediment) and morphology at both a flood-scale and over a longer period of time, in order to determine the controls of arroyo morphology. Channel-forming flow concepts, in the two senses described previously, are, therefore, incorporated into the revised arroyo evolution model.

1.4 STUDY AREAS

Particular care was taken in this study to ensure that certain criteria were met when selecting the arroyo systems for investigation in this project:

1. The sites are all entrenched, ephemeral arroyo systems, as defined in Section 1.1.
2. The sites have a minimum of 30 years' discharge record, up to and including the present day, with measured sediment discharge data.
3. The sites are in areas where historic data is readily available.
4. The sites are as free from human intervention as possible.

Only three arroyos met these stringent criteria: the Rio Puerco, New Mexico and the Santa Cruz and San Simon Rivers, Arizona (See Figure 1.2). These systems shared many of the same drainage basin and geomorphological characteristics, although differences between the three may also be noted.

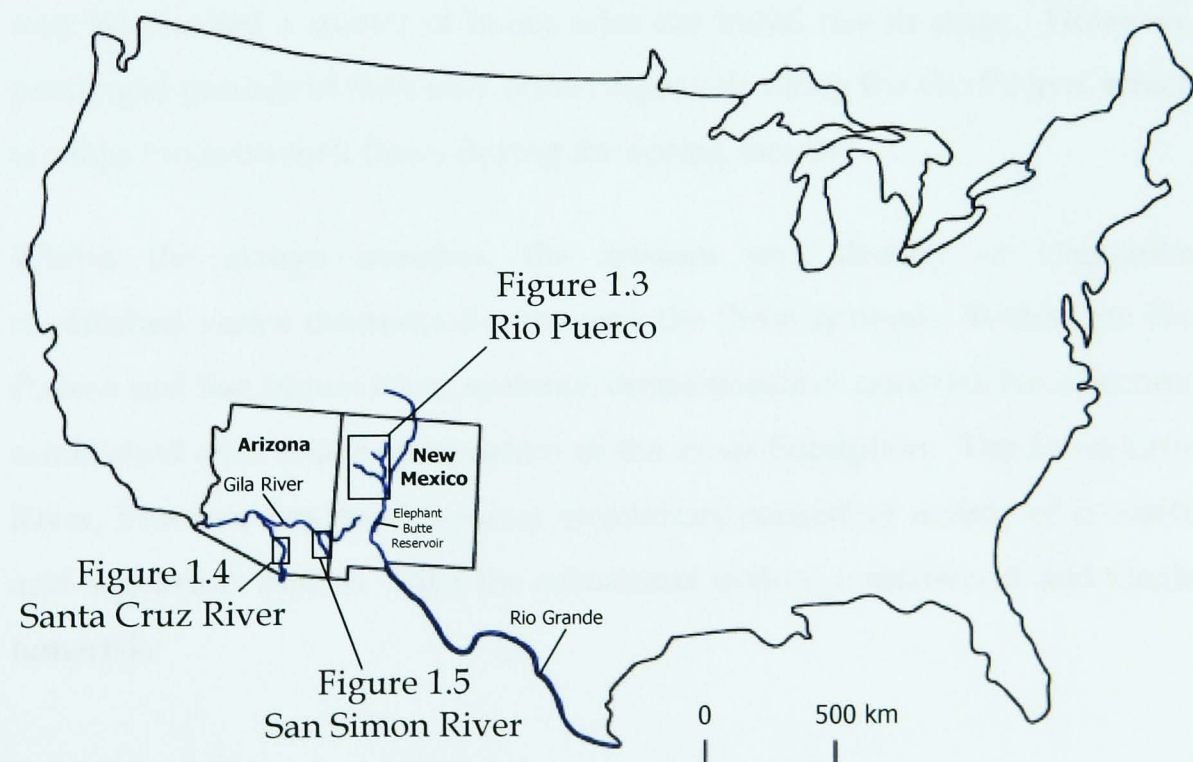


Figure 1.2 Location of study areas.

Note: Location maps may also be found in Appendix 2; Figures A2.1; A2.10 and A2.17

The three arroyos are all situated within large structural basins characteristic of the Basin and Range physiographic province, although the Rio Puerco drainage basin also has physiographic features characteristic of the Colorado Plateau and Southern Rocky Mountain provinces. The drainage basins are flanked by high mountain ranges, generally Tertiary in age, which rise to over 3,000 metres (Figures 1.3 to 1.5). The basin floors are characterised by early- to late-Quaternary alluvial terraces signifying the cycles of arroyo cut-and-fill which have occurred over recent geologic time. The geologic evolution of each drainage basin represents an element of the evolution of each arroyo system and is, therefore, presented in Chapter 5.

Precipitation within the basins varies with altitude, with higher elevations receiving up to three times the amount of rainfall than the lower elevations. Precipitation is generally bi-seasonal, with localised, intense summer "monsoonal" rainfall contrasting with more prolonged basin-wide storms during autumn and winter months.

Arroyo systems characteristically have flashy flow regimes and the regimes of the three arroyos studied are no exception. Peak discharges may be two orders of magnitude larger than the mean discharge and maximum flows may be reached a matter of hours after the initial rise in stage. However, prolonged periods of flow may occur, especially along the Rio Puerco, which is subject to snowmelt flows during the spring months.

Within the arroyo trenches, the amount and density of vegetation established varies dramatically between the three systems. Within the Rio Puerco and San Simon River systems, dense stands of tamarisk have become established over a large proportion of the inner floodplain. The Santa Cruz River, however has much sparser vegetation, consisting mainly of creosote and sagebrush bushes, with the occasional mature cottonwood and single tamarisk.

Rio Puerco

The Rio Puerco drains 18,892 square kilometres in west-central New Mexico, east of the Continental Divide (Love, 1986; 1992; Popp *et al.*, 1988). The headwaters of the system are in the Nacimiento Mountain range, with the mouth at the Rio Grande some 280 kilometres south (Figure 1.3). The Rio Puerco is joined by two major tributaries: the Arroyo Chico, which has a major influence on the geomorphology of the main arroyo; and the Rio San Jose, which does not. Of the smaller tributaries, only the Arroyo Chijuilla

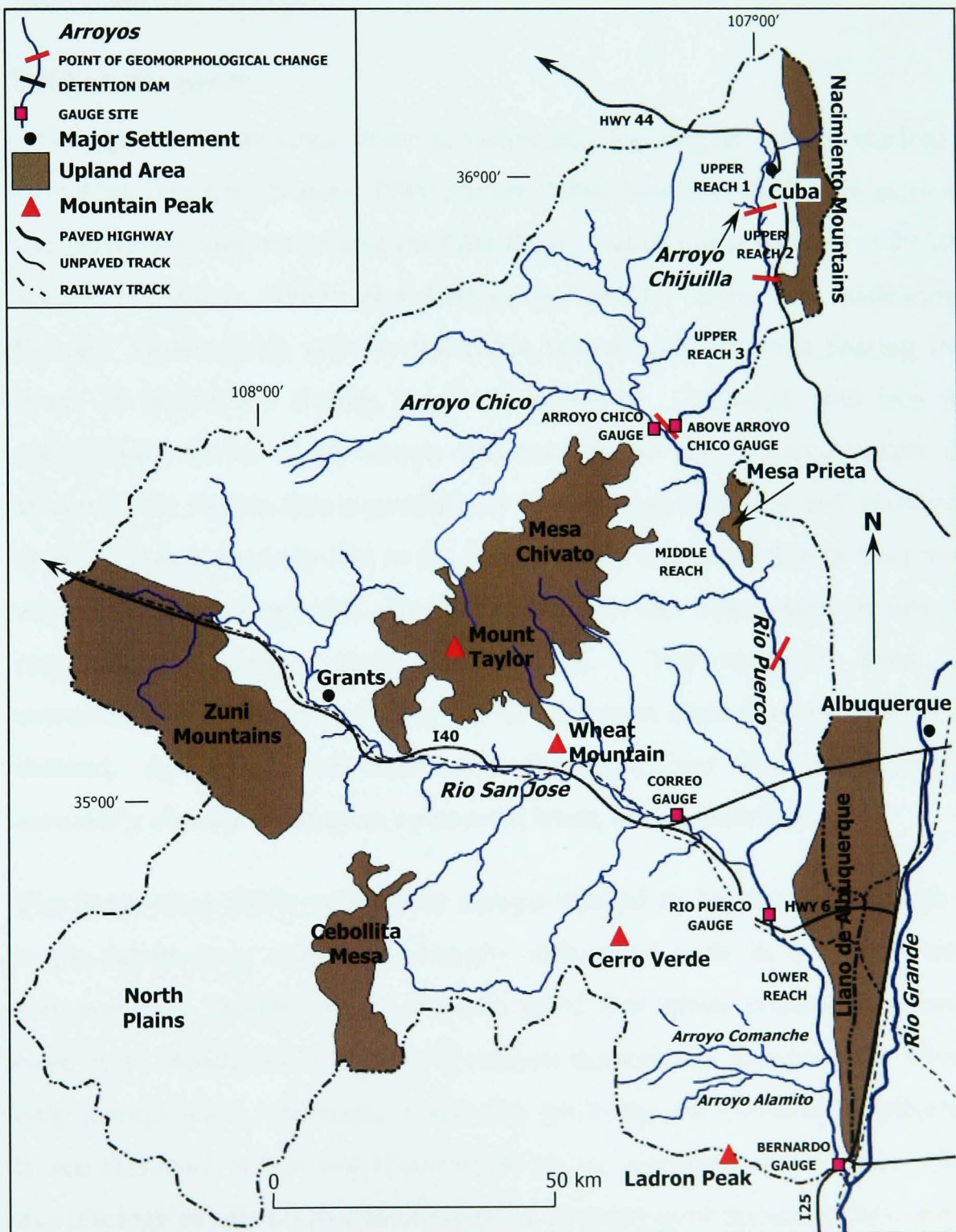


Figure 1.3 Major landforms, settlements and gauging stations of the Rio Puerco Basin.

has a significant geomorphological effect on the mainstem. The Rio Puerco was divided into five geomorphically distinct reaches, located in Figure 1.3. These reaches are separated by a combination of tributary confluences and knickpoints, both artificial and natural.

The Rio Puerco basin has the smallest population of the three arroyos studied and, therefore, has been subject to the least alteration. This arroyo is, therefore, for the purposes of this project, considered to represent a near-natural pattern of evolution.

Santa Cruz River

Although the Santa Cruz River is technically the largest system studied - stretching 390 km (Waters, 1988; Parker, 1996) between the headwaters in the Patagonia Mountains and the Gila River, and draining an area of 22,200 square kilometres (Webb and Betancourt, 1992) - these are misleading figures. Flows rarely activate the entire system, with Marana bearing the brunt of deposition during larger flow events. Although this lack of connectivity occurs in all arroyo systems, due to the localised nature of storms in the region, this is particularly pronounced in the Santa Cruz River system. This is partially due to the fact that only a short section of the river, where it cuts through the city of Tucson, fits the description of arroyo morphology specified above (Figure 1.4). The upstream limit of entrenchment is abrupt, whereas the downstream limit is much less well-defined. Apart from this short reach, the Santa Cruz River can be more accurately characterised as an ephemeral wash, and is unincised.

The Santa Cruz River is the only arroyo studied to be situated close to a major urban area, which has heavily influenced both its evolution and contemporary morphology. Artificial flood and grade control structures have been implemented to prevent erosion through the Tucson area. Thus, only a short reach, upstream of the city, has remained relatively unaltered. It was this reach which was investigated for the purposes of this study. The morphology of this reach was affected by an outcrop of resistant Pleistocene sediment, which defined the upstream limit of the arroyo. No major

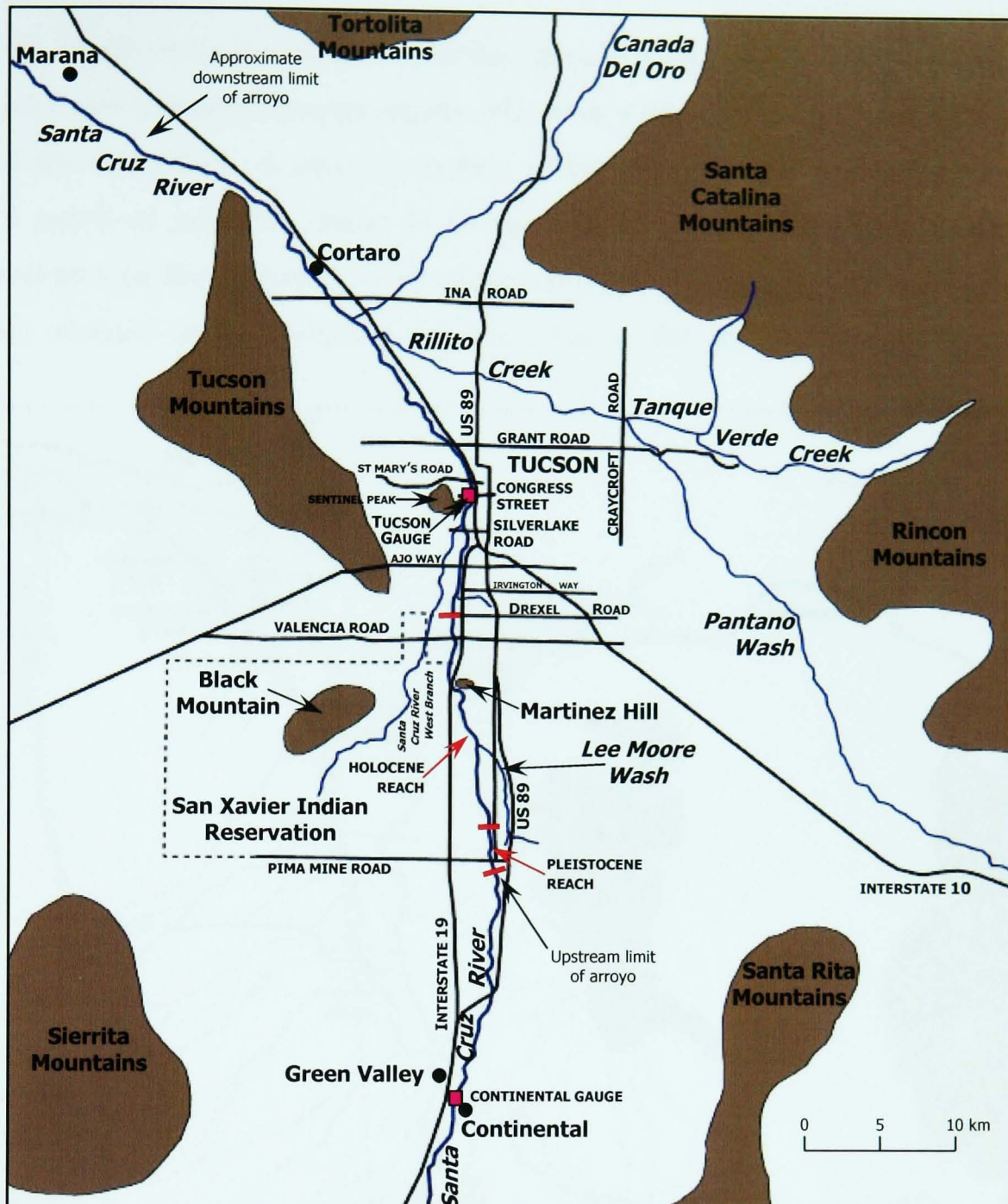


Figure 1.4 Major landforms, settlements and gauging stations of the Tucson Basin (See Figure 1.3 for legend).

tributaries enter the system along this incised reach. Thus, only two geomorphologically different reaches were identified, each distinguished by the predominant sediment type through which the arroyo is incising.

San Simon River

The San Simon River rises near the Arizona/New Mexico border, flowing over 170 kilometres to its confluence with the Gila river close to Safford (Figure 1.5). The drainage basin encompasses an area of approximately 6,000 square kilometres (Mathis, 1983).

The trench of the San Simon River has been heavily dissected by numerous gully and tributary arroyo systems, which have headcut, eroding large areas of the valley floor. It was this erosion which prompted the implementation of sediment detention dams: 15 on aggressively eroding tributary systems and four on the mainstem. Two of these mainstem dams, the Cienega Dams are situated in the upstream reaches, close to the state border, and their

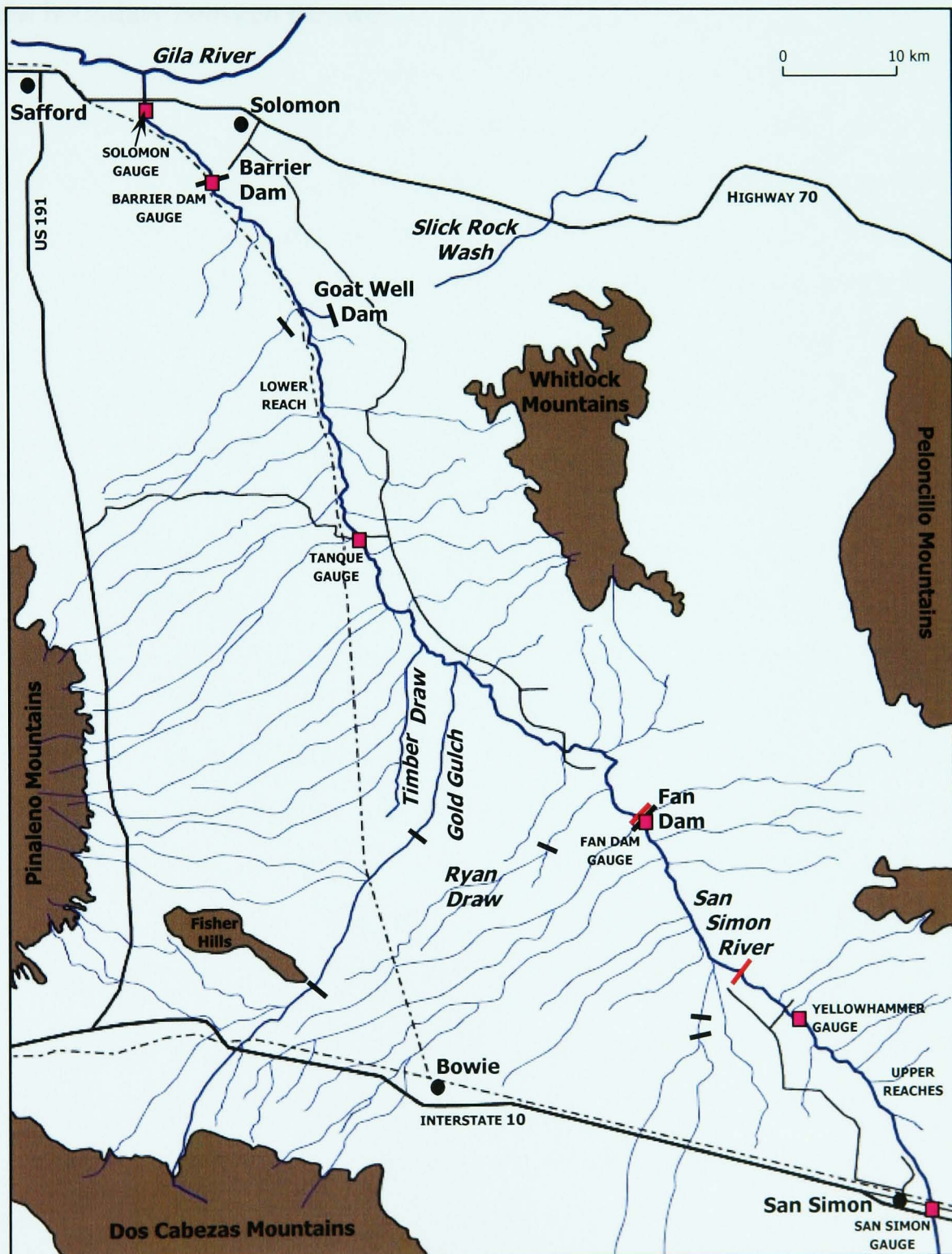


Figure 1.5 Major landforms, settlements and gauging stations of the San Simon Basin (See Figure 1.3 for legend).

effects were not included in this study. The other two mainstem dams, especially the Fan Dam, have had a marked effect on the geomorphology of the San Simon River, causing aggradation for some distance upstream. This project has concentrated on an investigation of the morphology of the arroyo between the town of San Simon and the Goat Well reach, just upstream of the aggraded Barrier Dam reach. Only two geomorphologically distinct reaches were identified for the San Simon River, with the Fan Dam acting as the boundary between the two.

CHAPTER 2

Channel-Forming Flow and Fluvial System Behaviour

2.1 INTRODUCTION

“Discharge is the most important variable controlling the size and shape of alluvial channels” (Hey, 1998, p1)

Any discharge which exceeds the critical shear stress required for sediment transport has the potential to change the channel morphology. However, certain discharges have been observed to have a greater effect on channel form than others. The geomorphological importance of an event is governed by both its magnitude and the frequency with which it occurs (Wolman and Miller, 1960; Wolman and Gerson, 1978). There has been much discussion in geomorphological literature as to whether less frequent, high magnitude flows or more frequent, lower magnitude flows carry out most work on stream channels. Dominant discharge theories proposed in the 1940s, originally for regime canals and later applied to natural channels, conclude that significant alluvial landforms are formed by more frequent events of moderate intensity (Wolman and Miller, 1960). The dominant, or channel-forming discharge is equal to the steady flow which produces the same regime channel as the naturally occurring sequence of events (Inglis, 1941 and Blench, 1951; in Wolman and Miller, 1960). Regime channels are, by definition, those which neither scour nor fill their channels (Leopold and Maddock, 1953), although this definition has been modified to include natural self-formed, alluvial channels which have achieved a state of dynamic equilibrium, with the channel dimensions fluctuating around average long-term conditions (Chang, 1979; Nouh, 1988; Hey, 1997).

The concept of dominant discharge is often confused with the concept of effective discharge. The effective discharge is defined as that increment of a river’s discharge which transports the largest fraction of the annual sediment load over a period of years (Wolman and Miller, 1960; Andrews, 1980; Leopold, 1992). Thus, the effectiveness of an event is the ability of that

event, or combination of events, to affect the landscape (Wolman and Gerson, 1978).

Channels in semi-arid and arid regions have been shown to be adjusted to very rare, extremely large floods, rather than the lower magnitude, higher frequency discharges suggested by dominant discharge theories (Wolman and Gerson, 1978; Osterkamp and Hedman, 1982; Graf, 1983a; Hey, 1997). Low frequency, high magnitude events, which have great destructive potential are generally termed “catastrophic” floods (Wolman and Miller, 1960).

2.2 THEORIES OF CHANNEL-FORMING FLOW

2.2.1 Effective and Channel-Forming Discharge

The geomorphological effectiveness of different flows was examined by Wolman and Miller (1960) and later by Andrews (1980), Thorne *et al.* (1993) and Biedenharn and Thorne (1994), amongst others. By quantifying the amount of material carried by flows of various magnitudes and then multiplying these amounts by the frequency of occurrence of these flows, the effectiveness of different flow classes was examined (Figure 2.1). Wolman and Miller (1960) calculated the percentage load carried by flows,

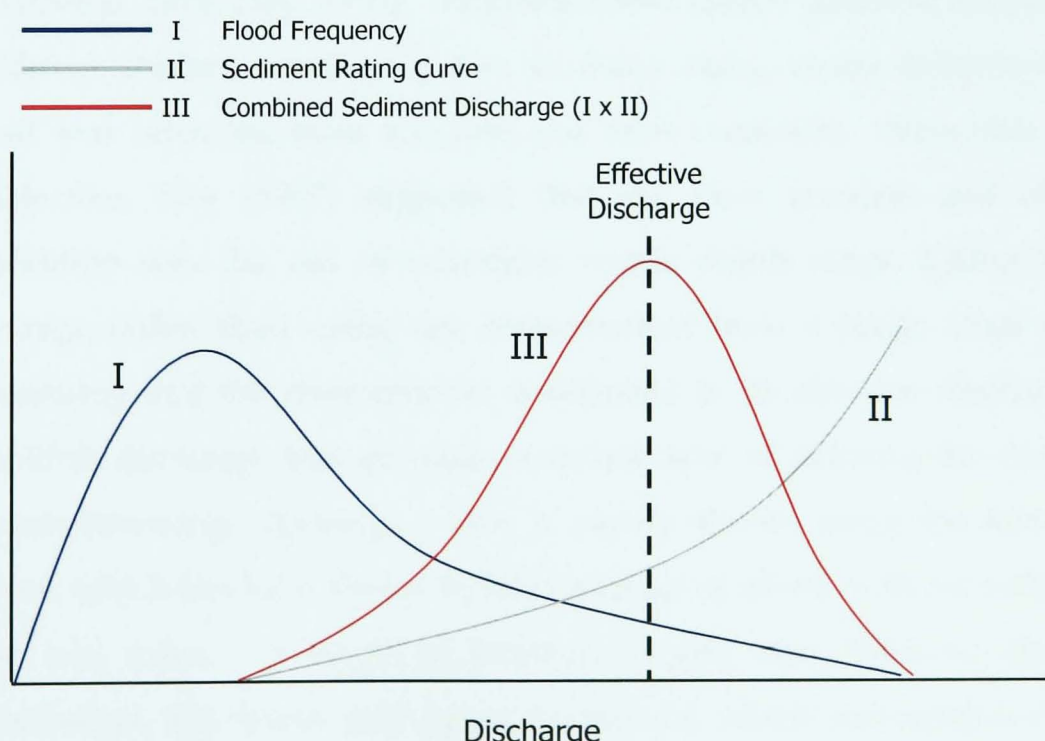


Figure 2.1 Schematic representation of effective discharge (after Thorne *et al.*, 1998).

discovering that, although catastrophic floods carry huge amounts of sediment, they occur so infrequently that their overall effectiveness is relatively low. It was observed that over 50% of the total suspended sediment load was transported by flows which occurred, on average, on one day or more per year. The majority of the remaining 50% was transported by floods which occurred at least once every five years, not by extremely large events.

Given that the effective discharge accomplishes most work in forming the channel, where work is defined by the amount of sediment transported, regime channels may be expected to adjust their channels to this flow. Thus, channel dimensions and form reflect the effective discharge of the system, assuming a stable flow regime. The channel capacity and bank-top elevation have been found to be strong morphological expressions of this effective flow, leading to the conclusion that the effective discharge equates to the dominant, channel-forming discharge. A regime channel, therefore, contains all flows up to and including the effective discharge (Biedenharn and Thorne, 1994).

There has, however, been much confusion over what constitutes “bankfull” (Williams, 1978; Hey, 1997). Williams noted eleven different definitions in different studies, concluding that, in many cases, visual definition in the field was often the most accurate and most consistent. Since this can be subjective, Hey (1997) suggested that the most accurate and objective definition was the use of minimum width: depth ratios, taking a reach average rather than using one measurement from a single cross section. Assuming that the river channel is adjusted to its effective discharge, the bankfull discharge thus provides a simple way of defining the dominant, channel-forming, discharge. This is clearly shown along the Mississippi River, which has been shown to have a range of effective flows, rather than just one value. A range of bankfull heights was observed along the Mississippi, the lower and upper bounds of which corresponded to the

dominant discharge at 30,000 cumecs and the upper limit of the effective range of flows at 40,000 cumecs (Biedenharn and Thorne, 1984).

Since the bankfull discharge corresponds to the effective discharge in many perennial rivers, it has been found useful to determine the return frequency of this dominant, channel-forming flow. Some researchers have found that a consistent return period of between one and two years represents bankfull flow frequency (Wolman and Miller, 1960; Dury, 1976; Andrews, 1980; Biedenharn and Thorne, 1994; Soar and Thorne, 2001). However, this frequency has been challenged by other researchers, who have found that bankfull return frequencies may be very variable between channels (Williams, 1978; Andrews, 1980; Nash, 1994). These studies have indicated that, although the modal bankfull frequency was found to be between one and two years, the actual return frequencies were highly variable and could be as long as thirty or more years, although this difference has been attributed to a poor threshold choice when determining partial duration series' (Hey, 1997). It has also been suggested that the variation in return frequency of bankfull flows reflects differences in the flow regime of natural channels (Hey, 1997). Care should, therefore, be taken when using $Q_{1.5}$ or $Q_{1.58}$ rather than the actual bankfull discharge, that this is truly representative of the dominant discharge, since channel management based on the 1.5 or 1.58 year flood may lead to seriously erroneous results (Hey, 1998).

The significance of using the bankfull flow as the dominant channel-forming discharge has been made apparent by observations that many other channel characteristics, such as pool-riffle spacing, meander geometry and channel width, are also closely related to bankfull discharge. These concepts are closely tied to the theory that all stream channels adjust their dimensions in order to achieve an equilibrium, where the total power per unit length of the stream is at a minimum (Chang, 1979; Baker and Costa, 1987; Simon, 1992).

2.2.2 Equilibrium and Threshold Concepts

Self-regulation, through negative feedback processes, has long been recognised as being a feature inherent in natural systems (Chorley *et al.*, 1984). The concept of negative feedback was initially applied to fluvial systems to explain the concept of a graded stream: defined as a channel which, over a period of time, neither aggrades or degrades but is instead adjusted to the sediment load supplied from the drainage basin (Chorley *et al.* 1984; Bull, 1988; Knighton, 1998). A graded stream tends to form and maintain a smooth equilibrium long-profile through the action of negative feedback effects. For example, steeper sections cause an increase in the flow velocity, leading to bed erosion until a lower slope is attained (Chorley *et al.*, 1984). Subsequent research has indicated that this concept is overly simplistic and equilibrium theories have, therefore, been adapted to include process-form interaction using a more quantitative approach (Chorley *et al.*, 1984; Knighton, 1998).

Systems which are in a state of equilibrium show a constant relationship between inputs to the system, outputs from the system and form. In a geomorphological context, this does not mean that the system is stable, but if observed over a long enough timescale, maintains the same relatively stable characteristics (Graf, 1979a; Chorley *et al.*, 1984; Renwick, 1992; Knighton, 1998). Adjustments to the channel occur as the river's ability to transport sediment balances the available sediment load (Chang, 1979; Baker and Costa, 1987). Thus, for given system inputs of water and sediment discharges, a particular channel geometry exists (Chang, 1979; Simon, 1992). If one link within a system in stable-equilibrium is altered through internal or external stimuli, all other links within the system respond through negative feedback mechanisms to re-establish the original balance (Graf, 1988a; Renwick, 1992). If the long-term form oscillates around an unchanging mean value, the system is said to be in steady-state equilibrium (Figure 2.2a) (Chorley *et al.*, 1984). However, if this mean itself shows a trend, the system is instead said to be in a state of dynamic equilibrium (Figure 2.2b) (Chorley *et al.*, 1984; Renwick, 1992).

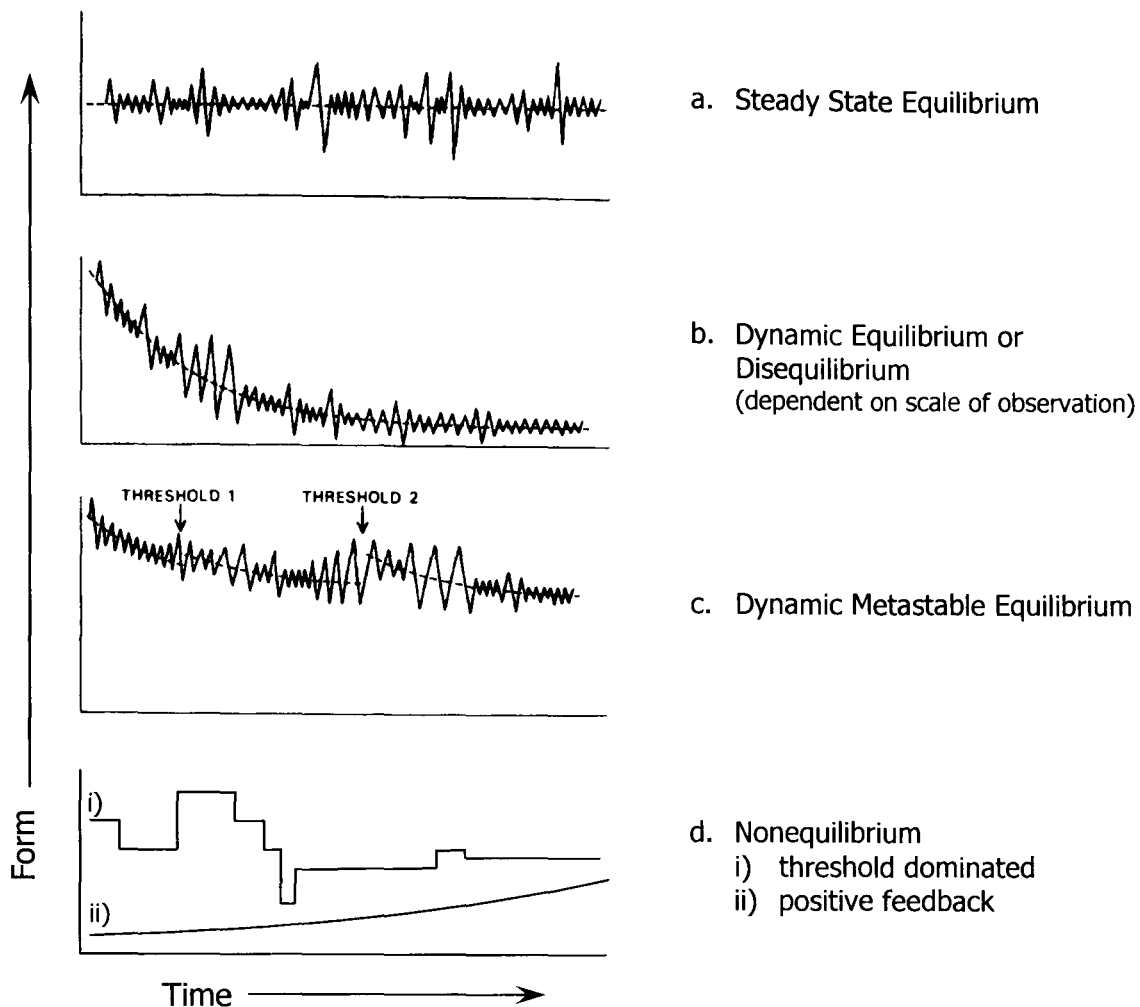


Figure 2.2 Types of equilibrium (after Chorley *et al.*, 1984; Renwick, 1992).

Systems in equilibrium are, therefore, in a constant state of flux, whereby the form fluctuates around an average condition. If inputs to the system are of sufficient magnitude, the system takes some time to return to its original form through negative feedback mechanisms. This is known as the recovery time of a system (Chorley *et al.*, 1984). For a system to remain in equilibrium, the recurrence interval of high-magnitude events must be longer than the recovery time.

The study of equilibrium concepts concentrated research on the periods of time when the system was stable (Graf, 1979a). However, it was recognised that importance should also be placed in the short changes seen in channel systems between periods of equilibrium (Schumm, 1973; 1979; Chorley *et al.*, 1984). Equilibrium concepts did not explain why, for example, some rivers responded to catastrophic flooding with devastating change (for example: Wolman and Miller, 1960; Anderson and Calver, 1980; Osterkamp and

Costa, 1987), whereas others apparently caused very little channel change (for example: Gupta and Fox, 1974; Moss and Kochel, 1978). Schumm (1973) recognised the failure of dynamic equilibrium concepts to explain these different responses to the same external influences and, therefore, put forward the concepts of geomorphic thresholds and complex response. It was suggested that the magnitude of system response depends on the proximity of the system to threshold conditions (Schumm, 1973). Large magnitude events are only able to cause significant modification if the system thresholds are passed. Thus, channels within the same region and subject to the same processes may have different resultant forms.

External influences causing abrupt changes within a system have been termed “extrinsic thresholds”. The threshold exists within the system but is not crossed without the influence of an extrinsic variable (Schumm, 1973). A second type of threshold was also recognised, whereby the external variables acting on a system remain relatively constant yet failure or dramatic change still occurs within the system. Schumm suggested that these intrinsic geomorphic thresholds develop due to changes within the system itself. Thus, a system may be observed to evolve slowly until a critical situation is reached, triggering sudden adjustment or failure (Schumm and Khan, 1972; Schumm, 1973). It may not always be clear whether a system is responding to an external influence or to an internal geomorphological threshold. However, if a change in slope is involved, the control is geomorphic and intrinsic to the system (Schumm, 1973). Since the periods of little change approximate steady equilibrium conditions, systems showing sudden short periods of change separated by longer periods of apparent equilibrium are said to be in dynamic metastable equilibrium (Figure 2.2c) (Schumm, 1975; Chorley *et al.*, 1984; Renwick, 1992).

The inherent thresholds built into a natural system enable one event to trigger several phases of complex channel response. This observation was based on a flume experiment in which base-level of a small drainage was lowered. The system responded by adjusting to a new equilibrium by

incising, aggrading and then re-incising (Schumm, 1973; 1975). Channel incision occurred at the mouth of the system, working progressively upstream into tributary headwaters. Sediment was, therefore, released in increasing quantities, eventually leading to aggradation within the newly incised channel. As the main channel and tributaries adjusted to the new base-level, sediment loads decreased, leading to a new phase of incision. Examples of complex response were subsequently observed in natural systems (for example: Womack and Schumm, 1977; Love, 1979).

System thresholds may also be defined in terms of stream power. If an initial disturbing event surpasses the sediment transport threshold of the system, the critical slope for entrenchment may be exceeded, in turn causing the critical bank threshold to be passed and so on. Bull (1979) expressed these threshold concepts in terms of a single critical power threshold (CPT), explaining that the CPT separates modes of net aggradation and degradation. Stream power is used as a surrogate for width, depth and velocity, which interact to determine the capacity and competence of the stream to transport sediment. The CPT is determined by the relative values of power required to transport the average sediment load and the actual power available to transport this load (Bull, 1979). Rather than determining the ratio of vertical to lateral erosion by the height of the banks or width of the channel, Bull suggests that this ratio is determined by the proximity of the system to the CPT.

The concept of stream power thresholds has been tied to the effectiveness concept in order to assess the effects of flood events (Baker and Costa, 1987; Macgilligan, 1992). Thus, rather than assessing the channel-forming properties of events, the channel *de-forming* properties have been examined (Macgilligan, 1992). Flood power concepts attempt to explain the lack of channel change observed after some very large catastrophic floods by suggesting that for change to occur, the stream power per unit area produced must be maximised. Baker and Costa (1987) stated that, while the magnitude of a flow is important in landscape modification, other factors

such as drainage basin area, flow depth and flow velocity may also be important. Alluvial channels subjected to very large floods are able to reduce their stream power relatively rapidly by increasing the channel width through overbank flow or channel erosion. This effectively reduces the flow depth and thus boundary shear stress, limiting channel change. However, in channels containing very large boulders or in channels composed of bedrock, especially deep narrow gorges, extremely high values of stream power have been recorded, since the channel is unable to adjust as rapidly. Flow depths and velocities are thus able to reach a maximum. Thus, in channels which have high resistant thresholds it is only the rare, high magnitude floods which are able to cause significant channel adjustment (Wolman and Miller, 1960; Wolman and Gerson, 1978; Baker and Costa, 1987; Baker and Pickup, 1987). Baker and Costa (1987) suggest that many rivers seem to be adjusted to lower magnitude, higher frequency flows due to the fact that these flows are powerful enough to overcome the much lower sediment transport thresholds of finer grained alluvial streams and are thus able to accomplish much geomorphological work.

Channel change in response to extremely large flood events tends to result in an increase of energy conditions in the system, thus “rejuvenating” it (Simon, 1992). Using the example of a channel subject to an extremely high magnitude debris flow after a volcanic eruption, Simon (1992) demonstrated that the amount of energy dissipated by a system decreases in a non-linear manner over time, generally exponentially, towards the new equilibrium state. The channel configuration immediately after the disturbance represents extreme disequilibrium and the channel subsequently evolves to re-establish a new equilibrium state, which may take a considerable amount of time. Systems in a state of disequilibrium show progressive change, since the total response, or relaxation, time of the system to a perturbation is longer than the return period between perturbations (Figure 2.2c) (Renwick, 1992). The form of disequilibrium systems is therefore out-of-phase with the processes acting on the system (Malanson et al, 1992; Renwick, 1992). Systems in a state of disequilibrium thus show time-dependent adjustment

(Simon, 1992). It is, therefore, difficult to distinguish between a system in dynamic equilibrium, where equilibrium is maintained, and disequilibrium. Systems which appear to be in disequilibrium when observed over short time-scales may be in a long-term state of dynamic equilibrium (Renwick, 1992).

2.2.3 Non-Linear Dynamical Systems Theory

It may be noted that all the concepts of channel development mentioned so far have relied on equilibrium or disequilibrium concepts, whereby the system is tending towards a steady state. However, it has been noted that some geomorphological systems do not tend towards any definable state and thus a characteristic condition cannot be identified. Systems in this state are said to be in a state of non-equilibrium and are often characterised by the presence of thresholds at rare, high magnitude levels of process operation, together with strong positive feedbacks and the capability for chaotic behaviour (Figure 2.2d i) and ii)) (Renwick, 1992). These systems thus have a high level of potential instability, display metastable characteristics and thus behave in a non-linear manner. Non-linearity exists wherever outputs of energy and matter are not proportional to inputs across the entire range of inputs (Phillips, 1992a). Phillips (1992b) suggests that these characteristics indicate that, given the inherent instability and non-linearity of a system, equilibrium models may provide useful, easy answers which are approximately correct but for the wrong reasons. Equilibrium concepts are criticised in particular for their time-independence and misleading implications regarding system behaviour. Similarly, Lane and Richards (1997) suggest that channel evolution models which rely on location-for-time substitutions are fundamentally flawed since there are no rigorous dating controls and formative mechanisms are often disregarded in favour of surrogate process variables.

Phillips (1992a) indicates that, although catastrophe theory utilised non-linearity, non-linear dynamical systems theory (NDS) should be applied to geomorphic problems in its place. NDS theories recognise that systems may

be dissipative structures and may exhibit chaotic behaviour, or deterministic complexity. Dissipative systems are those that dissipate energy maintaining order in states removed from equilibrium. Deterministic complexity describes apparently random behaviour that arises deterministically due to non-linearity in often relatively simple systems. Phillips (1992a) distinguishes deterministic complexity from stochastic complexity by stating that chaotic systems are extremely sensitive to initial starting conditions and diverge increasingly as progression away from the initial conditions occurs (asymptotic instability). However, systems may include both stochastic and chaotic behavioural characteristics.

Rather than assuming that landscape systems are constantly adjusting towards steady state, NDS studies use chaos theory concepts, which propose that systems evolve away from “repellors” and towards “attractors”. Repellors and attractors are, respectively, asymptotically unstable and stable states (Phillips, 1992a). NDS theories also suggest that after a perturbation, rather than moving back towards its original equilibrium state, a system will remain in disequilibrium or will move towards a new equilibrium state. This theory contradicts the concept that channels have a tendency to conserve channel adjustments that lead to equilibrium and dissipate adjustments that do not (Baker, 1988). These discontinuities in geomorphological systems, originally termed “thresholds”, have been redefined as “bifurcations” in NDS theory.

Phillips (1992a) proposed a NDS model, using inputs, outputs and storage of mass within systems, and an algorithmic approach, representing the system using numerical simulations. This mass flux model is based on the simple premise that the inputs to a system will equal the sum of the storage within the system and the outputs from that system. However, since this would result in a highly unstable system, due to the “competitive” relationship between storage and output, a feedback mechanism was introduced to mimic natural geomorphological systems. Natural fluvial systems will self-stabilise their mass storage, since with progressive entrainment, the amount

of stored material generally becomes less, until sediment becomes progressively more difficult to entrain. Similarly, catastrophic events are able to increase their output by transporting high-calibre sediment which smaller events are unable to transport. This self-limitation results in a non-competitive storage-output relationship. A power-resistance element was also added to the mass flux NDS model, which determines just how much sediment is allocated to storage or output. The NDS theory again uses the concept of critical power thresholds; if system power is higher than the resistance of the system, net erosion will occur, triggering a feedback whereby eventually the amount of sediment produced increases the resistance until it exceeds the power, thus causing net deposition. Thus systems which have a power resistance threshold are potentially unstable.

Phillips (1992a) defines the system attractors for geomorphic systems as being states where thresholds are not exceeded and where the power-resistance component is irrelevant. A fluvial system satisfies these conditions when it is actively aggrading or degrading, or when it is in a steady state (Phillips, 1992a). NDS theories can be seen to use the same basic concepts as equilibrium geomorphology, expanding them to include new, more up-to-date system theories. The use of chaos theories is particularly applicable if a system is viewed over gradually increasing periods of time: if a short period of time is observed, a system may appear to be in equilibrium. If gradually longer periods of time are observed, regularities will emerge until the pattern becomes dominated by the patterns of the attractors (Phillips, 1992a; Lane and Richards, 1997).

2.2.4 Catastrophe Theory

The concept of using force and resistance as the basic control variables in fluvial systems was the basis for development of a catastrophe theory model, describing the behaviour of change in geomorphic systems (Graf, 1979a; Thornes 1980). Equilibrium concepts are again a crucial starting point for catastrophe theory, since it is assumed that a system changes in space and time from one equilibrium state to another.

Graf (1979a) indicates that the most important implication of catastrophe theory is that geomorphological adjustments change according to topological singularities (catastrophes). Topology is the study of those geometric figures which are unaffected by deformation. Thus, the arrangement of variables rather than their magnitude becomes of prime importance. Catastrophe theory recognises that, even though system processes may quantitatively be extremely complex, qualitatively they may be simple and stable. This may be observed throughout natural stream channels since all channels have many similarities even though their formative characteristics (for example, lithology and climate) may be vastly different (Graf; 1979a; Thornes, 1980).

If force and resistance are used as basic control variables in fluvial systems, a behavioural variable, such as channel area, may be used to plot a three-dimensional smooth surface, or catastrophe, interrupted by a tuck, or cusp (Figure 2.3). For a given system, the cusp catastrophe describing that system remains stable and unchanging. Graf (1979a) discovered that this surface may be used to represent many of the most important behavioural change characteristics in ephemeral streams. First, the system behaves differently depending on the proximity of the system state to the cusp. A perturbation may cause very different outcomes, even though the starting points are very similar. Change may either be abrupt, if the system is close to the cusp, or gradual, if the system is far from the cusp or is at a point on the cusp where it can be bypassed rather than jumped across (Graf, 1979a; Thornes, 1980). Systems which have very similar starting points may exhibit divergence, where two stable, but very different, final conditions of the behavioural variable are possible. The cusp catastrophe concept also allows the possibility of hysteresis, a characteristic commonly observed in geomorphological systems, especially those experiencing regular increases and decreases in one (or more) controlling variable, leading to cyclic change. A fourth characteristic of cusp systems is bimodal behaviour. For any given values of the two controlling variables, two stable values of the behavioural variable are possible. All four characteristics of a cusp system are strongly

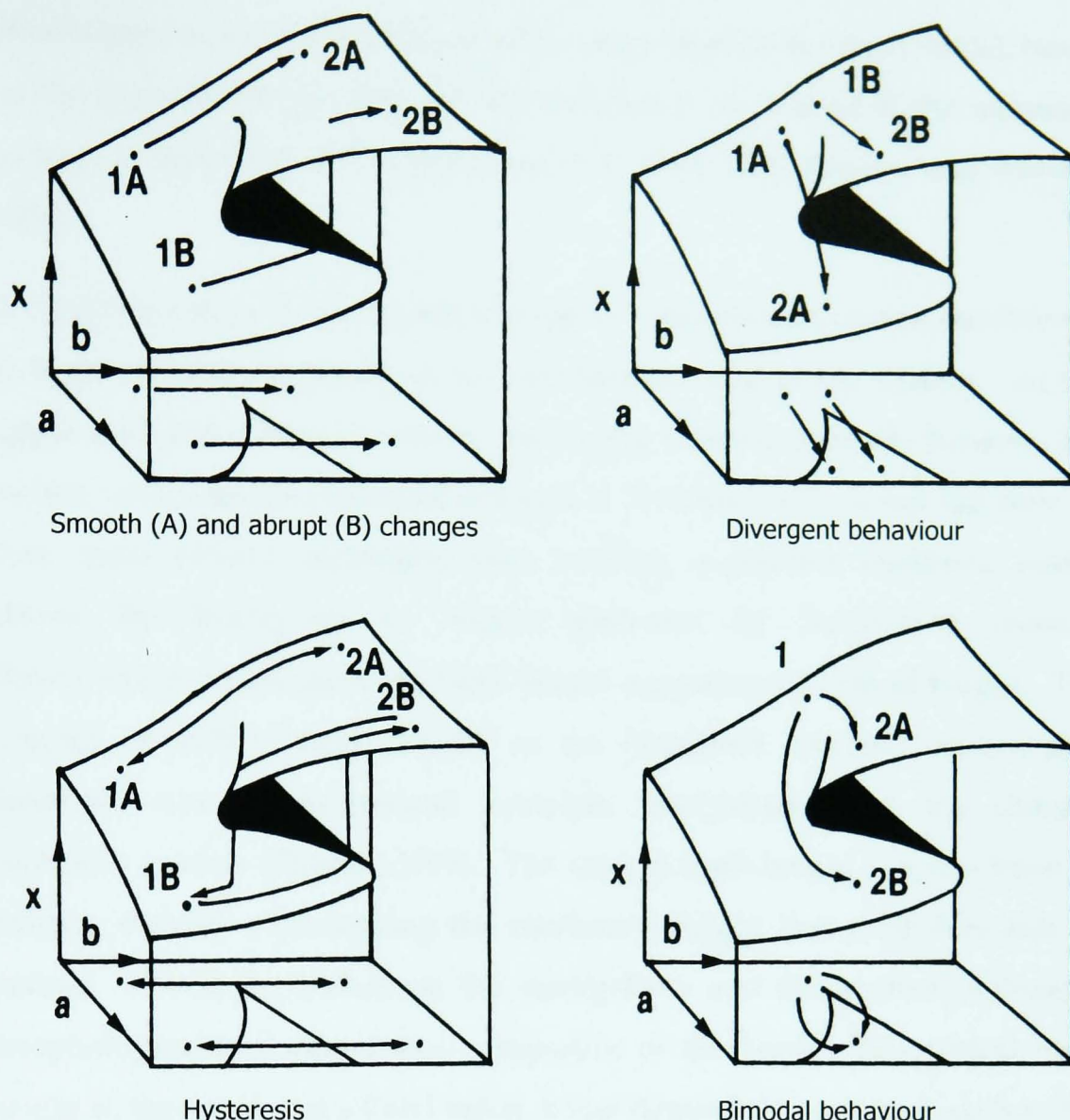


Figure 2.3 Diagrammatic representation of cusp catastrophe and different system behaviour according to initial proximity to cusp (after Graf, 1979a).

Axes a and b are control variables; x axis is a behaviour variable.

controlled by the antecedent conditions, which determine both the position of the system prior to a disturbing event and the path of the system to its final equilibrium.

2.2.5 Models of Channel Evolution

The observations of the pattern of morphological response to destabilising events led to the development of general channel evolution models for incised channels (Thorne, 1999). The most fundamental concept behind these models is that observations and data from different locations may be used to infer landform development through time (Harvey and Watson, 1986; Lane and Richards, 1997). Observations made along Oaklimiter Creek,

Mississippi were used to develop a five-stage location-for-time model, based on the assumption that distance downstream is equivalent to the increased passage of time (Figure 2.4) (Schumm *et al.*, 1984; 1987; Harvey and Watson, 1986).

A trigger event, such as climatic change or rejuvenation, causes the channel to begin incising, generally at the downstream end of the system. At the upper end of the incised section, the locally steepened divide between the incised and unincised channel (termed a “knickpoint”) causes the flow to have more erosive capability, thus creating a positive feedback, which allows the knickpoint to retreat upstream by headwards erosion. Downcutting occurs until the bank height surpasses its critical height. The concept of critical bank height as an important intrinsic geomorphic threshold was a fundamental principle incorporated into the channel evolution models (Thorne, 1999). The critical bank height is a condition of limiting stability representing the maximum height that a bank is able to sustain. This is dependent on the stratigraphy and the geomorphological, morphological and geometrical properties of the bank. The critical bank height is, therefore, not a fixed value, being dependent on factors such as the degree of bank material saturation, presence of failed material at the bank toe or presence of vegetation.

Once the critical bank height is reached, mass bank failure causes the channel to begin widening. As widening continues, the banks pass from a state of impeded removal, where the sediment transport capacity of the flow is more than sufficient to remove all failure material, to a state of excess basal capacity, where the channel has become so wide that the stream is no longer able to remove the failed sediment (Thorne, 1982). The build-up of sediment at the base of the banks may allow the channel to achieve a state of quasi-equilibrium, especially if vegetation is able to become established. Secondary knickpoints may cause a complex response to occur as the sediment supply to the system decreases. This allows terraces to form, which are subsequently abandoned as progressive knickpoints pass through the system (Womack and Schumm, 1977).

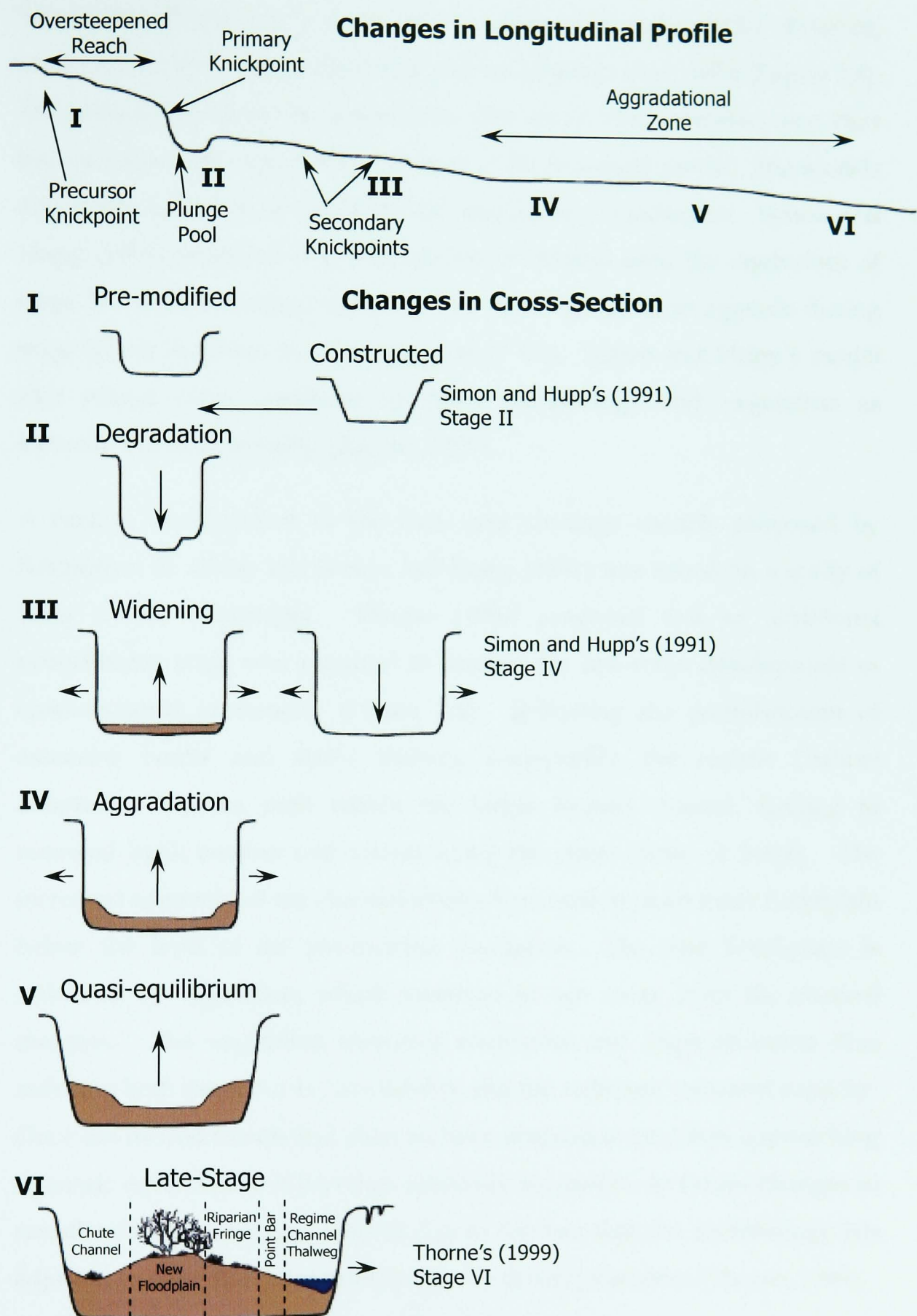


Figure 2.4 Composite incised channel evolution model (after Schumm *et al.*, 1984; Harvey and Watson, 1986; Simon and Hupp, 1991; Thorne, 1999).

Simon and Hupp (1991) proposed a similar, but significantly different, model to the five-stage model proposed by Schumm *et al.*, 1984 (Figure 2.4). This model was based on channelised streams in west Tennessee and thus has a construction stage prior to stage II of the five-stage model. The models also differ in the point at which bed aggradation commences. Simon and Hupp (1991) proposed that degradation continued until the equivalent of stage IV of the five-stage model, rather than beginning to aggrade during stage III, as proposed by Schumm *et al.* (1984). Simon and Hupp's model also placed more emphasis on bank morphology and vegetation as indicators of bank stability (Thorne, 1999).

A further development to the five- and six-stage models proposed by Schumm *et al.* (1984) and Simon and Hupp (1991) was based on a study of Long Creek, Mississippi. Thorne (1999) proposed that an additional evolutionary stage was required to account for late-stage development of cross-sectional asymmetry (Figure 2.4). Following the establishment of extensive berms and stable thalweg long-profile, the regime channel adopted a sinuous path within the larger incised channel, leading to renewed bank erosion and retreat along the outer curve of bends. The increased sinuosity of the channel allows the creation of an inner floodplain below the level of the pre-incision floodplain. The new flood-plain is stabilised by vegetation, which increases in age away from the channel margins. This vegetation increases roughness and traps sediment thus reducing both the sediment availability and the sediment transport capacity. Once the incised trench and channel have attained a condition approaching dynamic equilibrium, it becomes relatively insensitive to future changes in runoff or sediment yield. This is due to the fact that the morphology has adjusted to accommodate variations in the driving variables (Thorne, 1999).

2.3 CHANNEL-FORMING FLOW IN EPHEMERAL STREAMS

From the review of system change theories, it can be seen that there are many different ways in which the fluvial system may be simplified in order to understand its formative processes more clearly. However, fluvial

systems in different climatic regions have been shown to produce very different forms from similar sets of processes. For the purposes of this project, it is thus important to determine which system change theories are applicable to arroyo systems.

2.3.1 Flow Variability and Ephemeral Channel Form

Since arroyos are located in semi-arid or arid climatic regions, flow generally occurs only for a few days every year. Discharges also tend to be extremely variable, thus leading to a very high peak discharge to mean discharge ratio (Osterkamp and Hedman, 1982; Gupta, 1983; Webb, 1987; Schumann, 1989; Hey, 1997). This variability has a distinct effect on the channel form. If rivers have a very highly variable discharge, channels are not conditioned for large flows since these floods exceed the usual flood experience of the river (Wolman and Miller, 1960; Baker, 1977). Hence, large floods have a higher potential to cause catastrophic change as the system attempts to adjust (Kochel, 1988). Very large floods, therefore, leave a virtually permanent imprint on the system (Wolman and Gerson, 1978; Kochel, 1988).

Arroyo systems need to be considered in different ways according to the magnitude of the flood event. Low magnitude events rework sediment on the floor of the arroyo trench, creating an active channel pattern which is often very different from the overall channel pattern (Graf, 1988a). Guber (1988) has shown that this low-flow channel is not formed by catastrophic floods but instead reverts to an equilibrium form, which is likely to be adjusted to an undefined dominant discharge, possibly corresponding to bar-top level in braided low-flow channels and berm-top level in meandering low-flow channels (Thorne *et al.*, 1993; Biedenharn and Thorne, 1994). Thus after catastrophic events, this inner channel recovers rapidly to its former hydraulic geometry condition. However, the same cannot be said of the arroyo trench. It has been argued that channel form has a memory, reflecting all antecedent flows that have passed through the system (Yu and Wolman, 1987). Arroyos can be said to possess a strong memory, since the arroyo trench widens, becoming too large to be influenced by the vast

majority of flows (Hey, 1997). However, events are only “remembered” if they are larger than subsequent events, resulting in arroyo systems having a truncated memory (Yu and Wolman, 1987). This factor emphasises the importance of treating arroyos as “channel[s]-in-channel[s]” (Graf, 1988a).

Extremely high magnitude floods that cross resistance thresholds will cause large amounts of channel change, no matter the environment in which they occur (Wolman and Miller, 1960; Gupta, 1983; Webb, 1987; Osterkamp and Costa, 1987). The different channel responses thus relate to the rapidity with which pre-flood conditions are restored. Rivers in arid and semi-arid regions have been shown to have extremely long recovery times compared with perennial streams in humid climates. This difference in recovery time becomes crucial for channel development when compared with the frequency of extremely large events (Wolman and Miller, 1960; Gupta and Fox, 1974; Wolman and Gerson, 1978; Brunsden and Thornes, 1979; Newson, 1980; Graf, 1983b; Gupta, 1983; Osterkamp and Costa, 1987). If recovery times are long with respect to the frequency of large events, the system changes progressively since it has not returned to its pre-flood configuration by the time the next event occurs. Channels in humid environments may show width increases of up to 40%, but are fully restored to their pre-flood conditions within ten to fifteen years (Hey, 1997). In semi-arid regions, the channel remains widened after large floods and is unable to return to pre-flood configuration during the decades between floods. Surprisingly, however, relatively rapid recovery rates of less than five years have been noted in semi-arid regions, where fine sediments facilitated rapid revegetation (Osterkamp and Costa, 1987; Kochel and Ritter, 1990). Arid-region channels respond in a different way altogether, with floods leaving a virtually permanent imprint on the system. The width of these channels increases abruptly during successively larger storm events and does not recover during the intervening period.

There are several factors which strongly affect the recovery time of a system. Yu and Wolman (1987) note that cut and fill phases have incomparable

timescales, since channel filling takes much longer than the initial channel incision. This is due to the fact that aggradation is associated with low energy environments and thus takes longer to occur. Almost all researchers have cited the presence of riparian vegetation as being one of the most important factors affecting the recovery time of a system (for example: Harvey, 1969; Wolman and Gerson, 1978; Kondolf and Curry, 1986; Simon and Hupp, 1992; Hereford, 1993; Hey 1998). Unless vegetation is so heavy that it causes bank weakening, roots will lead to increased strength of the bank materials (Thorne and Osman, 1988b; Thorne, 1990). Thus, if the vegetation is able to become re-established rapidly after an event, as in humid environments, the channel stabilises rapidly and within-channel aggradation is encouraged, creating bars and berms (Osterkamp and Costa, 1987; Hey, 1997). However, in semi-arid regions, the recovery rate often reflects the occurrence of wetter or drier climatic periods (Burkham, 1972; Schumm and Lichy, 1963). The high stabilising effect that vegetation has on a system is reflected in the fact that Graf (1979a) used vegetation density as a surrogate for channel resistance in the application of cusp catastrophe theory to arroyo development.

2.3.2 Applicability of Channel-Forming Flow Theories

Single flood events in arid and semi-arid environments may cause large, progressive increases in channel width (Schumm and Lichy, 1963; Burkham, 1972; Wolman and Gerson, 1977). In these cases, the effective discharge is not related to bankfull discharges, since the bankfull discharge is constantly modified (Clarke and Davies, 1988). This non-linear progression of a non-equilibrium system results in a non-stationary mean discharge, making statistical analysis of channels in arid and semi-arid regions very difficult (Baker, 1984; Reich and Davies, 1987; Webb and Baker, 1987). The application of channel-forming discharge theories to these channels is, therefore, problematic. This problem is highlighted in Clarke and Davies' application of regime theory to wadi systems (1988). These researchers have been forced to use regime equations which reflect changes in channel width during and after a large perturbation. Different regime

equations are used depending on the width of the channel, contradicting research into dominant discharge in perennial streams, which aims to prove the existence of a single channel-forming flow or limited range of flows.

If channel-forming discharge theories are applied to arroyo development it may be seen that there are many anomalies (Wolman and Miller, 1960; Osterkamp and Hedman, 1982; Hey, 1997). First, arroyo trenches very rarely achieve “bankfull” flow as it is defined in perennial streams. The flashy nature of the flow regime in arroyo systems results in bankfull flow occurring infrequently, even within the inner channel. These events are, therefore, not very geomorphologically effective. The smaller, high-frequency discharges which occur between bankfull events are effective sediment transporting flows in terms of their channel reforming capabilities. Therefore, the effective discharge in flashy streams is of significantly lower magnitude than the bankfull discharge (Soar and Thorne, 2001).

Although dominant discharge theories may be altered to fit arroyo evolution, channel-forming theories developed specifically for ephemeral channels have since been developed, the most applicable of which is Graf’s cusp catastrophe model. Using stream power as a surrogate for force, vegetation density as a surrogate for resistance and using the cross-sectional channel area as the behaviour variable, the cusp catastrophe surface for montane arroyos in Colorado was calculated. This catastrophe surface indicates that the arroyo system has a distinct threshold whereby the same controlling processes may cause either a stable entrenched system, or a stable unincised system.

The cusp catastrophe theory also provides an explanation for similar floods in similar systems causing vastly different end results; the position of the system on the catastrophe surface prior to a perturbation is crucial. Thus the antecedent conditions leading up to an event are highly important. For example, if the system has been pre-wetted, its resistance may be significantly lowered, leading to a greater amount of change (Wolman, 1959). Equally, the antecedent order of events will be vital in determining

the initial catastrophe position (Graf, 1983b; Kochel, 1988; Hey, 1997). If a large event follows several smaller events, it will have a very different end condition to a system where the large event follows one, or several, large events (Graf, 1983b).

It can, therefore, be seen that, while naturally stable perennial streams in humid environments are adjusted to a dominant or channel-forming discharge, the long recovery period of ephemeral channels in semi-arid or arid environments results in catastrophic events having a far greater cumulative effect on the system. Thus, rather than the channel being dominated by one equilibrium state, non-linear progression from one equilibrium form to new, different equilibrium forms occurs. Criticisms levelled at the concept that large events are the channel-forming events are based around the evidence that some river channels have shown little change in response to high-magnitude floods. However, the introduction of threshold concepts and the incorporation of these concepts into cusp catastrophe theories can satisfactorily illustrate how both gradual and abrupt changes can be caused by very similar magnitude events in very similar systems. However, while useful for geomorphologists wishing to describe threshold phenomena in river systems, cusp catastrophe theory has severe limitations for any application beyond this. Similarly, NDS concepts have progressed conceptual modelling of process-form interaction and dynamic system behaviour but have little practical use within the scope of this project.

2.4 MODELS OF ARROYO EVOLUTION

The channel evolution models discussed in Section 2.2.5 were developed for perennial incised channels in a humid environment. However, researchers studying arroyo morphology in the south-western USA have noted a similar evolutionary pattern (Bryan and Post, 1927; Graf, 1983b; Gellis *et al.*, 1991; Ellis, 1993; Gellis, 1998a; Elliott *et al.*, 1999; Gellis and Elliott, 2001). Bryan and Post, although working many years prior to Schumm, noted the same progression of incised channel evolution: initial downcutting until a critical

bank height is reached, followed by widening of the main channel. These researchers recognised that this would cause rejuvenation of tributaries and consequently a huge increase in the amount of sediment. However, as was dictated by popular theory at the time, it was assumed that the sediment would exit the system, rather than being stored in it. Eventually, as the arroyo trench became too wide for flows to cause significant erosion, sediment production would decrease and the system would eventually become graded to a new lower level. The retarding action of vegetation during wetter years would hasten the attainment of a graded system.

Later researchers have directly applied the five-stage channel evolution model to arroyo evolution, with very little modification (Elliott, 1979; Hereford, 1983; Gellis *et al.*, 1991; Gellis, 1998a; Elliott *et al.*, 1999; Gellis and Elliott, 2001). In all these models the first stage of evolution corresponds to the initial incision (Figure 2.5), the cause of which has been hotly debated (discussed in Chapter 3). As the system progresses from unincised to actively downcutting, stream power, rather than decreasing, instead increases downstream as the flow conveyance is increased (Graf, 1983a; Macgilligan, 1992).

Downcutting (Stage 2) continues until the arroyo walls reach a critical bank height, at which point widening follows (Stage 3). As first vertical and then lateral erosion progresses headwards, a large amount of sediment is released as tributaries are degraded and subsequent widening occurs (Elliott, 1979). The volume of sediment released is sufficient to overload flows, causing a braided planform to develop. This braided channel is defined as a Type 1 reach by Elliott and represents an intermediate stage in arroyo evolution (Elliott, 1979). Type 1 reaches are sustained by variable discharges and high sediment loads and are subject to lateral shifting causing continued widening of the arroyo trench. The rate of sediment production was found to attain a maximum during widening (Schumm, 1973; Gellis *et al.*, 1991), with up to five times as much sediment produced during widening compared with the initial downcutting (Meyer, 1989).

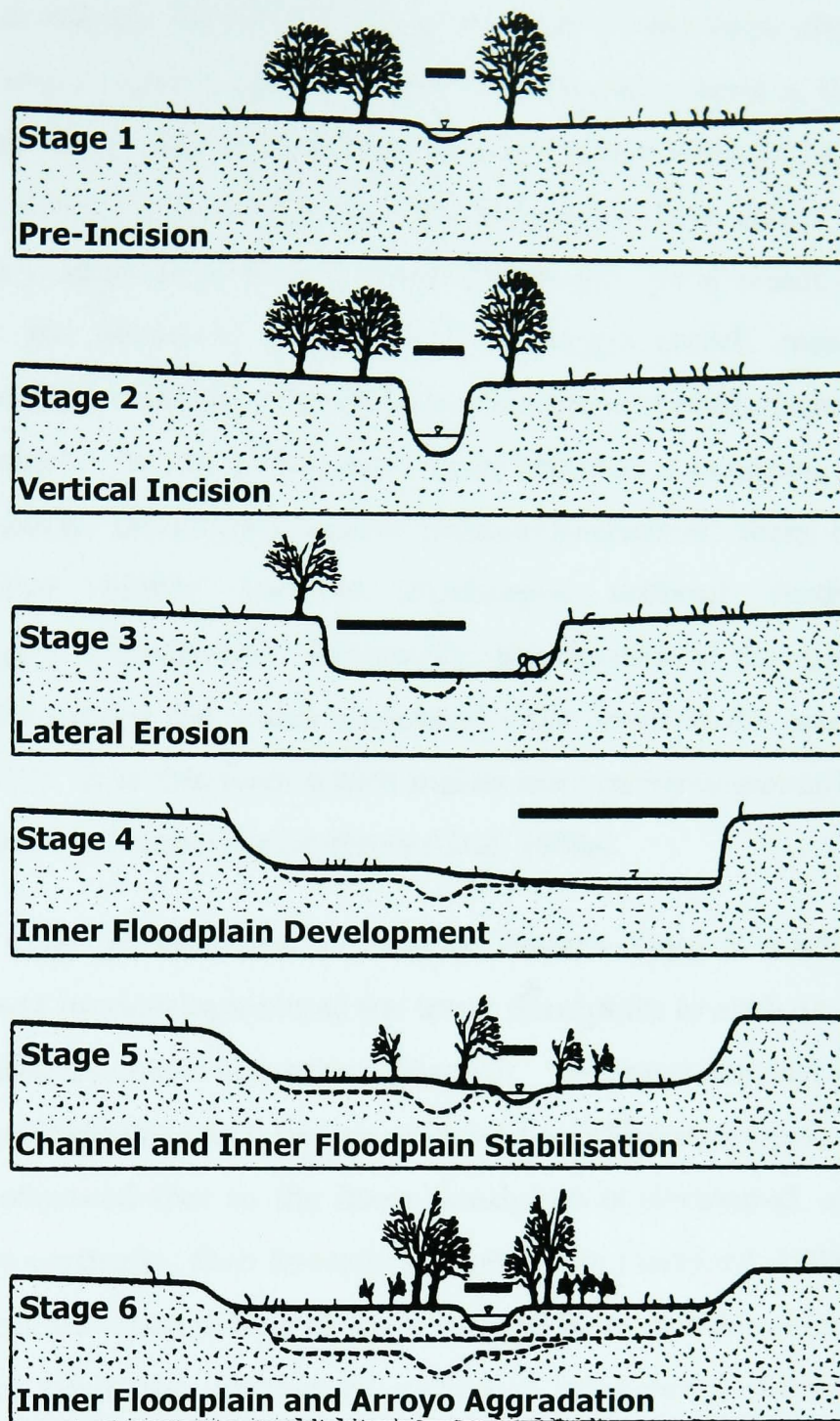


Figure 2.5 Hypothetical sequence of geomorphological evolution of large-scale arroyos (after Elliott, 1979; Elliott *et al.*, 1999).

After this maximum is attained, the quantity of sediment produced decreases logarithmically (Begin *et al.*, 1980; Gellis *et al.*, 1991). This pattern of development is characteristic of dissipative systems, where the most effective method of energy dissipation was found to be degradation in conjunction with widening (Simon, 1992). In arroyo systems, as the trench widens, the amount of sediment produced is eventually reduced as the width becomes too great for the walls to be frequently eroded laterally,

resulting in storage within the arroyo trench. It has been observed that channels which carry high sediment concentrations have a tendency to become narrower, deeper and more sinuous (Schumm and Khan, 1972; Qi and Zhao, 1993). This pattern of development has been noted as the next evolutionary stage in arroyo systems (Stage 4). As a result of channel widening, the increased storage in the arroyo trench results in the development of an incipient floodplain and a single-thread, narrow, sinuous active channel. At this point, the arroyo becomes a complex, compound channel system, developing Graf's "channel-in-channel" form in order to accommodate highly variable discharges without further major morphological adjustments. Eventually, the breadth of the arroyo trench may greatly exceed the width associated with flows in the active channel (Elliott, 1979). It is this form which makes arroyos fundamentally different from channels in humid-region rivers (Graf, 1988a).

The next stage in evolution represents Elliott's Type 2 reach, which is characterised by development of the inner floodplain to such an extent that it is stabilised by dense vegetation (Stage 5). The inner channel system of a Type 2 reach behaves much like an unincised equilibrium regime channel. It has been observed that as the inner floodplain is developed, aggradation first occurs vertically, then laterally (Elliott, 1979; Hereford, 1984). Vertical accretion occurs when sediment loads are still high and the inner channel is still wide. Once the amount of sediment transported decreases and a narrow, single-thread active channel is formed, fine sediments are deposited laterally along the channel margins. The commencement of lateral accretion is thought to indicate that the inner floodplain has achieved a critical height, at which floods of a given (but undefined) frequency are no longer able to overtop the banks. As a result, the dissipation of energy that would have occurred as the flow increases beyond bankfull stage no longer takes place. Thus the average flow velocity, and accordingly the stream power, is higher and the flow more efficient. Therefore, lateral accretion also indicates that renewed downcutting has been initiated and that complex response is occurring (Hereford, 1984).

Schumm's original model assumed that the channel develops quasi-equilibrium once Stage V is attained. However, the complex response observed by some researchers has led to modification of this stage of the model in arroyo evolution (Elliot, 1979; Love, 1979; Hereford, 1984; 1993). Gellis introduced an element of flexibility beyond stage V, whereby complex response may occur (Gellis, 1998a; Elliott *et al.*, 1999; Gellis and Elliott, 2001). Thus, after developing a pseudo-stable inner channel system, the arroyo system may continue aggrading until it has attained quasi-equilibrium or, more likely, re-incision of the active, inner channel may occur. It has also been noted that small arroyo systems tend to fill back to their original, pre-incision level before attaining quasi-equilibrium, whereas large arroyo systems create a valley-like trench below the pre-incision level capable of accommodating the highly variable flows (Elliott, 1979). This final phase of evolution, Stage 6, is synonymous with Thorne's (1999) late-stage modification.

Elliott (1979) proposed that intermediate Type 1 reaches would evolve into mature Type 2 reaches, assuming that location-for-time substitution was a valid supposition for arroyo systems. Thus, the upper part of the arroyo system would still be widening (Type 1) when the lower reaches had already developed a compound channel (Type 2). However, this may be an oversimplification, since erosion due to outer bank scour in meandering arroyos, rather than solely headwards erosion, has also been observed (Leighly, 1936; Love, 1979). There is also evidence that, in many arroyos, erosion occurred simultaneously along several separate reaches (Cooke and Reeves, 1976; Love, 1979; 1997).

As the arroyo evolves into a compound channel, peak flows have been observed to decrease and dense vegetation is established concurrently with the development of the inner floodplain (Elliott, 1979; Hereford, 1983; Gellis *et al.*, 1991). This has provoked speculation as to the order of events at this stage of evolution. In theory, a reduction in flood magnitudes allows vegetation, in particular tamarisk, to become established, which in turn

causes flow concentration and retardation, and the development of the inner floodplain. Tamarisk, or salt-cedar, are non-native in the south-western USA, and were introduced highly successfully, often as an erosion control measure. As a result, dense tamarisk can be found on the floors of many arroyo systems. The effect of this vegetation on the arroyo morphology is unclear. The synchronicity of tamarisk growth and floodplain development has understandably led to the conclusion that the changes in arroyo morphology are a direct result of the spread of tamarisk. However, Hereford (1984) has reviewed the available literature, noting that there are valid arguments against this theory. It has been observed that tamarisk is no more effective at stabilising sediment than the native riparian species it replaced. It has also been pointed out that there are arroyo systems which are devoid of tamarisk, but which have still developed a compound channel. Similarly, it was thought that the decrease in peak flows was a result of climatic trends, improved land use or increased water storage (Burkham, 1972; Leopold, 1976; Elliott, 1979; Hereford, 1984; 1993; Graf *et al.*, 1991). These researchers assumed that the frequency of large floods directly controlled the channel morphology. However, there is also the possibility that the changing morphology of the arroyo system caused this decrease, rather than the other way around (Popp *et al.*, 1988; Gellis 1998b). As the inner floodplain and channel developed and vegetation became established, roughness increases. This causes the velocity of high magnitude (overbank) floods to decrease. The increasing thickness of sediment in storage within the arroyo, combined with decreased flow velocities results in increased infiltration. The magnitude of flood peaks, therefore, declines due to this combination of flood-wave attenuation and infiltration leading to considerable loss of floodwater volumes.

The role of intrinsic thresholds are highlighted by other models of evolution. Meyer (1989) proposed a model of development, again noting the importance of the volumes of sediment being produced and transported, but also observing the effect of different alluvial grain sizes on the arroyo pattern (Figure 2.6). Meyer argued that the models of arroyo evolution

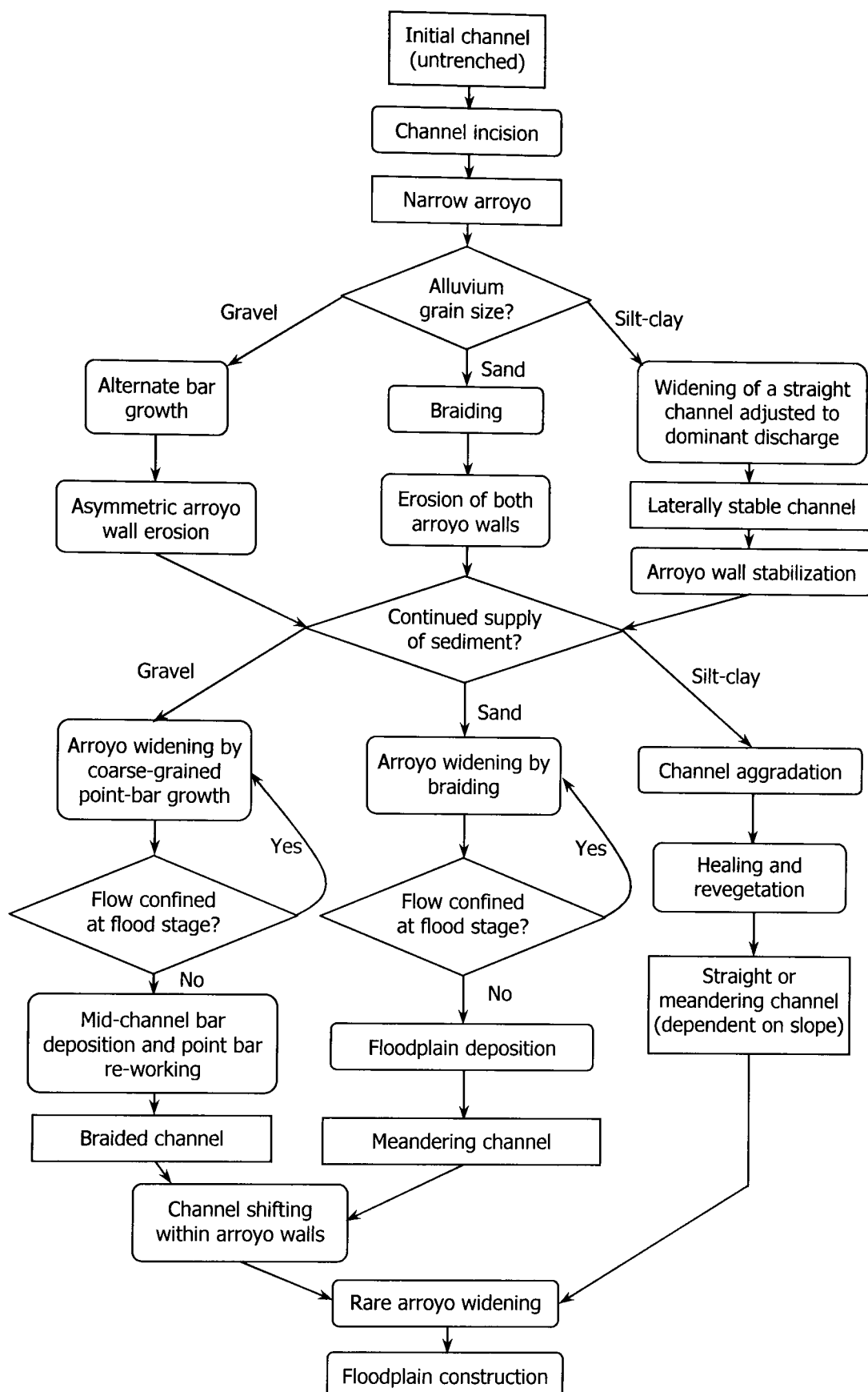


Figure 2.6 Model of arroyo development showing influence of sediment load and grain size on stability (after Meyer, 1989).

based on Schumm's V Stage model hold true for fine-grained alluvial channels. Arroyos transporting sand or silt-clay sized sediments develop a compound channel, although through different mechanisms. Sand transporting systems first develop a braided channel, until the arroyo

widens sufficiently that large magnitude floods are no longer confined. At this point finer-grained sediment is deposited in backwater, low-velocity areas become more abundant and a compound channel is formed. Arroyos transporting quantities of gravel, however, develop alternating coarse-grained point bars. Asymmetric widening occurs until flood flows are unconfined, at which point a braided gravel-bed channel forms through reworking during high flows. However, Meyer's study was partly developed by studying cross-sections surveyed along reaches of the Santa Cruz River which do not have the morphological characteristics of true arroyos, as defined in Chapter 1, and along the San Pedro, which is both perennial and has heavily bedrock-controlled morphology. Thorne (1999) noted that asymmetry may be observed in fine-grained, as well as gravel-bed, incised channels. Lastly, Meyer's model was based on a limited number of cross-sections, with little apparent reference to actual observations of arroyo system evolution.

Although arroyos are generally seen as erosional features, it can thus be seen that as their systems evolve, an aggradational phase is triggered. The vast majority of contemporary arroyos, after downcutting of 19th century have now reached this aggradational stage, and indeed began aggrading some decades ago. This aggradation has been generally attributed to climatic change (for example: Antevs, 1952; Tuan, 1966; Emmett, 1974; Leopold, 1976; Cooke and Reeves, 1976; Elliott, 1979; Love, 1979; 1997; Hereford, 1984; 1993; Gellis *et al.*, 1991). There is also irrefutable evidence that some arroyos were aggrading and had developed a compound channel even before the end of the 19th Century (Bryan and Post, 1927; Love, 1979; 1997). Thus it would seem unlikely that the climatic cause of such aggradation would have triggered this non-synchronous aggradation. While climatic fluctuation may have played its part in causing arroyo systems to switch from degrading to aggrading (Gellis *et al.*, 1991; Parker, 1996), there is no doubt that intrinsic geomorphic thresholds are a major cause.

CHAPTER 3

Arroyo Initiation

"The problem of the origin and dynamics of arroyos
has generated more interest ... than any other research question
in arid environments." (Graf, 1983, p279)

3.1 ARROYO INITIATION THEORIES

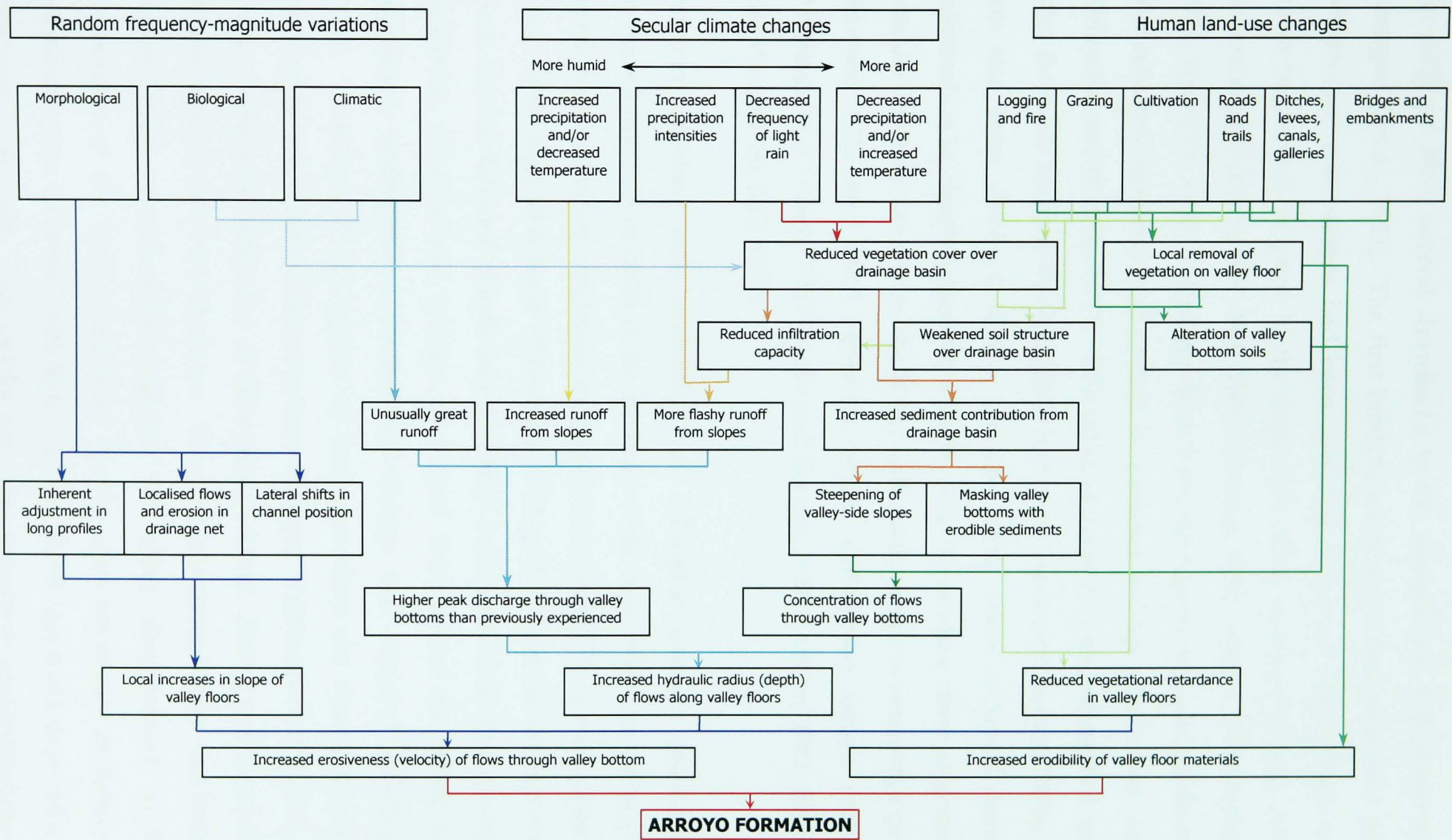
The widespread and semi-synchronous downcutting of arroyos at the end of the nineteenth century understandably created much interest in the then newly burgeoning field of geomorphology. This interest continued almost unabated for much of the next century leading to a vast amount of literature detailing arroyo initiation theories. This led to Graf commenting in 1979 that the "thread of research into questions of initiation seems to be completed, or at least to have reached a limit imposed by available data" (1979b, p1). Although the main emphasis of arroyo research is now focused on processes responsible for development rather than initiation, almost all recent publications have included some sort of summary of initiation theories (for example, Elliott *et al.*, 1999; Bull, 1997). This is in addition to several highly detailed and thorough reviews of the available arroyo initiation literature (Bryan, 1925; Antevs, 1952; Tuan, 1966; Cooke and Reeves, 1976; Graf, 1983b). These reviews have enabled geomorphologists to untangle the often confusing wealth of conflicting information. Theories were often based on patchy data, biased first-hand observations and considerable hindsight (Hastings, 1959; Cooke and Reeves, 1976; Betancourt, 1990; Bull, 1997). A correlation between the profession of the researcher and the conclusions drawn was also observed (Cooke and Reeves, 1976). However, the painstaking piecing together of data for individual arroyo systems cannot be dismissed lightly. Thus it must be assumed that different causal mechanisms in different locations can operate through the same processes to produce similar forms; arroyos are, therefore, essentially a product of equifinality (Cooke and Reeves, 1976; Graf 1979b, 1983b; Bull, 1997).

Although there is a large volume of literature describing theories of arroyo initiation, the range of proposed causal mechanisms is actually relatively limited. Almost all theories are based on the premise that the relationship between vegetation and runoff is the most important factor controlling arroyo initiation (Bryan and Post, 1927; Bailey, 1935; Antevs, 1952; Cooke and Reeves, 1976; Bull, 1997; Elliott *et al.*, 1999). Vegetation provides significant surface roughness, retarding the runoff velocity; intercepts water, reducing the runoff volume; binds valley-bottom soils, reducing erosion and also responds rapidly to changes in moisture, temperature and human impacts (discussed in Chapter 2). These environmental changes, whether intrinsic or extrinsic to the arroyo system, have been summarised in Figure 3.1. Most initiation hypotheses fall into three broad categories.

3.1.1 Human Land-Use Change

One of the earliest theories of initiation proposed noted the apparent correlation between the influx of Anglo-American settlers and the formation of arroyos (Rich, 1911). These settlers introduced large numbers of cattle into the southwest, which had a visibly detrimental effect on the environment. Overgrazing could be seen to have stripped vegetation from valley floors, trampling compacted soils and stock trails caused further compaction, concentrating runoff and reducing infiltration (Rich, 1911; Olberg and Schanck, 1913; Bryan, 1925; Bailey, 1935; Antevs, 1952; Hastings, 1959; Heede, 1974; Cooke and Reeves, 1976; Womack and Schumm, 1977; Dobyns, 1981). The end result was to cause a decrease in hydraulic roughness, increasing the flashiness of runoff and thus increasing the sediment load and peak discharge (Bryan, 1925; Webb and Baker, 1987; Bull, 1997). This theory remained highly popular for many years, mainly due to the demonstrable temporal coincidence of initiation and cattle introduction. Graf (1983b) lists 34 separate studies, ranging in date from 1902 to 1982, which emphasise grazing as a major causal mechanism of arroyo initiation, and his list is limited to representative papers only. In fairness, not all the studies cited by Graf propose overgrazing as the single cause of initiation.

Figure 3.1 Summary of environmental changes responsible for arroyo initiation (after Cooke and Reeves, 1976).



As early as 1911, several drawbacks to the overgrazing hypothesis had emerged (Bryan, 1925). The first limitation was noted by researchers who pointed out that arroyos had been observed in regions where there had never been cattle or prior to the large-scale cattle ranching (Bryan, 1925; Schumm and Hadley, 1957; Bull, 1964; Emmett, 1974; Leopold, 1976; Bendix, 1992; Hereford, 1993). Similarly there were river systems in the southwest that remained unentrenched despite the presence of large numbers of cattle (Schumm and Hadley, 1957). Still other systems became entrenched long after the cattle boom of the late 1800s had past (Cooke and Reeves, 1976). It has also been observed that a previous cattle boom occurred during colonisation by Spanish-Mexican settlers. The devastating effect of grazing was documented as early as the 1640s, with cattle numbers reaching a peak between 1790 and 1820, centuries before widespread arroyo cutting (Hastings and Turner, 1965; Cooke and Reeves, 1976; Dobyns, 1981; Balling and Wells, 1990; Bull, 1997).

Another problem with evaluating the ecological damage caused by increased numbers of cattle is the accuracy of the reports documenting pre-incision valley-bottom conditions in the south-western USA. Descriptions of grass "belly-high to a horse" (Hastings, 1959, p60); perennial streams with clear, beaver-dammed ponds and plentiful trout; and abundant ciénegas (marshes), swamps and springs all helped bring about the belief that significant, widespread environmental change had occurred (Hastings, 1959). However, if the reports of early travellers are examined more thoroughly, an entirely different picture emerges. Testimonies of thick lush grass are balanced with tales of inhospitable desert. Partly, this depended on the view-point of the observer. Those newly-arrived from the humid eastern states would understandably be rather disappointed in the appearance of the local vegetation. Partly, also, memories of fabulous grasslands were enhanced with time, leading to the "good-old days fallacy" (Hastings, 1959, p60). This patchy reporting is entirely understandable if related to the known environment of the semi-arid south-west, where periods of above average rainfall resulted in plentiful vegetation and vice



Figure 3.2 Palaeoarroyos exposed in the outer bank of XS-17, Rio Puerco (courtesy John Elliott).

versa. Similarly, spatial variation in the condition of the vegetation occurred depending on the proximity to permanent water. These temporal and spatial variations would thus strongly affect the appearance of the environment and its subsequent description (Hastings, 1959).

The final, and perhaps most conclusive, drawback to the overgrazing theory is that, in the cut banks of contemporary arroyos, buried, preserved palaeoarroyos may be found (Figure 3.2). These fossil trenches indicate that there were several cut and fill cycles during the Holocene prior to modern human habitation and the widespread introduction of cattle (Bryan, 1925, 1928; Antevs; 1952; Leopold, 1976; Tuan, 1966; Graf, 1983b). Since prehistoric farmers were not believed to keep livestock, grazing could not be responsible for arroyo initiation (Bryan, 1928; Antevs, 1952; Tuan, 1966; Love, 1997). The overgrazing theory was thus modified to take account of these drawbacks, leading to the hypothesis that, while grazing might not be the main cause of initiation, climatic changes could cause a system to become unstable. Grazing then acted as a "mere trigger pull which timed a change about to take place" (Bryan, 1928, p281).

Although grazing depletes vegetation cover, trampling and the creation of stock trails has been shown to cause far more destruction (Dobyns, 1981). The compaction of soils, especially in the valley-bottom where the greatest concentration of cattle were found, significantly impairs the re-growth of

vegetation. Stock trails, which could become two or more metres wide and half a metre in depth, similarly caused the destruction of protective vegetation (Dobyns, 1981). These trails also caused concentration and acceleration of runoff, thus increasing stream power. Similarly, artificial concentration of flow occurred along wagon trails, dirt roads and railroad and bridge embankments (Rich, 1911; Olberg and Schanck, 1913; Bailey, 1935; Antevs, 1952; Cooke and Reeves, 1976; Dobyns, 1981; Betancourt, 1990; Bull, 1997). A common practice by early settlers was to "develop ground water" (Olberg and Schanck, 1913, p8). This entailed digging a ditch which intercepted the water-table. Other ditches were dug in order to deliberately concentrate floodwaters and prevent destructive flooding (Cooke and Reeves, 1976; Dobyns, 1981; Bendix, 1992; Bull, 1997). Often ditches were started with the expectation that subsequent floods would save further labour and enlarge the ditches by headwards erosion. In some cases the ditches were enlarged far more than expected and this process can be directly related to arroyo initiation. Many contemporary arroyos owe their initiation at least partly to artificial drainage concentration features.

Other human actions which changed the desert environment have been linked to arroyo initiation. Placer and upland mining contributed indirectly by causing an increase in the number of trails and deforestation occurred due to the large amount of wood required for camps, smelting and shorings (Dobyns, 1981). Deforestation also occurred due to the large increase in population requiring fuel, timber for building and land for cultivation. Along some rivers, the decimation of the beaver population lead to the destruction of beaver dams, responsible for creating artificial pools. The removal of these dams changed the moist oasis environment and allowed the acceleration of floodwaters (Dobyns, 1981; Bendix, 1992). Cienega draining had a similar effect (Dobyns, 1981; Waters, 1988). Artificial dams, or rather their collapse, were also responsible for the initiation of some arroyos (Bryan, 1925; Love, 1997). Finally, the suppression of the Native American practice of using fire as a method of hunting may also have been responsible for changing the vegetation, and therefore, resistance of the

valley-bottoms (Hastings and Turner, 1965; Cooke and Reeves, 1976; Dobyns, 1981).

3.1.2 Climatic Change

As the overgrazing theory of initiation became increasingly suspect, climate change seemed to be the most likely explanation. This led to some highly conflicting theories of initiation being proposed, even by researchers using the same databases. Initially Huntingdon, in 1914, proposed that a change to a drier climate would cause a decrease in vegetation, which would in turn allow more sediment to enter stream channels, causing them to become overloaded, leading to aggradation. In contrast, a wetter climate causes increased vegetation coverage. This retards sediment transport, leading to highly competent clear-water streams and thus erosion. Thus arroyo incision was thought to be associated with a general increase in precipitation, with human activities then providing the trigger (in Antevs, 1952; Cooke and Reeves, 1976; Graf, 1983b; Betancourt, 1990; Bull, 1997). Although unpopular for many years, some more recent studies have provided evidence to support Huntingdon's hypothesis (Bull, 1964; Hereford, 1984; Bendix, 1992).

In direct contradiction to this view, Bryan agreed with the theory that drier conditions would deplete vegetation as Huntingdon had recognised, but this would actually cause significant increases in storm runoff (Bryan and Post, 1927) (wrongly attributed to Bryan, 1928 in Antevs, 1952; Cooke and Reeves, 1976; Betancourt, 1990). This model of increasing aridity came to be known as the "Bryan-Antevs climatic model" (Tuan, 1966), although the reference in which this was initially proposed seem to have been lost to posterity. While this hypothesis has a sound theoretical basis, there is little evidence in precipitation records of a climatic shift to drier conditions at the time of arroyo initiation. The only incidental evidence of a trend to a warmer, drier climate since 1800 is the migration of plant communities to higher elevations (Hastings and Turner, 1965). Complicating matters still further, Richardson,

in 1945, suggested that a shift to either a wetter or drier climate would cause arroyo initiation (Cooke and Reeves, 1976; Graf, 1983b).

Subsequent research has attempted to develop more sophisticated models by analysing changes in frequency, intensity or seasonality of annual climate data, rather than just investigating general climatic shifts. It was suggested that very subtle shifts in climate could cause very large changes in channel morphology (Emmett, 1974; Molnár, 2001). Leopold's (1951) pioneering study of New Mexico precipitation data established that, while the annual rainfall totals showed no trend, there were significant trends in the seasonality and frequency of precipitation of different intensities. The period 1850 to 1880, shortly prior to the establishment of many contemporary arroyos, was characterised by a decrease in low-intensity and an increase in high-intensity rains. Leopold argued that this would cause poor vegetation cover and higher incidence of erosive runoff. However, during the decade when most arroyos were actually initiated, between 1880 and 1890, the opposite was true, with a sharp increase in the frequency of low-intensity events and a decrease in high-intensity. Either, therefore, a lag occurred between the increased frequency of high-intensity storms (Elliott *et al.*, 1999), or it may be that this is a case of trying to make the data fit the theory, especially considering the many theories based on the rapidity of vegetation response.

Analysis of rainfall data from Arizona showed that, as in New Mexico, there was an increase in the frequency of light rains and a decrease in the frequency of heavy rains towards the end of the 19th Century (Reeves, 1974; Cooke and Reeves, 1976). It was, therefore, suggested that during the summer, the critical period for vegetation growth, the water available for grasses may have been reduced, thus possibly resulting in the vegetation cover being weakened at the time of arroyo initiation. However, other studies supported Leopold's theory that an increased frequency of high-intensity, high magnitude rains, especially during summer months, occurred

concurrently with arroyo initiation (Schumm and Lichthy, 1963; Bull, 1964, 1997; Tuan, 1966; Balling and Wells, 1990; Bendix, 1992).

3.1.3 Random Frequency-Magnitude Variations

It can be seen that there has been a prevalence of hypotheses which essentially attempt to explain arroyo initiation in terms of various factors controlling vegetation coverage either directly or via climate drivers. However, it has been suggested that undue emphasis has perhaps been placed on the role of vegetation (Betancourt, 1990). Rather than attempting to explain the condition of vegetation in drainage basins by observing climate data, many studies have noted the predominance of catastrophically large floods which have directly initiated arroyo trenches (Hastings, 1959; Hastings and Turner, 1965; Cooke and Reeves, 1976; Graf, 1983b; Webb and Baker, 1987; Betancourt, 1990, Hereford, 1993). A series of large floods over much of the south-west concurrent with the initiation of many arroyos may have been due to the prevalence of El Nino-Southern Oscillation (ENSO) conditions. During ENSO years, there is an increased variability of precipitation. Thus these years may be characterised by either unusually large floods or may have below average rainfall. The general effect, however, is for periods with a higher frequency of ENSO events to have marked increases in precipitation and increased flooding (Betancourt, 1990; Graf *et al.*, 1991; Webb and Betancourt, 1992; Molnár, 2001).

In some cases these abnormally large floods occurred during, or just after, periods of drier than average conditions. Analysis of precipitation data has shown that periods of at least three successive years of above or below average rainfall commonly occur and are not always coincident in each valley (Cooke and Reeves, 1976). These alternating periods are, thus, due to random climatic fluctuations rather than climatic change. The drier periods are often followed by periods of abnormally large rainfall (Cooke and Reeves, 1976; Balling and Wells, 1990; Bull, 1997). Yet again, these changes are thought to have affected the vegetation cover: drier periods being responsible for depleting the protective vegetation, with the subsequent wet

periods being responsible for increased runoff exploiting the increased erodibility of the drainage basin (Cooke and Reeves, 1976).

As with all theories, there are problems with the catastrophic flooding and random fluctuation hypotheses of arroyo initiation. Floods of similarly large magnitude and on similar streams have not always produced channel entrenchment (Hastings, 1959; Webb, 1983b). Equally, there is no evidence that there has been any historical change in the frequency of large floods or change in the pattern of wet/dry years (Cooke and Reeves, 1976; Webb and Baker, 1987). Thus, given that these events cannot be wholly responsible for arroyo initiation, other factors, such as land-use change, must still be taken into consideration.

All the above theories have proposed extrinsic causal mechanisms of arroyo initiation. In Chapter 2, the effect of intrinsic geomorphic thresholds on river systems was discussed. For an arroyo system to begin downcutting, thresholds must be crossed as a matter of necessity for the system to switch to a degradational trend. Once initiated, this progression may occur through mechanisms which are, to a degree, independent of environmental change. The point of initial headcutting has been found to occur at steeper sections of the longitudinal profile along some arroyos (Schumm and Hadley, 1957; Cooke and Reeves, 1976; Bull, 1997). It should be noted, however, that there is little specific data to support this theory, and this is not the case along other arroyos (Bendix, 1992). However, it has been observed that the relative importance of breaks in slope varies with drainage area. Smaller drainage basins require progressively steeper angles to initiate trenching since they generate smaller amounts of runoff, which in turn cannot generate as much stream power as larger discharges (Schumm and Hadley, 1957; Patton and Schumm, 1975; Bull, 1997). In larger drainage basins, the steeper reaches thought to have been responsible for arroyo initiation may be as little as a degree steeper and tended to occur downstream of ciénegas (Cooke and Reeves, 1976). Other reaches may become steepened as sediment is deposited by flows dissipating through

infiltration or evaporation (Schumm and Hadley, 1957; Patton and Schumm, 1975; Cooke and Reeves, 1976); when sediment-laden flows from tributary channels decelerate on reaching the main channel, forming a fan (Rich, 1911; Patton and Schumm, 1975); or when meanders cut-off (Womack & Schumm, 1977).

The documented evidence of Holocene periods of cut and fill has lent support to both climatic (Antevs, 1952; Tuan, 1966; Love, 1979, Waters, 1988; Bull, 1997) and intrinsic geomorphic threshold mechanisms of arroyo initiation (Love, 1979; Elliott *et al.*, 1999). As with the current period of incision, the evidence to support climatic change being the cause for past phases of incision is confusing, conflicting and relies on less-than-ideal data. In particular, some research has relied on questionable climatic interpretation of tree-ring data, with its emphasis on recording trends in summer precipitation (Tuan, 1966). Evidence has been put forward to support the theory that palaeorroyos incised during drier climatic periods, such as the Altithermal, a warmer, drier phase which occurred between 7500 and 4000 years BP and also between 850 and 750 BP (Antevs, 1952; Betancourt, 1990; Elliott *et al.*, 1999). However, it has also been suggested that the opposite was true (Bendix, 1992). One crucial piece of evidence for a widespread change in climate was the supposed synchronicity of aggradational phases throughout the south-west, although degradational phases were found to be only crudely synchronous (Bull, 1997). However, re-examination of the dates of downcutting have suggested an overemphasis on synchronicity (Tuan, 1966; Love, 1979; Betancourt, 1990; Elliott *et al.*, 1999), perhaps another case of trying to make the data fit the hypothesis. Even the widely held belief that the last period of arroyo cutting occurred during the last two decades of the 19th Century has been found to be incorrect, with evidence that some arroyos were entrenched as early as the mid-1800s and others as late as the mid-1900s. Elliott *et al.* (1999) reviewed the available dates of downcutting throughout the south-west, finding that most of the cut and fill episodes did not begin or end concurrently. In fact, it

was discovered that there was no instance after 15,000 BP where aggradation was not occurring at some location.

Lack of synchronicity of downcutting has several implications. Non-synchronicity could suggest that random climatic fluctuations, rather than general climatic shifts, were responsible for initiation (Bailey, 1935; Antevs, 1952; Schumm and Hadley, 1957; Waters, 1988). This is supported by tree-ring evidence of variable summer precipitation and the fact that pollen analysis shows no confirmed evidence of general climatic change (Tuan, 1966; Love, 1979). Historic and pre-historic ENSO episodes have also been documented (Waters, 1988). Non-synchronicity also favours intrinsic geomorphological thresholds controlling cut and fill cycles (Patton and Schumm, 1981; Elliott *et al.*, 1999).

As with evidence for synchronicity, the accuracy of the available data must be questioned. Since the periods of downcutting are almost an order of magnitude shorter than periods of aggradation (discussed in Chapter 2), errors or differences in dating techniques may give a false result (Elliott *et al.*, 1999). Arroyo systems may have different sensitivities to a climatic perturbation, even in adjacent drainage basins (Bull, 1997). The size of the basin may also have a significant effect, with larger basins damping the effects of climate change (Bull, 1997; Elliott *et al.*, 1999).

One other fact which should be mentioned is that the existence of palaeoarroyos has long been seen as evidence to support climatic arroyo initiation theories. However, it has been suggested that pre-historic farmers may have used methods that were not radically different from those used at the time of the most recent initiation, rather than using non-destructive techniques as was widely accepted in the past (Waters, 1988; Betancourt, 1990). The correlation between pre-historic occupation and alternating cut and fill periods is striking, although there is no direct evidence to support this hypothesis (Waters, 1988). Again, different basins may have been affected differently by these occupants, since other researchers have found

little evidence to suggest that an anthropogenic cause for past incision phases (Love, 1979).

The above discussion has shown that, in general, a combination of factors triggered arroyo incision. For one paper which proposed a certain hypothesis, it is almost certainly possible to find another which proposed the opposite, confirming the suggestion that arroyos are the result of equifinality. In the majority of cases, however, initiation can be pinpointed to a particularly large flood. Since there is no evidence that the frequency of high-magnitude floods has changed significantly, importance must also be placed on conditioning factors which help destabilize the system ready for the triggering event, ensuring that, geomorphologically, the system is ready for change.

3.2 ARROYO INITIATION IN STUDY AREAS

Rio Puerco

The location of historic sites in the Rio Puerco Basin are shown in Figure 3.3.

- 1540 Coronado first crossed the Rio Puerco area (Love, 1997)
- 1692 De Vargas described the Rio Puerco as being a flashy unentrenched channel (Love, 1997).
- 1752 Spanish settlers moved into the area, although human habitation dates back at least 1,500 years (Gorbach *et al.*, 1996; Love, 1997).
- 1765 The settlement of Los Quelites was established close to the Rio San Jose, which was thought to be perennial. Gullying soon developed nearby, eroding agricultural fields (Love, 1997).
- Pre-1800 All settlements were abandoned due to Navajo and Apache raids (Gorbach, 1996; Love, 1997).

The condition of the Rio Puerco during the early - mid 19th Century was described by topographical engineers accompanying the military on campaigns against the Apache and Navajo and on route-finding expeditions (Elliott *et al.*, 1999).

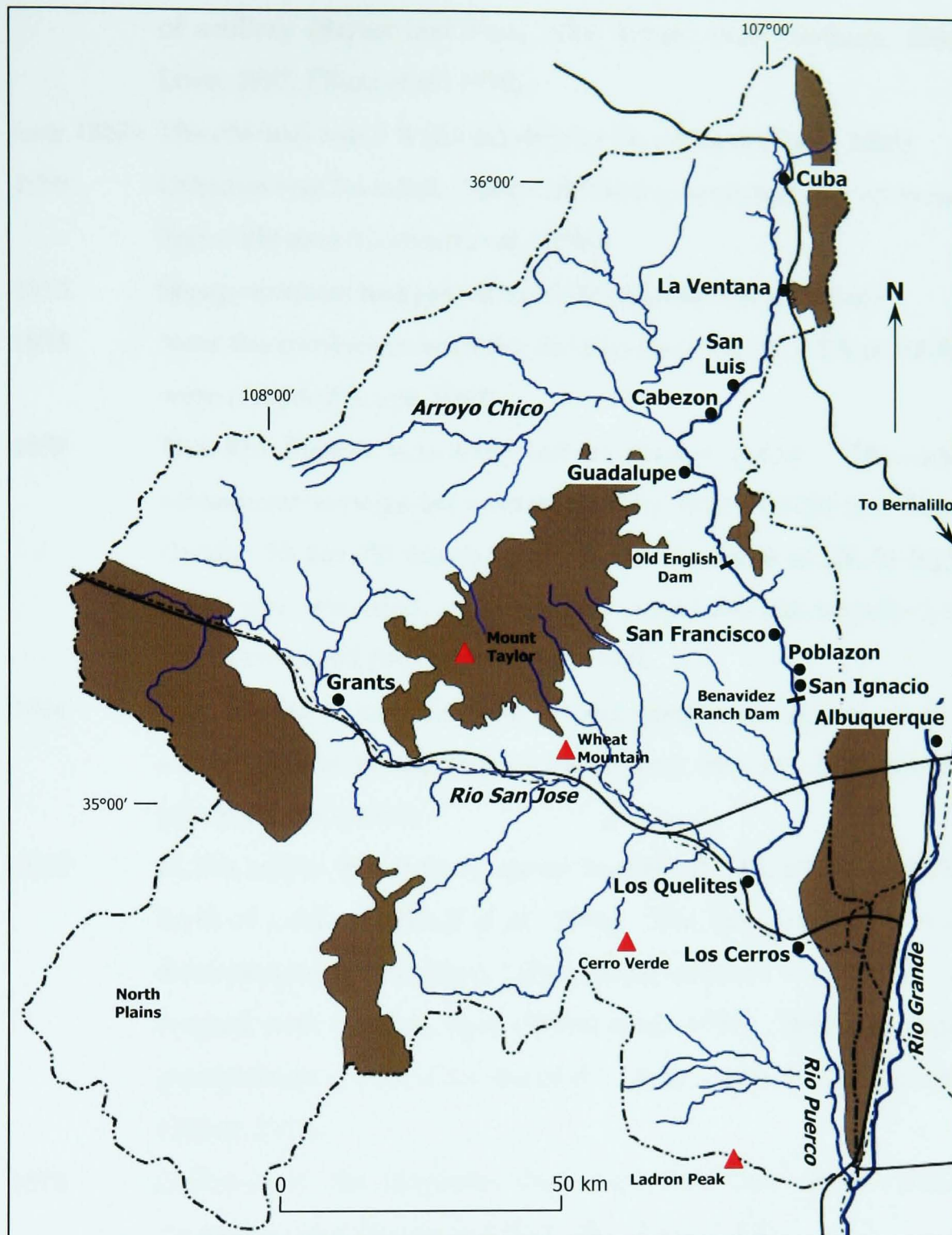


Figure 3.3 Location of historic sites of the Rio Puerco Basin (after Widdison, 1959).

- 1846 Army campaigners sent to the area to subdue the Navajo documented 9 m (30 ft) vertical banks near the ruins of Poblazon, on the Montaño Grant, and 3-4 m (10-12 ft) high banks elsewhere (Bryan and Post, 1927; Bryan, 1928; Tuan, 1966; Gorbach *et al.*, 1996; Love, 1997; Elliott *et al.*, 1999).
- 1849 5 miles above Cabezon, the channel was 30m (100 ft) wide and 6-9 m (20-30 ft) deep, which had to be graded to allow the passage

- of artillery (Bryan and Post, 1927; Bryan, 1928; Gorbach, 1996; Love, 1997, Elliott *et al.*, 1999).
- Early 1850s The channel was 8 ft (2.5 m) deep at La Ventana (Tuan, 1966).
- 1850 Cabezon was founded. 1,000–2,000 sheep were introduced to the Bernalillo area (Gorbach *et al.*, 1996).
- 1853 Sheep numbers had grown to 50,000 (Gorbach *et al.*, 1996).
- 1854 Near the confluence with the Rio San Jose, banks of 5.5 m (18 ft) were recorded (Love, 1997).
- 1855 The Rio Puerco was surveyed at several points. This and subsequent surveys are summarised by Bryan (1928) and Tuan (1966). 30 km (20 miles) south of Los Cerros, 6 m (20 ft) high banks were recorded, although the channel was still unincised at Los Cerros itself (Bryan and Post, 1927).
- 1864 The Navajo were defeated, encouraging resettlement of the valley. Diversion irrigation systems were constructed by farmers (Gorbach *et al.*, 1996).
- 1870 In the upper Rio Puerco, sheep numbered 240,000, with 9,000 head of cattle (Gorbach *et al.*, 1996). The Rio Puerco was still discontinuously trenched, since some reaches could still be crossed with small bridges (Elliott *et al.*, 1999). Below average precipitation occurred for the next 30 years, with few exceptions (Elliott, 1979).
- 1875 Collapse of the irrigation dam near San Luis caused some channel change (Bryan and Post, 1927; Love, 1997).
- 1877 Communities in the upper and middle Rio Puerco were thriving, with populations nearing their historical maximums (Bryan and Post, 1927; Bryan, 1928; Widdison, 1959). Floodwaters were diverted, creating a ditch, which was subsequently occupied as the main channel when a flood washed around the Cabezon dam (Bryan and Post, 1927; Bryan, 1928).
- 1880 The Santa Fe railroad was extended across the Rio Puerco valley, causing traffic through the crossroads at Cabezon to dwindle (Widdison, 1959). An artificial cut-off of the Rio Grande near

San Acacia shortened the channel by 2.4 or 3 km (1.5 or 2 miles). This may have resulted in base-level lowering of the Rio Puerco (Elliott, 1979).

- 1881 Above average precipitation occurred (Elliott, 1979).
- 1882 The Rio Puerco was still discontinuous, with a bridge lower than 1.5 m (5 ft) high reported near Cabezon. This was not designed for the floods which still overtopped the banks on occasion (Bryan and Post, 1927; Elliott *et al.*, 1999).
- 1883 The bridge near Cabezon was rendered useless as the channel had changed position (Bryan and Post, 1927).
- 1884 Above average precipitation occurred (Elliott, 1979). At Cabezon, the Rio Puerco was still unincised (Figure 3.4).
- 1888 A US Geological Survey map shows the Rio Puerco flowing on the east side of the valley 3 km (2 miles) south of San Ignacio (Love, 1997). Los Cerros, the settlement furthest south, was abandoned after a local dam washed out due to headcutting of the incised channel (Bryan and Post, 1927; Gorbach *et al.*, 1996).

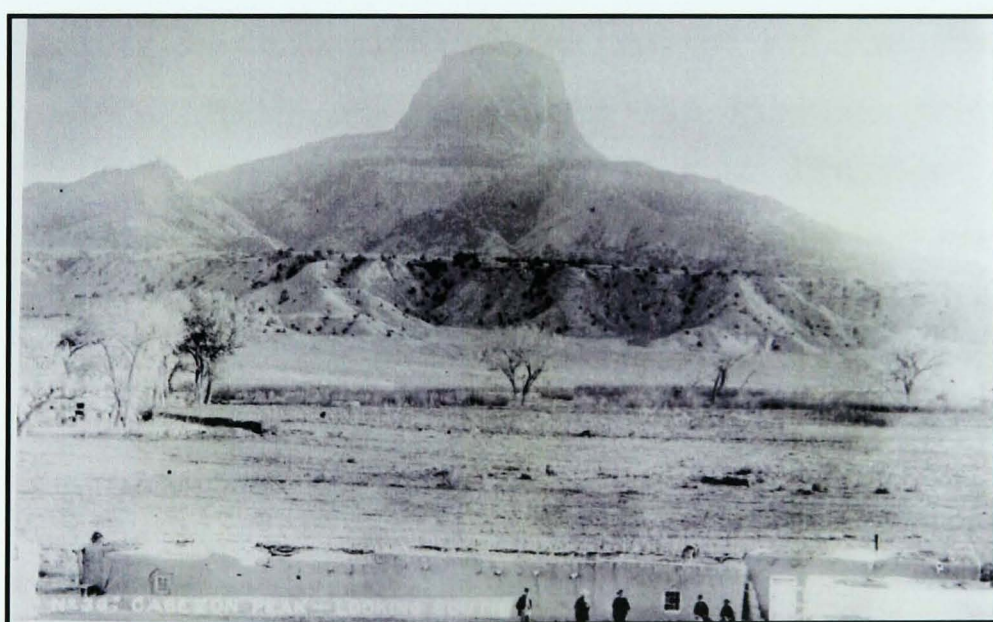


Figure 3.4 1884 photograph of the unincised Rio Puerco at Cabezon, looking south towards Cabezon Peak (EA Bass, courtesy of the Library of Congress Prints and Photographs Division Lot No. 3286).

- 1889 The Rio Puerco Irrigation and Improvement Company purchased land and water rights, planning to construct a 190 km (120 mile) long canal on the eastern floodplain from the headwaters to a dam on the Montaño Grant, close to Benavidez Ranch (Gorbach *et al.*, 1996).
- 1885-92 The channel at Cabezon was believed to have become incised, the water table dropped and wells dried up (Bryan and Post, 1927; Bryan, 1928). Discontinuously entrenched segments began coalescing (Elliott *et al.*, 1999)
- 1896 The Old English Dam, or Puerco Dam, was constructed by the Irrigation and Improvement Co.. Photographs taken by PE Harroun during the construction of this dam indicate that it was built on the site of a previous dam, the remains of which were estimated to be less than a decade old at that time (D Love, pers. comm., 2003). Although solidly built, with sandstone abutments infilled with timber, the margins of the Old English Dam were in unconsolidated alluvium which caused failure soon after it was finished, draining a lake 2.5 km (1.5 miles) long. Shortly after this, the settlements of San Ignacio and San Francisco (progressively further upstream) were abandoned (Bryan and Post, 1927; Bryan, 1928; Gorbach *et al.*, 1996; Love, 1997), although San Ignacio was only abandoned by farmers requiring irrigation water (Bryan, 1928). The arroyo at this point was 6 m (20 ft) deep and an abandoned floodplain containing mature cottonwoods existed between the valley floor and the arroyo floor. The collapse of the Old English Dam possibly caused a flash flood, triggering the collapse of a smaller, earthen dam downstream. The failure of this dam, the Benavidez Ranch Dam, is likely to be responsible for the subsequent avulsion of the Rio Puerco to the west side of valley south of former position of San Ignacio (D Love, pers. comm., 2003). The new channel was larger, following the course of a road to the southwest (Love, 1997).

1887	Above average precipitation occurred (Elliott, 1979).
1900	Migration from Cabezon was occurring due to problems with cultivation and lack of prosperity in the town (Bryan, 1928).
1910	The arroyo at Cabezon was 11 m (35 ft) deep (Bryan, 1928).
1911	San Ignacio was abandoned completely (Bryan, 1928).
1922	The dam at Cabezon was washed out (Gorbach <i>et al.</i> , 1996).
1927	Rio Puerco was reported as being continuously incised (Bryan and Post, 1927).

It was initially thought that headcutting had progressed upstream in one continuous push from mouth to Cuba (Bryan and Post, 1927; Bryan, 1928). However, further examination of records has indicated that localised headcutting of individual reaches was more likely (Love, 1997; Elliott *et al.*, 1999). The above chronicle of incision within the Rio Puerco system has provided incontrovertible proof that a discontinuous arroyo existed in the mid-1800s. There is also evidence that initiation proceeded headwards from the lower reaches. However, these two hypotheses are not mutually exclusive. It is, therefore, most likely that the discontinuous sections coalesced as headcutting of the continuous arroyo occurred.

The review of causes of arroyo incision in Section 3.1 indicated that a combination of factors was generally responsible for triggering downcutting. In this regard, the Rio Puerco is no exception. Unusually, incision on the Rio Puerco was not initiated by one particular flood, occurring piecemeal until the entire system was entrenched. The major cause of incision, especially in the discontinuously entrenched sections of the system, is most likely to have been the presence of intrinsic geomorphic thresholds, which were crossed prior to the first recorded descriptions. Coalescence of the discontinuously entrenched sections occurred through headward erosion of the upstream knickpoints, assisted by several other factors. Heavy grazing and poorly adapted farming practices, which included the construction of flow diversion ditches, in the upper and middle reaches caused flow concentration and depletion of protective vegetative cover. In the lower

reaches, flash flooding occurred due to the failure of the Old English Dam and, subsequently, the Benavidez Ranch Dam further downstream. The latter failure, especially, produced a great deal of geomorphological change, causing channel avulsion and initiation of downcutting in the reaches immediately downstream. A further likely cause of incision along the lower Rio Puerco was base-level lowering, due to the straightening of the Rio Grande in 1888.

Santa Cruz River

The location of historic sites pertinent to the development of the arroyo of the Santa Cruz River are shown in Figure 3.5.

- 350-1500 Prehistoric Hohokam farmers occupied the region, building irrigation channels and using similar farming methods to later settlers (Waters, 1988; Betancourt, 1990).
- 1689 The area was visited by Kino. The Santa Cruz River was known as the Rio Santa Maria de Soamca (Dobyns, 1981; Betancourt, 1990) and had a poorly-defined channel flowing across a grassy valley floor (Olberg and Schanck, 1913; Antevs, 1952). North Pimans practiced irrigation, using canals, close to springs and ciénegas, especially at Tubac and San Xavier (Cooke and Reeves, 1976, Dobyns, 1981; Betancourt, 1990). The area was under the control of the Spanish Presidio (Dobyns, 1981; Betancourt 1990).
- 1702 Missions were established at Tucson and San Xavier. The intervening land was covered in thick mesquite forest (Dobyns, 1981) (Olberg and Schanck (1913) reported that these missions were established in 1732).
- 1763 Cattle and sheep were brought into the area (Cooke and Reeves, 1976).
- 1768-1822 Increased prosperity in the region lead to increased development of irrigation near the San Xavier Mission and springs (Olberg and Schanck, 1913). Apache raids continued (Dobyns, 1981).

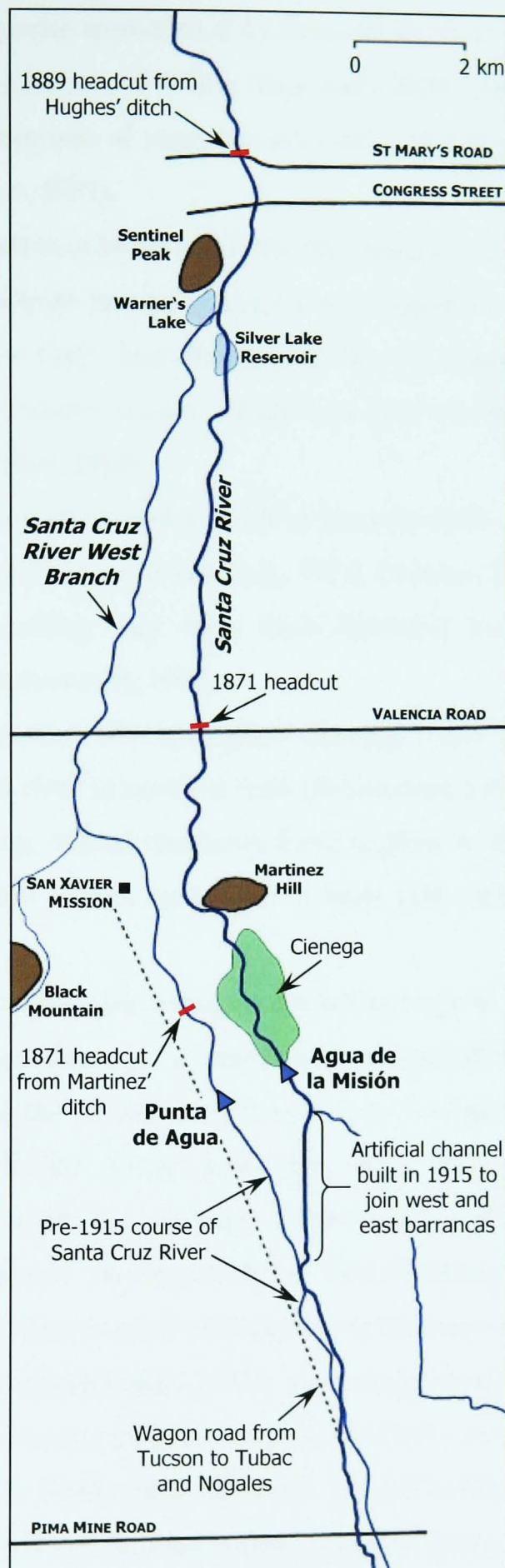


Figure 3.5 Location of historic sites of Santa Cruz River in the San Xavier and Tucson reaches (after Betancourt, 1987; 1990).

- 1830s The Apache were forced to fence off fields to prevent damage by grazing horses, of which there were 2000. Apache raiding led to abandonment of ranches and stock, allowing cattle to run wild (Dobyns, 1981).
- 1846 War between Mexico and the US brought soldiers into the Tucson area. Dense mesquite forests were reported, as their wood was used for fuel. Travellers noted that the Santa Cruz River was a discontinuous stream which sank into the sand (Dobyns, 1981; Betancourt, 1990).
- 1849-51 Martinez excavated a ditch to increase flows from the Punta de Agua (Olberg and Schanck, 1913; Dobyns, 1981; Waters, 1988). Downcutting may have been initiated immediately (Waters, 1988; Betancourt, 1990).
- 1857 Downstream of a spring-fed ciénega, Silver Lake Reservoir was created close to Sentinel Peak (Betancourt, 1990).
- 1858 Flooding caused the Santa Cruz to flow to the Gila River, with the Rillito River reportedly a mile (1.6 km) wide (Betancourt, 1990).
- 1862 Mexican farmers enlarged ditch headings to a mill-race, hoping to extend flows to beyond St Mary's Road (Betancourt, 1990).
- Pre-1870 80% of the 72 km stretch between Continental and confluence with Rillito River was dry, with two perennial reaches downstream of springs (Betancourt, 1990). Malaria was prevalent in Tucson (Hastings, 1959; Dobyns, 1981).
- 1871 The northern end of the San Xavier Reservation (actually created in 1874 (Betancourt, 1990)) was being dissected by headcutting discontinuous gullies. Vertical headcuts were recorded close to Valencia Road and at Martinez' ditch (Waters, 1988).
- 1873 Grass still covered the valley bottom (Olberg and Schanck, 1913). The Apache were finally conquered, although raids still occurred until 1886. A dramatic increase in the number of cattle occurred over the next two decades (Dobyns, 1981).



Figure 3.6 1885 photograph of Silver Lake Reservoir (courtesy of Arizona Historical Society, Tucson, AHS #18,335).

- 1874 Mesquite forested land was recognised as good-quality farmland, initiating clearance (Dobyns, 1981).
- 1877 Drought caused fires in the Santa Catalina Mountains and depleted grasses (Betancourt, 1990).
- 1878 Flooding occurred prior to recovery of the grasslands, although no channel change was reported (Betancourt, 1990).
- 1880 Resorts opened at Silver Lake (Figure 3.6) and other reservoirs, such as Warner's Lake. Farmers downstream complained that their water had been obstructed, depriving the oldest fields of water. Chinese farmers began growing water-intensive crops and were accused of stealing water from irrigation ditches (Betancourt, 1990).
- 1881 July flooding deposited cottonwood and willow seeds which grew rapidly, impeding flow and causing net aggradation (Dobyns, 1981).
- 1885 A drought occurred, although severe flooding occurred in August (Hastings, 1959; Betancourt, 1990).
- 1886 The Arizona Mining Index warned of building on the floodplain. Half the average annual precipitation, although floods in August

- damaged dams and enlarged the Santa Cruz River to 0.8 km (0.5 miles) wide (Hastings, 1959; Betancourt, 1990).
- 1887 The Bavispe earthquake occurred on May 3rd, measuring 7.3 on the Richter Scale (Betancourt, 1990). As a result, the position of groundwater and surface flows changed. The Agua de la Misión moved south (Waters, 1988). Subsidence caused groundwater to rise to the surface, fissures caused forcible ejection of water and unconsolidated alluvium was deformed. Subsequent flooding washed out dams and some river deepening occurred (Betancourt, 1990). The last reported fish was caught (Hastings, 1959). A large-scale irrigation ditch project was formulated (Dobyns, 1981).
- 1888 Hughes excavated a ditch to increase discharge by tapping groundwater 12 km north of Martinez Hill. As he ran out of funds before reaching the desired size, he intended to allow flooding to complete the ditch for him and, thus, left it unprotected (Waters, 1988; Betancourt, 1990). A ditch was also dug on the Silver Lake resort. Ditch building was the most popular method of securing near-surface throughflow (Betancourt, 1990).
- 1889 Flooding caused erosion of Hughes' ditch (Betancourt, 1990).
- 1890 Extensive flooding in August saw equally extensive erosion. Hughes' ditch was extended almost to Silver Lake, at rates of up to 30 m per hour (Hastings, 1959; Waters, 1988; Betancourt, 1990). Networks of headcutting gullies were reported, with irrigation canals and much agricultural land lost (Hastings, 1959). Eroded sediments were deposited downstream causing a wide, braided channel. Some fields were buried under sediment over 1 m deep (Betancourt, 1990).
- 1891 Hughes' ditch continued headcutting during floods (Betancourt, 1990).
- 1892 The ciénega at the site of Warner's Lake was drained (Betancourt, 1990).

- 1893 Falling water tables necessitated the digging of wells on the San Xavier Reservation (Betancourt, 1990).
- 1899-1904 Severe drought occurred (Betancourt, 1990).
- 1905 Severe flooding from heavy precipitation between January and April occurred (Betancourt, 1990).
- 1908 Flooding caused further headcutting (Olberg and Schanck, 1913).
- 1910 Greene's Canal was completed north of Tucson, in order to channel water to a reservoir for irrigation (Cooke and Reeves, 1976).
- 1912 The Tucson arroyo coalesced with the incised channel at Valencia Road, which reached 5 km into the San Xavier Reservation, where it had reached a resistant caliche layer (Olberg and Schanck, 1913; Dobyns, 1981; Betancourt, 1990). The Martinez ditch was reported as being filled with approximately 2–3 m (6–8 ft) of sand after each flood, requiring re-excavation to access water again. The incised arroyo was up to 30 m (100 ft) wide and 6 m (20 ft) deep at this point. Upstream of the caliche outcrop, the channel was still a broad, sandy channel (Figure 3.7) (Olberg and Schanck, 1913).

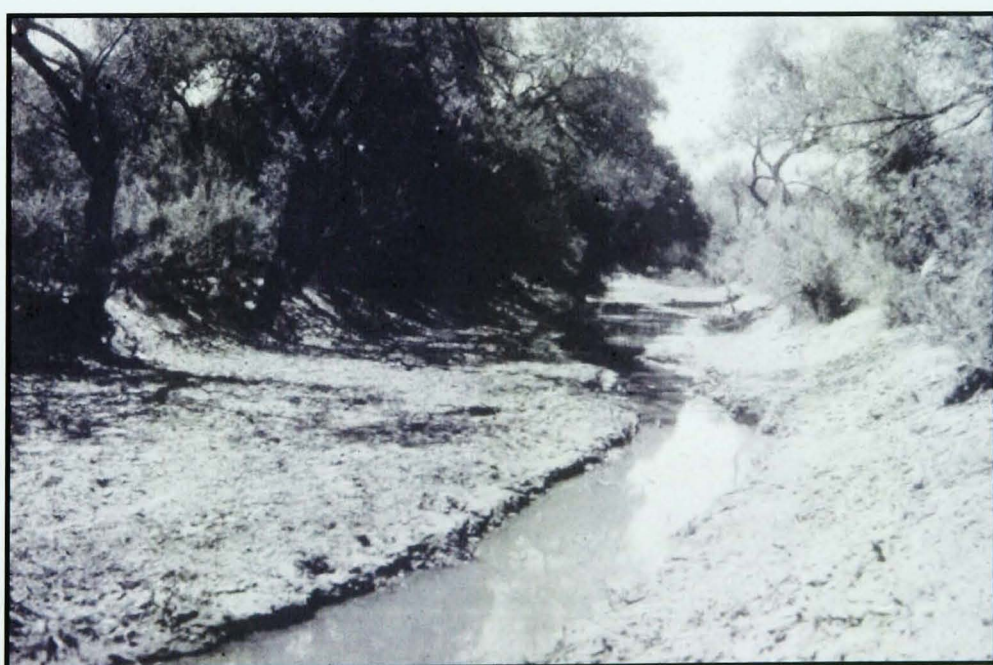


Figure 3.7 Unincised channel at the Punta de Agua on the west barranca of the Santa Cruz River, 1912 (Photographer unknown).

- 1914/15 Extremely large magnitude floods during the winter initiated lateral erosion along the incised Santa Cruz River and destroyed the ciénegas below the Agua de la Misión. Headcutting reached the east-side barranca (arroyo). Subsequently, an artificial ditch linking the entrenched channel with the unentrenched channel upstream was completed in 1915. Concentrating flow further, a dyke was built upstream from the incised Martinez ditch, known as the west-side barranca (proposed by Olberg and Schanck, 1913; Waters, 1988). The dam below Greene's Canal was washed out, causing the canal to erode (Cooke and Reeves, 1976).
- Pre-1917 80% of the mesquite forests within the Tucson Basin had been destroyed (Betancourt, 1990).
- 1930s The arroyo continued to headcut through the artificial ditch then along an old wagon road, until continuously entrenched for 70 km (Waters, 1988).

As with the Rio Puerco, a number of different causal mechanisms were responsible for the initiation of entrenchment of the Santa Cruz River system. However, documented observations of the Santa Cruz River date back several centuries and these causes are, therefore, better known. The major entrenchment trigger is likely to have been the creation of various artificial drainage concentration ditches and canals during the mid- to late-19th Century. These were either deliberately built to be enlarged by floods, or were under-engineered and could not, therefore, accommodate the highest magnitude floods. An old wagon road running from Tucson to Nogales also caused concentration of runoff.

The Santa Cruz River became discontinuously entrenched at the sites of the artificial runoff concentration features. These incised channels were enlarged rather more than anticipated by a series of large floods. Those which occurred in 1886, 1887 and 1889 caused little significant erosion. However, the 1890 flood caused an intrinsic geomorphic threshold to be crossed and incision began in earnest. High-magnitude flooding

subsequently occurred in 1891, 1905 and 1914/1915, causing further enlargement and coalescence of the discontinuously entrenched sections. The 1887 earthquake caused deformation of unconsolidated alluvium and hydrological changes, most likely contributing to the increased susceptibility of the Santa Cruz River system to incision. The incision of the Santa Cruz River system, therefore, occurred in the piecemeal manner observed in the Rio Puerco. Erosion progressed headward from several distinct points until a continuous arroyo had formed.

San Simon River

The historic sites of the San Simon River differ little from those seen today (shown in Figure 1.5 and Appendix 2, Figure A2.17).

- 1859 The Butterfield Stage Line was established at what is now San Simon, due to the existence of permanent water. There were few permanent settlers due to the Indian threat (Cooke and Reeves, 1976; Jordan and Maynard, 1970a). Cienegas were common in the valley (Meyer, 1989).
- 1862 Camp Bowie was established to give protection from hostile Apaches, encouraging more settlement, especially mining camps in the southern part of the San Simon Valley (Jordan and Maynard, 1970a).
- 1869 The San Simon River was reported as flowing through an unchannelled, almost imperceptible bed (Hastings, 1959).
- 1875/8 The valley was reported as being grassy with a seasonal water supply. No mention of entrenchment was made. (Cooke and Reeves, 1976; Dobyns, 1981; Jordan and Maynard, 1970a).
- 1882 The San Simon Valley, known as the Valle de Sauz (Willow Valley), was suitable for cattle farming (Jordan and Maynard, 1970a; Dobyns, 1981). The San Simon River was reported as being an intermittent, unincised stream with water holes, although it had become entrenched at the confluence with the Gila, with 0.9 m (3 ft) high banks and a channel less than 6 m (20 ft) wide (Cooke and Reeves, 1976; Jordan and Maynard, 1970a).

- Only infrequent large floods caused flow along entire length of the river (Cooke and Reeves, 1976). Reports of many springs, waterholes and lakes indicated that they were generally dried up by the end of April (Dobyns, 1981). Few cattle (Jordan and Maynard, 1970a).
- 1883 Settlers near Solomonville dug a flood concentration channel and built funnelling levees to prevent debris being spread across their land during large flow events (Bryan, 1928; Cooke and Reeves, 1976, Jordan and Maynard, 1970a). This is thought to be the date of first entrenchment, although there is some confusion over the exact date of construction of the artificial channel, which may actually have been as late as 1900 (Hastings, 1959; Meyer, 1989). Hay was harvested from meadows. Ore wagons from nearby mines were eroding wagon routes.
- 1884 The Gila, Globe and Northern Railway was extended through area, which followed the valley floor for over 30 km (20 miles) and possibly reduced flood widths by 40% (Cooke and Reeves, 1976).
- 1890 The first incidence of serious entrenchment was reported during flooding in July and August, although there was no evidence of downcutting any great distance south, upstream of Solomonville (Cooke and Reeves, 1976).
- 1895 An estimated 50,000 head of cattle grazed the valley (Jordan and Maynard, 1970a).
- 1902-5 Serious drought occurred (possibly since 1899) (Cooke and Reeves, 1976). The combined effects of artificial drainage and grazing were highly visible (Jordan and Maynard, 1970a). Water holes dried up causing migration away from the area (Jordan and Maynard, 1970a).
- 1905/6 Much erosion occurred during floods (Burkham 1972; Cooke and Reeves, 1976, Mayer, 1989). The artificial drainage ditch, wagon road and main channel of the San Simon River were all eroded.

- 1916/7 The 1916 flood caused further erosion and also followed a period of drought (Cooke and Reeves, 1976).
- 1930s The arroyo had extended headward over 90 km (60 miles), forming a channel up to 9 m (30 ft) deep and 60 m (200 ft) wide, although it was much smaller than this in places (Cooke and Reeves, 1976; Jordan and Maynard, 1970a; 1916 & 800ft wide in Dobyns, 1981). Erosion was thought to be the indirect result of landowners work to protect land. Entrenched tributaries were thought to be eroded cattle trails.

Incision of the San Simon River, as with the other two arroyos studied, was initiated by a number of different causal mechanisms, in a number of locations through the system. Entrenchment was first documented in the lower reaches of the system, most likely due to the construction of a drainage concentration gully and funnelling levees at Solomonville. Subsequent flooding in 1890, following a drought, caused localised downcutting in this reach. Wagon roads, cattle trails and railway embankments running along the valley floor provided avenues for runoff concentration, aiding the headward progression of erosion.

The San Simon River did not, however, incise solely through headward progression of erosion. Overgrazing and poorly-adapted farming practices increased the erodibility of the system. The simultaneous construction of runoff concentration features increased the erosive capability of flood-flows, causing localised incision in other reaches (Cooke and Reeves, 1976). The system became continuously entrenched due to a series of large floods. These were particularly destructive in 1905 and 1916, following periods of drought.

3.3 COMPARISON OF INITIATION PROCESSES

The review of causal mechanisms of arroyo initiation in Section 3.1 indicated that arroyo systems were products of equifinality. This statement has been shown to hold true, as differing factors were responsible for the initial entrenchment of all three arroyos studied. A further common feature was

that no one process was responsible for their initiation. As a generalisation, incision was initiated due to a combination of the presence of artificial flow concentration structures, such as ditches and trails; land-use changes within the drainage basin; and climatic fluctuations. This combination of factors caused a positive feedback response, leaving each system primed for entrenchment. Since arroyos are event-driven systems, flood events, by necessity, provided the final trigger to incision. For both the Santa Cruz and San Simon Rivers, this triggering flood has been pinpointed to 1890. However, no single flood has been deemed responsible for the Rio Puerco entrenchment.

The classic models of channel incision, discussed in Chapter 2, indicate simple headward progression of entrenchment. However, in all three systems studied, it was found that the arroyos were initially discontinuous. The Rio Puerco appears to have become entrenched, in places, significantly earlier than the Arizonan arroyos, prior to the mid-1800s. The Santa Cruz River became discontinuously entrenched during the mid-1800s. However, incision in reaches of the San Simon River was not documented until the late 1800s. Headward migration of knickpoints, at the upstream limit of each entrenched section, subsequently caused these incised reaches to coalesce. Again, the sequence of flooding within each system determined the rapidity with which this occurred.

CHAPTER 4

Flow and Sediment Discharge Variability

“Streams may be regarded as sediment-transporting machines”

(Bull, 1979, p455)

4.1 FACTORS CONTROLLING STORM EVENTS IN STUDY AREAS

The discharge regime of a river is controlled primarily by three interrelated factors: hydrometeorology, hydroclimatology and basin physiography, including vegetation. The mechanisms controlling short-term precipitation patterns may be discerned by examining the hydrometeorology of an area. However, short-term discharge fluctuations generated by weather-related events are superimposed on the seasonal, annual and decadal variability related to the longer-term and larger-scale hydroclimatology of the region (House & Hirschboek, 1995). The arroyos of the south-western USA have distinctly seasonal flow regimes, which are best explained by examining hydroclimatological fluctuations. Discharge variability has been closely linked to changes in the configuration of elements of the large-scale atmospheric circulation (Hirschboek, 1985; Webb and Betancourt, 1992). With respect to flood flows, three different atmospheric circulation patterns have been found to cause the majority of flood events, resulting in demonstrable differences in the associated flood hydrographs (Webb and Betancourt, 1992).

Winter storms are generally generated by frontal and cut-off low pressure systems. During the winter months the Aleutian low-pressure cell in the North Pacific may expand causing frontal systems to be pushed south. During wetter winters, a prevalent ridge of high-pressure, which sits off the west coast of the Pacific north-west during drier years, is displaced westward, causing a trough of low-pressure to develop over the western USA. If this high-pressure ridge is well-developed, the low-pressure system may stagnate to form cut-off low-pressure systems. If these lows intensify off the coast of California before moving inland, substantial rainfall may be produced in Arizona (Webb and Betancourt, 1992). In general, however, this

type of system is associated with widespread, low-intensity rainfall which may produce relatively prolonged floods, especially if several storms occur in succession (Slezak-Pearthree and Baker, 1987; Meyer, 1989; Parker, 1996). These frontal storms are more likely to cause floods on the Rio Puerco, since the two southern Arizona arroyos lie to the south of the usual main storm track (Hirschboek, 1985; Parker, 1996). Frontal storms generally occur between November and March, although they may occur as early as September (Parker, 1996). The timing of these storms is crucial since, if cut-off low-pressure systems stall over warm tropical waters during the autumn, they may steer dissipating tropical cyclones inland, thus creating conditions for the occurrence of the idealised probable-maximum precipitation (Saarinen *et al*, 1984; Webb and Betancourt, 1992).

During late summer and early autumn, the north-easterly penetration of dissipating tropical cyclones (either hurricanes or tropical storms) may cause widespread, intense rainfall over the south-west. In the southwest this type of storm releases maximum precipitation during September and October if interaction with cut-off low-pressure systems, which occur with maximum frequency in October, causes recurvature and dissipation over the region (Webb and Betancourt, 1992). This type of atmospheric pattern can produce high-intensity precipitation, high runoff and is associated with some of the highest-magnitude floods (Saarinen *et al*, 1994; Parker, 1996).

The third type of upper atmospheric circulation causes intense, short-lived precipitation and is generally termed the "summer monsoon" due to the (slight) similarity to monsoon rainfall elsewhere. The early summer typically has very low rainfall due to the southerly displacement of a subtropical high-pressure system. At the end of June or beginning of July, this system moves rapidly north, causing an abrupt end to this seasonal drought throughout the south-west (Betancourt, 1990; Webb and Betancourt, 1992). The storms caused by this type of circulation are generally convective. They are generally responsible for at least one flood each year and constitute the majority of annual flood peaks (Slezak-Pearthree and

Baker, 1987; Webb and Betancourt, 1992; Parker, 1996). The flood events produced by monsoonal precipitation are very flashy and localised, with magnitudes dependent on the precise location and duration of the most intense precipitation (Parker, 1996).

Since these atmospheric patterns are all of a large-scale, relative to the study region, all three drainage basins have similar rainfall patterns (Meyer, 1989) and values of annual average precipitation. The higher latitude of the Rio Puerco basin results in snow accumulation in the surrounding mountains. During the spring, snowmelt causes prolonged, low-magnitude flow events, especially in the upper reaches (Molnár, 2001). Average annual precipitation ranges from 180 mm in the south of the basin to 600 mm in the mountains in the Rio Puerco basin. The average annual basin-wide precipitation between 1948 and 1997 was 267 mm, using data from 14 rain gauges located in or close to the basin (Molnár, 2001). In the Santa Cruz River basin, precipitation records again correlate well with altitude. Average basin-wide annual precipitation is 430 mm, ranging from 195 mm to 757 mm at the summit of Mount Lemmon (although runoff from the Santa Catalina Mountains enters the Santa Cruz River downstream of the study area) (Parker, 1996). It should, however, be noted that the average annual precipitation at Tucson itself, which is more representative of the study area, was 287 mm between 1867 and 1997. Average annual precipitation within the San Simon basin ranges from 200 mm to 760 mm, again dependent on altitude (Mathis, 1983). At the San Simon rain gauge, the average annual precipitation between 1882 and 1997 was 221 mm.

Seasonal and annual fluctuations in the regional atmospheric circulation are superimposed on longer-term oscillations. Oceanic and atmospheric conditions have been closely linked to changes in oceanic temperature that precede atmospheric changes (Webb and Betancourt, 1992; Molnár, 2001). The most important long-term fluctuations are associated with ENSO (El Niño – Southern Oscillation) conditions, which occur every three to five years. During these events, anomalously warm water occupies the surface

layer of the eastern and central Pacific (El Niño). ENSO events are also accompanied by high pressure at sea-level close to Indonesia and low pressure over the central equatorial Pacific. Technically, the Southern Oscillation is the pressure difference between Darwin, Australia and Tahiti, with negative values indicating ENSO conditions (Figure 4.1) (Webb and Betancourt, 1992). The effect of ENSO conditions on the magnitude and variability of flooding has already been noted in Chapter 3. It has been observed that the frequency of both frontal storms and tropical cyclones affecting the south-west may increase during ENSO conditions, due to the associated deepening of the Aleutian Low (Graf *et al.*, 1991; Webb and Betancourt, 1992). Thus, warm-phase ENSO years have been associated with higher than average annual precipitation (Molnár, 2001). However, it should be remembered that ENSO conditions may also coincide with drought conditions, especially during winter months (Graf *et al.*, 1991).

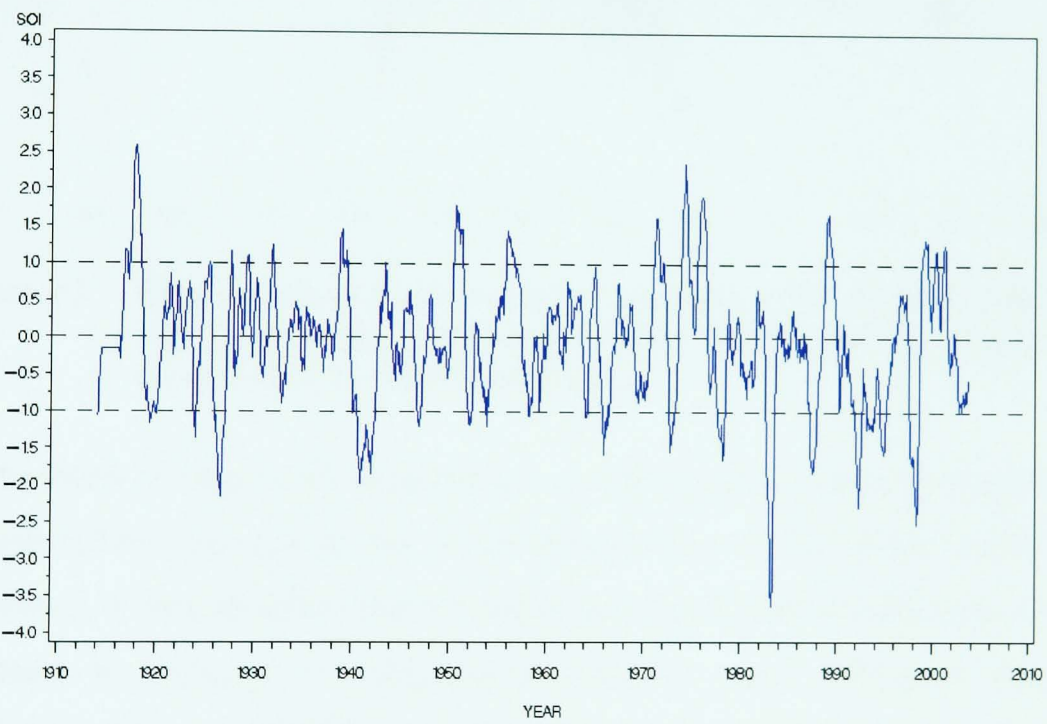


Figure 4.1 Southern Oscillation Index (Tahiti – Darwin), five month running mean for 1914 to present (after Dahm and Moore, 2003).

Fluctuations of sea-level pressure and temperature have also been significantly correlated with precipitation patterns in the south-western USA on a longer, decadal timescale. The most significant variation to affect the south-west is the Pacific Decadal Oscillation (PDO), which is, similar to

ENSO, based on Pacific sea-surface temperature anomalies, but which is characterised by more extreme regime shifts with a recurrence interval of between 50 and 70 years. Positive values of PDO indicate higher sea surface temperatures and a deepening of the Aleutian low-pressure anomaly, much the same as ENSO conditions, resulting in higher winter and spring precipitation (Molnár, 2001).

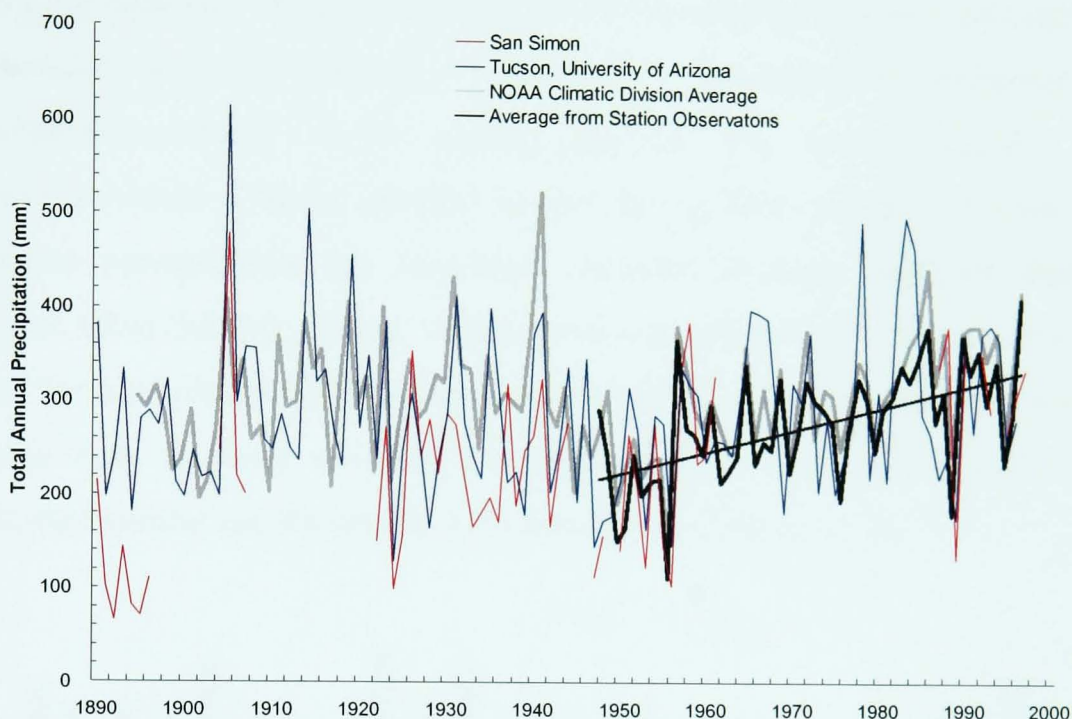


Figure 4.2 Time series of total annual precipitation (Rio Puerco data and NOAA climatic division data after Molnar (2001)). Linear trendline is for Rio Puerco data.

Fluctuations in large scale atmospheric conditions have, in turn, resulted in corresponding changes in the hydrometeorology of the study areas. In Chapter 2, it was observed that attempts have been made to attribute arroyo initiation to changes in precipitation intensity, since historical average annual rainfall records indicate no significant trend. The pioneering studies of precipitation patterns underpinning this conclusion were carried out several decades ago (Leopold, 1951; Cooke and Reeves, 1976). However, in recent years precipitation patterns have changed somewhat. While updating of Leopold's analysis of Santa Fe precipitation records indicates that the average annual rainfall continues to show no trend (Elliott *et al*, 1999; Gellis and Elliott, 2001), a statistically significant increasing trend can be observed for precipitation in the Rio Puerco Basin (Figure 4.2) (Molnár,

2001). This increase is paralleled by data from the Santa Cruz River and San Simon basins and is directly related to the variability of large-scale atmospheric circulation and, therefore global climate (Molnár, 2001). Since 1960, an increased frequency of ENSO conditions has been observed, which has caused an increase in the recurvature of both dissipating cyclones and frontal systems over the south-west (Webb and Betancourt, 1992). The changing pattern of large-scale atmospheric circulation has also affected the seasonality of precipitation in the southwest. The increasing frequency of precipitation-causing events during autumn and winter months has naturally caused a rise in average rainfall during these months. In contrast, summer precipitation has remained constant or even declined slightly (Figure 4.3.a) (Molnár, 2001). Although it was not possible to carry out the same form of trend analysis found in Molnár's Rio Puerco study, a simple comparison of mean monthly precipitation both before and after 1960 indicated similar results for the Arizonan basins (Figure 4.3.b).

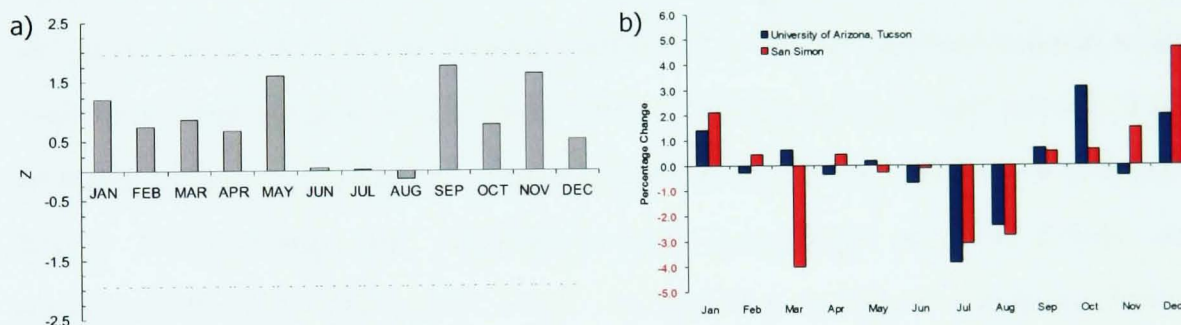


Figure 4.3 Variation in monthly rainfall data. a) Rio Puerco basin between 1952 and 1986 (after Molnár, 2001), with positive Z score indicating an increase over period of record, dashed line indicating statistically significant values. b) University of Arizona, Tucson, between 1868 and 1996, and San Simon, between 1882 and 1997, showing percentage change before and after 1960. Anomalous negative data for March at San Simon is due to unusually high rainfall during 1905 skewing average.

While a significant trend in annual average precipitation has been noted, rainfall intensity has continued to exhibit variability. Daily precipitation was divided into low, medium and high intensity purely by examining the total rainfall for that day (Leopold, 1951). After a peak prior to 1880, the frequency of high intensity precipitation fell during subsequent years, with a slight rising trend after 1950. In contrast, the frequency of low and medium intensity rainfall exhibited a peak between 1880 and 1930. The frequency of

low intensity rainfall has subsequently declined, whereas medium intensity precipitation shows similar increases to the frequency of high intensity rain after 1950 (Elliott *et al.*, 1999; Gellis and Elliott, 2001). This pattern corresponds to the increase in frequency of occurrence of atmospheric conditions likely to cause high intensity precipitation. Similar patterns of rainfall intensity were noted in southern Arizona (Hastings and Turner, 1965; Cooke and Reeves, 1976; Betancourt and Turner, 1993; Hereford, 1993).

4.2 DISCHARGE TRENDS

4.2.1 Seasonality of Flow

Although precipitation is an important factor affecting the initiation and evolution of arroyos, it is the runoff created by this rain which actually affects their morphology. Webb and Betancourt (1992) noted that streamflow is a less ambiguous measure of climatic variability than precipitation, due to the fact that weather phenomena are integrated and concentrated over space and time to produce a single variable. The study areas are situated in the semi-arid southwest, with low annual rainfall totals and very high evapotranspiration rates. Consequently, only two or three percent of the precipitation actually reaches the arroyo channels (Molnár, 2001). Occasionally, this rainfall-to-runoff percentage may fall below one percent (Olberg and Schanck, 1913). In addition to this, it has been shown that the rainfall-to-runoff percentage has changed over time. In the Rio Puerco Basin, a steady decline in this percentage at all gauges since 1967 was reported by Branson and Janicki (1986). As Figure 4.4 shows, this

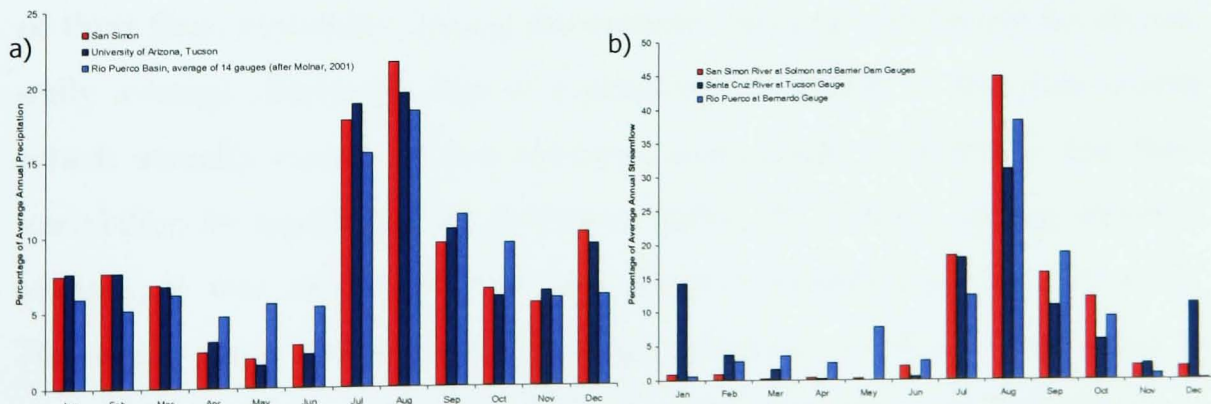


Figure 4.4 Percentage of a. average annual precipitation and b. average annual streamflow occurring each month, over entire period of record.

percentage is also variable throughout the year. Both precipitation and discharge monthly averages reach a peak during the summer months (July to September), averaging between 45 and 50 percent of the average annual rainfall but between 60 and 80 percent of the average annual discharge. This discrepancy indicates the different mechanisms controlling runoff that operate during each season. Thus, while a similar percentage of precipitation falls during the winter months (October to March), below 20 percent of the average annual discharge flows during the same period along the San Simon and Rio Puerco. However, the Santa Cruz River has a distinct winter peak not observed in the other two systems. This may be due to the rain-shadow effect and physiographic differences mentioned previously. A further inconsistency to note is the spring runoff in the Rio Puerco basin, due to the combined effect of precipitation and snowmelt, which is lacking in the Arizonan basins due to their lower latitude and altitude.

Figure 4.5 shows the average daily flow for the entire period of record at the gauges most significant to this study. This illustrates the seasonality of flow along each river far better than the monthly totals shown in Figure 4.4b. Thus, for analysis purposes, the Rio Puerco and Santa Cruz River were split into four distinct seasons, which showed significant statistical differences. Divisions for the Santa Cruz River were partially derived from those noted in Parker (1996). The San Simon River, however, does not display a significant spring period, and was, therefore, split into just three seasons.

Another defining characteristic of arroyos in the southwest is the flashiness of their flow, especially during the summer months. As Figure 4.6 shows, daily average discharge data is a poor representation of the flow events which actually occur. When attempts were made to quantify this flow variability, by examining the flashiness index, FI, of flows during different seasons, it was discovered that the summer months had the lowest FI. However, given the known hydrologic character of these flows, this is obviously incorrect. The FI is defined as the ratio between instantaneous peak discharge and associated mean daily discharge (Hey, 1998). If a

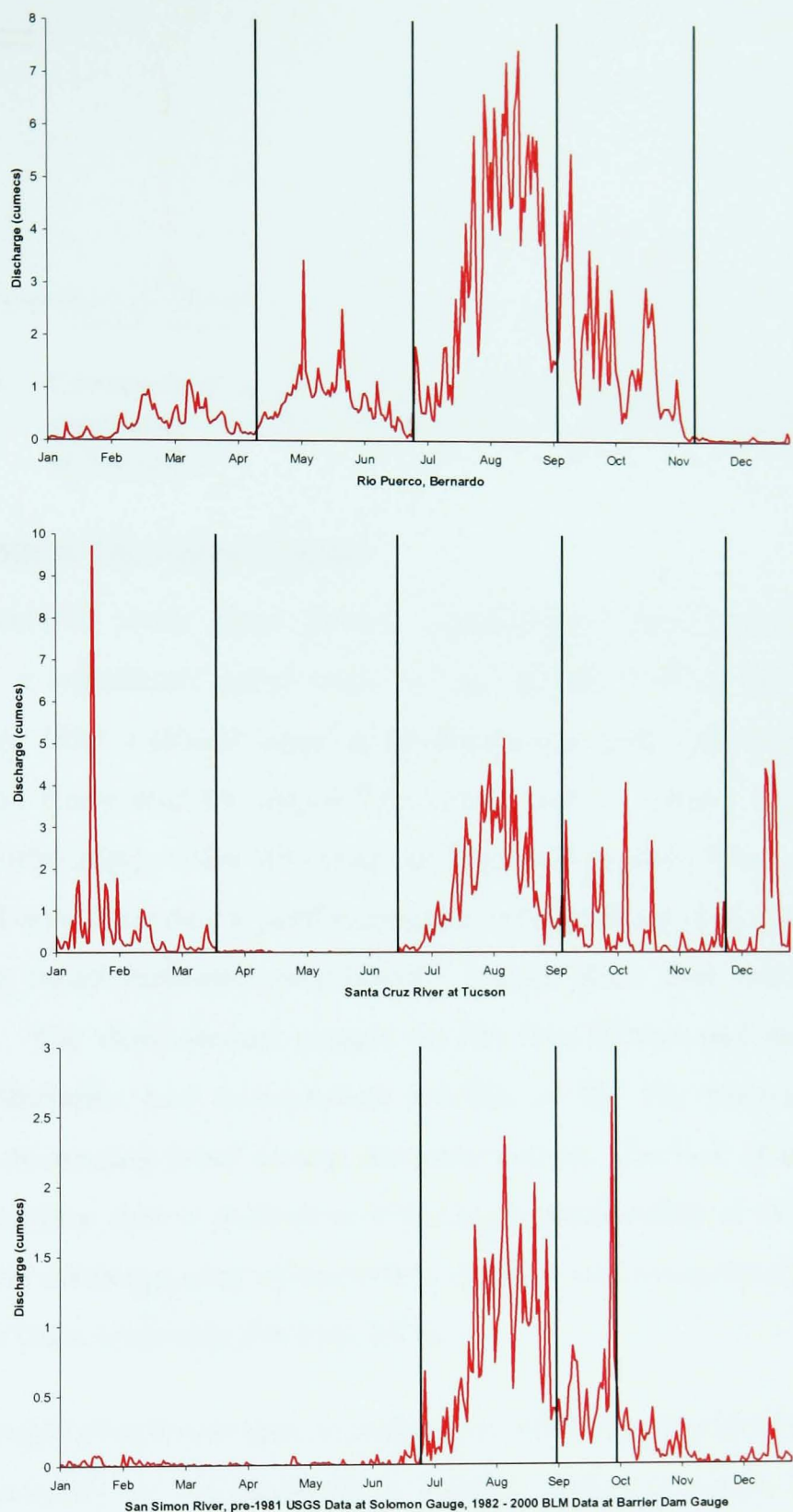


Figure 4.5 Average daily flow over entire period of record.

comparison is made between the daily average data and 15 minute discharge data, the reason for this inaccuracy is immediately obvious, since more than one flow event can occur during a single day (Figure 4.6). Therefore, the FI, when calculated with daily average discharges, is a misrepresentative statistic in ephemeral, flashy rivers.

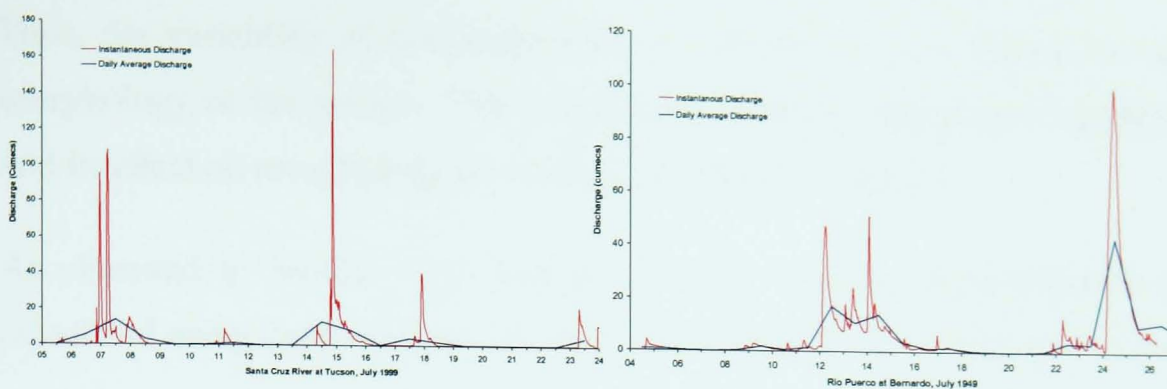


Figure 4.6 Comparison of daily average and 15 minute instantaneous discharge data, Rio Puerco at Bernardo and Santa Cruz River at Tucson.

4.2.2 Annual Discharge Trends

Annual runoff totals have varied considerably since records began. Although a significant rising trend in the annual precipitation has been noted since 1950, a similar trend in discharge was only observed along the Santa Cruz River and the upper Rio Puerco, above Arroyo Chico (Figure 4.7). Unfortunately, since the gauge at Tucson was abandoned during the 1980s and only recorded a partial duration series for some of the 1990s, the increasing trend indicated is probably smaller than that which actually occurred. The downstream gauges on the San Simon and those on the largest tributaries and downstream reaches of the Rio Puerco show an opposite, decreasing trend during the same period. The lack of any trend in the Rio San Jose data is indicative of the high permeability of the basin and the fact that discharges are influenced by springs and reservoir releases from Bluewater Dam upstream (Molnár, 2001).

It was thought that the decline in summer rainfall over the Rio Puerco basin was responsible for the decrease in annual discharge totals, due to the disproportionately high percentage of runoff occurring during these months (Molnár, 2001). However, the same change in seasonality was noted along the Santa Cruz River, with the opposite effect (Parker, 1996). It was observed that after 1960, the frequency of winter frontal storms and autumn tropical storms increased over the Santa Cruz River basin at the same time as annual totals increased. It is, therefore, doubtful whether the annual total discharge is related to either the annual or seasonal precipitation values.

Thus, the variability of discharge must be, at least in part, related to the morphology of the arroyo. The relationship between discharge variability and its effect on morphology is examined further in Chapter 5.

As observed in Section 4.2.1, values of the FI were misrepresentative if calculated using daily average discharge data. Thus, in order to discover the

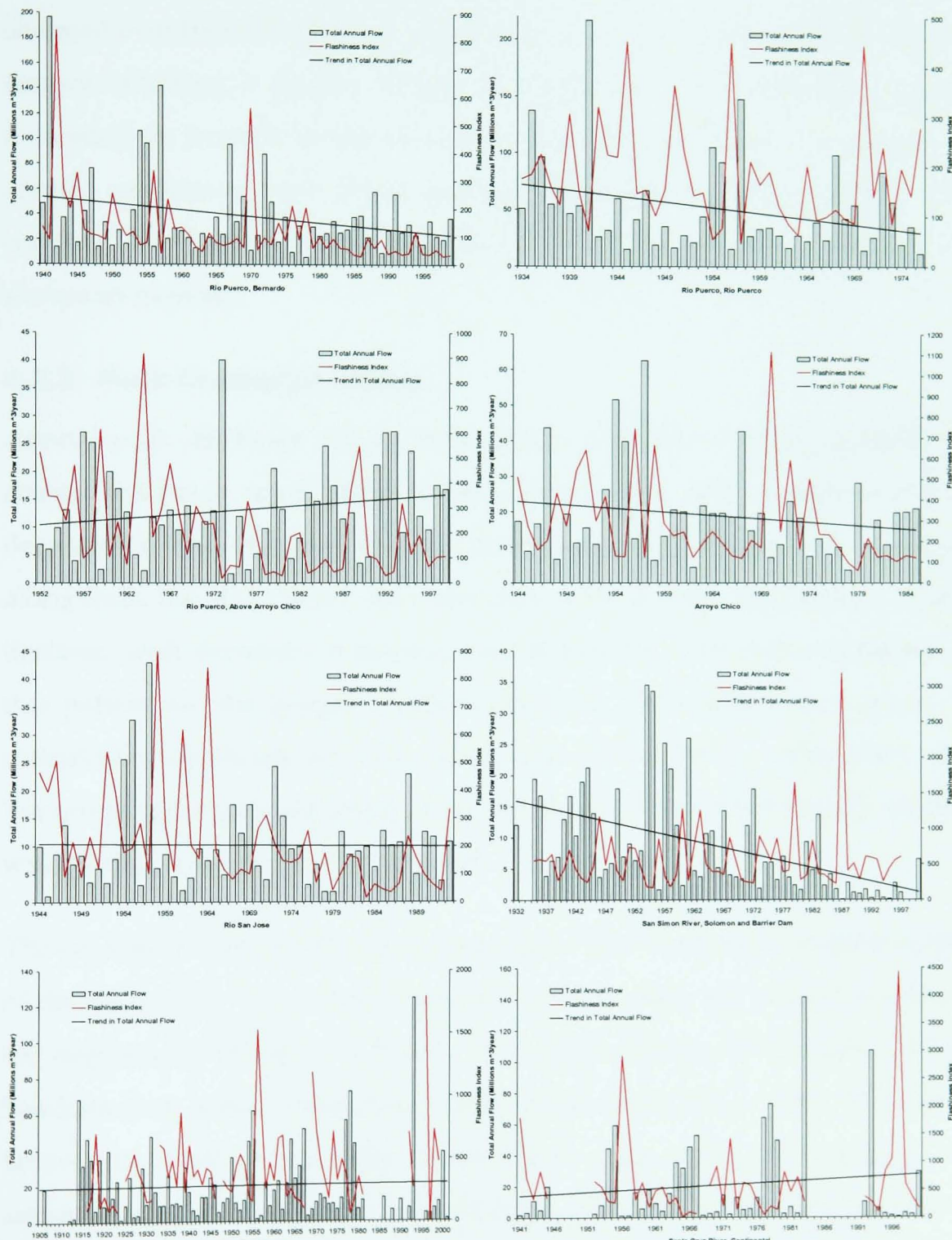


Figure 4.7 Total annual flow and annual flashiness index at all gauges along the Rio Puerco, Santa Cruz and San Simon Rivers for available period of record. Calculated from daily average discharge records. Note that scales and time periods are not the same at all gauges.

relative flashiness of the discharge regime along each of the three arroyos studied, the annual FI was calculated, using the ratio of the annual peak discharge and mean annual flow (Figure 4.7). As expected, the FI for all three arroyos was high, with peak discharges being well over an order of magnitude larger than the mean annual flow. The arroyos in Arizona were found to have far more flashy regimes than Rio Puerco. However, the FI has changed over time, in response to the changing flow regime. The Rio Puerco gauges exhibited a decline in the FI, especially at the Bernardo gauge, indicating an increase in the lower-magnitude flows and an attenuation of annual maximum peak flows (discussed further in Section 4.2.3). In contrast, the FI of the arroyos studied in Arizona has remained constant or shown an increase.

4.2.3 Peak Discharge Trends

Annual peak discharge values have shown a similar declining pattern to annual discharge totals (Figure 4.8). Since 1960, peak discharges have decreased by over 60 percent at the Bernardo gauge, although other gauges along both the Rio Puerco and San Simon River have experienced lesser declines, with decreases averaging over 40 percent. The only exceptions to this pattern are the gauges on the Santa Cruz River which have shown a statistically significant increase (Reich and Davis, 1987). After 1960, the Tucson gauge registered seven of the ten largest floods since records began, with peaks increasing over 30 percent.

The increase in both peak and average flows illustrates the non-stationarity of the Santa Cruz River flood frequency record, which has created problems for engineers wishing to calculate an accurate design flood (Baker, 1984; Saarinen *et al.* 1984; Hirschboek, 1985; Reich and Davies, 1987; Webb and Betancourt, 1992). Generally, when flood frequency is calculated, it is assumed that all floods are derived from the same statistical population (Webb and Betancourt, 1992). However, the change in the flood series after 1960 indicates that this is not the case for the Santa Cruz River, raising questions over the validity of applying statistical flood-frequency analysis to



Figure 4.8 Peak annual flows at all gauges along Rio Puerco, Santa Cruz River and San Simon River for available period of record. Note that scales and time periods are not the same at all gauges.

discharge data. Webb and Betancourt (1992) summarised the flood-frequency analysis of several researchers, showing the huge variability in estimates of the 100-year flood, which were calculated at between 575 and 2,780 cumecs. Taking the non-stationarity of the discharge record into

consideration, the 100-year flood was revised to 1,400 cumecs (Reich and Davies, 1987) and 1,660 cumecs (Webb and Betancourt, 1992).

Both increasing and decreasing discharge trends have been attributed to changes in large-scale atmospheric circulation (Saarinen *et al.*, 1984; Slezak-Pearthree and Baker, 1987; Roeske *et al.*, 1989; Graf *et al.*, 1991; Webb and Betancourt, 1992; Parker, 1992, 1996; House and Hirschboek, 1995; Molnár, 2001). There has been a distinct shift in the annual timing of flood peaks, which correlates with the shift in annual timing of ENSO events. Prior to 1960, ENSO conditions generally began in the early part of the year, whereas after 1960, ENSO conditions typically began mid-year, persisting into the early part of the next year (Webb and Betancourt, 1992). The flood peaks along the rivers studied have, therefore, changed from mainly summer monsoonal storm runoff prior to 1960, to mainly frontal or tropical cyclone-generated events after 1960 (Parker, 1996). The higher magnitude of the autumn- and winter-generated floods thus accounts for the increase in peak flows along the Santa Cruz River. However, given that flows along the San Simon and Rio Puerco have decreased under the influence of the same atmospheric conditions, it must be concluded that morphological differences play a dominant role in controlling the magnitude of peak flows. This is discussed further in Chapters 5 and 6.

Although the annual total and peak discharges have declined along the Rio Puerco, these flows are actually occurring over longer periods of time (Figure 4.9). The percentage of the year when flows are occurring has declined noticeably at all mainstem and tributary gauges. Given that the actual volume of flow has decreased over this time, this indicates that attenuation of flows is increasing. Molnár (2001) noted that the increase in annual flow duration had occurred due to increases in the volume of small to medium magnitude events, with large magnitude events actually declining in volume. It was also observed that the frequency of flows of all magnitudes had increased. Conversely, the duration of flows in the

Arizonan arroyos has remained very constant, averaging approximately 318 dry days per year, when averaged over the period of record (Figure 4.9).

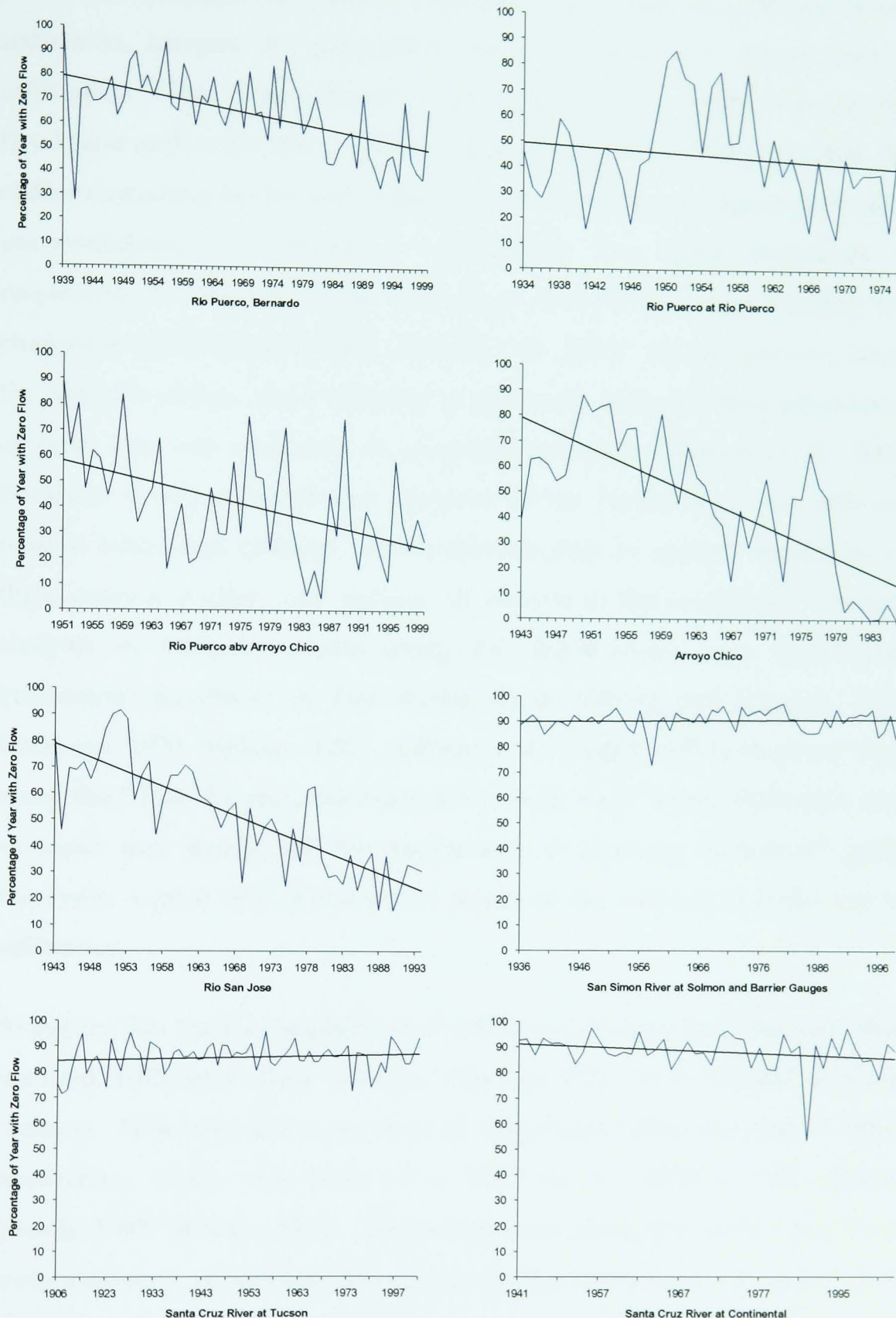


Figure 4.9 Time series showing percentage of year with zero flows for available gauges on Rio Puerco, San Simon River and Santa Cruz River Rivers. Calculated from daily average discharge records. Note that scales and time periods are not the same at all gauges.

4.2.4 Effects of Infiltration

Infiltration Rates

While the majority of alluvial channels lose water to bed and bank sediments, arroyos are particularly prone to large flow losses due to infiltration. This is as a result of low regional water tables beneath the floodplain and valley floor. These losses are high due to the fact that the sediment making up the bed of the trench is, in the main, highly permeable unconsolidated fine alluvium. Infiltration into these sediments is responsible for the loss of the vast proportion of the water entering the channel as runoff (Molnár 2000, Thomas *et al.*, 2000). For comparison, along the Santa Fe arroyo, also a tributary of the Rio Grande, less than ten percent of flow loss was attributed to evapo-transpiration (Thomas *et al.*, 2000. Burkham (1970) observed that channels in the Tucson basin are efficient natural infiltration galleries. This statement may be applied equally to all three arroyos studied and, indeed, all arroyos in the southwest. Various analysis of infiltration rates along the study rivers have noted that infiltration can absorb all flow during floods (Olberg and Schanck, 1913; Burkham, 1970; Molnár, 2001). Olberg and Schanck (1913) observed that, along the Rillito Creek, a tributary of the Santa Cruz River, infiltration was so rapid that floods had the appearance of "running backward" (p18). However, a great deal of variability occurs in the amount of water lost to infiltration.

Along the Rio Puerco, Stephens *et al.* (1988, in Constanz and Thomas, 1996) reported infiltration rates between 0.06 and 0.23 cm hr^{-1} (0.002 to 0.006 cumecs). However, this is an order of magnitude below the rates of other researchers, which vary from 1.8 to 137.5 cm hr^{-1} (0.05 to 3.82 cumecs) (Heath, 1983; Molnár, 2001). Infiltration rates along the Santa Cruz River were measured at between 1.75 cm hr^{-1} (0.05 cumecs) and 8.5 cm hr^{-1} (0.24 cumecs), although the lower value was measured during an anomalously long flow event of 1984/5 (Katz, 1987). The duration of the flow event is important in determining the amount of infiltration. This is due to the fact that, as flooding persists, the bed sediments become progressively more

saturated, thus reducing the infiltration rates. Katz' results indicate that the Santa Cruz River has a lower capacity for infiltration than the Rio Puerco. Unfortunately, no measured infiltration rates could be discovered for the San Simon.

It has been discovered that higher temperatures are conducive to higher rates of infiltration (Constanz *et al.*, 1994; Constanz and Thomas, 1996). Thus, infiltration rates during monsoonal floods are exacerbated by high summer temperatures. Along the Rio Puerco, between the Rio Puerco and Bernardo gauges, Heath (1983) recorded infiltration losses of 0.15 cumecs during the winter and spring, but this value doubled to 0.3 cumecs during the summer months. Thus, flows below these magnitudes were, on average, likely to be entirely lost. A small percentage of the seasonal difference was attributed to the rise in evapo-transpiration during summer months.

Infiltration During Flow Events

Infiltration rates indicate the rapidity with which water is lost to the bed and banks. However, since arroyos are event-driven, it is perhaps more important to determine the longitudinal flow connectivity within the arroyo system. Figures 4.10a and b show essentially the same data: the difference in flow volumes between consecutive gauges plotted in two different fashions; on the Rio Puerco, between the upper three gauges and Rio Puerco, and between Rio Puerco and Bernardo; and on the Santa Cruz River, between Continental and Tucson. When the data is plotted as a simple scatter graph of flow reaching the lower gauge versus the flow leaving the upper gauge (Figure 4.10a), there appears to be no relationship between the magnitude of flow and the amount of water lost to infiltration. However, if the flood volumes at the lower gauges are plotted as a percentage of the flow at the upper gauges (Figure 4.10b), a pattern becomes apparent. Above a runoff volume of approximately 1.5 million cubic metres, the variability of flow lost to infiltration decreases. This equates to a peak discharge of approximately 42 cumecs and an average discharge of 3.1 cumecs. Floods above this magnitude, are far more likely to remain constant or gain water

slightly as they pass through the system. Below this magnitude, infiltration losses are extremely variable, although care should be taken when using percentage differences, as a greater weight is placed upon the smaller values. Unfortunately, since 15-minute instantaneous discharge data was not available for all gauges it was not possible to examine infiltration using this more accurate data. This would undoubtedly give a far clearer indication of the true flow connectivity between gauges.

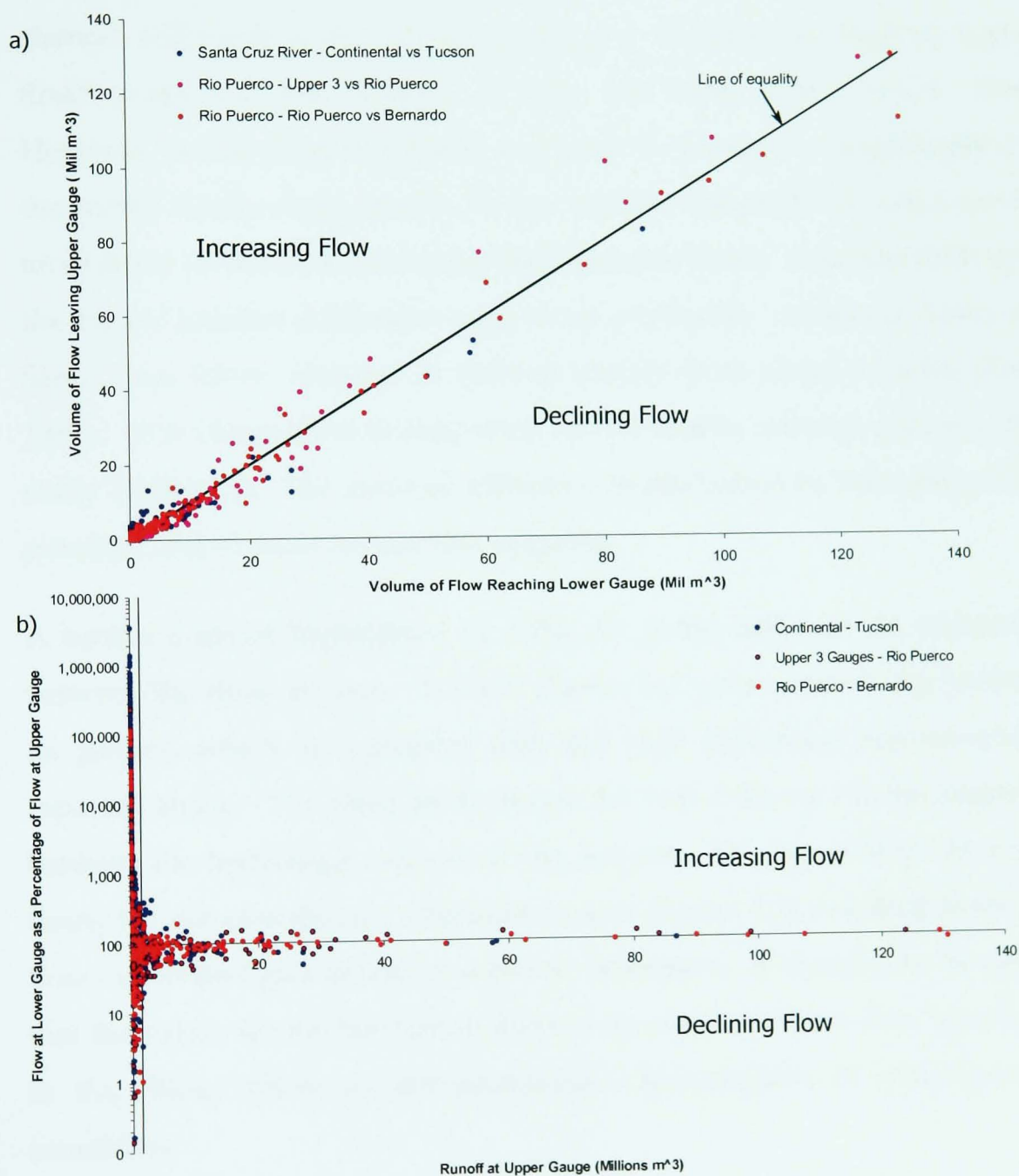


Figure 4.10 a) Difference in flow volumes between gauges along the Rio Puerco and Santa Cruz River. b) Volume of flow at lower gauge expressed as a percentage of volume of flow at upper gauge. Where flow has commenced below upper gauge, actual volume has been used.

The greatest amount of infiltration relative to the discharge magnitude is generally found during the smallest volume flows, with only the largest flows, with a recurrence interval of more than a few years, activating the entire system (Schick, 1974). Thus, the different magnitude and hydrograph shape of flows results in variable longitudinal flow connectivity. Flashy monsoonal floods, which tend to be of small magnitude, are theoretically subject to the most infiltration (Katz, 1987; Parker, 1996). The larger volume and longer duration of floods caused by tropical and frontal storms allows channel sediments to become saturated, thus resulting in relatively higher flood peaks and less volume of flow lost (Katz, 1987; Parker, 1996). However, as discussed previously and as Table 4.1 shows, surprisingly it is the winter floods along the Rio Puerco and San Simon River which are far more likely to be lost to infiltration than summer flows. This is at odds with the higher summer infiltration rates noted previously. However, along the Santa Cruz River, recharge is derived mainly from summer flows (Katz, 1987). This observation is supported by the results calculated during this study (Table 4.1). The seasonal difference in infiltration is, therefore, rather puzzling and requires further investigation.

A further contrast highlighted by Table 4.1 is the difference in infiltration between the three arroyos. The Rio Puerco has poor connectivity between its gauges, which is consistent with the high infiltration measurements reported above. The most likely reason for this difference is the disparity between the hydrologic regimes of the arroyos. The Rio Puerco has a less flashy regime than the two Arizonan arroyos (Figure 4.7), resulting in longer flow events and greater loss of water to infiltration. It should also be noted that the values for the San Simon River were calculated from data measured in the 1950s, which are not necessarily representative of contemporary conditions.

Season	Number of Flows	Percentage of Flows Showing Loss
Rio Puerco		
Between Upper Three Gauges and Rio Puerco Gauge, 1951 - 1986		
Winter	99	84.8
Spring	56	83.9
Summer	52	63.5
Autumn	48	64.6
All Data	255	76.5
Between Rio Puerco and Bernardo Gauges, 1939 - 1976		
Winter	163	95.1
Spring	71	71.8
Summer	101	62.4
Autumn	79	75.9
All Data	414	79.5
Between Upper Three Gauges and Bernardo Gauge, 1951 - 1976		
Winter	102	97.1
Spring	67	85.1
Summer	66	69.7
Autumn	60	75.0
All Data	295	83.7
Santa Cruz River		
Between Continental and Tucson Gauges, 1940 - 2001		
Winter	164	17.7
Spring	73	11.0
Summer	331	39.0
Autumn	162	35.2
All Data	730	25.7
San Simon River		
Between San Simon and Solomon Gauges, 1931 - 1941		
Winter	49	30.6
Summer	52	21.1
Autumn	28	28.6
All Data	129	26.4
Between Fan Dam and Solomon Gauges, 1955 - 1959		
Winter	14	14.3
Summer	13	0.0
Autumn	5	40.0
All Data	32	12.5
Between Fan Dam and Tanque, 1957 - 1959		
Winter	5	40.0
Summer	6	10.0
Autumn	5	20.0
All Data	16	18.8
Between Tanque and Solomon Gauges, 1957 - 1959		
Winter	14	14.3
Summer	12	33.3
Autumn	8	37.5
All Data	34	26.5

Table 4.1 Variability in infiltration rates between gauges on the Rio Puerco, Santa Cruz River and San Simon River.

Infiltration Trends

The variability in infiltration over the available period of record was examined to determine whether a trend could be observed. The flow connectivity between the majority of gauges has remained remarkably consistent, when averaged over the period of record (Figure 4.11). The data for the Rio Puerco gauges only overlaps until 1976, so this may be a misleading picture of contemporary conditions. However, the same consistent trend was observed on the Santa Cruz River, despite the changing flow regime. It is likely, therefore, that the variables controlling infiltration along each of the arroyos studied have remained the same.

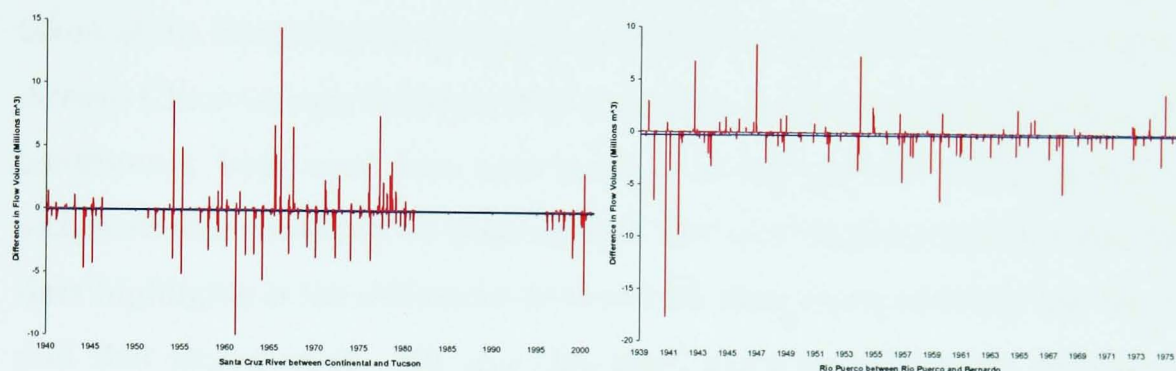


Figure 4.11 Time series showing consistency of infiltration.

4.3 SEDIMENT TRENDS

4.3.1 Nature of the Sediment Load

The sediment transported by a flow may be broken down according to its source and transport mechanism, which determines whether the sediment load is easily be measured using conventional suspended load samplers (Table 4.2) (Thorne *et al.*, 1998; Soar and Thorne, 2001). The bed material load is defined as the portion of the total load composed of grain sizes found

Sediment Source	Transport Mechanism	Measurement Method
Bed Material Load	Bed Load	Unmeasured Load
	Suspended Load	Measured Load
Wash Load		

Table 4.2 Classification of the total sediment load (after Thorne *et al.*, 1998; Soar, 2001).

in appreciable quantities in the bed of the channel. Sediment from the channel banks and the drainage basin finer than that found in the bed is termed wash load. The bed material load moves as bed load in gravel-bed rivers. The bed load is transported at or near the bed, through the processes of rolling, sliding or saltation (Thorne *et al.*, 1998). However, in sand-bed rivers, a significant portion of this load may be transported in suspension, whereby it is supported by anisotropic turbulence within the body of the flow (Thorne *et al.*, 1998).

4.3.2 Sediment Size

The particle size distribution was measured for suspended load samples taken at the Bernardo Gauge, between 1947 and 2000, and Rio Puerco above Arroyo Chico Gauge, between 1948 and 1996. Unfortunately this data is not continuous, both over time and method of calculation. Thus, trends in sediment size could not be determined. The most important factor that this data highlights is the difference between the data transported by the arroyo and that stored in it. Silt and clay-sized particles, which are defined as sediment finer than 0.062 mm (Roberts, 1990; Knighton, 1998), constituted approximately 80 percent of the sample by weight at Bernardo and approximately 85 percent above Arroyo Chico. Exact figures are not given due to the lack of data. Thus, suspended sediment sizes are frequently composed almost entirely of fines. However, during higher flows with higher sediment concentrations, more sand is transported. Bondurant (1951) noted that a flow with sediment concentrations of up to 680,000 ppm (parts per million) was composed of 75 percent sand (in Nordin, 1963a).

In contrast to this, the bed material stored in the arroyo is composed largely of sand. Elliott (1979) calculated an average D_{50} of 0.17 mm. Sediment larger than 2 mm is rarely found along the Rio Puerco. The downstream fining which occurs along many rivers is not observed along the Rio Puerco, with sediments sampled along the entire length showing clear homogeneity (Nordin, 1963a; Elliott, 1979; Heath, 1983; Molnár, 2001). The reason for the difference in transported and stored sediment size has been noted in

ephemeral channels in other regions and is thought to occur due to the difference in bed and suspended load sizes (Gerson, 1977; Frostick *et al.*, 1983). Since the suspended load is generally finer than the bed material load, the finer fraction is simply transported out of the system, whereas the coarser bed material load is deposited (Gerson, 1977; Frostick *et al.*, 1983; Leopold, 1992). It has also been suggested that fines may be removed from the channel by aeolian action (Lekach and Schick, 1982; Roberts, 1990).

Along the two Arizonan arroyos, far fewer sediment samples exist, especially along the San Simon River. Meyer (1989) calculated an average D_{50} of 0.4 mm along the active channel of the lower reaches of the San Simon River. The Santa Cruz River, although largely a sand-bed channel (Parker, 1986), contains a greater percentage of coarser sediments than the other two arroyos. Although some researchers, for example Roberts (1990), found that there was a distinct downstream coarsening of sediments, Parker (1996) notes that there is a great deal of downstream fluctuation in D_{50} . Meyer (1989) sampled sediments close to Martinez Hill, obtaining a D_{50} of 0.8 mm, although at Congress Street, Roberts (1990) calculated a much higher value of 4 mm. It is entirely likely that the grain size in any reach is highly dependent on the location and magnitude of the floods prior to sediment sampling.

Roberts (1990) measured the size of both suspended sediment samples and channel bed samples along the Santa Cruz River. The same disparity between suspended load and stored sediment sizes noted in the Rio Puerco was also found along the Santa Cruz River (Roberts, 1990). The bed load sampled during flood events had a maximum of 11 percent fines, the suspended sediment samples were on average 88 percent fines. It was discovered that both types of samples coarsened downstream. This is thought to be due to the fact that proportionally less water is lost to infiltration from the higher discharges in this arroyo, so that flows retain their transport competence further downstream. In this system, only high-

magnitude floods, which tend to extend for greater distances downstream, are capable of transporting the coarser sediment fractions.

Schumm (1960) developed a useful parameter which could be used to relate the sediment size within the bed and banks of the channel to the shape of that channel. It was discovered that, while there was no relationship between the D_{50} and the width:depth ratio, if a weighted percentage of silt and clay in the channel perimeter was used instead, a good relationship was obtained. This percentage, M, was calculated using the formula:

$$M = \frac{S_c \times W + S_b \times 2D}{W + 2D} \quad \text{.....Equation 4.1}$$

where S_c = Percentage of silt and clay in channel alluvium

S_b = Percentage of silt and clay in bank alluvium

W = Channel width

D = Channel depth

Schumm stated that channels with a higher percentage of silt and clay in the channel perimeter would be more likely to develop deep, narrow channels, when compared with those with a smaller percentage. It was calculated that the relationship between channel shape and sediment size could be expressed as:

$$F = 255 M^{-1.08} \quad \text{.....Equation 4.2}$$

where $F = \frac{W}{D}$

It was determined that aggrading channels were likely to have a higher width:depth ratio than indicated by M, whereas degrading channels had a lower width:depth ratio. Elliott (1979) calculated that the average value of M was 34.3 percent for the Rio Puerco. Meyer (1989) recorded an average value of M of 17.0 percent on the lower San Simon and 9.1 percent close to Martinez Hill on the Santa Cruz River. This gives a clear comparison of the relative channel composition of each arroyo. This is discussed further in Chapter 6.

4.3.3 Sediment Discharge

During flow events, arroyos carry sediment in very high concentrations, the Rio Puerco being the prime example of this. The highest recorded sediment concentration for the Rio Puerco was 680,000 ppm (1,156,000 Mg/l), reported by Bondurant in 1951 (Nordin, 1963a). The Rio Puerco is able to sustain such high concentrations of sediment for a number of reasons. Unconsolidated fine clay to coarse sand-sized sediment is abundant within the drainage basin, particularly within the arroyo itself. The sediment supply is, therefore, virtually unlimited and easily mobilised. Once some sediment is mobilised this has a positive feedback effect due to the fact that energy added by suspended sediment is approximately 130 times the energy required to support that sediment (Nordin, 1963a). Thus, the concentration can be increased indefinitely and “there is no upper limit to the concentration which may be found in natural streams transporting fine materials other than the static limit at which point the mixture turns into a mudflow” (Nordin, 1963a, p9). This theoretical maximum was calculated to be 800,000 ppm (Nordin, 1963a). As the concentration of fine sediment increases, the capacity for transport of sand is increased dramatically due to the increased viscosity of the flow. The percentage of sand transported in high-concentration flows is far higher than during low-concentration flows (Nordin, 1963a; Lekach and Schick, 1982).

Figure 4.12 shows the relationship between instantaneous discharge and sediment load at Bernardo and also at the Tucson gauge on the Santa Cruz River. It is immediately obvious that the Rio Puerco transports an appreciably higher sediment load than the Santa Cruz River, although the gradient of the regression curves are very similar. This is most likely due to the larger sediment sizes found along the Santa Cruz River, which inhibit entrainment.

The relationship between instantaneous discharge and sediment load along the Rio Puerco shows an interesting pattern in the upper values, exhibiting distinct hooks at approximately 150 and 3,000 million tonnes per day. Nash

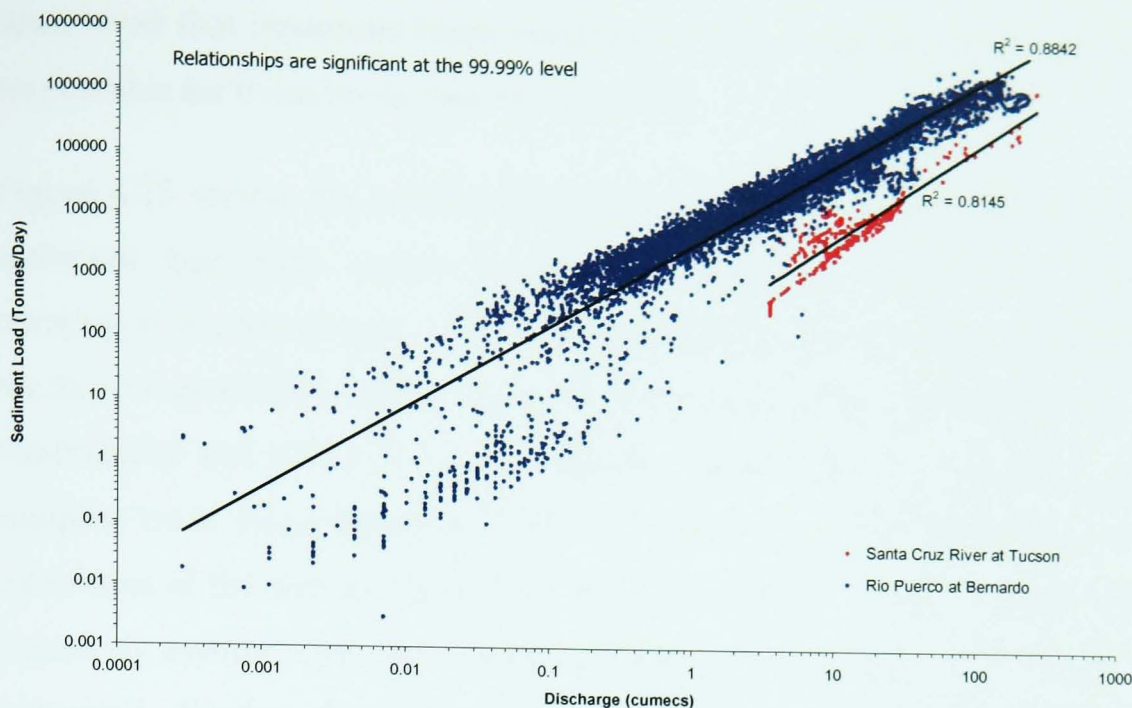


Figure 4.12 Relationship between instantaneous discharge and sediment loads, Rio Puerco at Bernardo Gauge and Santa Cruz River at Tucson Gauge.

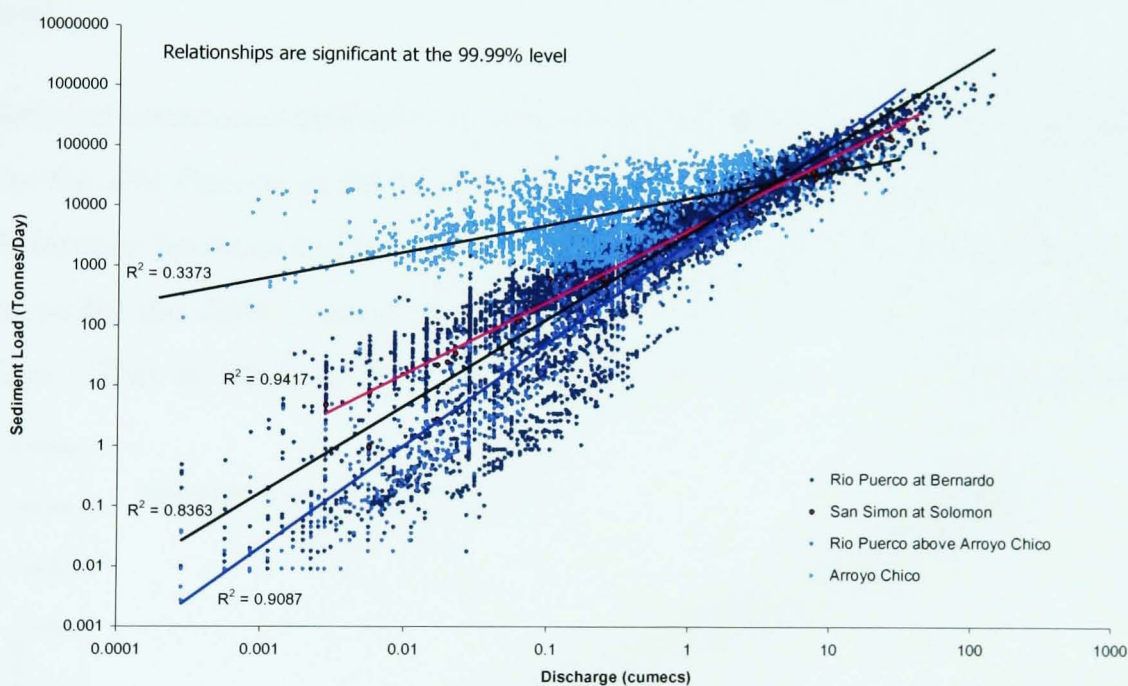


Figure 4.13 Relationship between daily average discharge and sediment loads, Rio Puerco at Bernardo and above Arroyo Chico Gauges, Arroyo Chico Gauge and San Simon at Solomon Gauge.

(1994) attributed this type of pattern to exhaustion of the sediment supply. However, given the almost infinite volumes of easily mobilised sediment available along the Rio Puerco, it must be concluded that different mechanisms are responsible for this pattern. Upon examination, it was

discovered that hysteresis loops occurring during single storm events were responsible for these hooks (see Section 4.3.4).

Figure 4.13 shows the relationship between daily average discharge and sediment load data, again showing an extremely good, and similar, correlation at most gauges. The only exception to this was the relationship for the Arroyo Chico, which shows a different discharge to sediment load relationship and also a poorer correlation between the two variables. The samples were taken between 1979 and 1986, at a time when the many tributaries of the Arroyo Chico were actively incising. Thus, it would seem logical to assume that the sediment supply to the gauge site would be unlimited. Further, the higher degree of bedrock control along the Arroyo Chico itself may cause limitations in the supply of sediment released by degradation, resulting in a much more variable and unpredictable sediment load.

Both instantaneous and daily average sediment discharge data was available for the Rio Puerco at Bernardo. As Figure 4.14 shows, there is very little difference between the two datasets, although the gradient of the regression curve for the daily average data is slightly steeper than for the instantaneous data. This is likely to be due to the smaller number of high-magnitude

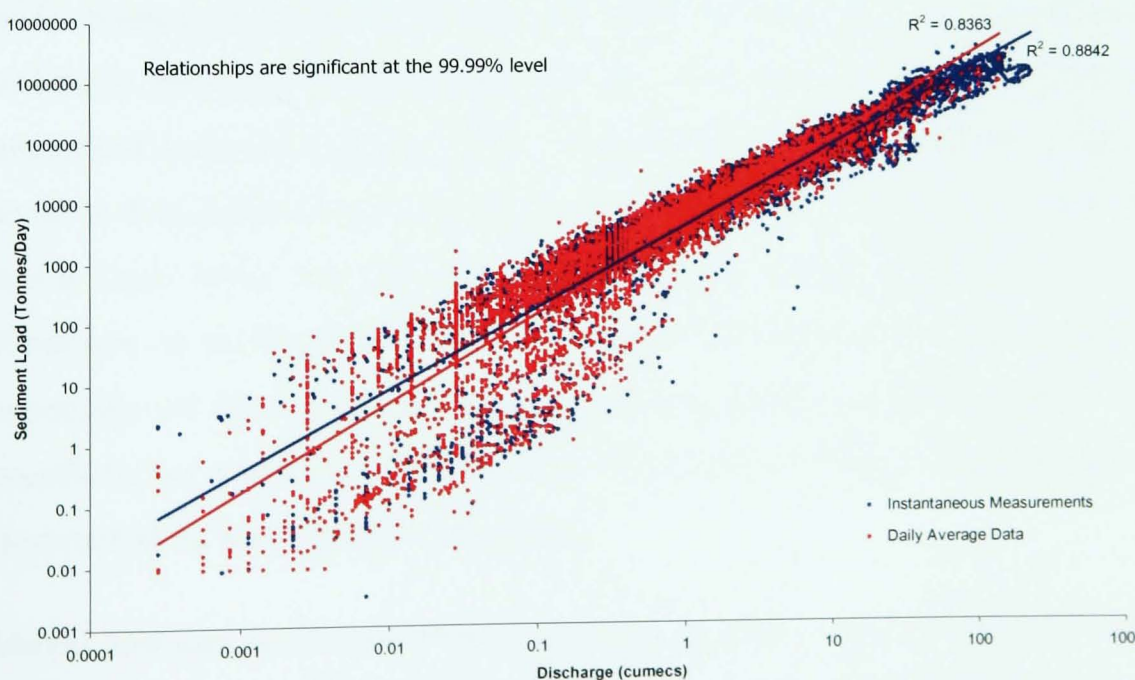


Figure 4.14 Comparison between instantaneous and daily average discharge and sediment load relationship, Rio Puerco at Bernardo.

points in the daily average dataset, which gives an increased weighting to the lower values, which have a large amount of scatter.

It should be noted that all discharge and sediment discharge relationships have been plotted using a double log scale and this tends to mask the considerable degree of variability: in fact, the sediment load for a given discharge at a gauge can vary by over an order of magnitude (Chorley *et al.*, 1984; Roberts, 1990; Nash, 1994). Sediment concentrations and, therefore, sediment loads are related to the discharge magnitude in a complex and non-linear manner. This is due to the fact that sediment transport rates depend on a number of factors, such as the antecedent conditions; hydrologic regime; flow conditions; spatial distribution of runoff; sediment supply and season (Chorley *et al.*, 1984; Knighton, 1998). Marked time-lags between the flow and sediment discharge peaks may also occur, giving rise to hysteresis. This is discussed further in Section 4.3.4.

The flow and sediment discharge relationship may vary due to the supply of sediment from the channel bed being limited by armouring or the presence of fine-grained drape deposits (Nordin, 1963a; Begin, *et al.*, 1980; Heath, 1983; Jobson and Carey, 1989; Roberts, 1990). Coarse sediment is deposited during the recession limb of floods competent enough to mobilize the entire bed. Subsequent smaller floods selectively winnow the finer fractions of sediment from the bed surface, leaving the coarse sediment to form an armoured layer (Knighton, 1998). Sediment supply from the bed due to scour is then limited in all but the largest floods. Of the arroyos studied, the Santa Cruz River was the only one in which armouring was observed. However, it is the point bars which tend to develop an armour layer, especially on the front face, rather than the channel bed (Ellis, 1993). This results in bar positions being fixed by the coarse sediments during periods dominated by lower-magnitude flows.

Drape deposits have been observed along all three arroyos, although they are most prevalent along the Rio Puerco and lower San Simon River. Along the Rio Puerco, it has been noted that the sand bed of the active channel can

be impregnated with silt and clay to depths of 0.3 metres (Nordin, 1963a; Heath, 1983). During flow events, especially during the recession limb, deposition of fines, combined with infiltration of flow carrying silt and clay particles into the matrix of the bed sediments, creates a virtually impermeable layer (Nordin, 1963a; Heath, 1983; Jobson and Carey, 1989). Transport of these fines beneath the channel bed while in suspension also occurs due to subsurface flow (Jobson and Carey, 1989). Drape deposits create an erosion-resistant cohesive layer which causes a reduction in both sediment transport and infiltration rates (Nordin, 1963a; Heath, 1983; Roberts, 1990). Nordin (1963a) observed an increase in sediment concentration of over 50 percent after the breaching of a clay drape layer along the Rio Puerco downstream of Bernardo. It was also noted that low concentrations were measured in flows which had originated in the upper part of the system, indicating that drape deposits along the entire 160 kilometre (100 mile) reach prevented mobilisation of the majority of channel bed sediment (Nordin, 1963a). During the rising limb of flow events, fines are rapidly mobilised, indicating that silt and clay armouring is a short-term phenomenon which affects the sediment discharge only temporarily (Molnár, 2001). Along the Santa Cruz River, the rapid mobilisation of fines was thought to be responsible for the disparity in bed material size observed by Roberts (1990), who noted that bed sediments measured during dry periods were finer than those observed during flow events.

As expected, given the flow regimes of the arroyos studied, a distinct seasonality occurs in the sediment discharge. At the Bernardo gauge on the Rio Puerco, the only gauge where sediment concentration measurements were recorded for a significant length of time, there is a distinct winter low, which is especially pronounced in December and January (Figure 4.15a). This is highlighted by the difference in discharge and sediment load relationship during the winter months (Figure 4.15b). When the percentage of the sediment load transported each month was calculated, this pattern is only slightly accentuated, with no significant difference between the discharge and sediment load, possibly due to the small percentage of flows

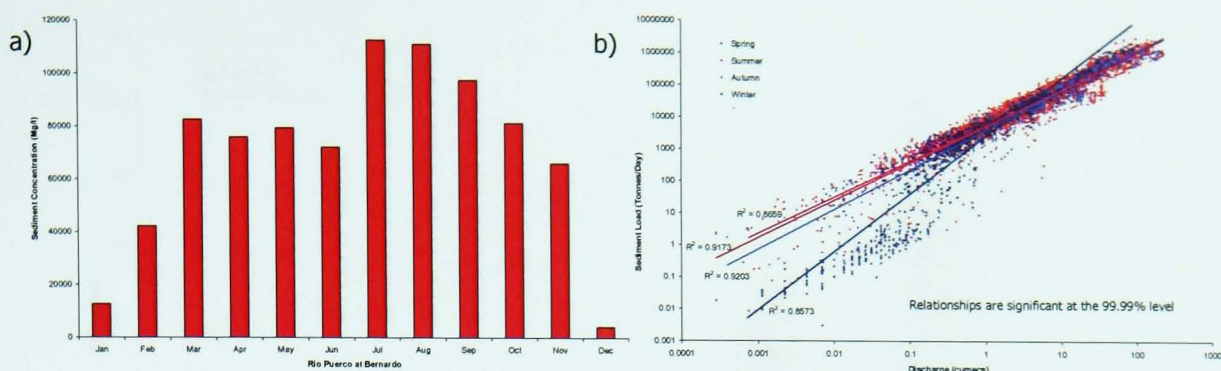


Figure 4.15 a) Variability in monthly sediment concentration and b) Seasonal variability in relationship between discharge and sediment load, from instantaneous measurements between 1948 and 2000, Rio Puerco at Bernardo.

which occur during the winter months (Figure 4.16). This pattern is different at the Arroyo Chico and Rio Puerco above Arroyo Chico Gauges, where there is a significant late winter to spring snowmelt runoff contribution, which is mirrored in the percentage of sediment load transported during these months. Sediment loads are also proportionally higher during the summer months, with flows between July and September accounting for 41 and 44 percent of discharge and 61 and 59 percent of the sediment load at the Arroyo Chico and Rio Puerco above Arroyo Chico gauges, respectively.

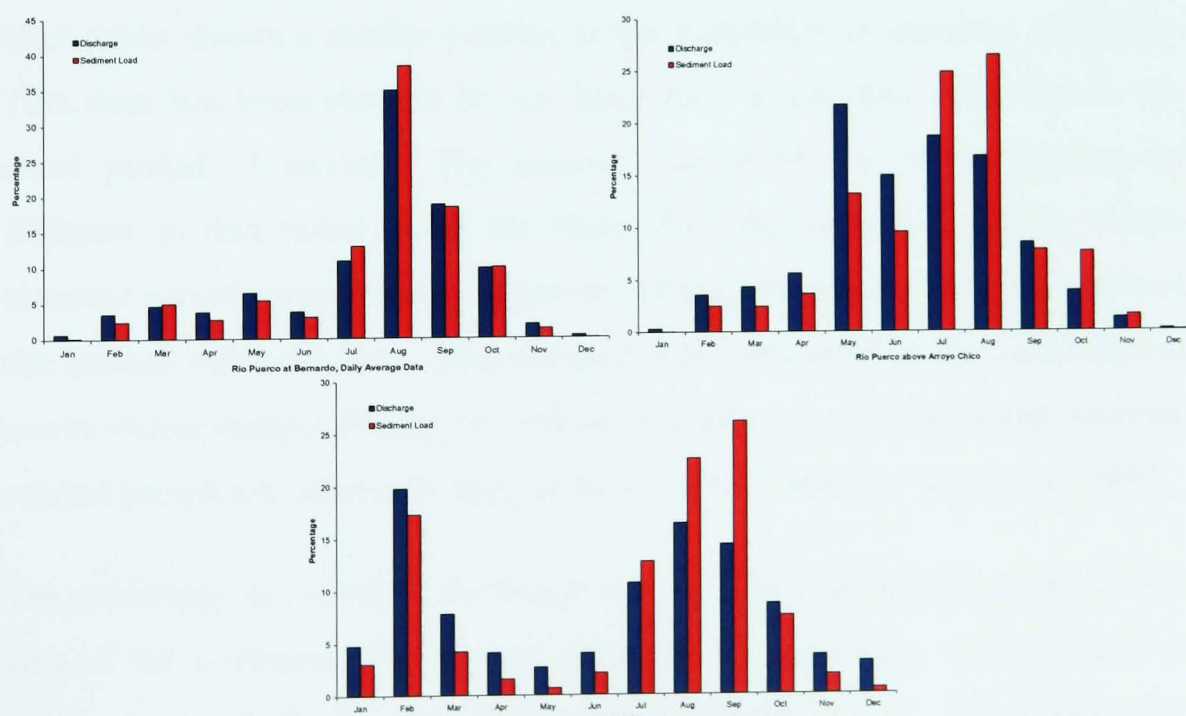


Figure 4.16 Average monthly discharge and sediment load over period of record, Rio Puerco at Bernardo (1955 – 2000), Arroyo Chico (1978 – 1986) and above Arroyo Chico (1994 – 1999).

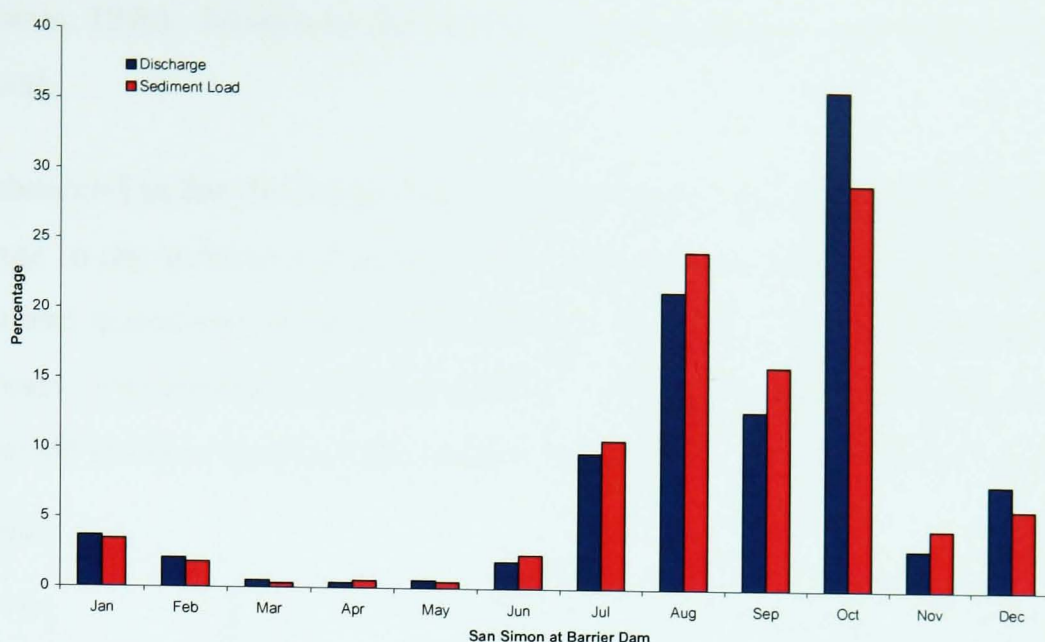


Figure 4.17 Average monthly discharge and sediment load between 1982 and 1995, San Simon River at BLM Gauge at Barrier Dam.

There is little data available for the Santa Cruz River. However, Parker (1996) found no significant difference between winter and summer sediment concentrations, although the sample size used was extremely small and probably not representative of average conditions. Similarly, samples taken along the San Simon River by the BLM since 1982 are limited and only monthly totals are available. However, as Figure 4.17 shows, the sediment load again shows a similar pattern to the variability in monthly discharge. This data has been skewed by the large flow in October 1983, due to the short period of record. The seasonal variability noted is significantly different to that noted along the Paria River by Graf *et al.* (1991), where summer runoff accounted for 48 percent of the annual flow but 91 percent of the annual sediment load. This anomaly was attributed to the variability in storm characteristics during the different seasons, with monsoonal summer storms producing extremely high sediment concentrations (Graf *et al.*, 1991).

The variability in sediment discharge may also be due, in part, to the source area of the sediment. Flows may originate far upstream, attenuating to a small magnitude by the time they reach the lower gauges. These flows are likely to have higher sediment loads than small flows generated locally

(Roberts, 1990). However, due to the lack of sediment data, this cannot be proved.

As observed in the discharge data, the Rio Puerco has displayed a significant change in the sediment discharge over time (Figure 4.18). At Bernardo, the sediment concentration has decreased noticeably, causing sediment loads to decrease exponentially (Figure 4.18.a). This decreasing trend has been observed in other rivers in the southwest (Gellis *et al.*, 1991; Graf *et al.*, 1991;

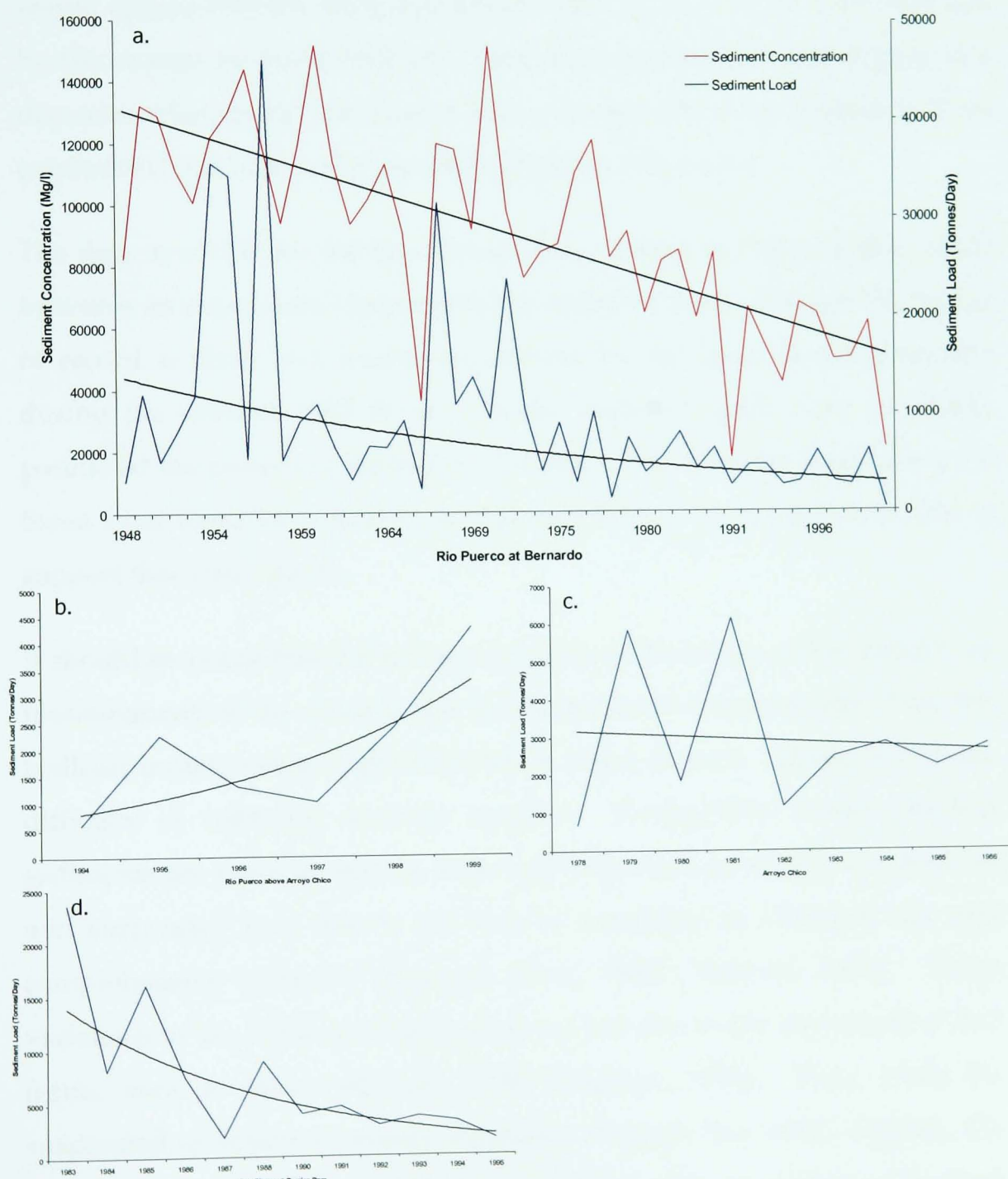


Figure 4.18 Trend in average annual sediment discharge (tonnes/day),
Rio Puerco at a. Bernardo, b. above Arroyo Chico, c.
Arroyo Chico and d. San Simon River at Barrier Dam.

Elliott *et al.*, 1999). As discussed in Chapter 2, the sediment load decreases once the maximum width has been attained. This occurs as a result of the increase in sediment storage within the arroyo as it aggrades (Gellis and Elliott, 2001). The effect of the changing morphology of the arroyo on the sediment discharge is examined further in Chapter 5.

At the Arroyo Chico and Rio Puerco above Arroyo Chico gauges, the length of record is not really long enough to show a clear pattern. However, it would appear that the discharge trends noted at these gauges are mirrored by the change in sediment load. Thus, the Arroyo Chico has displayed a decrease, whereas the Rio Puerco above Arroyo Chico has experienced an exponential rise in its sediment loads (Figure 4.18.b and c).

The data available for the San Simon River, shown in Figure 4.18.d, again indicates an exponential decrease in the sediment load, although the period of record is short and results are skewed by the large load transported during the October 1983 flood. As the sediment loads have so closely paralleled the pattern of discharge, it is likely that sediment loads along the Santa Cruz River have increased, although there is no independent data to support this assumption.

It should be noted that the sediment data described above relies entirely on measurements of the concentration of the sediment in suspension. Very few bedload measurements have been taken along arroyos, mainly due to the difficulty of collecting accurate samples. During flow events, the bed sediments are often in motion with very little distinction between bedload and suspended load due to the lack of variability in sediment size and comprehensive sediment dispersal (Graf, 1988b; Roberts, 1990). Large variations in the amount of bedload also occur due to the movement of bed forms, such as dunes (Roberts, 1990; Knighton, 1998). Thus, while the suspended sediment is evenly dispersed through the water column, the bedload is by no means uniformly distributed. The proportion of bedload was estimated to be, on average, 1.4 percent of the total load along the Santa Cruz River (Roberts, 1990). Similarly, it was estimated that only one percent

of the total load of the Rio Puerco is transported as bedload (Gorbach *et al.*, 1996). It has been shown that effective discharge calculations show no difference when either total load or suspended load are used (Thorne *et al.*, 1993; Biedenharn and Thorne, 1994; Nash, 1994; Hay, 1997; Soar and Thorne, 2001). Thus, for the purposes of this study, the available suspended load measurements were considered representative, when calculating the geomorphic effectiveness of the flows (Chapter 7).

4.3.4 Hysteresis

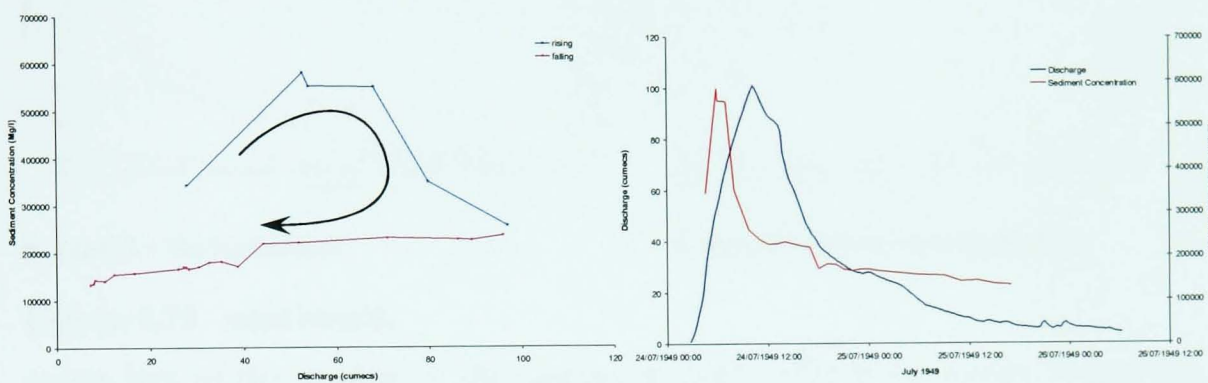
As mentioned above, stage and stage-change-related differences in the sediment concentration and load may be observed. Hysteresis so produced is responsible for a proportion of the scatter in the relationship between discharge and sediment load. Analysis of the instantaneous discharge and sediment discharge data was carried out to determine whether a consistent hysteresis pattern could be found. The data was split into different types, designated by Gellis (pers. comm., 2003). Type 1 signifies a clockwise hysteresis loop, where the sediment peak precedes the flow peak, thus giving higher concentrations on the rising limb than the falling limb (Figure 4.19.a). This is the most commonly observed hysteresis type and occurs due to a number of reasons. In most rivers, clockwise hysteresis occurs due to depletion of the sediment supply (Walling and Webb, 1982; Nash, 1994; Knighton, 1998). Dilution effects as the discharge rises may also have this effect (Walling and Webb, 1982).

Type 2, clockwise followed by anticlockwise hysteresis, occurs when the sediment peaks both before and after the flow peak, with a sediment minimum coinciding with the peak discharge (Figure 4.19.b). This may again occur due to dilution effects.

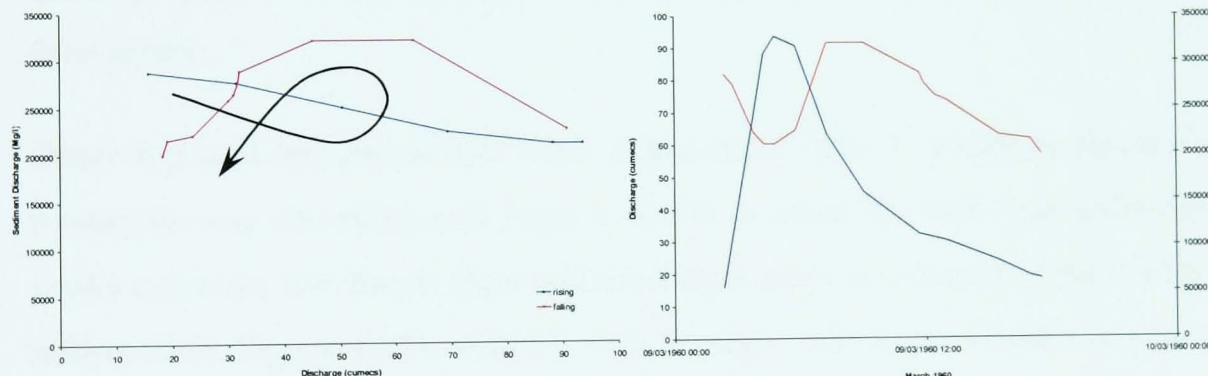
Type 3, anticlockwise hysteresis, is rarely found along perennial rivers. Of 30 rivers studied by Nash (1994), only 2 showed anticlockwise hysteresis, which occurs when the peak discharge appears prior to the sediment peak (Figure 4.18.c). This is due to the fact that the flood-wave moves up to 70 percent faster than the water carrying most of the sediment (Knighton,

1998). If flows originate far upstream above a gauge, the sediment peak may lag the discharge peak as the upstream sources continue to supply the bulk of the load (Knighton, 1998). Type 3 hysteresis may also occur as the sediment concentration remains high until the threshold for deposition occurs as flow velocities decrease during the falling limb (Thornes, 1980).

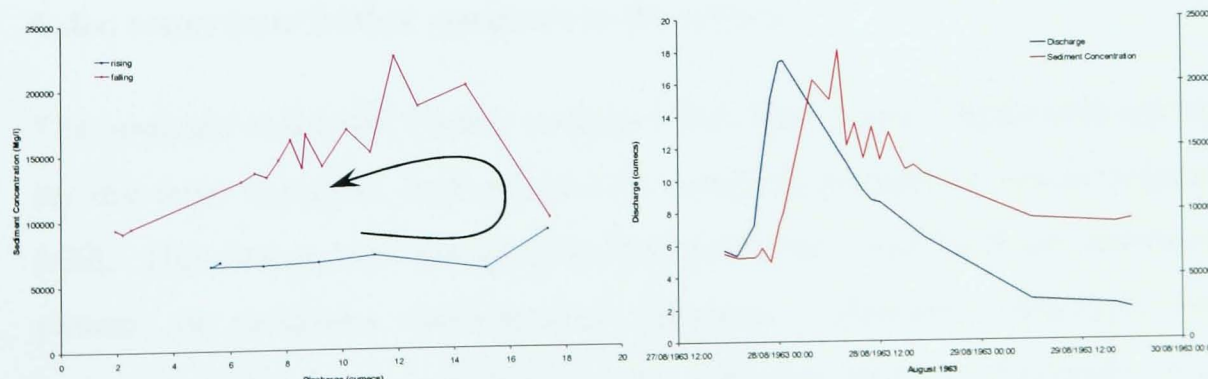
Type 4 hysteresis occurs when anticlockwise then clockwise hysteresis is observed (Figure 4.19.d). In this situation, the sediment concentration shows a similar pattern to Type 2 hysteresis over time, in relation to the flow discharge pattern. However, the significant difference between the two



a. Type 1 – Clockwise hysteresis

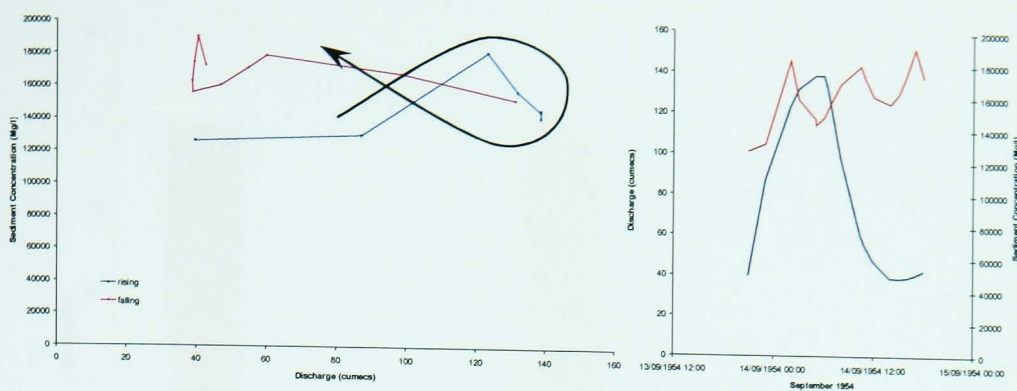
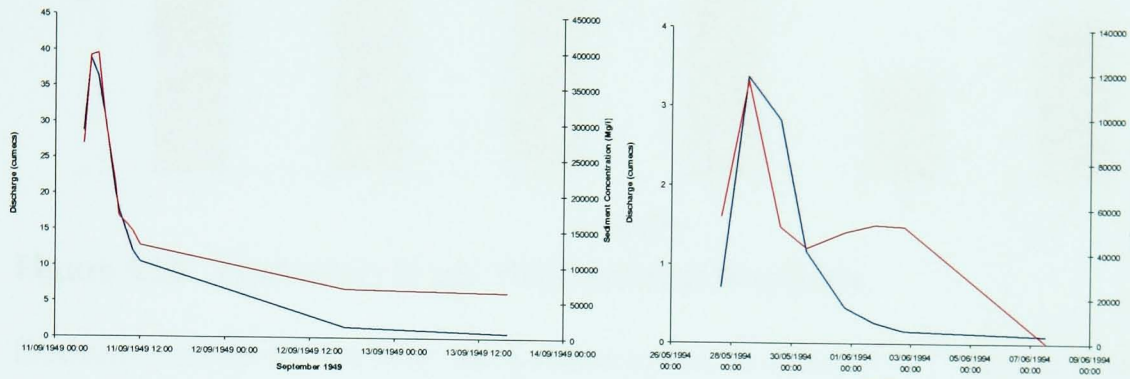


b. Type 2 – Clockwise then anticlockwise hysteresis



c. Type 3 – Anticlockwise hysteresis

Figure 4.19 Examples of different hysteresis types from instantaneous data at Bernardo, Rio Puerco (continued over).

**d. Type 4 – Anticlockwise then clockwise hysteresis****e. Type 5 – No hysteresis****f. Type 6 – Anomalous hysteresis****Figure 4.19 continued.**

types lies in the timing of the sediment peaks and is far easier to identify from the plot of discharge against sediment concentration, rather than the time series.

Other types of hysteresis that were noted were Type 5, which is when no hysteresis was observed, and Type 6, which is when the flow and sediment peaks coincide, but this is then followed by a second sediment peak on the falling limb (Figure 4.19 e. and f.). It is thought that Type 6 hysteresis may be caused by erosion of an armouring layer, or the late arrival of sediment-laden water from further upstream in the system.

The analysis of the Rio Puerco indicates that Type 1 and 3 hysteresis are by far the most common, each evident in nearly 30 percent of events (Figure 4.20). This researcher attempted to determine the controls of the observed pattern of sediment concentration changes. However, although the hysteresis types were compared to the different seasons; maximum and average flows; the antecedent conditions, including the number of dry days prior to the flow event and the size and length of the previous event; and the

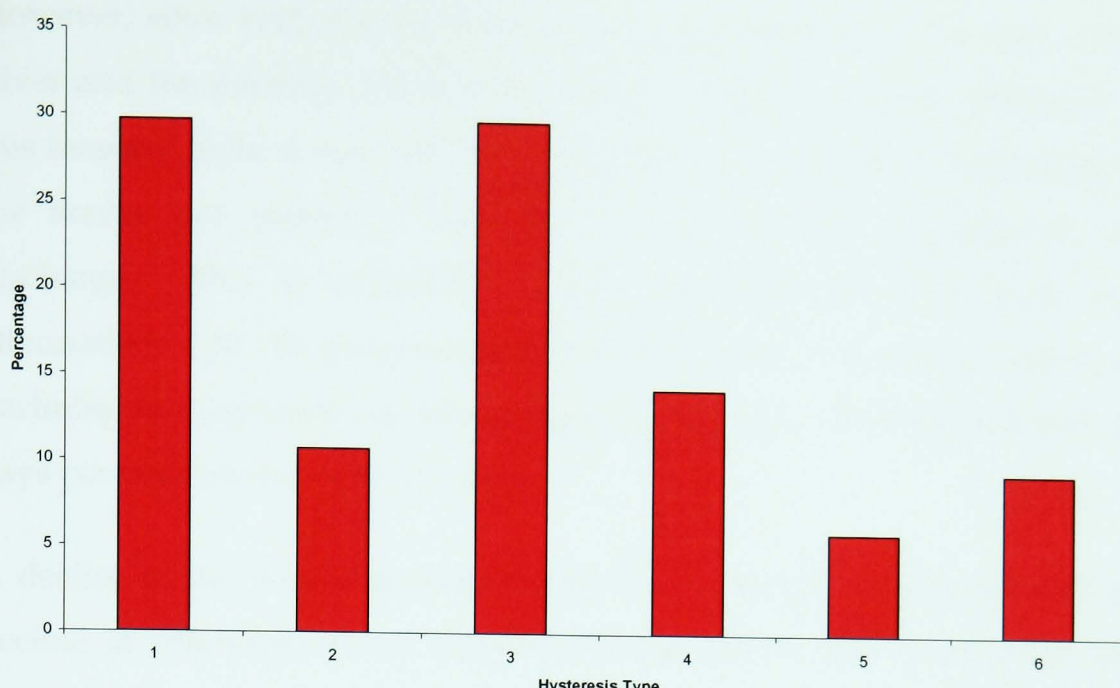


Figure 4.20 Hysteresis types, Rio Puerco at Bernardo.

flashiness index of the flow, no pattern could be discerned. Thus, it must be concluded that other factors, which are not easily discernable, such as the presence of armouring, must be responsible for the pattern of sediment concentration during flows. The unusually high percentage of Type 3 hysteresis along the Rio Puerco is thought to be due to the relatively unlimited supply of sediment.

4.4 COMPARISON OF FLOW VARIABILITY IN STUDY AREAS

Analysis of available data for the three arroyos studied has emphasised similarities and differences in the precipitation, flow and sediment regimes. The change in large-scale atmospheric circulation patterns, due to an increase in the frequency of ENSO conditions since 1960, has resulted in an increase in total annual precipitation over the entire south-western USA. Despite this, discharge totals and annual peak discharges over the same time period have only followed this rising trend in the Santa Cruz River. Gauges on the other two arroyos exhibited a marked fall in these variables, indicating a complex precipitation-runoff relationship. This is emphasized by the fact that the discharge did not begin to decline along the Rio Puerco until the mid-1970s, indicating that other controls are responsible. A proportion of this decline is attributed to the changing seasonality of storm events. Since 1960, the frequency of winter storm events has increased.

However, since both the increase in discharge observed in the Santa Cruz River and the decrease observed in the Rio Puerco have been attributed to this seasonal shift, it can only be assumed that the changing morphology of the arroyo has played a vital role in disassociating precipitation and discharge. This is supported by the concurrent trend in peak flow attenuation. At all gauges, except on the Santa Cruz River, flows are declining in magnitude but increasing their duration, resulting in fewer dry days per year and lower FI values.

A decline in the sediment concentration has occurred, concurrent with the decline in discharge at the Bernardo Gauge on the Rio Puerco, the only gauge where this data was available for a sufficiently long period of time that a trend could be established. Thus, the sediment load, which combines both the discharge and sediment concentration, has seen an exponential decline. Sediment load data for the Arroyo Chico and San Simon River also showed the same trend. However, at the Rio Puerco above Arroyo Chico gauge, an increase was observed, although the period of record was too short to establish whether this trend was significant.

A further characteristic of the flow regime in the arroyos studied is the downstream decrease in flow magnitude. This is in contrast to perennial rivers, which generally see an increase in discharge with distance downstream. It was observed that, if the volume of flow during an event exceeded 1.5 million cubic metres, the discharge was more likely to remain constant, or even increase in volume. However, below this volume, a good deal of variability was noted, emphasizing the poor flow connectivity due to the localised nature of flooding. Sediment is, therefore, transported and deposited sporadically, dependent on the location of flow within the system. This emphasizes the event-driven nature of geomorphological change within arroyo system.

CHAPTER 5

Evolution of Study Arroyos

5.1 GEOLOGICAL EVOLUTION OF STUDY AREAS

Rio Puerco

The Rio Puerco drains an area along the physiographic boundaries between the Colorado Plateau, the Nacimiento Mountains (Southern Rocky Mountains) and the Basin and Range province (Love, 1986). The shape of the basin reflects the lithology, tectonics and maturity of the development of the headwater areas (Figure 5.1) (Love, 1986). The early geologic history of the basin is not well known. Exposures of extremely resistant Precambrian igneous and metamorphic rocks may be found outcropping in the highland regions of the Puerco basin, in the Nacimiento and Zuni Mountains and the Sierra Ladrones (Bryan and Post, 1927; Elliott, 1979; Gorbach *et al.*, 1996). It is, however, estimated that exposures of Cretaceous sandstone, shale and mudstone account for over 40 percent of the basin area (Popp *et al.*, 1988). These sediments, when combined with similar outcrops deposited during other periods, make up over 80 percent of the exposed bedrock and are highly erodible. Thus, the drainage basin has an almost unlimited supply of sand, silt and smectite clays (Bryan and Post, 1927; Popp *et al.*, 1988; Gorbach *et al.*, 1996). Cenozoic outcrops dominate the geology of the upper and mid-Puerco basin (Gorbach *et al.* 1996).

The modern Rio Puerco and Rio San Jose drainages probably developed much later than the Cretaceous, as the Albuquerque structural basin began to subside during the Basin and Range disturbance of the late Oligocene, approximately 27 Ma (million years ago) (Love, 1986). At this time, the Rio Puerco basin was closed, with sediments from the highlands to the west and north collecting to form alluvial aprons around these margins, clay-rich playa deposits at the centre and common aeolian deposits (Bachman and Mehnert, 1978; Love and Young, 1983; Love, 1986). These thinly bedded sandstones, interbedded with volcanic flows and sills, are well over 6,000 metres deep and are known as the Santa Fe formation (Heath, 1983). It is

thought that initially a single large basin may have formed, which was later broken up into progressively smaller basins, which developed over pre-existing structures (Bachman and Mehnert, 1978). The later stages of this fragmentation, during the late Miocene, caused the creation of basins recognizable as those seen today and faulting and volcanism became common (Bachman and Mehnert, 1978).

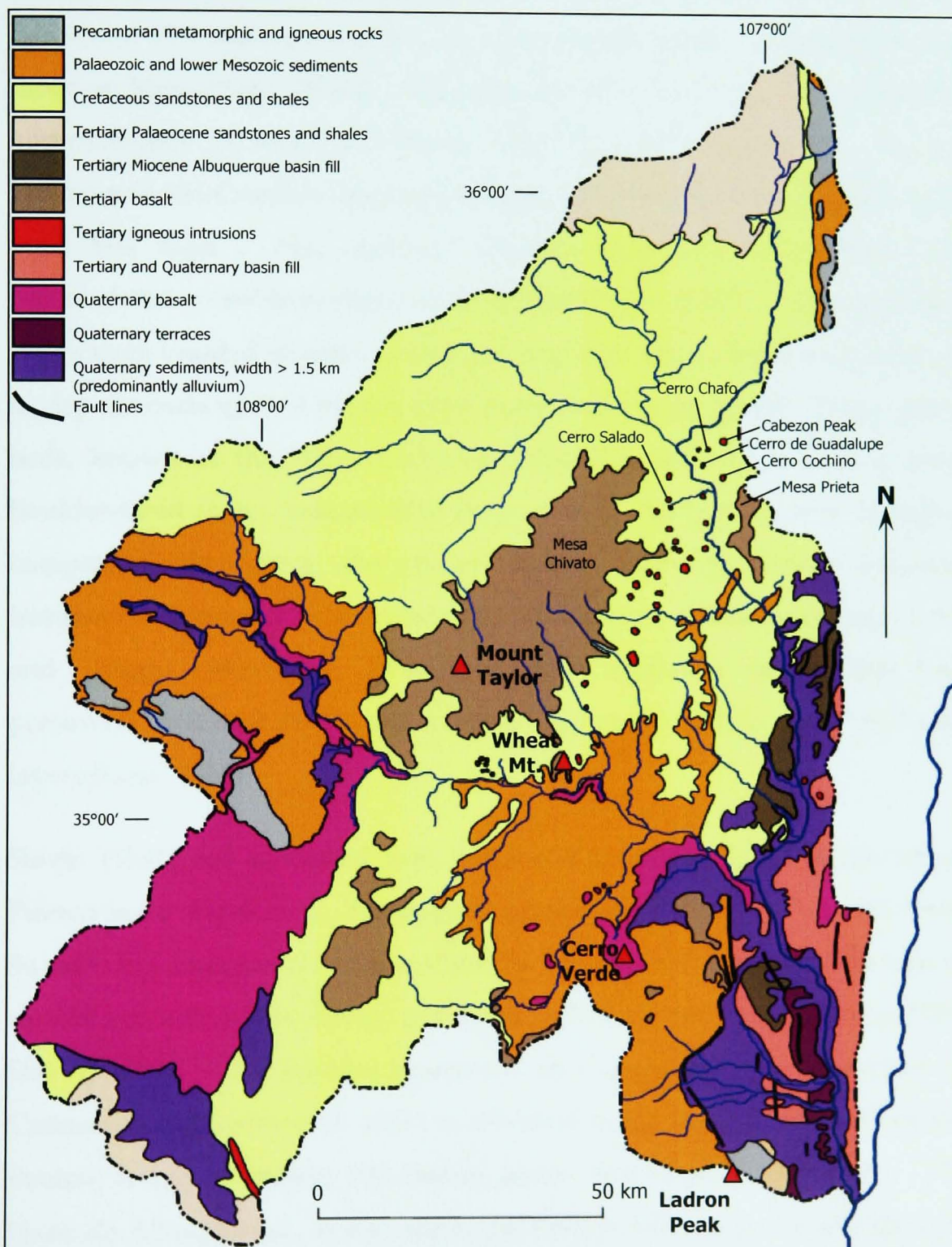


Figure 5.1 Generalised geology of Rio Puerco Basin (after Love, 1986; Gorbach, 1996).

The Basin and Range disturbance continued into the early Pliocene, approximately 5 Ma. During this period, the Albuquerque basin continued to subside and accumulate sediments (Love, 1986). After 5 Ma, the Rio Grande penetrated and traversed the lower third of the basin, where it was intersected by the Rio Puerco and its western tributaries, which flowed across wide, low-relief alluvial plains (Bachman and Mehnert, 1978; Love, 1986). Between 4.5 and 3 Ma, the Mount Taylor - Mesa Chivato volcanic field covered a major part of the upland area, with smaller eruptions such as those on Mesa Prieta, Wheat Mountain and Cerro Verde occurring between approximately 2.5 and 2 Ma (Bryan and Post, 1927; Love, 1986). The Rio Puerco and Rio Grande continued to aggrade within the Albuquerque basin until less than 1 Ma, burying volcanic plugs and soils which had accumulated on stable portions of the pediplain (Love, 1986). The aggrading rivers were braided in pattern, transporting sufficient quantities of sediment to deposit beds up to 4 metres thick (Love and Young, 1983). These gravel beds, known as the Sierra Ladrones formation and which include some boulder-sized clasts, indicate that flows during this period were of higher competence than along the present system, although overall sediment transport efficiency was reduced by inter-channel sediment storage (Love and Young, 1983; Love, 1986). Volcanic eruptions during this time preserved erosional levels by covering the surface with resistant basalt layers (Love, 1986).

Slavin (1991) has identified four preserved erosional levels in the upper Puerco basin (Figure 5.2). The uppermost surface, defined as S_1 , or the Ortiz Surface, has been dated at approximately 3 Ma and is defined by the tops of several volcanic necks (Bryan and Post, 1927; Bachman and Mehnert, 1978; Slavin, 1991). This surface represents an extensively graded surface of Cretaceous sediments and, when normalised to the level of the modern Rio Puerco, is approximately 530 metres above this base (Slavin, 1991). The Llano de Albuquerque, to the east of the Puerco basin, was initially thought to be a remnant of the this fill but is now thought to be much younger, at between 500,000 and 1 million years old (Bachman and Mehnert, 1978; Love

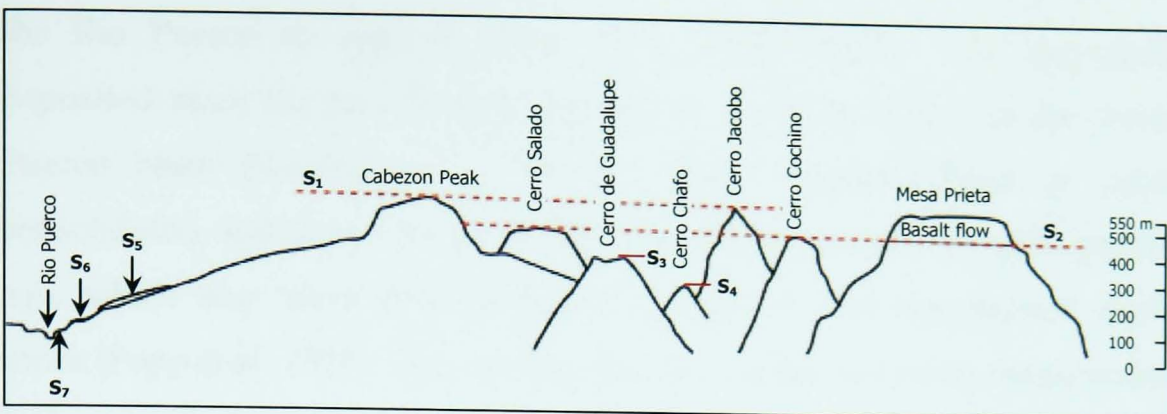


Figure 5.2 Schematic diagram showing erosional levels preserved by successive basalt flows in the Cabezon area of the Rio Puerco Basin (after Slavin, 1991). Figure 5.1 shows location of peaks.

and Young, 1983; Slavin, 1991). A second surface, S_2 , which is at least 2.2 Ma is defined by volcanic necks with an elevation of approximately 400 metres above the Rio Puerco base level (Slavin, 1991). Slavin (1991) has included the Mesa Prieta in this surface due to the fact that the basalt flow overlying the surface has been dated at 2.2 Ma. Other authors, however, have included Mesa Prieta in the Ortiz surface classification (Bryan and Post, 1927; Bachman and Mehnert, 1978). This surface represents a period of renewed downcutting and re-stabilisation (Slavin, 1991). The younger two surfaces, S_3 and S_4 , represent further periods of incision and stabilisation at elevations of approximately 300 and 200 metres above base level respectively (Slavin, 1991). No dates have been given for these surfaces, and it was not possible to correlate these with dated surfaces observed by other authors. All four surfaces have a similar gradient to the contemporary channel of the Rio Puerco indicating a lack of tectonic influence (Slavin, 1991)

After 1 Ma, the Rio Puerco system began incising episodically, duplicating similar fluctuations in the Rio Grande (Love, 1986). These periods of incision created terraces along both river valleys. The Rio Puerco developed its north-south orientation during this period, in part due to the development of faults (Love, 1986). It is thought that this faulting may be, in part, responsible for the initial incision, due to the fact that drainages were diverted southward into the Puerco system (Love and Young, 1983). Base level lowering due to incision of the Rio Grande is also likely to have caused

the Rio Puerco to degrade (Love and Young, 1983). The sediments deposited since the late Tertiary, 5 Ma, are generally found in the lower Puerco basin (Gorbach *et al.*, 1996). These unconsolidated or semi-consolidated sediments are generally reworked material of much greater age, which may have been previously deposited and re-entrained many times (Popp *et al.*, 1988). This sediment recycling also occurs at many scales, from episodic transport and deposition within the active channel to erosion of the valley fill by incising channels (Popp *et al.*, 1988).

Outcroppings of early Quaternary deposits indicate a relatively continuous fall in base level (Slavin, 1991). Thus, the stable periods which did occur have left few remnants, especially in the upper basin. Slavin (1991) noted four further surfaces, which were represented by fluvial landforms, rather than being preserved by volcanic flows. Approximately 70 metres above the Rio Puerco base level, the S₅ geomorphic surface remnants consist of pediments and strath terraces. This surface is characterised by large calcium carbonate clasts, up to seven centimetres in diameter, indicating the extensive stripping of the surface. Despite this, some soil development has been observed. A similar, but more continuous surface, S₆, approximately 40 metres above base level was also noted (Bryan and Post, 1927; Slavin, 1991).

Approximately 15,000 years ago, at the end of the Pleistocene, both the Rio Grande and Rio Puerco were incised at least 30 metres deeper than their present levels, representing the maximum depth of erosion (Heath, 1983; Love, 1986). Since this time, superimposed onto a general aggradational trend, there have been numerous cut-and-fill cycles along the Rio Puerco, which have been preserved within the valley fill (Love, 1986; Slavin, 1991). This recent period of aggradation, although interrupted by the periods of incision and refilling, was responsible for the level of the pre-incision valley floor and was defined as surface S₇ by Slavin (1991). The exact chronology and number of these incision phases has not been determined (Love, 1986). However, dating of archaeological sites has improved the knowledge of both channel and valley bottom levels. Between 2,000 and 3,000 years ago,

the Rio Puerco had aggraded almost to the level of the pre-incision valley floor (Heath, 1983; Love and Young, 1983). Since this period, at least three major episodes of cutting and fill have occurred (Love and Young, 1983). Other major channels have been discovered more deeply buried in the alluvial fill, indicating yet further cut and fill episodes (Love and Young, 1983).

The youngest palaeoarroyos within the valley fill sediments are, in some places, over 8 metres deep and 40 metres wide, filled predominantly with sand (Love and Young, 1983). The largest of these arroyos has been dated at approximately 2150 B.P.. Sedimentary structures preserved within this palaeoarroyo suggest similar conditions to the modern inner channel and floodplain, without the presence of tamarisk and other non-native contemporary types of vegetation (Love and Young, 1983). A further difference between the most recent palaeoarroyos and the modern channel is that the older arroyo appears to have been filled by a braided, rather than a single-thread channel, in discrete horizontal units, which may be up to a metre thick (Love and Young, 1983).

As recently as 600 years ago, during the Pueblo IV occupation, incision to depths of 6m has been documented (Heath, 1983; Love, 1987). The pattern of pre-historic human occupation of the basin declined sharply over this time, especially along the Rio Puerco itself, from a peak during the Pueblo II phase between 1100 and 900 BP, possibly associated with the change in environment (Larsen and Herzog, 2000). The region was still tectonically and volcanically active, such that ancestral inhabitants in the Rio San Jose basin were said to have witnessed an eruption close to Grants approximately 3,000 years ago (Bryan and Post, 1927; Gorbach *et al.*, 1996). The recent volcanic activity in the Rio San Jose has resulted in its sediments being less erodible than those in the rest of the Puerco basin (Bryan and Post, 1927). The tectonic activity does not appear to be affecting the long-profile of the modern Rio Puerco or its tributaries (Slavin, 1991).

The recent period of incision and subsequent aggradation has, therefore, continued the pattern of cut and fill which has characterised the recent geological evolution of the Rio Puerco. This phase is still ongoing.

Santa Cruz River and San Simon River

The geological evolution of the Tucson and San Simon basin are thought to be similar. While much literature exists describing the evolution of the Tucson basin, very little research available in the public domain has been carried out on the development of the San Simon basin. However, given their physiographic similarity, and the fact that researchers such as Melton (1965) and Parker (1996) have directly correlated structures in both basins, some insight into the evolution of the San Simon basin should be gained from analysis of the evolution of the Tucson basin.

The Tucson basin is a sediment-filled structural depression, situated entirely within the Basin and Range physiographic province (Katzer and Schuster, 1984; Miller, 1987; Parker, 1986), as is the San Simon basin. The Basin and Range disturbance has had the most influence on the modern drainage basin and very few outcrops dated prior to this period are found in the Santa Cruz River basin (Parker, 1996). However, outcrops of Precambrian gneiss, into which younger Precambrian to early Tertiary granite has been extruded, have been observed in the Catalina mountains (Olberg and Schanck, 1913, Parker, 1996).

Prior to the Basin and Range disturbance, southern Arizona was subject to an extended period of tectonic upheaval (Parker, 1996). Outcrops predating the subsequent block faulting tend to be metamorphic, heavily contorted, faulted and tilted, with interbedded igneous intrusions (Anderson, 1987). This entire sequence, containing rocks from late Eocene, Oligocene and early Miocene in age, unconformably overlies rock of Precambrian to early Tertiary age and is known as the Pantano formation (Melton, 1965; Anderson, 1987). The uplands surrounding the Tucson basin are part of a section of metamorphic core complexes dating from this period (Anderson, 1987; Parker, 1996). The Oligocene climate of southern Arizona was thought

to be both warmer and more humid than the present day climate (Melton, 1965).

Synchronous with the commencement of the Basin and Range disturbance, a second discrete unit, known as the Lower Tinaja Bed, was formed (Anderson, 1987; Parker, 1996). This formation is early to mid-Miocene in age, between 26 and 12 Ma, and contains some volcanic tuffs and flows (Anderson, 1987). The contorted modern appearance of the mid-Tertiary Pantano and lower Tinaja outcroppings is almost entirely due to alteration during the crustal extension of the Basin and Range disturbance (Anderson, 1987). During the mid-Miocene, the block faulting caused a regional topography of closed tectonic basins, creating the mid-Tinaja formation (Anderson, 1987; Parker, 1996).

The Basin and Range disturbance occurred during two phases, separated by a lull during the late Miocene and early Pliocene (Melton, 1965; Anderson, 1987). These events, particularly the second phase of block faulting, transformed the landscape from moderate to extreme relief, with numerous basins and complex morphology (Anderson, 1987; Miller, 1987; Parker, 1996). This disturbance was also sufficient to cause the climate of southern Arizona to become semi-arid, due to a diversion of the humid air stream by the newly uplifted mountains (Melton, 1965). The fault scarps have since been eroded a considerable distance, creating a sinuous mountain-front with many bedrock canyons eroded into the horst blocks (Katzer and Schuster, 1984).

Cessation of the Basin and Range disturbance at the start of the Pliocene caused a further period of stability, allowing the formation of a major erosional surface. This period of stability is thought to have lasted between eight and ten million years, due to the presence of pediments of this age occurring at the summit of the Tortolita Mountains (Melton, 1965). Erosion of the fault scarps during this period caused up to four kilometres of retreat (Parker, 1996). The eroded sediment was deposited creating the upper Tinaja beds (Davidson, 1973; Anderson, 1987; Parker, 1996). Southern

Arizona is thought to have had a wetter and more temperate climate during this period, thus conducive to enhanced weathering and erosion of lower elevation bedrock (Parker, 1996).

The unconformable units of the three Tinaja beds are thought to be several thousand metres thick (Anderson, 1987). Above the Tinaja beds, the early to mid-Pleistocene Fort Lowell formation underlies much of the Tucson basin, although it only outcrops close to the Santa Catalina and Rincon Mountains (Anderson, 1987). A similar formation, known as the Upper Gila formation, may be found in the Safford area of the San Simon basin (Parker, 1986). This formation is over 100 metres thick and is composed of larger quantities of sand and gravel than the older formations, indicating a wetter local climate during the early Quaternary (Melton, 1965; Anderson, 1987). It is thought that the Santa Cruz River did not become through-flowing until the mid-Pleistocene (Davidson, 1973; Anderson, 1987; Miller, 1987; Parker, 1996). The climatic conditions in southern Arizona had, by this time, become cooler and drier (Melton, 1965; Parker, 1996).

As observed in the Rio Puerco basin, several well-defined Quaternary surfaces and terraces have been identified (Figure 5.3) (Melton, 1965; Katzer and Schuster, 1984; Anderson, 1987; McKitterick, 1988; Jackson, 1989; Parker, 1996). Three Pleistocene terraces have been identified in the Tucson basin, although they have an elevation difference of only a few metres. Although terraces are found along every major stream course in southern Arizona, including the San Simon River, the number, age and elevation show considerable differences (Parker, 1986).

The University terrace is thought to be early to mid-Pleistocene in age, thus representing a period of erosion during long-term base-level stability during and after the deposition of the Fort Lowell formation (Anderson, 1987; Parker, 1996). This corresponds with Jackson's T5 terrace (1989). Parker (1986) has noted that this terrace has not been correlated with any other surface outside the Tucson basin. The lower elevation Cemetery, or T4, terrace is mid-Pleistocene in age and outcrops the central Tucson area

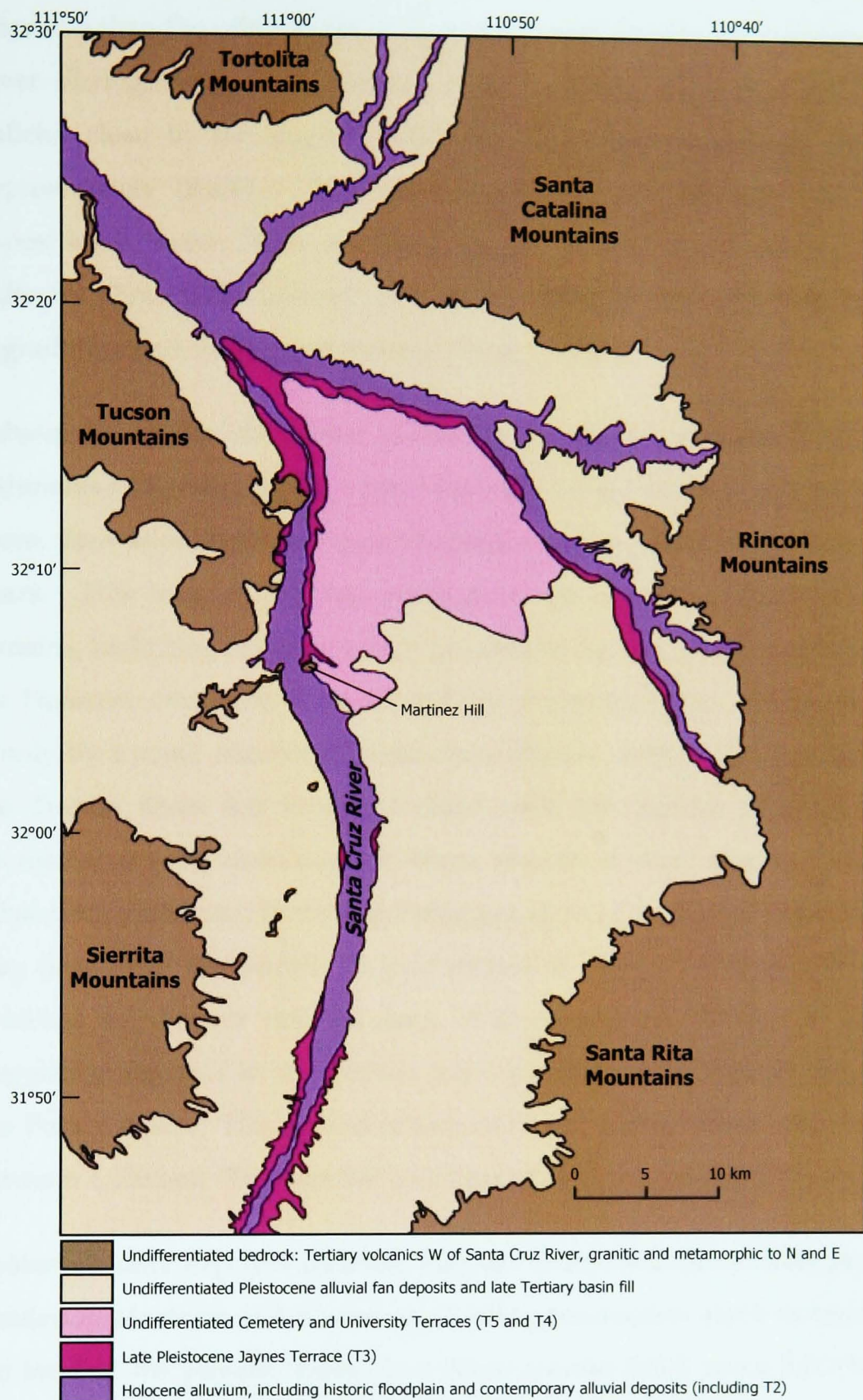


Figure 5.3 Surficial geology of the Tucson Basin (after Parker, 1996).

(Anderson, 1987; Jackson, 1989). Caliche deposits above gravels in this terrace have been dated at $25,900 \pm 840$ years B.P., although this date is a minimum due to contamination by water leaching into the older caliche (Haynes and Huckell, 1986). The youngest Pleistocene terrace is the Jaynes, or T3, terrace (Anderson, 1987; Jackson, 1989). This terrace is far less

extensive than the other terraces, due to renewed erosion by the Santa Cruz River during the early Holocene, which commenced around 8,000 B.P.. Caliche close to the upper surface of this terrace has been dated at approximately $18,400 \pm 120$ years B.P. (Haynes and Huckell, 1986). The depositional, rather than erosional, nature of the two younger terraces indicates climatically induced periods of sediment delivery with ensuing aggradation and subsequent incision (Parker, 1996).

Subsequent to the deposition of the Jaynes terrace, the oldest Holocene sediments have been dated at approximately 8,000 years B.P.. In the Tucson basin, there is evidence of human habitation dating back as much as 12,000 years. This long record has resulted in the presence of archaeological remains, including fire-pits, which are able to be radiocarbon dated. Thus the Holocene evolution of the Santa Cruz River has been well-documented, if only by a small number of researchers (Parker, 1996). The population of the Tucson Basin has been correlated with the periods of cut and fill: decreases, or even abandonment, being associated with incision. Although it has been postulated that the farming practices of these prehistoric farmers may have been responsible for past phases of arroyo initiation, there is no evidence to support this (Waters, 1988; Betancourt, 1990). Prehistoric population maxima in the Tucson basin parallels the Pueblo II maxima of the Puerco basin. This period is known as the Rillito phase and occurred between 1,150 and 950 years B.P. at a time of channel stability (Waters, 1988).

Coarse channel deposits indicate that the Santa Cruz River was probably braided in planform and flowed at a level approximately eight metres below the level of the present Santa Cruz River around 8,000 years B.P. (Waters, 1988). Cienega deposits overlying the coarse channel deposits indicate a cool, wet climate which caused a high water table (Waters, 1988). After 8,000 B.P., the climate changed to the hot, arid conditions of the Altithermal. The period of erosion triggered by this change in climate effectively removed a great deal of sediment and prevented further deposition until 5,500 B.P. (Katzer and Schuster, 1984; Haynes and Huckell, 1986; Jackson,

1988; Waters, 1988). The subsequent backfilling of this valley represents the pre-incision floodplain of the Santa Cruz River and has been termed T2 by Jackson (1988).

After the cessation of downcutting, slopewash from the ancient bajada, an alluvial piedmont consisting of deposits from the surrounding mountains, caused channel filling between approximately 5,500 and 4,500 B.P. (Haynes and Huckell, 1986; Waters, 1988). Between approximately 4,000 and 2,500 years B.P., a second period of fluvial then ciénega deposition occurred (Haynes and Huckell, 1986; Waters, 1988). Materials deposited prior to 2,700 B.P. are coarser than those subsequently deposited, suggesting a transition from a higher to a lower energy environment (Katzer and Schuster, 1984). This is consistent with the fact that the uppermost layers of this unit represent a former stabilised floodplain, seven metres below the level of the contemporary pre-incision valley floor (Waters, 1988). Thus, around 2,500 years B.P., the climate in southern Arizona became semi-arid and has remained so until the present (Waters, 1988).

Since 2,500 years B.P., four epicycles of cut and fill have been observed in the Tucson basin (Waters, 1988). These cycles have been superimposed on a general pattern of filling, causing the floodplain to aggrade seven metres. During this time, the climate has remained relatively stable, indicating intrinsic thresholds were responsible for the periods of incision (Waters, 1988). It has also been noted that the preserved palaeochannels are very narrow with overlapping radiocarbon dates. This indicates that incision occurred very rapidly, with prolonged re-filling occurring almost immediately. Local gradient adjustments due to sediment deposition and erosion are thought to be responsible for the change in channel environment (Waters, 1988). The preserved sediments of all four cycles show the same aggradational pattern. Coarse sand and gravel, fining upwards into silty sand indicate ephemeral discharge and aggradation during large storms, with ciénega deposits completing the sequence (Waters, 1988).

The first phase of cut and fill took place between 2,500 and 2,000 B.P. and caused the floodplain to aggrade four metres (Waters, 1988). The next phases of incision were followed by periods of aggradation lasting between approximately 1,900 - 1,000 B.P. and 1,000 - 650 B.P. (Haynes and Huckell, 1988; Waters, 1988). The penultimate epicycle saw entrenchment initiated approximately 530 years B.P., with refilling completed at the time European travellers first entered the basin in 1692 (Haynes and Huckell, 1988; Waters, 1988; Parker, 1996).

It is not known whether cut and fill cycles along the San Simon River have mirrored those along the Santa Cruz River. However, the most recent downcutting phase was synchronous between the two basins, with initiation occurring at the end of the 19th Century. Since then, however, the evolution of the two arroyos has been significantly different.

5.2 RECENT ARROYO EVOLUTION

The only major external influence on the arroyos studied, other than the climatic changes discussed in Chapter 4 and geological influences discussed above, has been human alteration of the river system. The extent of this alteration has been very different in each of the three basins. The specific anthropogenic influence on the evolution of each arroyo has, therefore, been examined where pertinent. The location of places mentioned in the text are shown in Appendix 2, Figures A1, A10 and A17.

Rio Puerco

Factors Affecting Evolution

As discussed in Chapter 1, the Rio Puerco is the only one of the three arroyos studied that has not had significant artificial alteration and thus represents an example of near-natural evolution. The structures which had the most geomorphological impact on the arroyo were those built during the population boom of the mid- to late-1800s. However, these had more impact on the initiation, rather than the subsequent evolution of the Rio Puerco. As noted in Chapter 3, a series of dams and irrigation ditches, particularly around the San Luis – Cabezon – Guadalupe reach, were constructed during

the 1880s (Bryan and Post, 1927; Bryan, 1928; Widdison, 1959; Love, 1997). These dams were generally locally built by farmers and tended to be washed out during major floods and rapidly rebuilt (Widdison, 1959). The San Luis dam was destroyed and rebuilt in 1877, 1880 and 1926/7 (Widdison, 1959). It was then rebuilt for the last time in 1936, in this instance properly engineered and built by the Soil Conservation Service. When the San Luis dam was finally destroyed in 1951, it was the last artificial structure remaining on the mainstem of the Rio Puerco (Widdison, 1959; Gorbach *et al.*, 1996). Further downstream, the Cabezon Dam had been breached by 1927, leaving a 16 by 4 metre (52 by 13 foot) gap (Bryan and Post, 1927). Along the middle Rio Puerco, the dam-breach flood following the collapse of the Old English Dam in 1893 and the subsequent collapse of the Benavidez Ranch Dam potentially caused the most geomorphological change due to artificial causes (discussed in Chapter 3; Love, 1997).

As discussed in Chapter 3, the initiation of the arroyo caused rapid depopulation of the Rio Puerco basin, making large flood control schemes or detention dams unnecessary. However, the construction (in 1915) and subsequent rapid sedimentation of Elephant Butte Reservoir, on the Rio Grande, prompted research into the source of material causing this infilling. It was discovered that 83 percent of the total sediment load of the Rio Grande at San Marcial, 84 kilometres (52 miles) downstream of the junction with the Rio Puerco, was supplied by the Rio Puerco between 1948 and 1973 (Gellis, 1998b). This compares with only 5.6 percent of runoff over the same period. Between 1973 and 1996, however, the proportion of both flow and sediment discharge supplied by the Rio Puerco had declined to 2.3 percent and 64 percent respectively. Given the disproportionate amount of sediment produced by the Rio Puerco, many studies have been carried out to determine the optimum method of reducing this sediment supply.

Bryan and Post (1927) produced the first of these comprehensive reports, suggesting that a system of interactive check dams be implemented: 1099 along small tributaries; 99 on larger tributaries, such as Arroyo Torreon; 68

on major tributaries, such as Arroyo Chico; and 80 on the main stem. It was intended that the tributary channels would be dammed first, thus severing an important source of sediment. This would ensure that the works on the main channel were more manageable and more likely to succeed. Similar schemes were proposed by the Soil Conservation Service and other government agencies between the 1930s and the present day (Tuan, 1966; Gorbach *et al.*, 1996). These system-wide proposals have never been implemented since they were not deemed cost-effective. Instead, flood control and channel stabilisation levees were built along the Rio Grande (Gorbach, *et al.*, 1996). However, since the early reports, a natural reduction in sediment concentration and load has occurred (discussed in Chapter 4). Thus, there is now no economic benefit for the implementation of major sediment control structures.

The lack of structured erosion control measures prompted token efforts that were both piecemeal and sporadic (Tuan, 1966). The Bureau of Land Management (BLM) implemented over 650 small-scale detention dams during the 1950s and 1960s to control a basin described in 1963 as “more seriously deteriorated than any other formerly productive land in the nation” (Gorbach *et al.*, 1996, pE-3). This was combined with the application of improved basin management practices in order to improve vegetation coverage and reduce soil loss from the valley floor (Gorbach *et al.*, 1996). It was noted that in one study basin, Cornfield Wash (a tributary of Arroyo Torreon), a 380 percent increase in vegetation cover occurred between 1958 and 1979. Within the same basin, grazing impacts were also studied and it was discovered that grazing did not significantly affect the improvement in vegetation (Branson and Janicki, 1986). These programmes, together with similar programmes by other agencies, may have had some success as sediment loads have decreased. However, the lack of comprehensive monitoring and quantification of results means that there is no direct proof of success or otherwise (Gellis, 1998b).



Figure 5.4 Artificial cut-off at Ventana, 1968 (photographer unknown).

The largest artificial change to the Rio Puerco since the collapse of the Old English dam was the straightening of a reach at Ventana during 1965 and 1966 (Figure 5.4) (Gorbach *et al.*, 1996; Coleman *et al.*, 2003). This rerouting was carried out in order to avoid having to build two or more bridges over the arroyo channel during the construction of a new route for Highway 44 (Coleman *et al.*, 2003). The 1.8 kilometre (1.1 mile) long channelised reach was far smaller, when constructed, than shown in the original engineering plans. This is thought to be due to the resistant bedrock outcropping in the area (Coleman *et al.*, 2003). The former channel was isolated by bulldozed dams, diverting flow into the artificial channel, which was over seven times narrower than the natural channel.

Lastly, a discussion of the artificial changes to the Rio Puerco cannot be complete without mentioning the introduction of tamarisk at three locations by the Middle Rio Grande Conservancy District in 1926 (Bryan and Post, 1927; Heath, 1983; Gorbach *et al.*, 1996). This scheme was undertaken in order to check erosion by stabilising the arroyo floor. The tamarisk multiplied very rapidly and have become widespread, with particularly dense stands along the margins of the active channel.

Arroyo Evolution

The evolution of the Rio Puerco appears to have occurred by both continuous headwards erosion of knickpoints superimposed over the earlier discontinuous erosion of specific reaches. As noted in Chapter 3, some reaches of the arroyo were incised prior to the mid-1800s. Photographs taken by P.E. Harroun in 1896, during the construction of the Old English Dam, indicate that a compound channel, with a vegetated inner floodplain and abandoned terrace levels, had already begun to develop (Love, 1997). During the late 1800s, more artificial geomorphological change occurred than at any time before or since. In particular, the collapse of the Old English Dam in 1896 had far-reaching consequences. The failure of this dam caused a lake 2.4 kilometres (1.5 miles) long to be entirely drained, resulting in a reversal of the arroyo evolution along this reach and possibly causing avulsion of the river from the east to west side of the valley downstream of the smaller Benavidez Ranch Dam (Love, 1997). Although the arroyo was already at least six metres (20 feet) deep in the 1896 photographs, the ensuing flood caused further entrenchment, resulting in an arroyo closer to nine metres (30 feet) deep (Love, 1997). Further downstream, the newly avulsed channel was much larger than the former, eastern, channel, most likely in response to the high-magnitude dam-burst flood (Figure 5.5). The old channel had a width of between 9 to 30 metres (30 and 100 feet), whereas the post-avulsion channel had widened significantly to between 30 metres (100 feet) and several hundred metres. The meander geometry had also changed noticeably: the radius of curvature and amplitude adjusted by an order of magnitude from a few hundred feet to a few thousand; and the new channel developed a more sinuous pattern, with sinuosity values changing from 1.36 to 1.66 (Love, 1997). This change in morphology illustrates the rapidity at which arroyo change occurs, with major alteration occasionally occurring during single floods.

By the time of Bryan and Post's investigations in 1927, the three dams left on the mainstem of the Rio Puerco had varying effects on the arroyo morphology. The largest of these, at San Luis, had caused the channel to

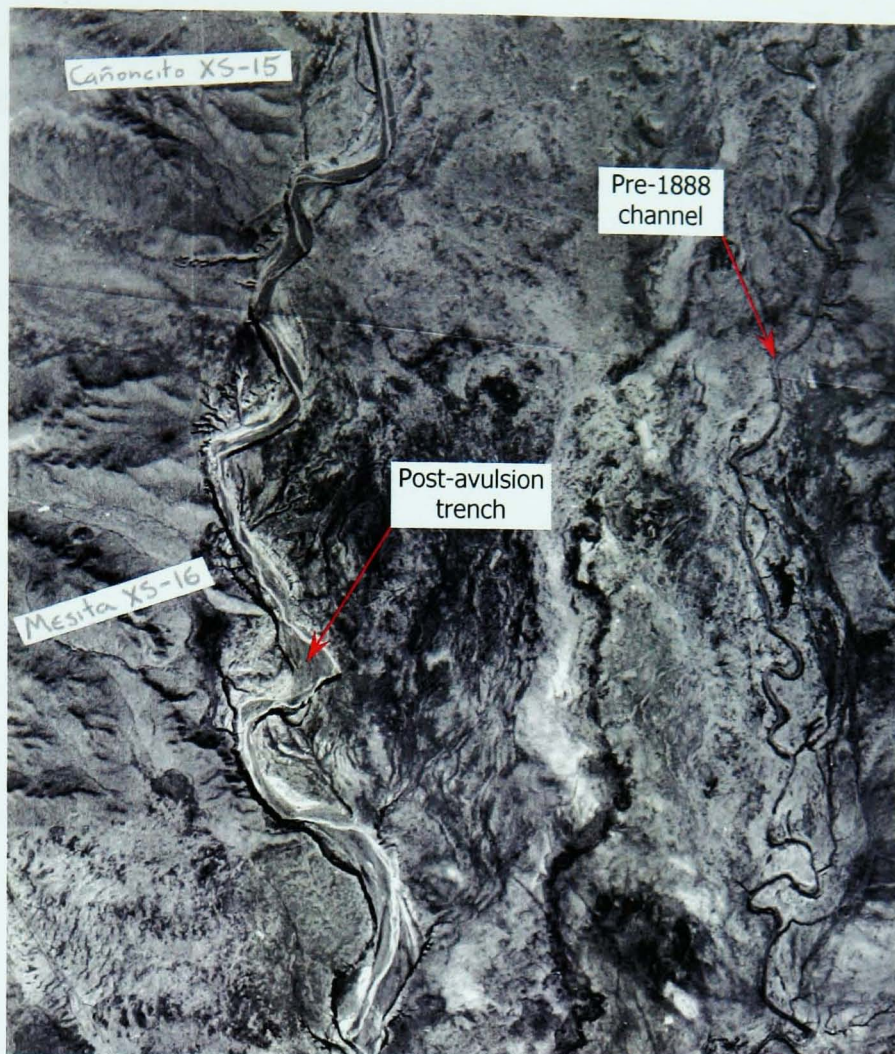


**Figure 5.5 Pre- and post-avulsion channels, 1935 aerial photograph.
Numbers refer to Elliott's cross-sections (see Appendix 2).**

aggrade approximately three kilometres (10,000 feet) upstream. The gradient of the channel above the dam was low, at 0.17 percent, corresponding to the lowest gradients found along the mainstem, which were between 0.13 and 0.8 percent (Bryan and Post, 1927). The dam had also prevented both mainstem and tributary erosion. A nearby tributary had aggraded approximately 5 metres (17 feet) and the mainstem and tributaries had begun to become stabilised by vegetation. Further downstream, the Cabezon Dam, although breached and, therefore, not as effective as the San Luis Dam, had still caused upstream aggradation. Upstream of Cabezon, several abandoned irrigation channels were noted, up to 3 metres (10 feet) deep and 46 metres (150 feet) wide, presumably left unusable after the dam breach (Bryan, 1928). The Guadalupe Dam, still further downstream, was primarily intended to divert water for irrigation purposes and its effect on the channel is not recorded, although at 7.6 metres (25 feet) high, some sediment accumulation must have occurred.

As well as the artificial changes to the Rio Puerco observed by Bryan and Post (1927), the geomorphology of the 1927 arroyo was also noted in detail. The upstream limit of incision had reached almost to the headwaters, some distance above Cuba. The upper Rio Puerco was very sinuous, with actively eroding meanders. Vegetation had begun to be established on the meander point bars, berms and mid-channel islands, indicating some stabilisation and the development of a braided low-flow channel. Between San Luis and Guadalupe, the arroyo, although incised to 6 metres (20 feet) deep, was considerably narrower and less deep than the remainder of the mainstem, due to outcrops of resistant shale in this reach. However, the geomorphological effect of bedrock was localised. The remnants of the Old English Dam could still be observed on a ledge above a 6.7 metre (22 foot) high bedrock knickpoint, which also provided a hindrance to headward erosion. The middle Rio Puerco was generally wide and deep, with a gentle gradient (averaging 0.15 percent), although several smaller shale outcrops had been observed to have checked erosion.

It was noted that many of the tributary channels along the middle Rio Puerco were, at the time of Bryan and Post's research, as yet unincised. It was, however, observed that incision was imminent and would cause much destruction of grazing land, as well as hugely increasing the amount of sediment supplied to the lower reaches of the arroyo. Below the Rio San Jose, the Rio Puerco was over 12 metres (40 feet) deep and over 300 metres (1000 feet) wide in places. The larger dimensions of the arroyo along this reach were thought to be due to the additional flow provided by the Rio San Jose. However, the lower 9.7 kilometres (six miles) of the Rio Puerco were observed to be considerably less-incised, presumably due to the controlling effect of the Rio Grande.

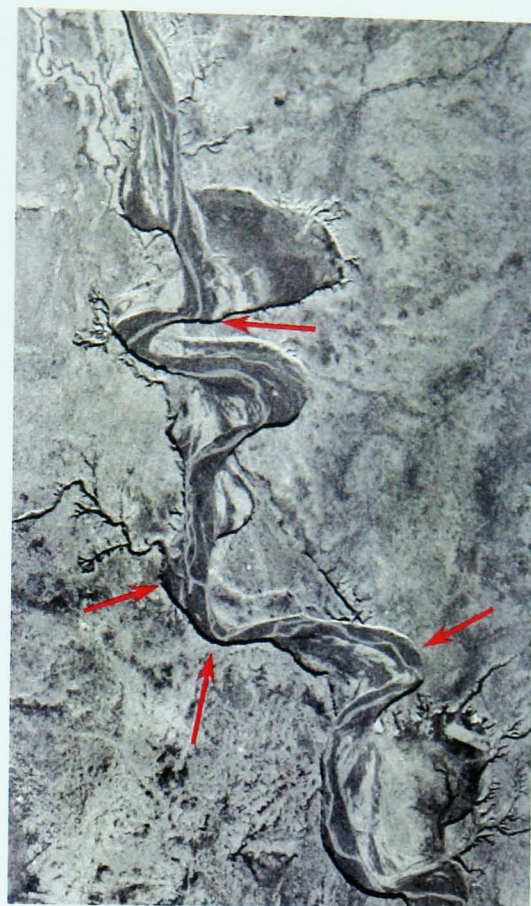
The 1935 aerial photographs were the next significant documentation of the Rio Puerco, taken almost half-a-century after continuous incision commenced (Elliott, 1979). The arroyo at this time appears choked with sediment along nearly the entire course and there is a distinct lack of

vegetation within the arroyo trench. The change in geomorphology from that observed by Brian and Post is easily explained by observing the flood series for the intervening period. Two large floods occurred in 1929, which peaked very close together on August 12th and September 23rd (Heath, 1983). The first of these reached 892.3 cumecs (31,509 cfs) at Rio Puerco and 867.8 cumecs (30,643.7 cfs) at Bernardo. The second of these is the flood of record at both gauges, peaking at 1,068 cumecs (37,700 cfs) at Rio Puerco and 991 cumecs (35,000 cfs) at Bernardo. These were the only two gauges in operation at the time. The third largest recorded flood occurred in 1935, which reached approximately 800 cumecs (28,000 cfs) on August 21st. The monsoon season of 1935 also produced three other large floods with peaks estimated at 450 cumecs (15,490 cfs) on 5th August; 590 cumecs (20,780 cfs) on 30th August; and 240 cumecs (8590 cfs) on 28th September. Prior to these floods, the largest recorded flood between 1915 and 1925 had a magnitude of 400 cumecs (14,000 cfs), less than half the 1929 values. (Bryan and Post, 1927; Bryan, 1928). The floods during 1929 and 1935 were, therefore, larger than any flood previously recorded and undoubtedly caused a great deal of geomorphological change, which included a reversal of the evolution of the arroyo. Reaches which had previously been observed to have developed an inner floodplain reverted back to having a trench-width braided, broad active channel due to the amount of sediment mobilised during these floods.

Interestingly, the 1935 aerial photographs appear to have been taken at different dates, since there are three sets of flight and photograph numbers. Unfortunately, the exact dates of the flights have not been recorded. However, there is a distinct change in the morphology of the Rio Puerco between the three sets. It should, however, be noted that the overlap between the different sets of photographs is very short and it is, therefore, difficult to distinguish between apparent changes due, for example, to the difference in the time of day that the photographs were taken, and actual geomorphological change. However, examination of the changes in the morphology of the active channel have led to several conclusions.



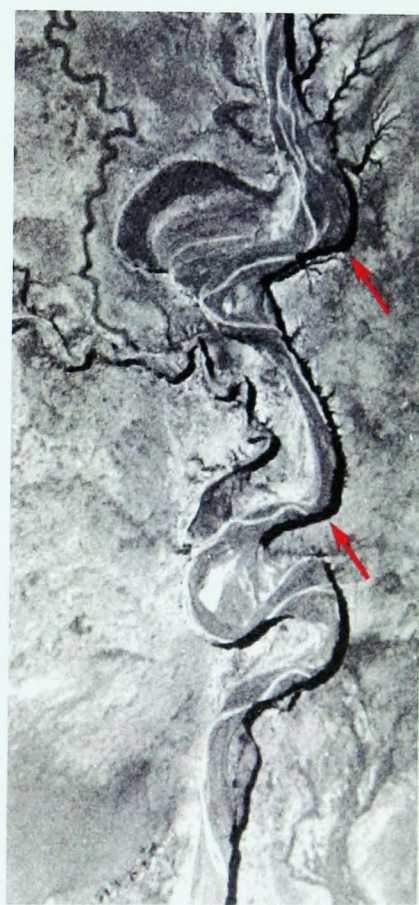
Upper reach sequence



Middle reach sequence



Lower reach sequence



Middle reach sequence

Figure 5.6 1935 aerial photographs showing the difference in morphology due to different over-flight dates. Arrows show sites of erosion.

The upper Rio Puerco was photographed first (Figure 5.6A). This active channel along this reach was wide and braided. Freshly deposited sediment may be observed covering much of the base of the arroyo trench, indicating a recent large flood. The lower reach was photographed prior to the middle reach (Figure 5.6C), and may have been over-flowed at the same time as the upper reaches. However, given the different photograph numbers, this seems unlikely. Given the difference in planform morphology, it is more likely that the lower reach was over-flowed after the upper reach. The active channel along the lower reaches is fairly wide, with a well-defined braided channel with distinct unvegetated or sparsely vegetated lateral bars. The middle reaches must have been photographed shortly after the lower (Figure 5.6B and D), since in some places, the former position of the active channel is visible. A large flood probably occurred between the flights over the upper and middle reaches, since significant outer bank erosion has occurred (Figure 5.6B). However, the middle reaches have developed a very clear, narrow active channel, which is mainly single thread.

The morphological differences between the reaches is puzzling, since it might be assumed, from casual observation, that the lower and middle reaches were over-flowed after a series of low flows, to create the small low-flow channel, with the upper reach representative of conditions after a high-magnitude flood. However, since this is clearly not the case, it must be concluded that the upper reaches were over-flowed shortly after the first large flood that occurred during the summer of 1935. It is presumed that the middle and lower reaches were over-flowed after the largest flood, since this was then followed by several days of much lower flow, which would account for the creation of the narrow active channel. This distinct change in the planform of the active channel illustrates the rapidity at which geomorphological change occurs in arroyos. This also highlights the fact that photographs only show a snapshot of the existing conditions, which may appear significantly different depending on the sequence of floods preceding the date of observation.

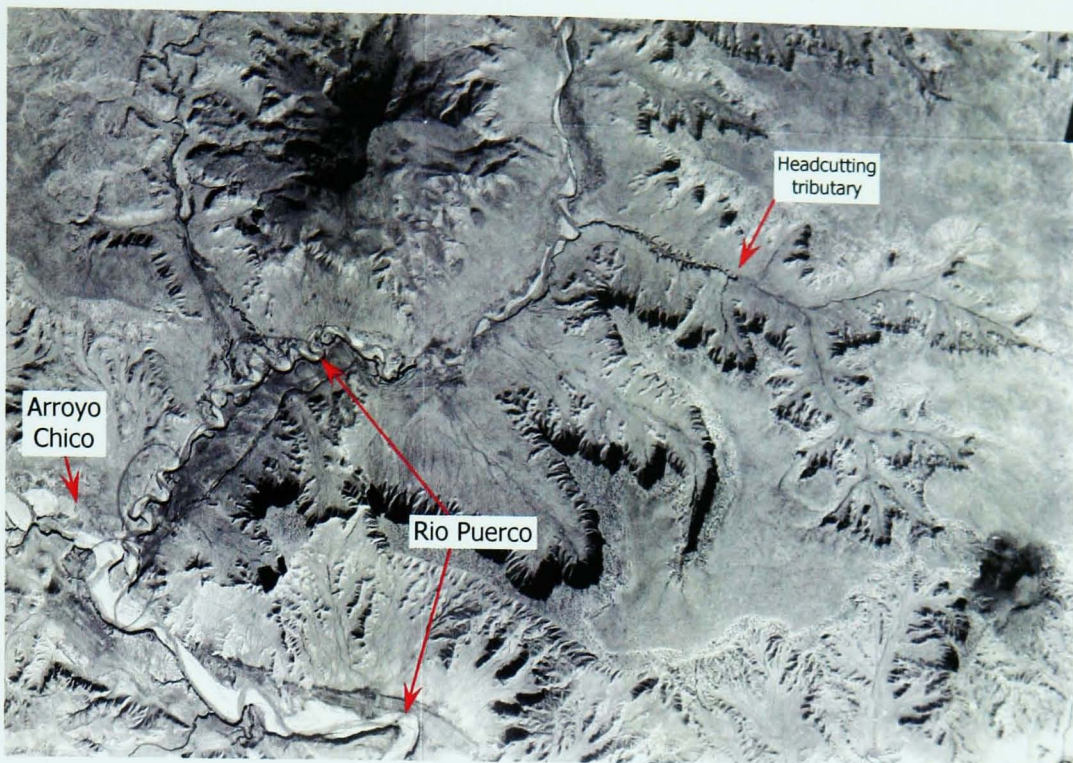


Figure 5.7 Change in morphology at the confluence with Arroyo Chico, 1935 aerial photograph.

The arroyo shows two distinct changes in the morphology of the active channel. The most obvious change occurs due to the effect of the Arroyo Chico, which, in reality, should be re-classified as the mainstem of the Rio Puerco, due to their morphological similarity (Figure 5.7). Above the confluence, the Rio Puerco itself is considerably smaller, although further upstream, the arroyo becomes significantly wider along some sections. The narrower reaches of the arroyo possibly coincide with a narrow river valley.

Previous studies have generally split the Rio Puerco into three reaches (Elliott, 1979; Love, 1986; Gellis and Elliott, 2001; Molnár, 2001): the upper Rio Puerco defined as the smaller channel above the Arroyo Chico; the middle Rio Puerco between the Arroyo Chico and the Rio San Jose; and the lower reaches below the Rio San Jose. However, this study has found that, aside from the obvious effect of the high sediment and flow discharge input from the Arroyo Chico, aerial photographs show a distinct and abrupt geomorphological change in the Benavidez Ranch reach. The reason for this change is not immediately apparent, although the most likely cause is a change in bedslope. The valley width at this point is also distinctly narrower than upstream, which may also have affected the arroyo. Unfortunately, the inaccessibility of this site has resulted in no field

observations of the arroyo at this point, both by other researchers or during this project, an omission which should be remedied by future studies.

The exact point of the second morphological change, in the Benavidez Ranch reach, has been obscured by the changes due to the different dates of the 1935 aerial photographs. Thus, the abruptness of this change cannot be observed. The reach upstream of this point has a broad, shallow channel which meanders around broad terraces and point bars, which are mainly unvegetated. However, the reaches downstream appear to have a very narrow, mainly single-thread channel, again with clear meander terraces and point bars. This may represent a recent low-flow channel and, although clearly visible, appears unconfined. Tamarisk had progressed upriver a great distance, with a far higher density along the lower reaches, especially within abandoned meander terraces (Heath, 1983). Along both reaches, the meander geometry is still largely scaled to the arroyo, although along the lower Rio Puerco, there are very short reaches which have developed smaller-scale meanders which appear to be adjusted to the narrower inner channel. The active channel pattern through the upper reaches is more chaotic than that observed along the lower reaches.

The 1935 aerial photographs indicate that the trench of the Rio Puerco alternated between highly sinuous reaches, interspersed with straight reaches. There is no obvious reason for this difference in planform. Straight reaches of the active channel may occur often where the active channel has cut-off several meanders to create abandoned channels and terrace remnants, or where the arroyo itself has remained straight. Meander cut-offs have also been created where the active channel has progressively retreated, leaving visible scroll bars or different terrace levels as evidence of this retreat. Compressed meanders may be found upstream of bedrock outcrops, generally in the upper reaches, and along the large tributaries, due to backwater effects. These factors both cause a reduction in the arroyo gradient. Arroyo meanders in the middle and upper reaches are distinctly smaller, perhaps due to the lower valley width along these reaches.

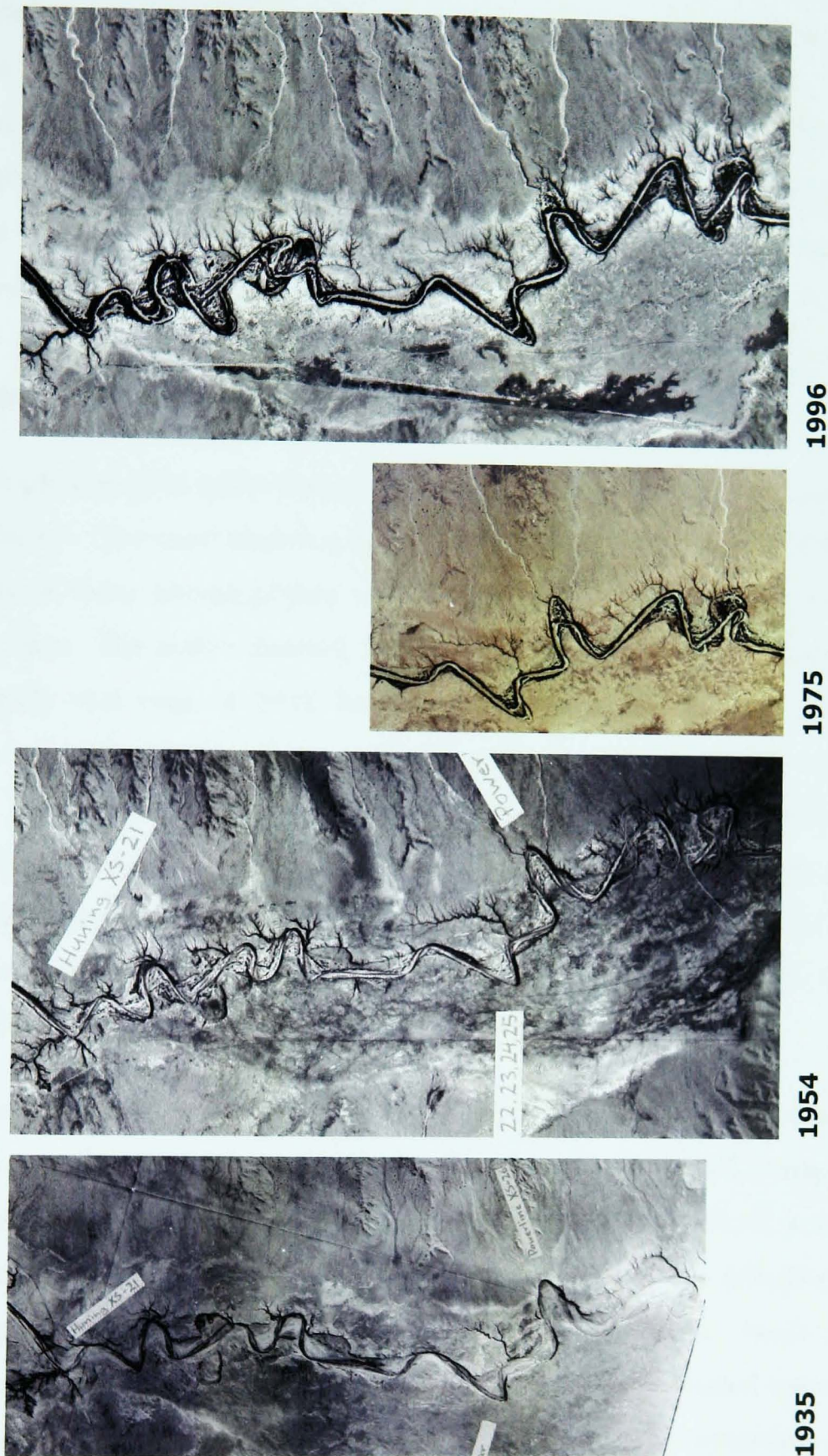


**Figure 5.8 Arroyo evolution between 1935 and 1996, Lower Reach.
Numbers refer to Elliott's cross-sections (see Appendix 2).**

Actively incising tributary arroyos may be observed along the entire arroyo, with considerable smaller-scale gully networks eroding headward, especially around the outer banks of meanders and along terrace fronts. These gullies were less common above the confluence with the Arroyo Chico, indicating that outer bank erosion along this reach was sufficient to prevent gully formation. This reach was, therefore, still undergoing the initial phase of lateral erosion at the time of the 1935 aerial photographs. The sediment supplied to the lower reaches by this tributary arroyo and gully erosion was undoubtedly partly responsible for the morphological changes of these reaches.

Aerial photographs taken during the 1940s are available only for the lower Rio Puerco. The most obvious change since 1935 is the increase in tamarisk. Stands of these phreatophytes may be observed growing along meander scroll bars. The active channel, despite high-magnitude floods during the extremely wet year of 1941, has become better-defined, wider and has distinct braiding tendencies, compared with the active channel noted in 1935. Observations of the hydrograph at Rio Puerco indicate that the 1947 photographs were taken after a series of low- to medium-magnitude floods. It is thus presumed that the 1947 photographs were taken shortly after a higher-discharge flood than those taken in 1935. This again indicates the rapidity with which the arroyo adjusts to the sequence of floods.

By the mid-1950s, the Rio Puerco had developed a clearly defined narrow single-thread active channel below the Benavidez Ranch reach (Figure 5.8). Tamarisk development along scroll bars on meander terraces and point bars was widespread along this reach, although densities were still low, with individual stands of trees still apparent. The upstream reach has a noticeably wider active channel, which has distinct unvegetated lateral and point bars. Tamarisk had, by this time, reached as far upstream as the confluence with the Arroyo Chico. The Arroyo Chico again had a distinct effect on the arroyo morphology. Above this point, the Rio Puerco was mainly single-thread, although braided reaches may be observed, especially

downstream of the Arroyo Chijuilla. Below the confluence with the Arroyo Chico, along the Guadalupe reach, the Rio Puerco was far wider, with a distinctly braided low-flow channel, indicating a high sediment input from the tributary arroyo, although the effects appear to be relatively localised. The 1953/4 aerial photographs show a general decrease in the dimensions of the active channel along the Rio Puerco, especially in the lower reaches, which was likely to have occurred due to the low incidence of high-magnitude floods during the late 1940s and early 1950s (Elliott, 1979).

In 1961, Nordin studied the Rio Puerco intensively, just downstream from the Bernardo gauge. It was noted that the arroyo along this reach had been aggrading steadily for a number of years (Nordin, 1963a). This affected the stage/discharge relationship at Bernardo. In 1960, the stage was 0.76 metres (2.5 feet) higher than in 1950 (Nordin, 1963b). Localised scour at the confluence with the Rio Grande caused a headcut to work upstream through the reach during August and September (see Appendix 2, Figure A2.9). This affected the stage/discharge relationship significantly, with low flows reverting back to the 1950s relationship, although at high flows it was unchanged. It was noted that during high flows, when the headcut might be expected to migrate upstream more rapidly, the cut channel actually filled with sand, thus preventing migration. During low and medium flows, however, upstream migration occurred at speeds relative to the discharge magnitude (Nordin, 1963b). Although this reach was only studied for a few months, rapid geomorphological change within the arroyo trench occurred, again illustrating the rapidity at which adjustments to the prevailing conditions occur.

The most significant change during the 1960s was the construction of the artificial channel at Ventana in 1965 and 1966 (Figure 5.4). This channel effectively doubled the channel gradient from 0.004 to 0.0074, thus increasing the stream power and erosive capability of flows through this reach (Coleman *et al.*, 2003). The immediate response of the arroyo was to incise, creating a series of bedrock knickpoints. The geomorphology of the

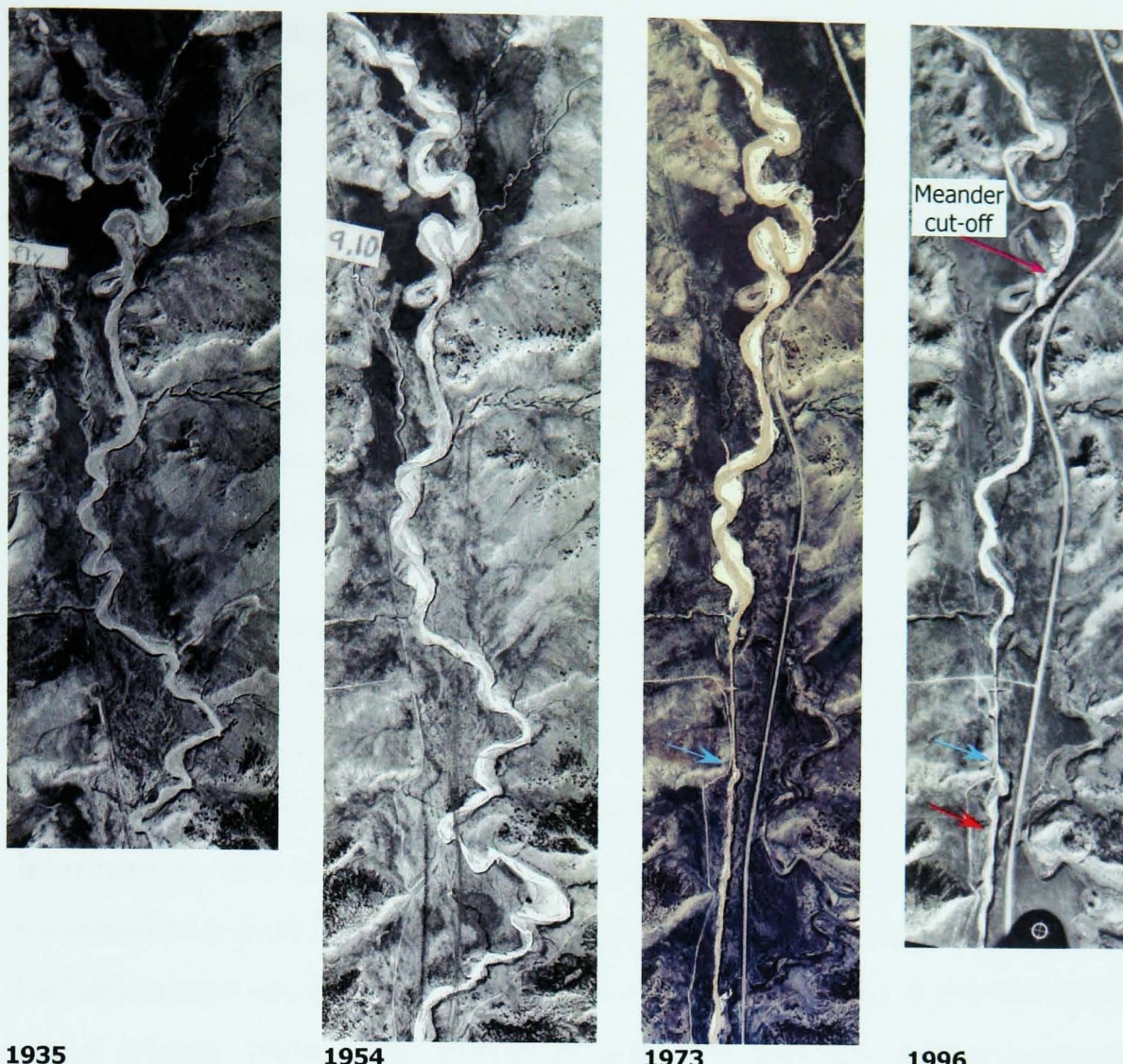


Figure 5.9 Morphological change due to the construction of artificially straightened reach at Ventana.

Red arrow shows point at which breakthrough to former position of arroyo is likely to occur. Blue arrows show position of largest waterfall/knickpoint.

reaches upstream of the Ventana channel have been significantly affected since initial construction. This is clearly illustrated in Figure 5.9. Upstream of the artificial cut, by the 1970s, the active channel had become wide and braided, meandering at arroyo-scale to create mainly unvegetated point bars. Some lines of tamarisk had begun to develop. Further upstream still, the arroyo was even wider and the wide, shallow active channel covered the entire base of the arroyo trench. Few meander terraces existed along these reaches, indicating that the meander pattern had not yet had time to mature and create cut-offs. Downstream of the straightened reach, the active channel was considerably narrower, with far less bare sediment in storage. The majority of point bars and meander terraces had been stabilised by tamarisk. Thus, the upstream reaches appear to have been changed far more

significantly than those downstream. The substantial change in morphology in the reaches upstream of Ventana occurred due to the effective rejuvenation of the system above this point, since the base level was lowered due to the increase in the gradient of the arroyo. The record flood on the closest gauge, at the Rio Puerco above Arroyo Chico, occurred on July 29th 1967, with a peak discharge of 197 cumecs (6,940 cfs). In all probability, much sediment was mobilised by this flood. The knickpoints created along the artificial channel provided a barrier to sediment, thus causing loss of competence and deposition.

During the 1960s and 1970s, the wide reach downstream of the confluence with the Arroyo Chico changed little. The flood of record at the Arroyo Chico gauge occurred on September 12th, 1972, reaching 430 cumecs (15,200 cfs). Sediment was thus supplied to the Guadalupe reach in abundance. Interestingly, the 1972 flood, which started in the Arroyo Chico basin, increased to a peak of 629 cumecs (22,200 cfs) at the Rio Puerco gauge, but had attenuated dramatically to only 261 cumecs (9,220 cfs) at the Bernardo gauge (Heath, 1983). This pattern of gain then loss reflects the changing morphology between the three gauges. The middle reaches of the Rio Puerco had a meandering, but very wide, active channel. The 1975 aerial photographs again show a clear change in arroyo morphology at the Benavidez Ranch reach. Below this point, the lower reaches had developed a very narrow, tamarisk-lined active channel (Figure 5.8). Thus, the majority of the arroyo between the Arroyo Chico and Rio Puerco gauges consisted of wide, unvegetated meanders. Between the Rio Puerco and Bernardo gauges, however, the active channel had effectively been channelised by tamarisk, providing ideal conditions for the attenuation of large flows. It was estimated that, between 1954 and 1979, 90 percent of the active channel had shifted along the lower Rio Puerco, again illustrating the rapidity of change within the arroyo trench (Heath, 1983; Popp *et al.*, 1988).

As discussed in Chapter 2, Elliott (1979) split the Rio Puerco into two morphological types: Type 1 indicating laterally eroding reaches with a

Variable	Type 1	Type 2
Width/Depth Ratio	78.3	12.2
Slope	0.0032	0.0014
Schumm's M (%)	23.7	44.9
Bend Radius of Curvature (metres)	97.7	69.6
Sinuosity	1.6	1.5
Valley Slope	0.0032	0.0019
Mean Grain Size of Channel (mm)	0.22	0.11

Table 5.1 Morphological difference between Elliott's Type 1 and Type 2 reaches.

braided active channel; and Type 2 indicating the development of a stabilised compound channel. This division was based on fieldwork carried out during 1977 (summarised in Appendix 3, Table A3.1). It was discovered that the two types had significantly different morphological characteristics (Table 5.1). The upstream, Type 1 reaches also had far more variability than those downstream. It was noted that cross-section 11, between San Luis and Cabezon, exhibited morphological characteristics of both arroyo types. However, Elliott's findings over-simplify the evolution of the Rio Puerco, possibly due to the fact that the cross-sections surveyed for his research are located at points which are not representative of each geomorphologically different reach. The underlying premise of the proposed evolution hypothesis is that progressive upstream change from Type 1 to Type 2 morphology will occur. It was observed that, in 1977, the upstream, Type 1 reaches were similar to the morphology of the 1935 lower reaches, thus apparently confirming this theory (Elliott *et al.*, 1999; Gellis and Elliott, 2001). However, cross-section 11 is situated upstream of the Guadalupe reach, which has been included in Type 1. Thus, other considerations must be taken into account, such as the presence of natural and artificial knickpoints, such as those in the artificial Ventana reach, and the considerable effect that the Arroyo Chico has on the morphology of the Rio Puerco.

A cross-section, initially surveyed by Brian in 1936, was re-surveyed by Hadley in 1966 and 1972 and included in Elliott's analysis. It was observed

that although lateral accretion had occurred, the level of the bed had changed little (see Appendix 2, Figure A2.6). It was noted in Chapter 2, that aggradation tends to occur vertically at first, then laterally. This progression of vertical then lateral aggradation may have occurred as the arroyo created a narrow, deep channel in response to the high sediment concentrations. Thus, although vertical, then lateral aggradation of the inner floodplain occurred, bed aggradation did not, in order to maintain the depth of channel.

By 1989, the rejuvenation of the reach above Ventana had possibly caused the cut-off of a major bend, in response to a minor knickpoint working headwards through the system (Figure 5.9) (Love, 1992). This bend is synonymous with Elliott's "Horsefly" cross-sections 8, 9 and 10 (Appendix 2, Figure A2.3). This enabled the processes involved to be examined in detail. Love (1992) states that only one or two real cut-offs, as opposed to the gradual retreat of the active channel, occur per century. This type of cut-off leaves a core of unincised sediment, which is visible from aerial photographs. Contrary to Love's findings, inspection of the 1935 aerial photographs during this study revealed that 12 such cut-offs had occurred since the incision of the Rio Puerco. By the 1996/7 over-flight, a further nine bends had been cut-off, including the Horsefly meander. These figures are probably an underestimation of the true number of cut-offs, since it is often difficult to pick out the meander cores. Thus, it would seem that this is a relatively frequent occurrence. Figure 5.10 indicates the effect of large

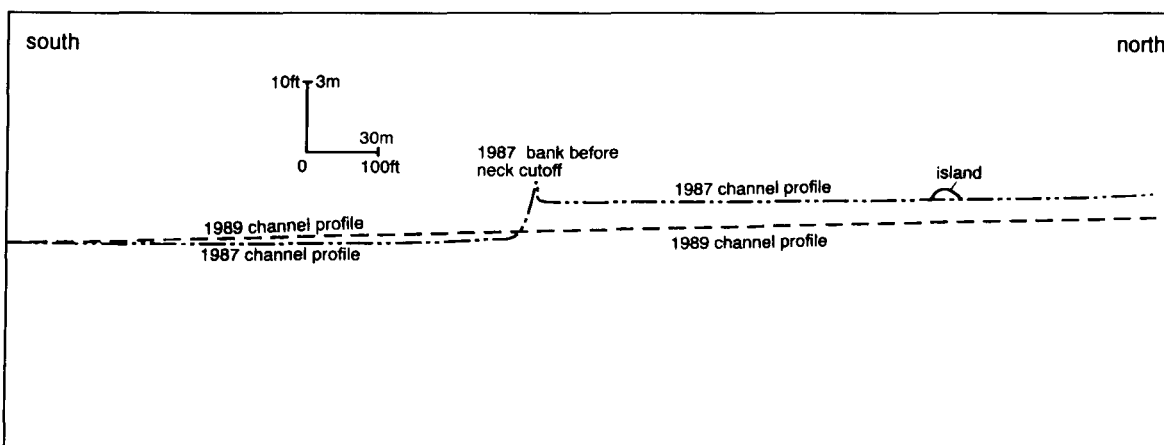


Figure 5.10 Longitudinal profiles across the neck of Horsefly meander before and after its cut-off in 1989 (after Love, 1992).

meanders on the gradient of the channel. It can be seen that, prior to cut-off, the head loss around the meander was 1.7 metres (Love, 1992). When the active channel broke through the neck of the meander, very rapid adjustment to the new planform occurred. The cut-off actually occurred in February 1988. By June 1989, the bed had totally readjusted. The breach actually occurred during a minor event, indicating both the crossing of an intrinsic threshold and the importance of the timing and duration of events (Love, 1992).

The 1989 aerial photographs are only available for the Guadalupe and upper Rio Puerco reaches and show a wide, braided active channel. The only exception to this is between the straightened reach at Ventana and the confluence with the Arroyo Chico, where the arroyo was still small with a single-thread active channel, which meandered at arroyo-scale around unvegetated point bars. A narrow constriction above the Guadalupe reach is very clear in these photographs and serves to illustrate the abrupt widening and change in planform morphology along this reach (Figure 5.11). Along the entire upper reach, tamarisk had stabilised abandoned meander terraces and higher bar areas. The artificial cut at Ventana had developed clear meanders, but only along the centre of the reach (Figure 5.9). The upper and lower sections still remained very straight. This difference is presumably due to the controlling effects of knickpoints, which are not visible on the aerial photographs.

During the mid-1990s, the re-surveys of Elliott's 1970s cross-sections seemed to reaffirm the headwards progression of evolution. There was a general stabilising trend, with the upper reaches, therefore, showing the greatest change since 1977 (Elliott *et al.*, 1999). The geometrical changes in the channel and arroyo dimensions are summarised in Appendix 3, Table A3.3, with the actual cross-sections shown in Appendix 2, Figures A2.2 to A2.9. The only reach that had continued to widen was at the Horsefly meander due to the 1988 cut-off (Figure A2.3). It was also noted that the effect of the Arroyo Chico on the Guadalupe reach had prevented it from evolving a

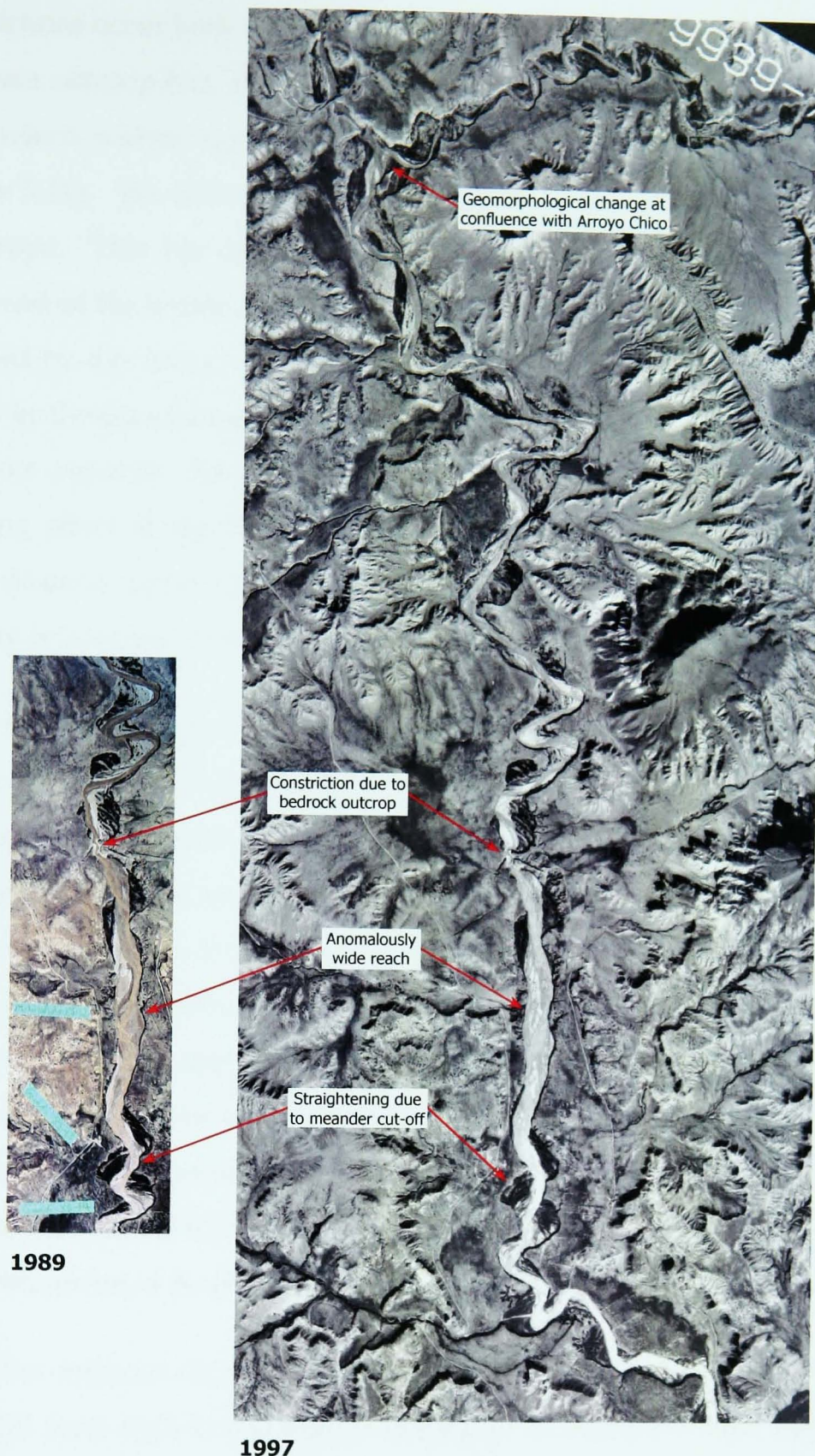


Figure 5.11 Anomalous morphology of Guadalupe sub-reach and point of geomorphological change at confluence with Arroyo Chico.

Type 2 morphology (Figure A2.4) (Gellis and Elliott, 2001). However, the reaches just downstream of the Arroyo Chico do not show the marked difference in morphology seen along the Guadalupe reaches. This indicates that there are other factors contributing to this difference. Bedrock

constrictions occur both up- and downstream of the wide braided reach. The upstream outcrop has, as noted previously, caused a very narrow section to form, which widens rapidly as more easily erodible sediments are reached (Figure 5.11). The downstream outcrop has caused an abrupt diversion of the arroyo. This has caused a series of compressed meanders to form at either end of the braided reach. It, therefore, seems likely that the sediment supplied by the Arroyo Chico has overloaded the sediment capacity of the arroyo in the Guadalupe reach. Flows in this reach have a lower sediment transport capacity than corresponding meandering reaches, due to the checking effect of the abrupt changes in flow direction downstream. As flows disperse upon reaching the wider section, the sediment transport capacity is lowered, thus causing the deposition of sediment.

Aside from the Arroyo Chico, only one other tributary has a significant effect on the arroyo morphology. The Arroyo Chijuilla has also caused the reaches of the Rio Puerco downstream of its confluence to remain braided, although the effect is nowhere near as marked as downstream of the Arroyo Chico (see Appendix 2, Figures A2.2 and A2.3). Above this confluence, the active channel has become deeper and narrower, with a sinuous planform. However, although the active channel below the confluence has narrowed somewhat and become better defined, it is still shallow, with a braided low-flow channel. This braided reach extends downstream as far as the Ventana artificial channel. It is, therefore, likely that the gradient steepening caused by the straightened reach is partly responsible for the braided planform.

Along the artificial Ventana reach itself, the arroyo has developed a 4.6 metre (15 foot) high knickpoint, resulting in 15 metre (50 foot) high walls downstream of this point (Coleman *et al.*, 2003). This knickpoint has migrated only slightly over 21 metres (70 feet) since 1973, indicating the resistance of the bedrock through this reach, especially compared with the rapidity at which regrading occurs along reaches of the Rio Puerco cut into alluvium (Figure 5.9). It is downstream of this waterfall that the arroyo has widened laterally due to the development of meanders, as noted in the 1989

aerial photographs. It should be noted that the widening of the straightened channel has brought it very close to the old meandering channel. Therefore, unless bank protection measures are implemented, it is highly likely that the arroyo will break through into its former channel. This may be hastened by the migration of an upstream meander, which has been steadily eroding down-valley. This is discussed further in Chapter 6.

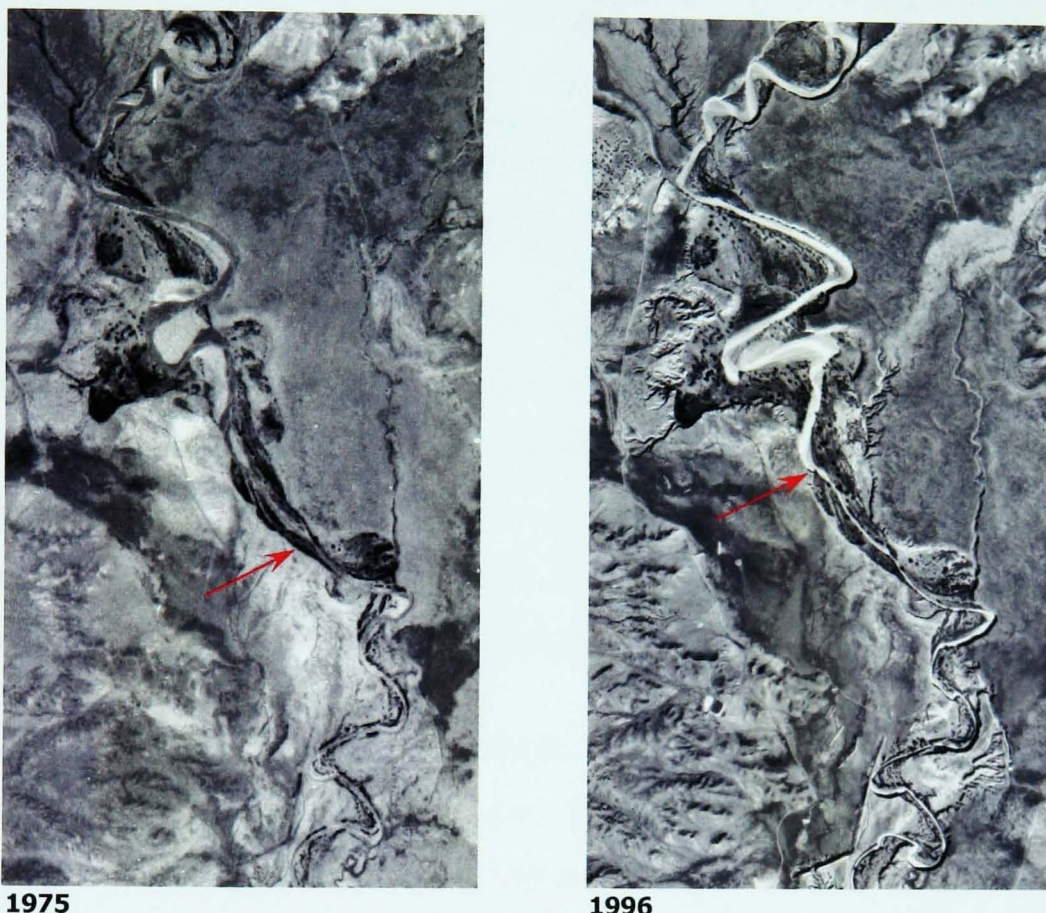


Figure 5.12 Geomorphological change at the Benavidez Ranch reach, arrow indicating point of change.

The change in geomorphology along the Benavidez Ranch reach is very distinct in the mid-1990s aerial photographs, although its position has not changed dramatically over time (Figure 5.12). This may indicate that the cause of this change is either a very slow-moving knickpoint, or that another, unknown, factor is responsible.

By the mid-1990s, the active channel along the lower reaches, downstream of the Benavidez Ranch reach, had effectively become channelised, forming a distinct trapezoidal shape (Figure 5.13). Tamarisk lining the channel are especially dense, forming an almost impenetrable barrier. This has caused



Figure 5.13 View downstream from Highway 6 bridge, Rio Puerco at Rio Puerco, showing morphological change. (1936 photograph courtesy H. Yeo, Ms 94 Box 16/76, Rio Grande Historical Collections, New Mexico State University Library; 1996 photograph courtesy J. Wall, BLM).

natural levees to be deposited along the bank margins. The middle and upstream reaches, however, have not developed this density of vegetation. Tamarisk along these reaches are more commonly found on abandoned meander terraces, leaving the active channel still relatively unconfined. Above the Arroyo Chijuilla, the introduction of Russian Olive has been effective in suppressing tamarisk, which are rare along this reach.

The active channel of the Rio Puerco, by the mid-1990s, had generally developed a highly sinuous planform. In some reaches these had become compressed, forming a hooked or recurved shape. Particularly tortuous meanders may be observed just downstream of the Benavidez Ranch reach, close to the remnants of the Benavidez Ranch Dam (Figure 5.14). In general, hooked meanders have only developed along the lower Rio Puerco, downstream of the Benavidez Ranch reach. The active channel along this reach has been narrow for some decades. Thus, the meanders, rather than developing their geometry at the arroyo-scale, have begun to adjust to this narrow channel. The radius of curvature has, therefore, become far smaller. However, as tamarisk and natural levees have fixed the position of much of the active channel, the meanders are not able to entirely adjust to the reduced width and discharge. Meanders along the lower reaches have thus formed at several scales, giving the compressed, tortuous pattern observed today.

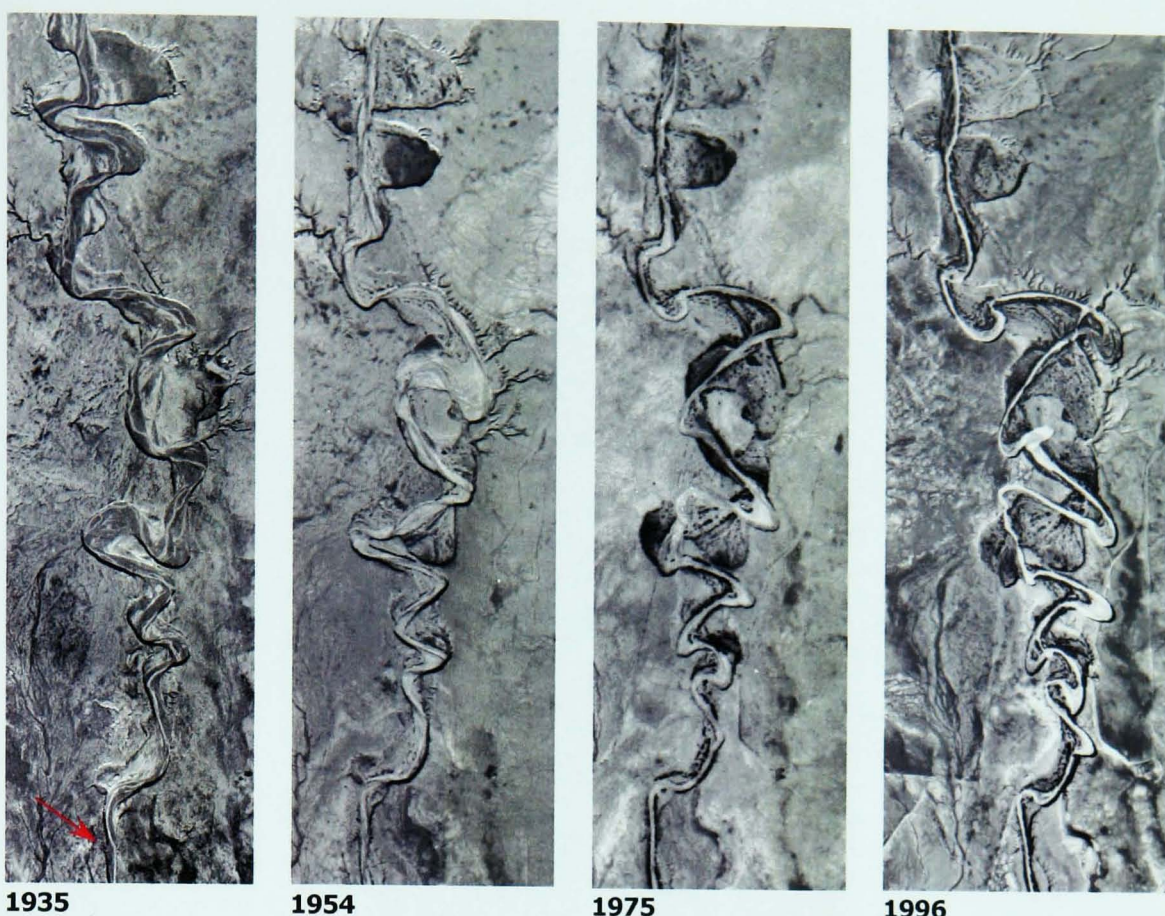


Figure 5.14 Development of hooked meanders downstream of the Benavidez Ranch reach. Arrow indicates remnants of Benavidez Ranch Dam.

Another factor which may have resulted in the pattern of recurved meanders along the lower reaches is related to the incision of the arroyo. As the active channel abuts the arroyo wall, which may be well over 10 metres high, it becomes fixed by the relative resistance of the sediments (Elliott, 1979). Thus the upstream limb migrates at a faster rate than the fixed downstream limb, causing a reduction in the radius of curvature. However, this hypothesis may not apply to the hooked meanders of the Rio Puerco, since upstream meanders, which formed at a similar time to those downstream, have not developed this pattern, even though they too impinge on the arroyo walls. It may be that the narrower active channel along the lower reaches is unable to carry sufficient discharge to erode the walls sufficiently to prevent the meanders from becoming distorted.

Compressed meanders just upstream from the Rio San Jose, and along the Rio San Jose itself, have punched laterally into the valley fill to such an extent that the tributary may soon enter the main arroyo considerably

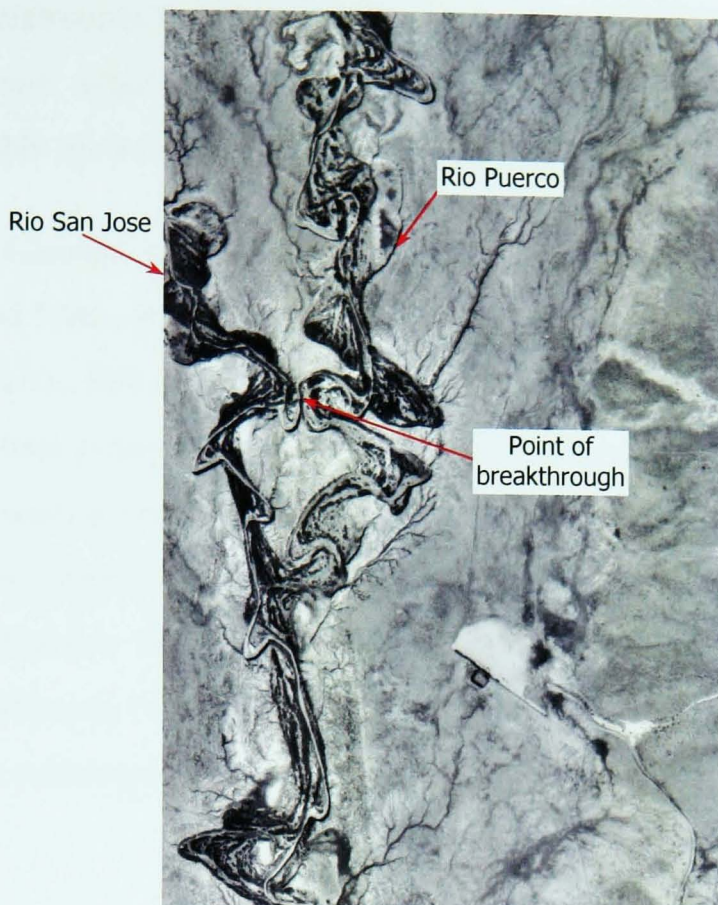


Figure 5.15 Lateral erosion of meander bends causing breakthrough of the Rio San Jose to the Rio Puerco, 1996.

further upstream. The mid-1990s aerial photographs show a very thin wall of sediment separating the two arroyos, with the active channel impinging this wall from both sides (Figure 5.15). Figure 5.15 also shows the lack of planform change as the Rio San Jose enters the Rio Puerco. Other large tributaries, such as the Arroyo Comanche and Arroyo Alamito entering the Rio Puerco along the lower reaches have a similarly minor effect, emphasising the geomorphological importance of the Arroyo Chijuilla and Arroyo Chico. It is likely that the downstream tributaries have evolved sufficiently that they are now aggrading, contributing far less sediment to the main arroyo system than the still-actively eroding upstream tributaries.

The headcutting observed by Nordin during the 1960s has continued to occur in the Bernardo reach. This reach has developed a deep, narrow active channel, which was still incising during the mid-1990s (see Appendix 2, Figure A2.9). However, this renewed incision does not seem to have progressed far upstream. This apparent “complex response” may actually, therefore, be adjustments to the local base-level of the Rio Grande, rather

than adjustments to intrinsic thresholds. Nordin (1963a) arrived at similar conclusions after his 1961 study: that local base-level changes were responsible for localised headcutting (Nordin, 1963a).

The Rio Grande has been evolving parallel to the Rio Puerco. During the 1930s and 1940s, the active channel of the Rio Grande was braided and wide. By the 1950s, this channel had become far less chaotic, meandering through unvegetated point and braid bars. During the 1960s and 1970s, these bars became semi-permanent, developing dense vegetation. By the mid-1990s, the active channel of the Rio Grande had developed into a wide, single-thread channel, with a braided low-flow planform. This morphological change affected both the gradient of the Rio Grande and also the point at which it converged with the Rio Puerco, thus causing the changes in base-level.

Santa Cruz River

Factors Affecting Evolution

The contemporary morphology of the arroyo reach of the Santa Cruz River is affected significantly by the surface geology of the Tucson basin, in particular through the upstream reaches. At Pima Mine Road, resistant Pleistocene sediments outcrop, with Holocene sediments confined to the uppermost metre. The dominance of Pleistocene sediments along this section of the arroyo is thought to be due to the fact that incision initially took place along a wagon trail along this reach, as discussed in Chapter 3, thus causing the channel to be diverted from its natural floodplain (Betancourt, 1990; Parker, 1996). In this reach, the arroyo is significantly narrower than reaches cut into less-indurated Holocene sediments.

Further downstream, the igneous cores of Martinez Hill and Black Mountain sandwich the arroyo. The position of Martinez Hill is particularly crucial for the geomorphology of the arroyo, since it causes abrupt deflection of flow. The natural course of the arroyo is from south to north, directly towards the outcrop. The abrupt deflection has caused sediment deposition and a reduced stream gradient at this point, causing the only significantly sinuous

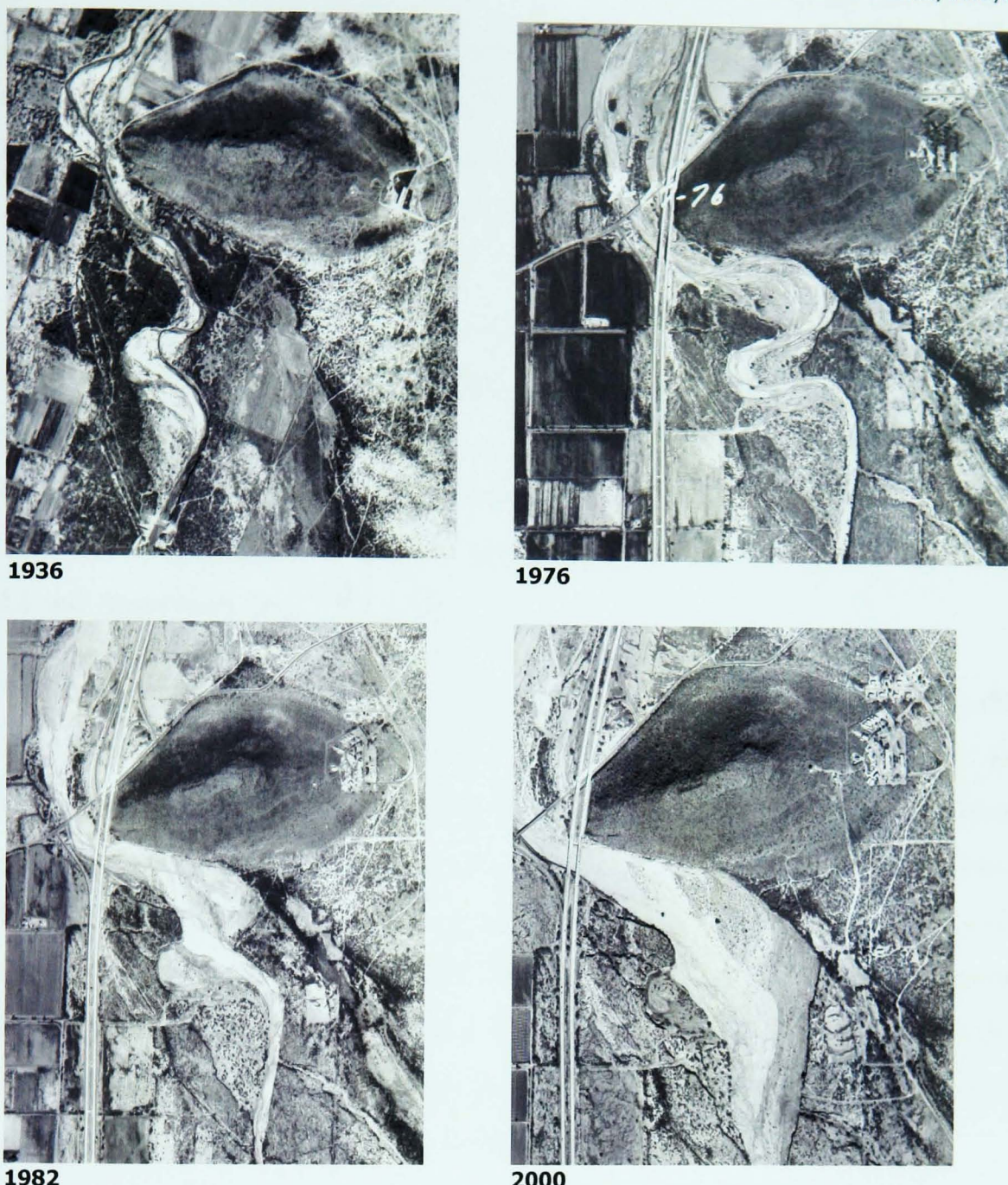


Figure 5.16 Aerial photograph showing compression of meanders against Martinez Hill and subsequent straightening during series of large floods.

entrenched reach. Since the meanders have been prevented from migrating downstream naturally, they have become compressed against Martinez Hill, although the sequence of large floods in recent decades has caused a significant reduction in sinuosity (Figure 5.16).

As discussed in Chapter 1, the Santa Cruz River is the only river studied with a major urban area situated close to the arroyo. The trench of the Santa Cruz slices straight through the city of Tucson. The population of the metropolitan area has been growing rapidly during the 20th century and in recent years. Between 1965 and 1985, Tucson saw an influx of 195,000

people (Slezak-Pearthree and Baker, 1987). United States census data indicated a 20 percent rise in population and a 24 percent increase in urban area between 1990 and 2000. This rapid growth is not ceasing, with a projected six percent growth over the last three years, to give a population of nearly 520,000 in September 2003 (City of Tucson Planning Department, 2003). The population expansion has, both directly and indirectly, had a significant effect on the morphological evolution of the Santa Cruz River, prompting the comment that “a major portion of the severe erosion which has occurred along the Santa Cruz River can be directly attributed to man’s activities within the river environment during the past 100 years” (Simons, Li and Associates, Inc., 1986, p56).

The trigger effect of irrigation and water-supply ditches and wells on the initiation of the arroyo was discussed in Chapter 3. The acquisition of an adequate water supply for the increasing population of Tucson has been problematic ever since. As early as 1895, falling water tables were reported by the Tucson Water Company, even with recharge due to a large flood on the Rillito River (Betancourt, 1990). Between 1940 and 1965, the water table lowered 21 metres (70 feet), with a cone of depression forming around the Tucson area. The last documented year that groundwater recharge equalled removal was in 1940 (Anderson, 1972).

The major consequence of groundwater removal has been the loss of vegetation and its stabilising effects (Baker, 1984; Saarinen *et al.*, 1984; Reich and Davies, 1987). Many mature cottonwood and mesquite trees within the arroyo trench have died, producing a far higher capacity arroyo trench (Reich and Davies, 1987; Betancourt, 1990). The loss of vegetation was further exacerbated early on in the 20th century by clearance of mesquite forests (detailed in Chapter 3), approximately 80 percent of which were destroyed by 1917 (Betancourt, 1990). Recovery of this vegetation was made impossible by the reduction in water table levels. The continued occurrence of high-magnitude floods, which cover the entire base of the arroyo trench, has also prohibited the growth of mature vegetation. For these reasons, the

Santa Cruz River was the only arroyo studied in this project which did not have dense stands of tamarisk established within the arroyo trench.

The rapid growth in population has caused increasing pressure to develop the river margins (Slezak-Pearthree and Baker, 1987). Unfortunately, flooding has had devastating consequences on these developments, requiring flood protection schemes to be implemented. The first major scheme to be implemented was the construction of an artificial channel in 1915. As discussed in Chapter 3, this channel joined the east- and west-side barrancas, which were already both entrenched (Betancourt, 1990). The design of this structure was proposed in 1913 by Olberg and Schanck, with the purpose of preventing land on the San Xavier Reservation being ruined by overbank flow (Betancourt, 1987). More recently, the arroyo between Martinez Hill and Congress Street was straightened to minimise lateral erosion, with the outer banks of severe bends being protected by revetments (Saarinen *et al.*, 1984).

The increased occurrence of large magnitude floods since 1960 exposed the vulnerability of construction and land close to the arroyo margins. This was exacerbated by the fact that the primary mechanism of adjustment of the contemporary Santa Cruz River is lateral erosion (Baker, 1984; Saarinen *et al.*, 1984; Parker, 1996). The Federal Emergency Management Agency (FEMA) guidelines on floodplain zonation were developed for perennial rivers, which tend to flow overbank during floods, rather than eroding laterally (Simons, Li and Associates, Inc., 1986; Parker, 1996). Bank protection of various forms was first utilized during the 1950s. The lateral shifting of the Santa Cruz River during large flow caused flood protection schemes, developed by planners unused to the regime behaviour of arroyos, to be woefully under-engineered. The bank protection implemented during the 1950s to 1970s was designed for a 850 cumec flood. The 1983 flood had a peak of 1,500 cumecs, equating to a return period of close to 1000 years if calculated using the entire flood series (Reich and Davies, 1987). Planners



Figure 5.17 Aerial photograph showing collapse of I19 during 1983 flood.

had not taken in to account the non-stationarity of the flood series (discussed in Chapter 4).

The most widely used method of bank protection has been the emplacement of a soil cement lining along much of the arroyo downstream of Valencia Road, extending north of the Tucson metropolitan area. Unfortunately, the effects of this protection on the arroyo have not been entirely positive. Since the primary mechanism of adjustment of the Santa Cruz River is lateral erosion, the implementation of soil cement effectively prevents this occurring. Thus, the only subsequent mechanism of adjustment is bed scour, which may lead to unprotected banks reaching or exceeding their critical bank height. Consequently, a higher degree of lateral erosion than expected occurs along these reaches. Piecemeal soil cement flood protection causes unprotected reaches to be subject to phenomenal scour, especially along the outer banks of meanders (Baker, 1984; Saarinen *et al.*, 1984). During large floods, such as the 1983 and 1993 floods, this scour caused the undermining of bridge revetments and piers, causing them to become unsafe and even to collapse (Saarinen *et al.*, 1984). Three major bridge failures, including the major I19 crossing, occurred during the 1983 flood (Figure 5.17) (Simons, Li and Associates, Inc., 1986). Similarly, inadequately

keyed-in soil cement was flanked by upstream lateral erosion, leaving it abandoned in mid-channel (Saarinen *et al.*, 1984). As Saarinen *et al.* noted in 1984, “partial bank protection will beget the need for more bank protection”.

The presence of a convenient dumping ground close to a large urban area has resulted in the channel of the Santa Cruz River being used as a landfill site along some reaches. This effectively constricts the channel, in much the same way as soil cement (Betancourt, 1990). However, landfill material is far less resistant than either the original bank material or soil cement bank protection, and it is thus preferentially eroded (Simons, Li and Associates, Inc., 1986). Parker (1996) has noted that the increase of landfill operations south of Tucson corresponds with a period of degradation.

The increase in both the urban area and the constriction of the arroyo with bank protection has had an undeniable effect on the hydrologic regime of the Santa Cruz River. The low permeability of the built-up valley bottom combined with artificial drainage channels and pipes has, therefore, reduced infiltration, causing a greater percentage of precipitation and runoff to reach the arroyo (Saarinen *et al.*, 1984). The amount of sediment available for transportation has also been reduced, thus causing flows to become more competent and erosive (Parker, 1996). This has had the most effect at the Tucson gauge, as well as those downstream that are not pertinent to this study. Reich and Davies (1987) noted that peaks at the Tucson gauge were only 60 percent of those recorded at Green Valley during the late 1940s, but magnitudes had increased to 85 percent of the Green Valley peaks between 1960 and 1980. By the 1983 flood, the Tucson gauge recorded a peak 20 percent larger than that upstream. However, this is perhaps not entirely due to urban effects, since, as discussed in Chapter 4, larger magnitude flows are far less likely to decline in volume downstream.

Flood flows passing the Tucson gauge are thought to have increased in velocity due to the accelerating effects of soil cement, channel straightening and reduced lag times (Reich and Davies, 1987; Parker, 1996). This resulted in extremely rapid flow during the 1993 flood, with velocities reaching seven

metres per second (Parker, 1996). Therefore, the 1993 flood did not reach the peak discharge as the 1983 flood and was actually not significantly greater than other large winter floods. However, the volume of flow during this flood reached record levels, the difference being that flows during the 1993 event were more rapid and also more prolonged than previous floods (Boyd *et al.*, 1993; Parker, 1996). Unfortunately, the discontinuous records at this gauge make it impossible to substantiate this statement.

A further consequence of the expansion of the Tucson metropolitan area has been the need for larger roads. Both major interstates, I10 and I19, were raised on embankments, constructed from sand and gravel taken from the Santa Cruz River bed. Over 700,000 cubic metres was removed from the San Xavier reach during the 1960s for the construction of the I19 embankment (Figure 5.18) (Reich and Davies, 1987). Similarly, over 1.2 million cubic metres (920,000 cubic yards) of material was removed from between Grant Road and Silverlake Road during the construction of I10 (Simons, Li and Associates, Inc., 1986). Sand and gravel extraction for construction and other purposes is still ongoing due to the ease of removal and has had a significant

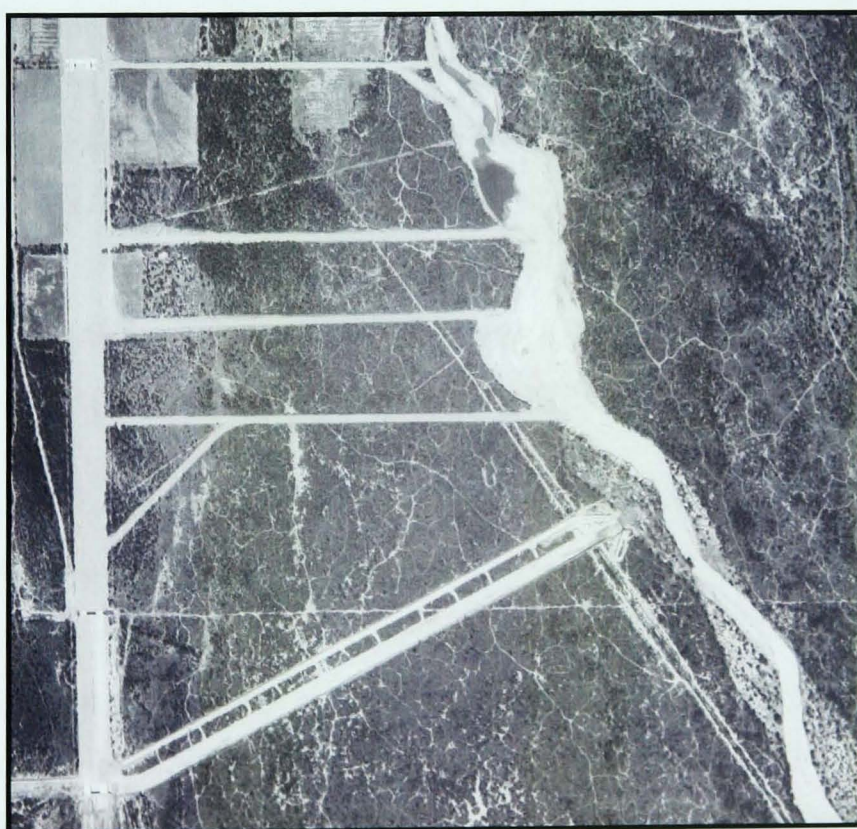


Figure 5.18 Aerial photograph of mid-San Xavier reach showing sediment extraction for construction of I19, 1967.

effect on the morphology of the Santa Cruz River over the past few decades (Bull and Scott, 1974; Baker, 1984; Saarinen *et al.*, 1984; Simons, Li and Associates, Inc., 1986). Mining from the stream bed causes artificial degradation, which works upstream during flow events (Bull and Scott, 1974; Baker, 1984; Saarinen *et al.*, 1984). Thus, similar effects to natural degradation, including scour of bridge abutments, bank protection and natural banks, may be sufficient to cause failure as banks exceed their critical bank height (Simons, Li and Associates, Inc., 1986). Temporary bank protection structures are often implemented to divert water away from the mining pits (Baker, 1984; Saarinen *et al.* 1984). Failure of these structures can cause significant local morphological change. During the 1983 flood, failure of one such structure triggered the capture of a sand and gravel pit, which caused lateral migration of over 200 metres (700 feet) (Simons, Li and Associates, Inc., 1986).

The effects of bed scour during flood events, both due to the prevention of lateral erosion by bank protection and sand and gravel mining are thus problematic. Further channel modification was, therefore, implemented to prevent this. Grade control structures were built at several places on the channel, although some have since been washed out. Approximately 0.8 kilometres (0.5 miles) upstream of Martinez Hill, a concrete dam was built to control degradation. This was washed out during the 1977 flood (Reich and Davies, 1987). Structures also prevent degradation downstream of Congress Street and Grant Road. As a result, the course of the arroyo through Tucson is effectively fixed, preventing the natural morphological evolution.

Parker (1996) suggested that the predominance of different storm types had a direct effect on the morphology and, thus, evolution of the Santa Cruz River. Periods when monsoonal storms produce the majority of significant streamflows are dominated by local erosion and general deposition. Since these floods are generated by local convective storms, with little downstream flow connectivity, they have little system-wide impact. Thus, sediment transport is also discontinuous, both spatially and temporally.

Sediment within the active channel is the most mobile, leading to the lateral accretion of semi-permanent bars and berms. It, therefore, follows that the dominance of monsoonal flows generally leads to a decrease in cross-sectional area of the active channel, aggradation of the channel bed and relatively low rates of erosion. The Santa Cruz River was dominated by monsoon-storm-generated floods between 1930 and 1959 (discussed in Chapter 4)

Prior to 1930 and between 1960 and the present day, the dominance of frontal and tropical storm-generated flows had the opposite effect on the arroyo morphology. Parker (1996) noted that when 30 percent or more of floods are generated by these types of storm, the amount of sediment mobilised from storage increases. Flows generated by frontal and tropical storms tend to be longer-lasting and are more likely to activate long reaches of the system. However, Parker (1996) has noted that tropical storms, as well as being longitudinally continuous, are also subject to localised, intense energy pulses, similar to monsoonal flows but with far higher magnitude. Tropical storm-generated flows were also discovered to be the only type over the period of record which continuously gained stream power in a downstream direction. While the majority of frontal storms increase their stream power downstream, a significant proportion were found to attenuate, causing a decrease in power. The continuous nature of floods generated by both frontal and tropical storms, combined with the high associated stream power, thus results in highly competent flows which efficiently transport sediment through the arroyo system. Therefore, a predominance of frontal and tropical storm flows causes significant sediment reworking, with even the coarsest fractions being mobilised. During these periods, the cross-sectional area of the active channel tends to increase, with accompanying bed degradation and high rates of bank erosion.

Arroyo Evolution

After the initial degradation of the Santa Cruz River (documented in Chapter 3), the Santa Cruz River followed the evolutionary pattern

described by incised channel evolution models (summarised in Chapter 2) and began eroding laterally. During the December 1914 flood, which peaked at 425 cumecs, 60 metres of lateral erosion during a single day occurred close to Congress Street, causing the channel to double in width (Saarinen *et al.*, 1984). By the 1920s and 1930s, despite large floods during 1926 (323 cumecs) and 1929 (295 cumecs), aggradation had begun occurring at this site as sediment from the still-eroding arroyo reaches further upstream began to accumulate, indicating that the morphology of the arroyo was again evolving in a pattern concurrent with that suggested by incised channel evolution models.

After the 1920s, the monsoon-dominated hydroclimatic regime also encouraged aggradation (Parker, 1996). Aerial photographs taken in 1936 indicate a relatively narrow arroyo trench with a significant amount of vegetation stabilising the bed. At this point, the upstream reaches of the San Xavier Reservation had only just begun degrading in response to headwards migration of knickpoints, with downstream reaches as yet unincised. The construction of the artificial link between the east- and west-side barrancas

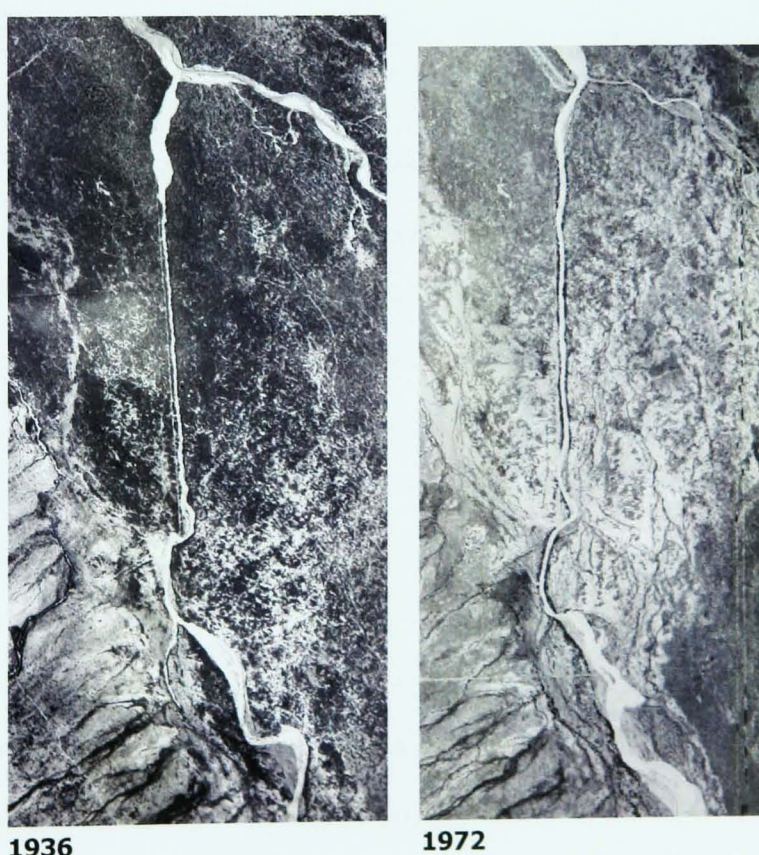


Figure 5.19 Artificial channel between east- and west- branches of Santa Cruz River, 1936 and 1972.

in 1915 undoubtedly contributed to the rapidity of headwards knickpoint migration. By 1936, the artificial channel showed remarkably little change (Figure 5.19). Close to the former east branch of the Santa Cruz River, a short, widened reach had formed due to sediment deposition. This occurred due to backwater effects since the former channel of the Santa Cruz River, now renamed Lee Moore Wash, was still the dominant channel. The arroyo incision, working headwards at this time, caused much sediment to be released into the system, which would be preferentially deposited in low-velocity areas. At the upstream end of the artificial straight reach, very little meander modification had occurred.

During the 1940s and 1950s, the active channel width continued to narrow, indicating continued stabilisation. During this period, however, the arroyo trench continued to enlarge during rare high-magnitude floods, such as those in August 1940, August 1945 and August 1955, which were all above 300 cumecs. This difference illustrates the compound behaviour of the arroyo system, whereby the arroyo trench and the inner channel evolve independently of each other.

A combination of factors during the 1950s caused a reversal of the aggradational phase (Saarinen *et al.*, 1984). The lowering of the water table; the increase in size of the urban area and the implementation of flood protection schemes, causing both straightening and constricting of the arroyo, have all combined to cause renewed degradation along the Santa Cruz River. Since 1960, degradation has been exacerbated by the change in flow regime, which caused an increase in the frequency and magnitude of frontal and tropical storm generated floods. The construction of interstate highways during the 1960s resulted in huge quantities of sand and gravel being mined from the arroyo bed, again causing degradation to occur. At Pima Mine Road, approximately 7.5 metres of incision occurred between 1936 and 1976, with up to 6.5 metres of this entrenchment occurring after the mid-1950s (Parker, 1996). Morphological change since the 1960s has, however, not been consistently degradational in character. Active channel

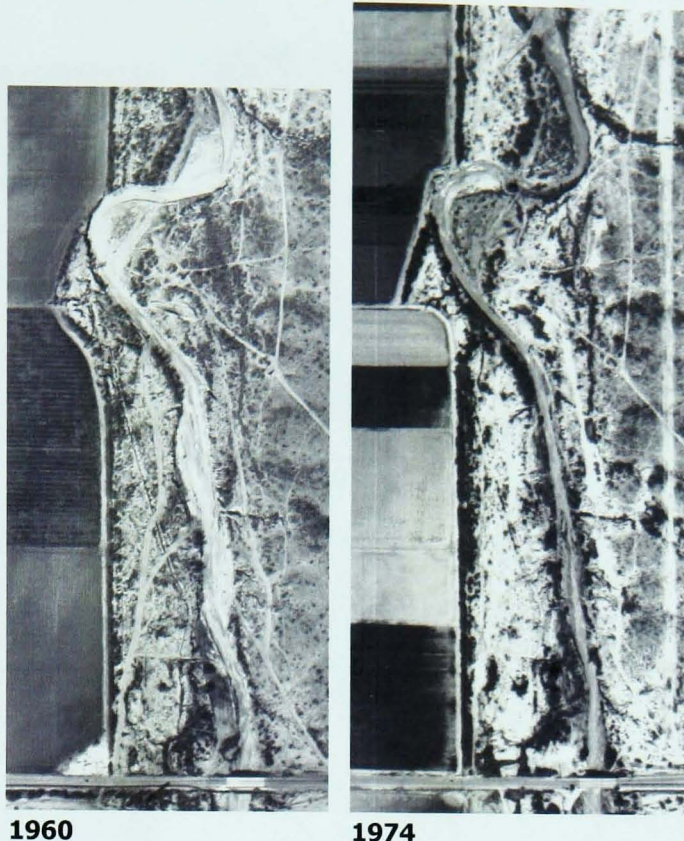


Figure 5.20 Aerial photographs showing narrowing and inner channel stabilisation of the Santa Cruz River between 1960 and 1974 at Valencia Road.

narrowing occurred during a period of lower-magnitude flooding during the early 1970s (Figure 5.20).

Since the high-magnitude flood of October 1977, the Santa Cruz River has experienced a historically unprecedented series of high-magnitude floods, which have resulted in the greatest amount of channel change subsequent to arroyo initiation. Major geomorphological changes occurred during the 1977 and December 1978 floods. Interestingly, although the 1978 flood, with a peak of 382 cumecs at the Tucson gauge, was close to half the size of the previous flood (671 cumecs), aerial photographs indicate that larger amounts of channel change occurred due to this flood through the upstream reaches of the arroyo (Figure 5.21). It is likely that the greater width change during the second flood was due to significant degradation during the 1977 flood, causing the arroyo walls to surpass their critical bank height. A grade control structure upstream of Martinez Hill washed out, thus causing a new knickpoint to begin working headwards through the system, which also contributed to the amount of degradation that occurred. During the 1978 flood, therefore, lateral erosion predominated. This erosion released larger

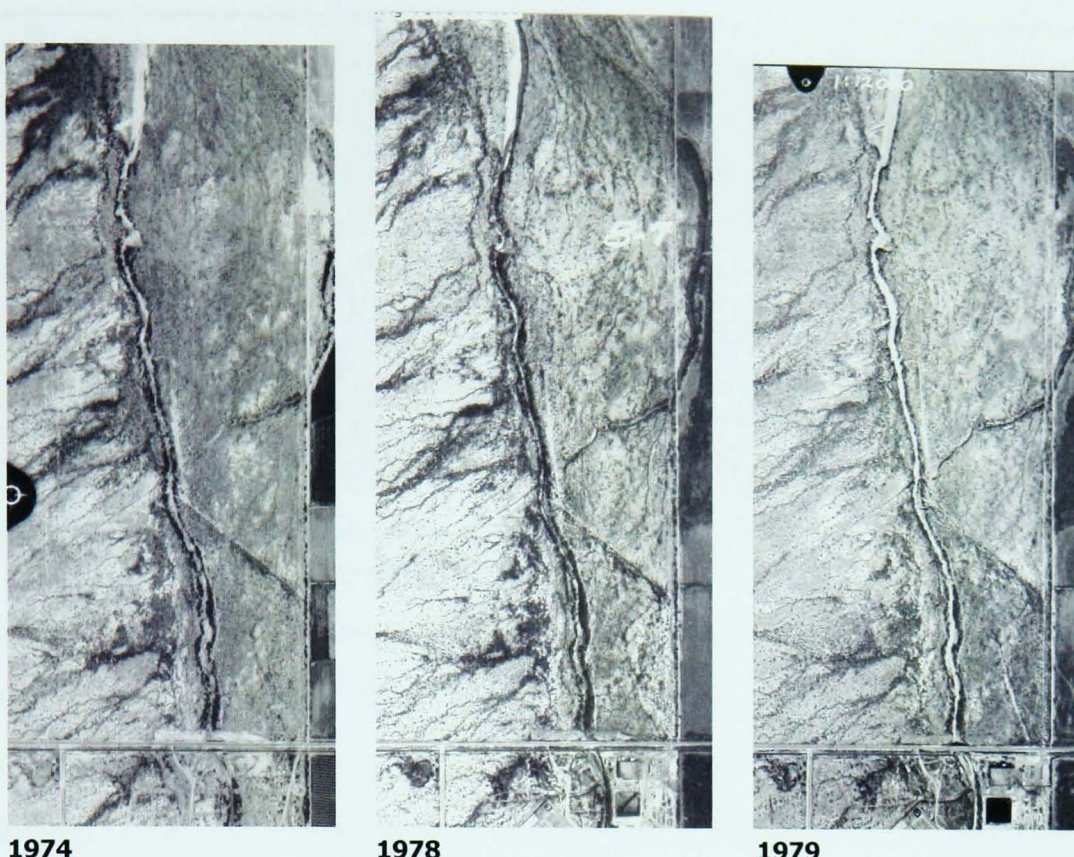


Figure 5.21 Aerial photographs showing geomorphological changes of the Santa Cruz River at Pima Mine Road due to high-magnitude flooding in October 1977 and December 1978.

quantities of sediment into the system downstream. The increase in the rate of bed degradation, especially through the San Xavier Reservation, caused tributary gullies to begin headcutting in response to the drop in base-level, again contributing to the increase in sediment supply.

The floods of the late 1970s were followed in quick succession by the flood of record in October 1983 (1,492 cumecs), and another large flood in December 1984 (282 cumecs). The 1983 flood, designated a “superflood” due to its extreme magnitude and geomorphic effect, caused the most channel change ever wrought by a single flood on the Santa Cruz River. The stream power of this flood was increased by the constrictions imposed on the arroyo due to flood protection schemes, such as soil cement, bridge revetments and grade control structures. These constrictions prevented the natural lateral adjustment of the arroyo, causing flood levels to become perilously close to trench-full, especially through the urban reaches (Figure 5.22). The relatively low channel capacity due to the outcropping of resistant Pleistocene sediments at Pima Mine Road and artificial



Figure 5.22 View upstream from St. Mary's Road before and during 1983 flood (courtesy P. Kresan).

constrictions in the channel upstream caused overbank flooding to the east of the Santa Cruz River. The overbank flow was heavily sediment laden and caused much destruction, flowing across orchards and roads, before entering Lee Moore Wash through a network of rapidly headcutting gullies.

The 1983 flood caused a great deal of both lateral erosion and degradation along the unaltered reaches, essentially causing a clean-out of stored sediment. At Valencia Road, up to three metres of net degradation occurred (Saarinen *et al.*, 1984). Lateral erosion was greatest along the outer bank of meander bends. During large floods, the thalweg straightens in order to increase the water surface slope, in turn increasing efficiency. Thus, during the 1983 flood, the apex of many meander bends shifted downstream significantly, causing large amounts of material to be eroded. The natural obstruction of Martinez Hill caused deflection of the flow and significantly higher rates of outer bank erosion along meander bends through this reach. It was this factor which caused the undermining and eventual collapse of the I19 bridge (Figure 5.17).

Downstream of Tucson, in Marana, where the Santa Cruz River is unconstricted, flood-flows were able to spread out, causing a deceleration, loss of competence and thus deposition of the huge quantity of transported suspended sediment. The destruction of farmland in this area was compounded by headwards erosion of gullies, created by oversteepened reaches at the downstream limit of deposited sediment.

The second largest flood of record, in January 1993, again caused a significant amount of geomorphological change. During the intervening 10 years, large monsoonal flows had been recorded during the summers of 1988, 1990 and 1992. Flow peaks during the 1993 flood showed the effect of extrinsic and intrinsic factors. At the Continental gauge, upstream of the entrenched arroyo reach, peak discharge was 1,014 cumecs. By the time the flow had reached Valencia Road, this peak had attenuated to 623 cumecs (Boyd *et al.*, 1993). Part of this loss occurred due to overbank flow upstream of Pima Mine Road bridge. However, some of this water re-entered the system through Lee Moore Wash, as had occurred during the 1983 flood, causing significant headcutting of the contributing gullies. Downstream, at the Tucson gauge, the discharge peaked at 1,059 cumecs, indicating the increased runoff due to the impermeability of the urban area.

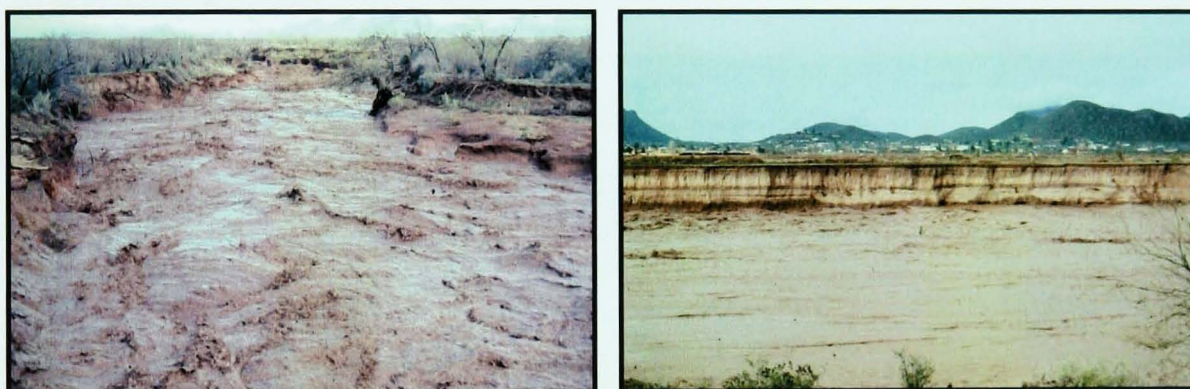


Figure 5.23 Trench-full flow at Pima Mine Road and significantly lower flood stage at Valencia Road, January 1993. Photograph taken during recession of flood, just after peak (courtesy J. Parker).

During the 1993 flood, near-trench-full flows occurred at Pima Mine Road and at Congress Street. At Valencia Road, however, although flows were bank-to-bank, the stage was nowhere near trench-full (Figure 5.23). The arroyo just downstream of Valencia Road was studied in both 1991 and just after the 1993 flood. Despite the extremely high-magnitude flow, little geomorphological change as a result of the 1993 flood could be discerned along this straight reach (Ellis, 1993). At the outer banks of meander bends, however, lateral erosion was substantial. For example, at the outer bank of a meander bend just downstream of Grant Road, over 50 metres of lateral erosion occurred. Although the geomorphic changes along the arroyo were

significant where the thalweg impinged against the arroyo walls, far less damage to property, bridges and roads occurred, when compared with the 1983 flood. Flows downstream of Martinez Hill, where damage was likely to have occurred, were sufficiently protected to prevent significant damage. Thus, from a commercial point of view, the bank protection schemes implemented through Tucson were highly successful. However, in Marana, downstream of Tucson, large quantities of sediment were again deposited as flows dispersed, causing damage to property, farmland and roads (Boyd *et al.*, 1993).

The removal of the grade control structure upstream of Martinez Hill in 1977, followed by the sequence of large floods during the 1980s and 1990s caused the reach downstream of Pima Mine Road to degrade appreciably (Figure 5.24). Once this degradation had caused the arroyo walls to reach a critical height, widening commenced, replicating the pattern of development which had previously occurred in downstream reaches.



Figure 5.24 View from Pima Mine Road bridge after 1983, 1993 and 2000 floods (1983 photograph courtesy J. Parker).

Since the 1993 flood, the sequence of high-magnitude floods has again continued, especially during the summers of 1998 and 1999. The November 2000 flood was the most recent, with a peak of 326 cumecs at the Tucson gauge. During these floods, wall-to-wall flows occurred at the constricted reaches downstream of Pima Mine Road and through Tucson. A similar

pattern of geomorphological change was observed as a consequence of each flood, the amount of change depending on the size of the flood (discussed further in Chapter 6). However, aggradation, rather than basal scour occurred during the smaller floods, indicating their lower sediment transport capacity and longitudinal connectivity.

San Simon River

Factors Affecting Evolution

The San Simon River has, like the Santa Cruz River, been subject to a great deal of artificial alteration which has significantly affected the evolution of the arroyo. As discussed in Chapter 3, an aggressively headcutting arroyo had caused the incision over 97 kilometres (60 miles) of the river by the 1930s. However, the main problem for land managers in the San Simon River basin were the networks of tributary gullies and arroyos radiating from the main trench, combined with significant amount of sheetwash erosion from the valley floor (Figure 5.25). Thus, during the 1930s, the Civilian Conservation Corps built a series of rock barriers on the valley floor, combined with small diversion dams, dykes and gully plugs, in an attempt



Figure 5.25 Headcutting tributary gullies, 1963 (courtesy of Safford BLM).

to halt this erosion. Many of these rudimentary sediment detention structures were too small to be effective and they were not maintained for a long period of time (Cooke and Reeves, 1976; McClure *et al.*, 2000). By the 1940s, the severe headcutting during each major flood meant that the San Simon basin was “recognised as one of the most degraded [sic] watersheds in the United States” (Molitor, 1997, p3).

Channel incision caused lowering of the water table, die-off of perennial vegetation and an increase in the amount of sheet erosion. This prompted the Soil Conservation Service to construct three large detention dams. The upper and lower Cienega dams were built across the main channel close to the Arizona/New Mexico border in order to prevent further headcutting of the mainstem. Goat Well dam was built across Slick Rock Wash in 1940, a large tributary, above the actively eroding headcut, again to prevent further headwards erosion (Figure 5.26).



Figure 5.26 Goat Well Detention Dam a) looking upstream at aggraded channel, b) looking down drop structure into Slick Rock Wash arroyo.

After the Bureau of Land Management (BLM) took over the management of 49 percent of the drainage basin area in 1949, further detention dams were built. In 1953, the first major dam, the Fan Dam, was built across the mainstem of the San Simon River. This failed during a large flood in 1954 and was subsequently rebuilt successfully in 1955. Dams continued to be built until a government stop order, imposed by the Secretary of the Interior halted further construction between 1957 and 1965, then between 1972 and 1980, since water-users downstream objected to possible interference of their

water-supply (Mathis, 1983; BLM, 1990; Molitor, 1997). Despite these interruptions, a total of 19 detention dams have been built throughout the arroyo system. The majority of these were constructed across eroding tributary channels. A second major dam, the Barrier Dam, was built across the main arroyo, close to the confluence with the Gila River, in 1980. Both mainstem detention dams have caused significant upstream regrading of the bed.

In addition to the construction of detention dams, the BLM has also implemented range and livestock management schemes to restore vegetation coverage within the watershed (Molitor, 1997). During the 1960s and 1970s, trial seeding areas were planted, generally unsuccessfully. The only successful seeding occurred at the Contest Well site, just upstream of the Fan Dam. Here, planting facilitated aggradation, causing a negative feedback, which allowed further re-vegetation and arroyo infilling (BLM, 1990). By 1970, livestock numbers in the watershed had been reduced to 5,000, ten percent of their 1900 figures (Jordan and Maynard, 1970). In 1980, these figures were reduced by a further 23 percent (Molitor, 1997). In addition, rotational grazing was implemented, with some areas, particularly just upstream of the newly built Barrier Dam, excluded entirely to allow recovery of vegetation. Watering areas were also dispersed to prevent trampling erosion by livestock.

As in the Rio Puerco arroyo trench, tamarisk are also found in dense stands on the San Simon arroyo floor. However, the date of introduction of this species has not been documented, indicating that the tamarisk within the drainage basin may be as a result of natural invasion. Inspection of the available aerial photographs of the arroyo system indicate that tamarisk numbers gradually increased from virtually zero in the 1935 photographs to the dense stands observed in the contemporary arroyo. The effect of tamarisk on the morphology of the San Simon River has not been addressed by other researchers, although it has been recognised that this type of shrubby vegetation is responsible for concentrating, rather than dissipating,

runoff on the valley floor. The BLM has root ploughed test seeding areas in order to remove tamarisk and other woody shrubs, such as mesquite. At the Contest Well seeding, undesirable tamarisk and mesquite were replaced with grasses (Mathis, 1983; BLM, 1990).

Arroyo Evolution

Very few geomorphological studies of the San Simon River have been made, with the exception of BLM monitoring, thus aerial photographs have mainly been used to determine the evolution of the arroyo. By the time the first aerial photographs were taken in 1935, the arroyo had incised and widened considerably. Much lateral erosion is likely to have occurred during the flood of record in 1931, which peaked at 765 cumecs (27,500 cfs). The 1935 channel still showed the effect of this flood, with a broad, unvegetated, braided low-flow channel covering the base of the arroyo trench.

Entrenchment of the main San Simon River channel triggered a huge amount of erosion in large networks of tributary arroyos and gullies. Depleted vegetation cover across the valley floor resulted in sizeable areas being eroded by sheetwash, which are clearly visible from the aerial photographs. However, of the two largest tributaries, Timber Draw and Gold Gulch, only Gold Gulch was incised to any degree in 1935, although a gully network had begun working headward from the mouth of Timber Draw.

The San Simon River was generally of low sinuosity, except through several short meandering reaches. Downstream of Gold Gulch, the heavy load of sediment from the newly incising tributary, combined with a natural bedrock constriction had lowered the gradient sufficiently to cause a short series of tortuous meanders (Figure 5.27). Other meandering reaches were also located in reaches constricted by bedrock outcrops. The longest of these reaches occurs between Tanque and Goat Well, where the San Simon valley is narrow. This is the only reach with a well-developed, continuous series of meanders. In this reach, particularly large meander bends are inevitably situated slightly upstream of a resistant outcrop.

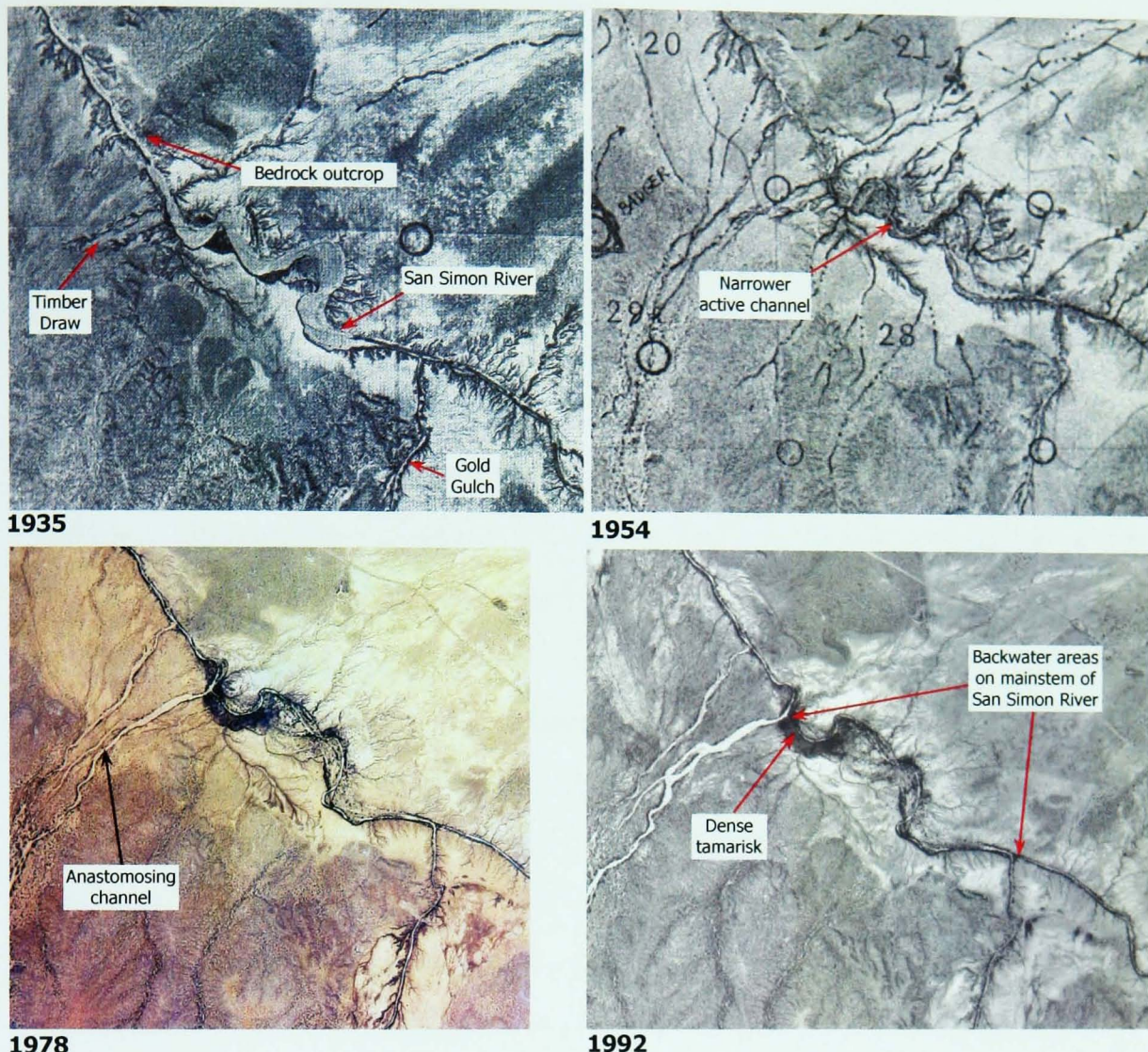


Figure 5.27 Arroyo evolution between Gold Gulch and Timber Draw, 1935 - 1992.

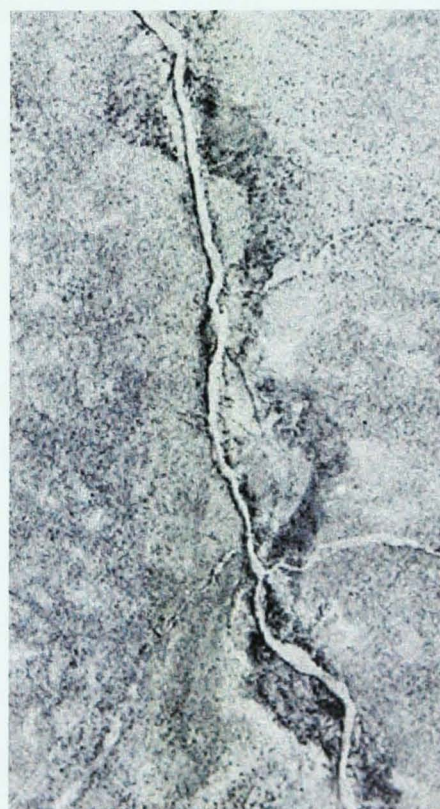


Figure 5.28 Straightened arroyo trench along Yellowhammer reach, 1941.

The arroyo through the Yellowhammer reach had clearly straightened during incision (Figure 5.28). The meandering path of the former, pre-incision channel can clearly be observed on the aerial photographs, indicating a significant steepening of the channel gradient. In this reach, several east-bank tributaries were actively eroding by the time of the first aerial photograph in 1947.

The 1953 aerial photographs indicate that the San Simon River had begun to stabilise. Deposition within the arroyo trench had caused narrowing of the active channel, creating point bars and berms. This narrowing was especially noticeable in the wider meandering reaches, such as between Gold Gulch and Timber Draw (Figure 5.27); and in the Goat Well reach (Figure 5.29). In these meandering reaches, outer bank erosion had caused more angular meanders to form, with significantly reduced radii of curvature. This is likely to have been in response to the decrease in channel width, with the meander geometry partially adjusting to the reduced conveyance of the active channel, as seen in the Rio Puerco meanders.

By 1953, Timber Draw had become incised, developing an anastomosed channel with very few actively eroding tributary gullies (Figure 5.27). In contrast, the gully network radiating from Gold Gulch had continued to erode headward. There was still very little vegetation established within arroyo, although tamarisk had become established on some point bars in meandering reaches. The Fan Dam had just been completed and sediment deposition had not, therefore, commenced upstream from this structure. However, sedimentation behind Goat Well detention dam had effectively prevented continued headcutting of Slick Rock Wash.

Significant development of the arroyo had occurred by 1963. A compound channel had clearly developed. However, the active channel, while well-defined, was still braided in sections and was still relatively wide. An inner floodplain had developed, which had been stabilised by dense tamarisk. This had preferentially colonised point bars and abandoned terraces along

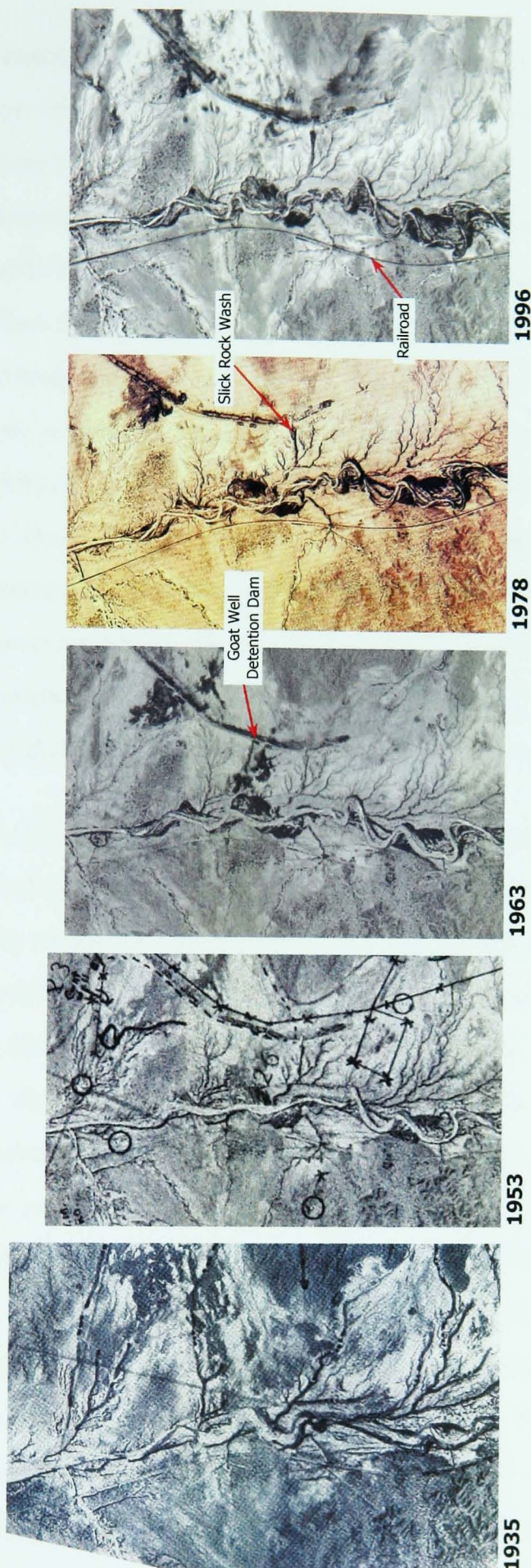


Figure 5.29 Arroyo evolution between 1935 and 1996, Goat Well Sub-Reach, Lower San Simon.

the meandering reaches. This vegetation was growing in clearly visible lines along the position of former meanders, as observed along the Rio Puerco. Meander evolution had continued to cause outer bank erosion where the active channel impinged against the arroyo wall. It is noticeable that the active channel still flowed around outer edge of meanders, rather than adjusting its radius of curvature and wavelength to the narrower channel dimensions. Actively eroding tributaries were, by this time, contributing considerably more sediment than the main San Simon arroyo. Backwater areas can be observed upstream of major tributaries, such as Gold Gulch, although Timber Draw was not yet having the same blocking effect. The tributaries themselves were often considerably broader than the mainstem, indicating that these systems had not yet become wide enough to trigger the deposition of sediment in bars and berms. Headward erosion of gully networks continued to be a cause for concern for the BLM (Figure 5.25).

By 1978, the San Simon River had developed a mainly single-thread active channel, which had narrowed further but still remained relatively wide. The decreased capacity of the evolving arroyo had apparently resulted in trench-full flows during the 1975 flood, which peaked at approximately 100 cumecs (3,500 cfs) at the Solomon Gauge. The Arizona Republic reported that the flow was “just about all the San Simon River could handle without overflowing everywhere... the brush [had] grown in so much that it [couldn’t] handle what it used to” (12th September, 1975). However, it is extremely unlikely that a flood of this magnitude was anywhere close to trench-full stage, although floodwaters may have covered the arroyo floor. Significant vegetation growth had stabilised point bars, abandoned meander terraces and berms, thus creating an inner floodplain. The active channel still generally flowed around the outer bank of meander bends, although the pattern of active channel sinuosity had been complicated by downstream migration of the apex through some bends, which reduced the radius of curvature (Figure 5.29). In comparison, major tributaries still had broad, braided, mainly unvegetated channels. Timber Draw, by this time, was

significantly larger than the main San Simon River (Figure 5.27). However, the rapid headcutting of tributary gully networks observed during previous years appeared to have slowed.

By the 1970s, the Fan Dam had proved very successful in trapping sediment. In 1970, the arroyo had aggraded some 13 kilometres (eight miles) upstream (Jordan and Maynard, 1970). By 1977, the effects were noticeable 19 kilometres (12 miles) upstream, almost to the Yellowhammer reach. It seems likely that a major source of sediment for this aggradation was the east bank tributaries along the Yellowhammer reach, which were still actively eroding during this period. The infilled area had been stabilised with naturally occurring and planted vegetation, which included grasses, cottonwood and willow, which, as discussed previously, were far more desirable species than the invading tamarisk (Mathis, 1983; BLM, 1990). Since the reaches above the Fan Dam had not begun to widen significantly prior to dam construction, rapid stabilisation occurred, with aggradation and narrowing of active channel. However, the Fan Dam was not entirely successful since by 1978, gullying was occurring at the upstream end of the aggraded reach (Figure 5.30) (Mathis, 1983). This suggests that a complex response mechanism had been triggered.

Although a second major detention dam was constructed across the main trench of the San Simon River in 1980, aerial photographs taken in 1992 and 1996-8 indicate that aggradation had not reached far upstream by this time. This lack of infilling is most likely due to the reduction in flow magnitudes, which are required to transport sediment and undoubtedly transported much of the sediment now deposited behind the Barrier Dam. The 1983 flood, which peaked at 146 cumecs (5,147 cfs), occurred during this period. Although this individual flood accounted for 90 percent of both streamflow and sediment volumes during that year, this flood was not of sufficient magnitude to cause a great deal of geomorphological change (Molitor, 1997). However, some erosion of gully networks and sheet erosion of the valley floor did occur, supplying sediment to the downstream reaches. By 1989,

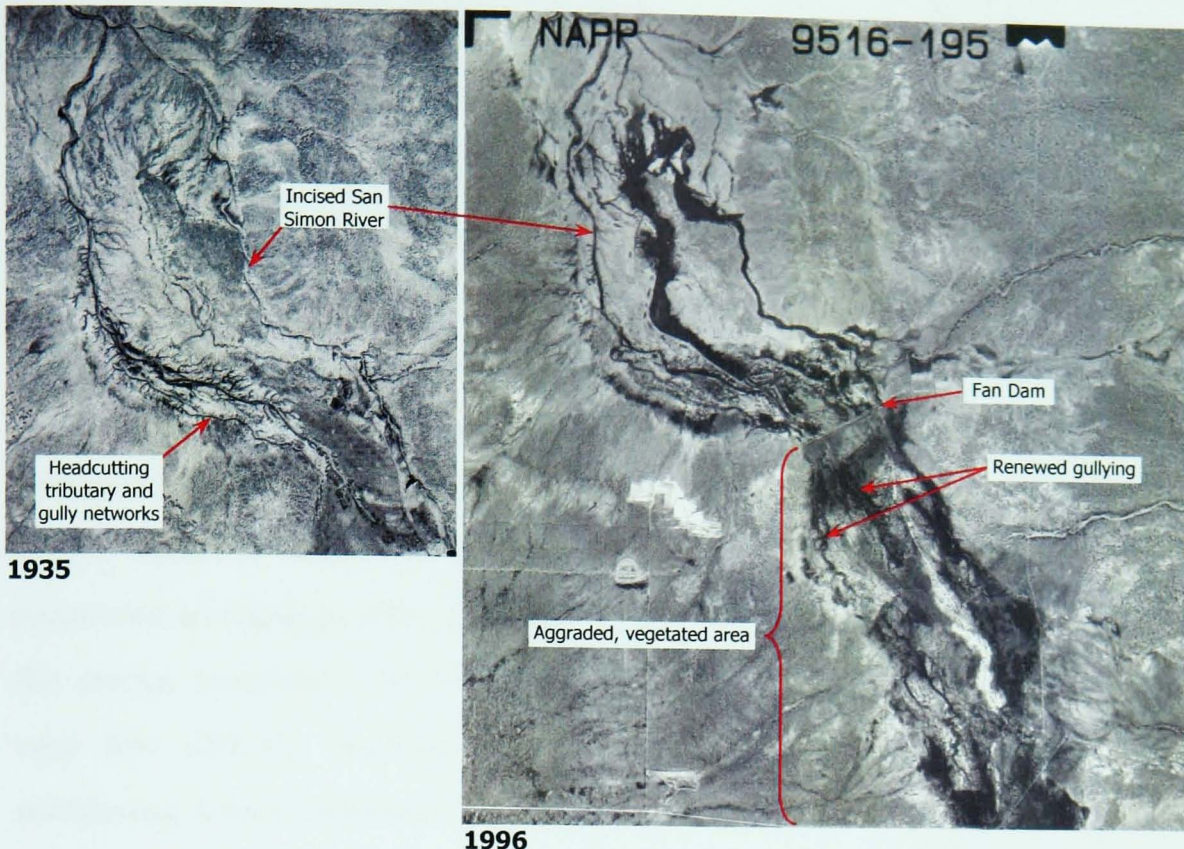


Figure 5.30 Morphological change caused by the Fan Dam.

the active channel upstream of the Barrier had aggraded 4.7 and 1.3 metres, 1.3 and 1.8 kilometres behind the dam respectively (Molitor, 1997).

1990s aerial photographs show that sedimentation behind the Fan Dam had not progressed much further upstream since 1978, suggesting that the channel through this reach had regraded to the new base-level (Figure 5.30). Meander evolution had continued, especially through the Goat Well reach (Figure 5.29). These meanders had become more convoluted, some even developing hooked, recurved apexes, similar to those observed along the Rio Puerco. Along the whole mainstem, meanders had tended to decrease their radii of curvature still further, indicating some adjustment to the reduced active channel width. However, in general, the wavelength and planform geometry of the meandering active channel was not adjusted to this decreased width, instead maintaining similar dimensions to the former, larger channel. The active channel planform had thus become superimposed onto the arroyo pattern. The density of vegetation cover within the arroyo, especially tamarisk, may have prevented significant migration of the active channel.

The two major tributaries, Timber Draw and Gold Gulch, in contrast to the San Simon River, showed continued morphological evolution between the 1978 and 1990s aerial photographs (Figure 5.27). Gold Gulch had begun to narrow, developing a distinct active channel with a vegetated, stabilised inner floodplain. However, significant tributary gully erosion had occurred since the 1978 image, probably during the 1983 flood. Timber Draw, although entering the San Simon River very close to Gold Gulch, had continued to develop a substantially different planform. The anastomosing arroyo network that was observed in the 1978 aerial photograph had continued to enlarge, with a braided low-flow channel covering the floor of the arroyo trenches. Timber Draw also differed from Gold Gulch in that very few actively eroding tributary gully networks radiated from the wandering arroyo channels. The difference in planform pattern between the neighbouring tributaries suggests that there is a significant difference in upstream sediment supply, with the supply to Timber Draw being far greater.

Observation of aerial photographs taken in 2001 show minimal change, indicating that stabilisation had continued. Narrowing of the active channel has continued very slowly, creating a very well-defined channel along the entire San Simon River. This is true even along the aggraded reaches upstream of both the Fan and Barrier Dams. Minor changes in the position of the active channel around large meander bends has occurred, with a small number showing retreat towards the inner bank or developing cut-off channels. One factor which it is interesting to note is that the artificially straight channel connecting the San Simon River to the Gila River, which was a contributing factor causing initial incision, is still straight and narrow. Thus through all the upstream arroyo evolution, this reach has remained relatively unchanged, even during the period of maximum sediment production during the mid-20th Century.

5.3 COMPARISON OF EVOLUTION IN ARROYOS STUDIED

Despite the fact that the Rio Puerco has been relatively unaffected by artificial alteration, evolution has not progressed headward in the simple manner proposed by Elliott (1979) and later by Gellis and Elliott (2001). Five geomorphologically distinct reaches were identified. The longest reach, between the Benavidez Ranch Reach and the confluence with the Rio Grande, together with the upstream reach, above the Arroyo Chijuilla, have evolved most rapidly, developing a quasi-stable morphology by the mid-1970s. This is characterised by a deep, well-defined active channel and a mature inner floodplain which has been stabilised by dense vegetation.

The reaches of the Rio Puerco downstream of the Arroyo Chico and Arroyo Chijuilla have responded to the additional input of flow and, more importantly, sediment from these tributaries. Overloading of the sediment transport capacity downstream of each confluence has caused the active channel to remain wide and shallow, effectively slowing the progression of morphological evolution. Abrupt boundaries between geomorphologically distinct reaches were also observed at the Ventana reach and the Benavidez Ranch reach, most likely due to a similarly abrupt change in bed-slope. Each reach along the Rio Puerco has, therefore, become adjusted to the flow and sediment discharge; gradient and vegetation conditions imposed (Love, 1997).

The pattern of natural evolution of the Santa Cruz River has been severely disrupted by artificial alteration. The initial evolution of the arroyo, directly following incision, appeared to follow the pattern of evolution proposed in incised channel and arroyo evolution models, whereby a degradational phase was followed by widening and the eventual creation of a stabilised inner floodplain and active channel. However, the bank protection schemes, when combined with other factors such as a decline in vegetation coverage due to water table lowering; removal of significant quantities of sediment for highway construction and the increase in the built-up area, have reversed this stabilisation process. Natural factors, especially the hydroclimatic shift

after 1960, have exacerbated this reversal. The resistant outcrop of Pleistocene sediments in the Pima Mine Road reach has resulted in the arroyo being far less adjustable than those reaches cut into the more erodible Holocene sediments. The Pleistocene reach is, therefore, still in the predominantly widening phase of evolution.

The evolution of the San Simon River has, like the Santa Cruz River, been significantly affected by anthropogenic alteration. However, the end result could not be more different. Detention dams have reversed the active erosion along much of the arroyo by effectively choking sediment from both the mainstem and large tributaries. The only major tributaries which are still producing significant amounts of sediment are Timber Draw and Gold Gulch. Seeding schemes have also stabilised the valley floor, reducing the amount of sediment entering the channel through sheetwash erosion. Thus, although there are huge areas with a high potential for erosion, by headwards and lateral erosion of tributary and gully networks, this potential is not realised due to the stabilising effect of increased vegetation both on the valley floor and within the arroyo. Many of the gully networks have remained virtually unchanged since the 1970s.

As discussed in Chapter 4, precipitation levels in the south-western USA have been increasing over the entire region. However, this increase has not been reflected in the flow and sediment discharge regime. There are perceptible relationships between arroyo morphology and the magnitude of these variables. Reaches which have developed a quasi-stable form have seen a concurrent reduction in discharge and sediment load. As the arroyo evolves, the width of the trench is increased until a maximum is reached and aggradation predominates. A negative feedback mechanism is subsequently triggered, whereby vegetation is able to become established on the newly-formed bars and berms. This, in turn, causes the attenuation of larger flows, promoting continued aggradation. Thus, a larger volume of sediment is stored within the system until a mature inner floodplain is constructed.

In the Rio Puerco and San Simon River systems, peak discharges at gauges in the increasingly stable lower reaches have been declining steadily since the recorded maxima in the late 1920s/early 1930s. The decline in both peak and mean discharge has been particularly marked since the mid-1970s in the Rio Puerco and since the early 1960s in the San Simon River. This is coincident with a significant proportion of each system achieving a degree of stability. At this point, flow patterns and magnitudes no longer control the arroyo morphology, but are controlled by it.

The progression of evolution along the Rio Puerco and San Simon River indicates that, had sufficient widening been allowed to occur, the morphological development of the Santa Cruz River would have prevented the damaging effects of the recent floods. This is supported by fact that a similar increase in precipitation has been observed over all three study areas in recent years, but record floods have only continued to occur along the Santa Cruz River. The prevailing arroyo morphology of the Rio Puerco and the San Simon River controls the flood magnitude and hydrograph shape. However, along the Santa Cruz River, the opposite is true, with individual floods controlling the morphology of the arroyo.

The entrenched section of the Santa Cruz River is fixed at its upstream end by the resistant sediments in the Pleistocene reach and at its downstream end by the artificially narrow channel through Tucson, both horizontally by bank protection and vertically by grade control structures. It is possible, therefore, that the flood protection schemes implemented, although highly successful in protecting the urban area of Tucson in the short term, may have prevented the arroyo from achieving a stable morphology.

While there is no doubt that the anthropogenic alterations of the Santa Cruz River have had a great deal of morphological effect, it has been suggested that the change in flow regime since 1960 noted in Chapter 4, in particular the increase in both magnitude and frequency of peak flows, may only be due in part to these alterations. Webb and Betancourt (1992) hypothesised that floods which had occurred in the embryonic arroyo system, when

routed through the contemporary channel would be much larger if the artificially altered morphology was a significant controlling factor in determining the flow regime. Conversely, if modern floods were routed through the incipient arroyo system, it was thought that peak discharges would be significantly lower. It was reported that routing of the 1983 flood through the discontinuous 1915 arroyo system caused a reduction of the peak discharge of 1,490 cumecs by between only 15 to 20 percent (Webb and Betancourt, 1992). The largest recorded flood at that time, in December 1914, had a significantly lower magnitude, peaking at 425 cumecs. Thus the change in hydroclimatology observed since 1960, in particular the shift in storm seasonality noted in Chapter 4, was thought to be, to a large extent, responsible for the change in flow regime (Webb and Betancourt, 1992). However, observations of the other two arroyos examined during this study indicate that, had the arroyo been left to develop naturally, it would have evolved into a channel form which attenuated flows, rather than increasing peak magnitudes. Perhaps a more revealing test to determine the effect of artificial morphological alteration would have been to compare the relatively unaltered, stabilising arroyo system of the late 1940s or early 1950s with the contemporary form.

The timing of the maximum recorded floods along the three arroyos raises an important point. At the two downstream gauges of the Rio Puerco, at Bernardo and Rio Puerco, the flood of record occurred in 1929. At this time, the arroyo along the lower reaches had just begun to achieve a defined compound channel and was, therefore, close to the maximum dimensions attained during this phase of incision. Further upstream, however, flood maxima were not recorded until 1967 along the smaller section of the Rio Puerco, above Arroyo Chico, and until 1972 along the Arroyo Chico itself. The arroyo along these reaches during these years had also just commenced the creation of a stabilised compound channel. This would, therefore, seem to suggest that as the arroyo evolves, the maximum discharge potential changes, with the highest magnitude discharges occurring when the active channel has begun to form bars. This hypothesis is confirmed by the timing

of the highest magnitude floods along the San Simon River and Santa Cruz River. The San Simon River achieved its highest recorded peak in 1931, when channel widths were at their greatest. Along some gauges of the Santa Cruz River the maximum recorded flood occurred during 1983, although at others this was during 1993. Since the Santa Cruz River has evolved to a stage at which the discharge potential is at a maximum, and has been prevented from evolving further, it is highly probable that larger discharges will occur, if atmospheric conditions give rise to a large storm event.

Along all three arroyos studied, the flood of record caused a significant but temporary reversal of the progression of evolution. It may be that arroyos are only able to evolve significantly after the maximum flood has occurred. This flood scours out the channel, eroding bed and banks and mobilising stored sediment. During the falling limb, therefore, huge quantities of sediment are deposited. After this superflood has ceased, smaller floods are only able to rework the deposited sediment within the active channel, thus feedback mechanisms occur, whereby aggradation begins to predominate.

Observations of the Rio Puerco, Santa Cruz and San Simon Rivers have indicated that the incised channel evolution models discussed in Chapter 2 are not entirely applicable. Instead, it was discovered that geomorphologically distinct reaches could be identified, each having a clear up- and downstream boundary. Reaches which have no complicating influences develop in the manner proposed, with upstream progression of deepening, then whole-scale widening of the arroyo trench and the subsequent formation of a narrow active channel with a stabilised, vegetated floodplain. However, natural influences, such as tributaries, knickpoints and outcrops of bedrock or resistant alluvium, have been shown to hinder the upstream progression of this evolution. Similarly, the implementation of poorly considered flood protection schemes, which restrict the natural adjustability of the arroyo, retard the natural progression of evolution. In contrast, the judicious implementation of sediment detention dams has the opposite effect, accelerating evolution to a point where stabilisation occurs.

The different controlling variables acting on each reach have caused them to evolve at different rates. There is actually little evidence to suggest that upstream progression of morphological change is a significant factor in arroyo evolution. Observations during this study have indicated that each reach evolves at approximately the same rate along its entire length. Since arroyos are systems in which changes are event-driven, and given the poor longitudinal flow connectivity, there is no reason to assume upstream progression. Within the general pattern of morphological change, sub-reaches adjust rapidly, assimilating to short-term, small-scale variations in input variables, causing localised fluctuation around an equilibrium form, indicating a system in dynamic metastable equilibrium.

CHAPTER 6

Contemporary Arroyo Morphology

"One of the most startling paradoxes of the world's drylands is that although they are lands of little rain, the details of their surfaces are mostly the products of the action of rivers" (Graf, 1988b, p4)

6.1 CONTEMPORARY PROCESSES

The previous chapter examined the evolution of the three arroyos studied. These observations were made at the basin and arroyo-system scales, over long timescales. However, basin-scale morphological change that occurs through the long-term evolution of arroyos represents the summation of numerous, much smaller-scale adjustments and modification that occur during individual floods. The rapidity with which arroyos are able to adjust to changes in their external, driving variables, such as high discharges during flooding, meander cut-off and engineering or other artificial interventions, was discussed in Chapter 5. It follows that, to comprehend fully process/form interactions which occur to create the contemporary arroyo system, these short-term, smaller-scale adjustments and modifications must be observed and explained.

The contemporary processes acting on the arroyo can only be explained by examining the changes which occur both during flooding and during the intervening dry periods. Ellis (1993) developed a behavioural model of arroyo modification at the flood-event-timescale based on observations of the Santa Cruz River (Figure 6.1). However, the model is a general one and can apply equally to the other arroyos studied.

6.1.1 Modification During Periods without Flow

As discussed in Chapter 4, the arroyos studied are highly ephemeral, with dry conditions representing the norm (Figure 6.1.A). Geomorphic processes acting on the arroyo during the majority of the time are, thus, not associated with fluvial action. However, research on perennial streams has indicated that the majority of geomorphological change occurs as a direct result of flow attack on the bed and banks (Hooke, 1979; Thorne and Lewin, 1979).

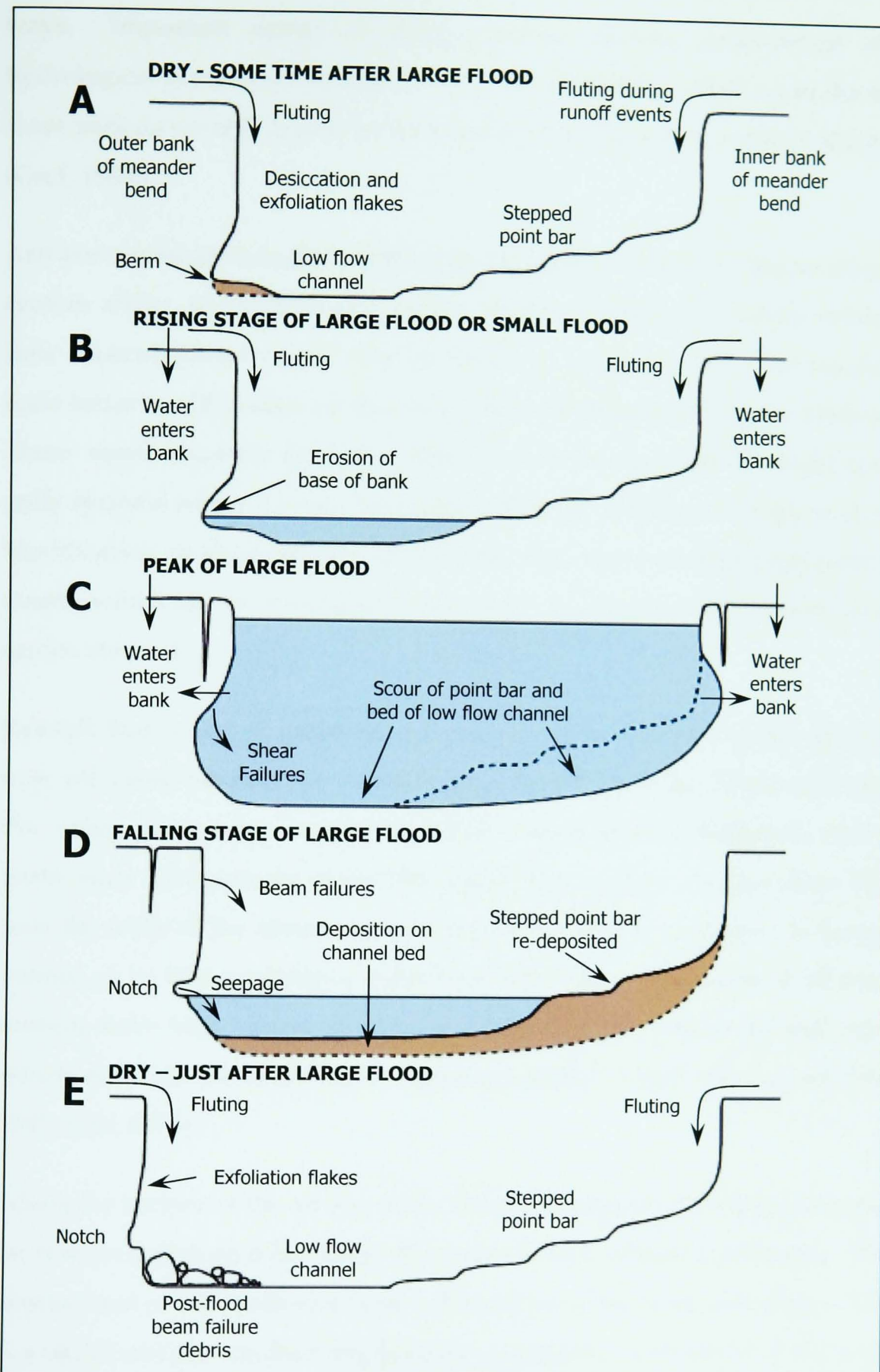


Figure 6.1 Model of arroyo behaviour during flow events, developed for the Santa Cruz River (after Ellis, 1993).

While this statement also holds true for the main features of ephemeral arroyos (Ellis, 1993; Parker, 1996), nevertheless, during periods of zero flow, the morphology of the arroyo trench may still be modified in significant

ways. Important agents of change include aeolian, geotechnical and hydrological processes, although most of the alterations which occur during these periods are still driven by the action of flowing water on the landscape (Graf, 1988b).

Arroyos are large-scale geomorphological features created by the increased erosive ability of concentrated surface runoff. Within the arroyo system, flow concentration features may be found at various scales. The smallest scale features, rills, occur on the valley floor or abandoned terrace surfaces. These small channels generally form networks upstream of larger-scale gully systems which, in turn, lead into a tributary, then main arroyo system. Modification of these small-scale features may occur during precipitation events which are of insufficient magnitude to generate flow in the main arroyo channel.

Rainfall that is not of sufficient quantity to cause flow within the arroyos may still cause modification of the arroyo trench, however. Sheetwash over the valley floor may entrain significant quantities of sediment and is particularly predominant in the San Simon River valley. As this water falls over the walls of the arroyo the entrained fines may be deposited to form a veneer up to two centimetres thick (Twidale, 1964). The walls of all three arroyos have been observed to have a covering of rainwashed sediment, which obscures the sedimentary layering usually visible (Bryan and Post, 1927; Ellis, 1993).

Along the surface of the arroyo walls, flakes of material of various sizes may be observed (Figure 6.2). These form due to two different processes. The intense heat of the southwest causes desiccation of the bank sediments. This is a significant pre-conditioning process, causing the outer layers of the walls to become finely cracked and weakened (Bryan and Post, 1927; Andrews, 1982; Lawler, 1992). Larger flakes are created due to the unloading of weight from the surface of the walls. As a flood recedes or as surface materials fail, the lateral pressure is reduced, thus promoting exfoliation of thin layers of material. Rainwash subsequently transports sediment and

water behind these flakes, eventually causing failure. As each surface fails, the arroyo wall is again unloaded, thus encouraging the creation of a new exfoliation flake.



Figure 6.2 Desiccation and exfoliation flakes along the arroyo walls, Goat Well Sub-Reach, San Simon River.

Modification due to aeolian action has a smoothing effect on the arroyo morphology. Gusty conditions, especially during the dry spring months, are ideal for mobilising fine, unconsolidated sediment found within the arroyo and on the valley floor (Bryan and Post, 1927; Ellis, 1993). In the Rio Puerco basin, it has been observed that aeolian reworking of valley floor is gradually obliterating evidence of past non-arroyo channels on the valley floor (Love, 1997).

The most significant modification of the arroyo system, other than by the action of flows within the channel, occurs through seepage processes. As discussed in Chapter 4, only a tiny percentage of effective precipitation is converted into streamflow. The vast majority of rainfall that is not intercepted or evaporated infiltrates into the basin sediments. As this water percolates through the sediments, a variety of geomorphological features may be formed. Sink holes and pipes are found in abundance along the study arroyos, although large seepage features are not generally found along the San Simon River. These features differ morphologically, the main difference being that pipes have a visible outlet, whereas sink holes do not.

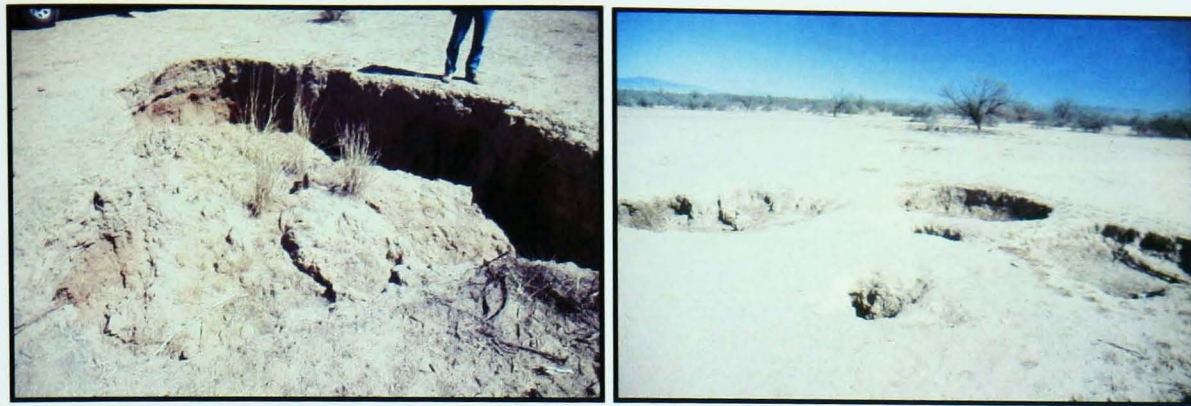


Figure 6.3 Sink holes along western valley floor of San Xavier Sub-Reach of the Santa Cruz River.

Sinkholes are thought to develop due to the exploitation of pre-existing desiccation and tension cracks formed predominantly in clay and silt sediments due to falling water tables (Hoffman *et al.*, 1998). Subsequently, percolating water entrains and transports the finest grained sediments through these cracks, causing voids to form. These voids propagate towards the surface as further entrainment occurs, leading to shallow surface depressions. Precipitation collects in and then infiltrates from these depressions, causing a positive feedback and void enlargement. Eventually void collapse causes the creation of a sink hole at the surface (Figure 6.3) (Hoffman *et al.*, 1998).

Pipes initially form an inlet on the valley floor where water percolates into the underlying sediments (Figure 6.4) (Graf, 1988b). This water tends to exploit differences in the hydraulic conductivity, whether due to cracks or alluvial layering (Grissinger, 1982; Graf, 1988b). The interface between two layers may be almost imperceptible and the layers may themselves be relatively permeable (Cosio, 1988; Hagerty, 1991). However, this difference may be sufficient to cause horizontal hydraulic conductivity an order of magnitude more rapid than the vertical conductivity (Cosio, 1988). As sediment entrainment continues, the pipe is enlarged, thus creating a positive feedback. The pipe exit is generally at the free face of the arroyo wall (Figure 6.4). This type of feature is not found along the banks of the active channels within the arroyo trench due to their low angle and cohesiveness.



Figure 6.4 Large pipe and pipe outlet, Guadalupe Sub-Reach, Rio Puerco.

6.1.2 Flood Modification

During flow events, a different sequence of driving processes and morphological responses occurs depending on the morphology of the arroyo and the magnitude of the flood (Ellis, 1993). During small floods, little geomorphological change occurs, although some modification occurs due to seepage erosion, sheetwash and direct flow erosion where the active channel impinges against the arroyo walls (Figure 6.1.B). Generally the most significant change during a small flood is the reworking of sediment within the active channel. However, even this may not occur if the active channel is protected by armouring or drape deposits (discussed in Chapter 4). The presence of large volumes of easily-mobilised sediment along the active channel bed results in a braided planform during the lowest-magnitude flows. As the stage and, therefore, competence and transport capacity of the flow increases, a single-thread channel is formed (discussed in Chapter 1).

Larger floods are responsible for greater amounts of geomorphological change (Figure 6.1.C). The high amount of precipitation required to produce

sufficient runoff to cause a large flood also results in significant amounts of seepage erosion and enlargement of flow concentration features. As the flood stage rises, direct flow erosion causes scour of bed and bank sediments, especially along the outer banks of meanders. As stage increases, the locus of bank attack shifts downstream within meander bends concentrating near or downstream of the bend exit during large floods (Ellis, 1993).

Bank failure commences once the arroyo walls reach a critical height with respect to their wet bank condition. This depends entirely on the degree of saturation, the bank angle and amount of undercutting (Thorne and Tovey, 1979; Osman and Thorne, 1986). Bed scour may also be responsible for causing the arroyo walls to surpass their critical bank height threshold for stability. The pattern of antecedent precipitation and flow is, thus, vital in determining the location of erosion.

The specific processes and mechanisms of bank erosion that occur during flood events along arroyo channels have been discussed in detail by Ellis (1993). Bank erosion may occur due to two main processes. Where flow impinges against the arroyo walls or channel banks, usually along the outer banks of meander bends, direct entrainment may occur (Bathurst, Thorne and Hey; Thorne and Osman, 1988). However, the majority of flows, especially along the Rio Puerco and San Simon River, are of insufficient magnitude to reach a significant height up the arroyo wall. The majority of bank erosion thus occurs due to sediment overloading, as the bank becomes saturated or undercut sufficiently to create a cantilever block (Hooke, 1979; Lawler, 1992; Thorne and Osman, 1988).

During large flow events the arroyo walls become saturated or partially saturated. Plane slip failures and shear failures are most likely to occur at this stage, since the tensile forces within the walls are minimal and shear exerted by the water is high (Ellis, 1993). As the floods subside, or during smaller flow events, the arroyo walls contain less water. Cohesion is, therefore, restored and tensile forces are far greater, leading to a

predominance of beam failures. The steep and often overhanging banks sustained by the cohesive arroyo walls may cause the formation of tension cracks a short distance behind the wall edge. Tension crack formation causes significant bank weakening, both due to the destruction of sedimentary bonds and due to the weight of water and sediment which may accumulate within the crack, thus accelerating failure (Thorne, 1981; Luzbetak *et al.*, 1988; Lawler, 1992). Once formed, these cracks are then exploited by sheetwash and seepage erosion, often creating pipes or seepage holes.

During flood events, water along the wetted perimeter seeps into the arroyo walls. As the flood recedes, this water seeps back out of the walls and seepage erosion occurs, creating a horizontally continuous notch (see Figure 6.5). The level of the notch thus represents a stable phase of the hydrograph, where the stage remains constant for sufficient time to allow erosion. Originally, it was thought that this level represented a boundary between sedimentary layers within the arroyo walls (Ellis, 1993). However, observations along the Santa Cruz River during the 2000 flood indicated that it is the flood stage which controls the notch level. However, it is possible that notch formation requires the stable phase of the hydrograph to coincide with a boundary between two layers. This would explain why these features are not more widespread.

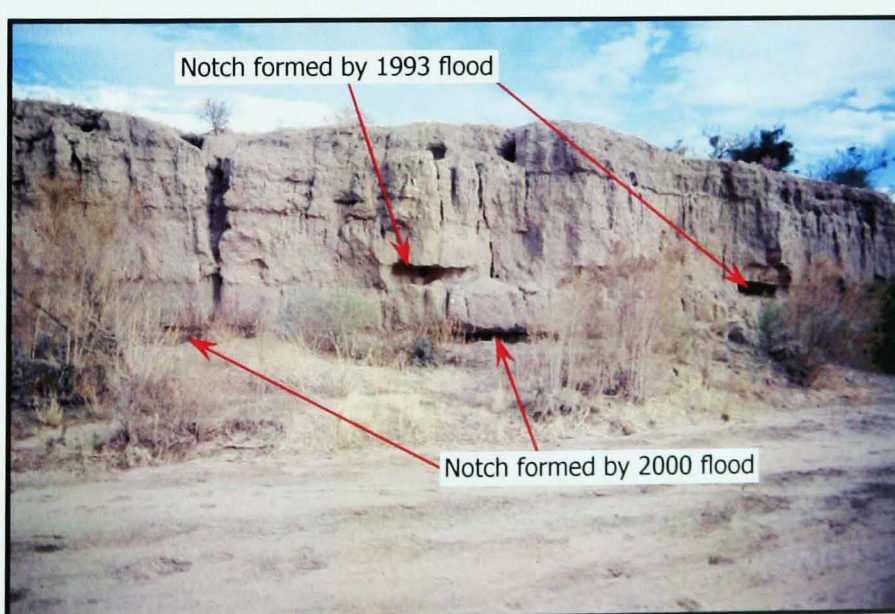


Figure 6.5 Seepage notches along the Santa Cruz River, upper level representing 1993 flood, lower level representing 2000 flood.

As the flood stage falls, sediment transport competence decreases, causing the re-deposition of entrained sediment (Figure 6.1.D). Point bar sediments are often deposited in discrete steps, corresponding to more stable phases of the hydrograph and indicating rapid width adjustment to the decrease in discharge. Shifts in the position of the active channel during the falling stage may also generate different bar surface levels, each level corresponding to the stage at which it was deposited. Lateral migration of the active channel also causes the recently deposited flood sediments to be exposed, revealing thick layers of parallel laminated sands (Figure 6.6).

After the flood, post-flood modification occurs (Figure 6.1.E). The flashy nature of storm hydrographs along arroyos causes steep recession limbs and, consequently, steep hydraulic gradients at the free-face. This leads to positive pore-water pressures and a reduction in the friction component of the resisting force (Leopold and Miller, 1956; Thorne and Tovey, 1981; Thorne and Osman, 1988; Parker, 1996). Therefore, a great deal of recession limb and post-flood failure occurs, often close to the apex of meander bends (Ellis, 1993). Post-flood failures may often be found blocking the low-flow channel, indicating that failure has occurred after flow had ceased. It has been suggested that post-flood bank failure may account for the most lateral erosion in arroyos (Leopold and Miller, 1956; Parker, 1996). However,



Figure 6.6 Parallel laminated sediments deposited in the San Xavier Reach of the Santa Cruz River during the October 2000 flood.

observations of contemporary arroyos have indicated that this statement is questionable, as the majority of lateral erosion actually occurs during high-magnitude flow events.

After the channel has returned to its usual, dry state following a large flood, modification by weathering, runoff and seepage erosion occurs, until the arroyo morphology has reverted back to that seen in Figure 6.1.A. Smaller floods cause narrowing of the widened active channel through the deposition of lateral berms, which become vegetated over time. The removal of material deposited across the active channel by post-flood failures also occurs. Sediments which crumbled during failure are entrained by even the lowest-magnitude floods. However, larger cohesive blocks of failed bank materials require correspondingly larger floods before they are removed. Desiccation of fines deposited during the final stages of the flood become cracked, occasionally forming mud-curls. Over time, sedimentary layering within the arroyo walls exposed by fresh bank failures becomes obscured by rainwash. Guber (1988) indicated that along the Santa Cruz River, recovery of the active channel to pre-flood widths occurs over approximately four years.

6.1.3 Flood Modification along Channelised Reaches

The presence of artificial bank protection along the arroyo walls prevents lateral adjustments from taking place thus causing a different pattern of morphological response during flow events (Ellis, 1993). Natural channelisation of the active channel, as observed along the Rio Puerco and San Simon River, has a similar effect. The main response to floods along reaches of the arroyo with this type of morphology is bed scour during the rising limb and re-deposition during the falling limb. However, the response to larger floods is significantly different along the two types of confined channels. Along reaches where the active channel has become naturally channelised, the arroyo morphology has adjusted to cope with the high variability in discharge. Thus, on the rare occasions when floods are of sufficient magnitude to cause overtopping of the active channel, inundation

of the inner floodplain occurs with no obvious lateral erosion of the active channel. The dense vegetation on the floodplain surface causes attenuation of the floodwaters, loss of competence and deposition of entrained sediment, particularly the coarser sand-sized fractions. Up to 10 centimetres of floodplain aggradation occurs by this process each year along the lower Rio Puerco (Love, 1986).

Along reaches where the arroyo has been channelised by bank protection, the natural lateral adjustment mechanisms have been removed. Since it is the arroyo, rather than the active channel, which is laterally fixed, adjustments to higher-magnitude floods are only able to occur through continued bed scour. The presence of grade control structures along artificially controlled reaches does, however, prevent further bed adjustments. This significantly affects the stage-discharge relationship along these channelised reaches. Since the arroyo is unable to adjust morphologically, flood stage and velocity increases occur in response to the increase in flow magnitude.

6.2 ARROYO MORPHOLOGY

As discussed in Chapter 5, the three arroyos can be divided into morphologically distinct reaches. Surveys of arroyo cross-sections were carried out in order to identify these morphological differences (shown in Appendix 2). The scale and inaccessibility of the Rio Puerco made it impossible to survey that arroyo during this project. However, repeat surveys of Elliott's 1977 cross-sections were carried out during the mid-1990s by Allen Gellis and John Elliott, and are used courtesy of J. Elliott. The basis of this survey, therefore, differs from that of the other two arroyos. Along the arroyos in Arizona, several cross-sections were surveyed in representative reaches, which were determined previously from observations made during reconnaissance fieldwork (Appendix 1 and 2). Multiple cross-sections were used to measure the longitudinal continuity of morphological features, in order to determine which characteristics were important in the context of this study. Along the Rio Puerco, single cross-

sections were surveyed at a greater number of sites, although multiple cross-sections were surveyed around occasional large bends.

Rio Puerco

General Observations

The Rio Puerco is the longest of the three arroyos studied and also shows the most morphological variability. As discussed in Chapter 5, five geomorphically distinct reaches were identified, separated by either tributaries entering the main arroyo or knickpoints, both artificial and natural. The arroyo and the inner channel cross-sections are shown in Appendix 2, Figures A2.2 to A2.9 and their geometry is summarised in Appendix 3, Table A3.2.

The contemporary morphology of the Rio Puerco was established from field observations in 1999 and 2000 and from the cross-sections surveyed by Elliott and Gellis during the mid-1990s as previously mentioned. During October 2000, a flood was observed at the Bernardo gauge. This flood originated from the same storm that generated one of the largest floods on record in the Santa Cruz River. However, along the Rio Puerco, the flow was of significantly lower magnitude and did not come close to overtopping the active channel. Thus, very little geomorphological change was observed as a result of this flood.

The arroyo trench of the Rio Puerco has generally become stabilised through natural processes and is not widening to any great extent, as discussed in Chapter 5. The arroyo walls are, therefore, generally weathered and degraded, except where the active channel impinges, most commonly along the outer banks of large meander bends.

Upper Reach 1 – above Arroyo Chijuilla

This reach, the furthest upstream, has developed a compound arroyo morphology with a mainly trapezoidal active channel, although some asymmetry occurs around the outer bank of meanders (Figure 6.7). Migration of meanders in the active channel has caused the formation of



Figure 6.7 Active channel and stabilised inner floodplain at Elliott's XS-1, Upper Reach 1, 1996 (courtesy J. Elliott).

several terraces. These were cleared of tamarisk by local inhabitants and the vegetation is now dominated by far less dense stands of Russian Olive (discussed in Chapter 5). Although this reach is close to the headwaters of the system, the arroyo trench is not appreciably smaller than it is in the majority of downstream reaches.

In the upstream reaches, the active channel is perennial due to treated sewage water being pumped into the channel from Cuba. Discussion with local inhabitants has indicated that the development of a deep, narrow active channel was concurrent with the commencement of perennial flow. It is likely that the increased moisture enabled vegetation to become well-established within the arroyo trench, causing flow concentration and floodplain stabilisation.

Upper Reach 2 – between Arroyo Chijuilla and Ventana artificial channel

The increased inputs of flow and sediment discharge from the Arroyo Chijuilla have caused the active channel of the Rio Puerco to switch from a narrow, deep, meandering planform to a much wider, shallower planform (Figure 6.8). The arroyo has achieved sufficient width that the active channel no longer flows wall-to-wall but is instead flanked by berms and point bars, which have been stabilised by permanent vegetation. Some recently eroded failure debris was observed along the outer walls of



Figure 6.8 Broad, braided low-flow channel of XS-9, Upper Reach 2, 1997 (courtesy J. Elliott).

meandering sections of this reach. This failed material had generally built up into a protective wedge at the base of the arroyo wall, creating a state of impeded removal and so preventing further erosion. Thus, stabilisation and narrowing of the active channel and inner floodplain are occurring along this reach. As discussed in Chapter 5, the artificially straightened Ventana sub-reach, which represents the downstream limit of this reach, is still actively eroding laterally. This lateral erosion is, however, occurring slowly due to the high resistance of the valley bottom sediments into which the arroyo is incised. Similarly, the bedrock knickpoint within the artificial Ventana sub-reach is migrating upstream only very slowly.

Interestingly, funding has been obtained by the Rio Puerco Management Committee to re-route the arroyo into its former meandering channel, in the hope that this will increase the stability of the Rio Puerco through this reach (M. Coleman, pers. comm., 2003). Lateral erosion of the straightened reach has bought the artificial and former natural arroyo trenches very close to each other (discussed in Chapter 5). Measures have, therefore, been implemented to prevent future break-through back into the artificial trench after flows have been re-directed into the former channel.

Upper Reach 3 – between Ventana and Arroyo Chico

Downstream of the artificially straightened reach at Ventana, the active channel is still distinct and braided, being flanked by vegetated berms and point bars (Figure 6.9). No cross-sections were surveyed along this reach, since Elliott's XS-11 could not be re-located during the 1990s survey, so exact dimensions are not available. However, both the arroyo and active channel are narrower than observed along the reaches immediately up- and downstream. Morphologically, this reach is similar to Upper Reach 2, above Ventana, with the exception of the high sinuosity of the active channel, which has developed meanders with a wavelength scaled to the arroyo trench. The radii of curvature of these meanders are generally large, although they become smaller towards the downstream end of reach, as the meanders are compressed due to the controlling effect of the Arroyo Chico, which prevents further downstream meander migration. Active outer bank erosion of the arroyo walls was observed, although the majority of the walls were in a state of impeded removal due to the accumulation of failure debris at their base. In places along this reach, the arroyo cuts through bedrock outcrops, for example close to San Luis, causing the trench to remain narrow.

It has been suggested that headcutting and lateral erosion of the artificial Ventana sub-reach caused a large increase in the sediment supply to this



Figure 6.9 Broad, shallow active channel of Upper Reach 3, 1997
(courtesy J. Elliott).

reach. This was thought to have accelerated downstream floodplain aggradation and channel incision (Mike Coleman, pers. comm., 2001). However, using average annual values of the sediment load at the Rio Puerco above Arroyo Chico gauge, it was found that, over a 30 year period, approximately 21 million tonnes of sediment was moved through the system. It has been estimated that, over the same time period, 600,000 tonnes of sediment was eroded from the artificial Ventana reach (Coleman *et al.*, 2003). Since this is only three percent of the total sediment load, the effect on the downstream morphology cannot have been significant.

Middle Reach – between Arroyo Chico and Benavidez Ranch Reach

In the middle reach of the Rio Puerco, the arroyo winds between erosion-resistant volcanic cores and crumbling mesas, within a narrow valley. As discussed in Chapter 5, this reach is very different morphologically from the other reaches of the Rio Puerco, almost entirely due to the influence of the Arroyo Chico. The high sediment input from this tributary has caused the active channel to remain wide and shallow, with a highly sinuous planform, which meanders at the arroyo scale (Figure 6.10). The only exception to this is the broad, straight sub-reach close to Guadalupe, just downstream of the confluence with the Arroyo Chico. As discussed in Chapter 5, the active channel within this anomalous reach is considerably wider than at any other point along the Rio Puerco. The Guadalupe sub-reach has formed where meander bends have cut-off, leaving abandoned meander terraces (Figure 6.11). Within these terraces, lines of dense tamarisk, following meander scroll bars, have become established.

A large number of actively eroding tributary systems may be observed along this reach. These arroyos are narrow and are still actively eroding both headwards and laterally through the valley bottom, supplying large quantities of sediment to the Rio Puerco. Many of these arroyos are themselves tributaries of the Arroyo Chico, which is consequently the most active sub-basin found within the Rio Puerco catchment.



Figure 6.10 Upstream limit of Middle Reach, showing broad, straight Guadalupe Sub-Reach and more representative sinuous planform, 1997.

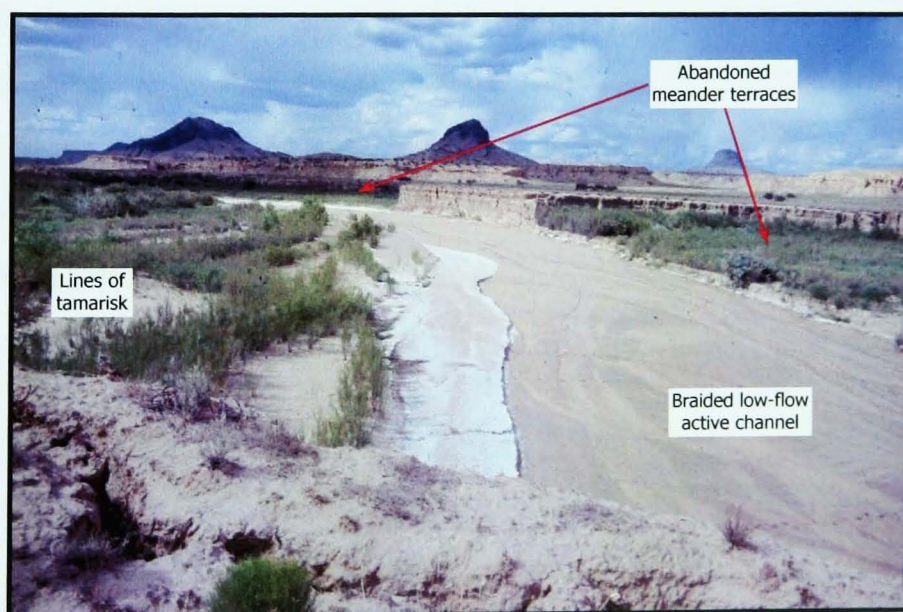


Figure 6.11 Guadalupe Sub-Reach, Middle Reach, 1999.



Figure 6.12 Arroyo wall dissected by piping, behind stabilised berm, Guadalupe sub-reach, 1999.

Piping of the valley floor close to the arroyo walls was particularly common in this reach. Those observed in this study extended no more than 3 metres from edge of arroyo, but observations have been made of piping systems extending hundreds of metres (J. Elliott, pers. comm., 1999). Some pipes along this reach extend almost the entire height of the arroyo walls (Figure 6.4). The collapse of large pipes leaves deep embayments in the arroyo wall, which may subsequently erode headwards to form tributary arroyos. It was observed that piping systems are found behind protective vegetated berms, bars and abandoned terraces (Figure 6.12). This is, perhaps, expected since these features are slow-forming and thus are unlikely to develop behind actively eroding banks. At the base of arroyo walls with active pipe systems, sediment fans have been deposited through the accumulation of material eroded from pipes.

Cross-sections surveyed in this reach indicate that the active channel, although still far wider than observed in other reaches, has narrowed and deepened since the 1970s. Deepening of the active channel has occurred through point bar and berm accretion, rather than incision, following the evolutionary pattern seen along other reaches of the Rio Puerco. However, the cross-sections surveyed are located in the Guadalupe sub-reach, which is not representative of the typical morphology of the Middle Reach.

Unfortunately, reaches downstream of this are very hard to visit due to the poor state of the unpaved roads. Much of the reach is also on private land. Not only are cross-sections unavailable for the majority of the Middle Reach, but it was also impossible to source ground level photographs. Therefore, it must be assumed from the similarity of planform, observed from aerial photographs, that the arroyo morphology, if not the scale of the features, remains relatively consistent.

Lower Reach – downstream of Benavidez Ranch Reach

This reach is by far the longest but its morphology is fairly uniform, as noted in Chapter 5. A trapezoidal active channel, bordered by tamarisk-lined levees may be found on the floor of the arroyo trench, indicating a quasi-equilibrium form, as defined in the channel evolution models discussed in Chapter 2. However, on closer observation, this is an oversimplification, as the width and depth of the active channel shows some variability and the active channel in some reaches retains an asymmetric planform.

The active channel is well-defined along the entire reach and, although point bars and berms have aggraded, causing deepening and narrowing of the channel, this has, in places, been insufficient to result in a trapezoidal cross-section. Observations indicate that the active channel tends to remain shallow and asymmetric close to the apex of meander bends, possibly due to large quantities of sediment still being input from failures along arroyo



Figure 6.13 Difference in active channel morphology within Lower Reach a) Trapezoidal channel at XS-15, situated in a low-sinuosity sub-reach, 1997 (courtesy J. Elliott). b) Asymmetric channel at XS-17, located in a sinuous sub-reach, 1999.

walls at points where the active channel impinges against the arroyo wall. Elliott's cross-sections indicate that straighter sections of the arroyo had trapezoidal channels, whereas those situated in meander bends showed far more shape variability (Figure 6.13). However, rather than the channel cross-section being larger at meander bends, the opposite was found to be true. These differences in morphology are also reflected in the arroyo geometry relationships (see Appendix 3, Table A3.2). As expected, arroyo widths in the straight sections were substantially lower than those in the meandering reaches, which have been widened by lateral erosion.

Other sources of sediment, in particular from large tributaries such as the Rio San Jose, Comanche and Alamito Arroyos, do not perceptibly affect the planform geometry of the arroyo trench (discussed in Chapter 5). The great length of this reach made it logically impossible to perform detailed observations along the entire reach. This statement is, therefore, based on inspection of aerial photographs. The exact nature of the geomorphology and geometry up- and downstream of these confluences is to some extent conjecture from observations of those reaches where it was possible to visit the arroyo.

The planform of the Lower Reach is characterised by hooked, recurved meanders, which have developed short radii of curvature superimposed on an arroyo-scale wavelength, indicating complex controls on planform geometry (discussed in Chapter 5, Figure 5.15). The point bars of these meanders exhibit different depositional levels, associated with accretion during the recession limbs of recent floods (Figure 6.13b). Generally point bars along this reach consist of a sparsely vegetated or unvegetated band close to the active channel, backed by parallel lines of willow and with dense lines of tamarisk higher up the bar, representing the former position channel (Figure 6.14). This pattern contrasts with the straighter reaches, where the trapezoidal active channel has little or no vegetation within its boundaries but is flanked by very dense tamarisk (Figure 6.13a).



Figure 6.14 Large meander at XS-17, showing increase in age of vegetation with distance from active channel.

The dense stands of tamarisk are dying, along some reaches. This is thought by Elliott to be due to the fact that such a large amount of aggradation has occurred that groundwater can no longer be accessed by the vegetation (J. Elliott, pers. comm., 2001). At the Hidden Lady meander (XS-18), an overbank flood, most likely during August 1994, caused deposition on the abandoned meander terrace. Subsequently the tamarisk established on this terrace died, leaving a broad expanse of cracked, desiccated, unvegetated sediment. If the current aggradational trend continues to occur, the floodplain may, in the future, no longer be stabilised by this vegetation. In turn, this may reduce the attenuation of flows, causing a reversal of the historical decline in the flow regime and allowing higher-magnitude floods and renewed incision to occur. The same pattern of deposition and decline in vegetation has also been observed on other meander terraces, for example just downstream of Interstate 40. Abandoned meander terraces are periodically occupied under the current flow regime, even if only rarely, and are, therefore, still part of the active flood-plain. Hence vegetation die-back and resulting increases in peak flows have the potential to drive future changes in arroyo morphology.

As noted along the upstream reaches, the arroyo walls, except where being actively eroded, are dominated by weathering, causing fluvial features to

become smoothed and generating a desiccated, brittle outer layer. Lack of erosion has enabled development of piping networks, although these are nowhere near the size of those observed along the Guadalupe reach. Lines of small sink holes and pipes were observed above, and directly in line with, tributary gully headcuts, indicating the mechanism by which these features erode headwards. These gully networks have caused the valley bottom close to the arroyo walls to become dissected, forming badlands in places.

Santa Cruz River

General Observations

The arroyo of the Santa Cruz River is incised into very different sediments from those of the San Simon River and Rio Puerco, featuring a far higher degree of Calcium Carbonate cementation. This has resulted in significantly different geomorphological features along the Santa Cruz River. When dry, the arroyo walls are incredibly cohesive and are geotechnically very stable (Ellis, 1993). However, when the arroyo wall sediments achieve any degree of saturation, the cohesive bonds due to the Calcium Carbonate cementation disperse rapidly. Thus, the critical bank height is significantly lower for saturated conditions than that for dry conditions (Ellis, 1993). As it is the critical bank height for saturated conditions that limits the arroyo wall height, the maximum height of the arroyo walls along the Santa Cruz River is considerably lower than the maximum height of the Rio Puerco and San Simon River.

Flow concentration features, known as flutes due to their similarity with similar features found in karst regions, may also form in the arroyo walls (Ellis, 1993; Parker, 1996). Flutes are vertically elongated cavities, which may extend the entire height of the arroyo wall. These features were found mainly along the Santa Cruz River, principally where the arroyo is incised into predominantly Holocene sediments, which have a higher degree of Calcium Carbonate cementation. Although flutes are predominantly formed due to surface runoff draining into the trench over the arroyo walls, some sedimentary layers are differentially exploited by seepage erosion (Figure



Figure 6.15 Preferential erosion of different sedimentary layers in flutes, Valencia Road Sub-Reach.

6.15). As with horizontal flow concentration features, flutes may also be found at different scales, representing different stages of development. The smallest flutes are only a few millimetres in diameter, generally forming in palaeosol layers within the arroyo walls (Ellis, 1993). The extent, depth and density of these flutes depends entirely on whether the arroyo walls are being eroded by flow in the active channel, with the greatest concentrations being found along reaches where steep walls are protected by bars, terraces, berms or vegetation. However, those banks which have been inactive for some time no longer develop flutes due to their reduced bank angles. The largest flutes may erode headwards, eventually enlarging sufficiently to form gullies and tributary arroyos.

Sink holes along the Santa Cruz River tend to have no outlet and may be located many hundreds of metres away from the arroyo trench. In the Tucson basin, sink holes are particularly common on the pre-incision floodplain to the west of the Santa Cruz River on the San Xavier Reservation (Figure 6.3). These holes range in size from a few centimetres to features with diameters and depths exceeding six metres (Hoffman *et al.*, 1998).

The arroyo reach of the Santa Cruz River is far shorter than the other two arroyos studied. However, external influences have generated a great deal of morphological diversity (discussed in Chapter 5). The most obvious

difference occurs between the Pima Mine Road reach, where the arroyo walls are composed predominantly of Pleistocene sediments, and the other reaches, which are composed predominantly of Holocene sediments. Within the Holocene sediment reaches, morphological differences occur due to the influence of the bedrock outcrop of Martinez Hill; the artificially straightened channel and the flood protection schemes implemented through the Tucson metropolitan area. Even without these external influences, a great deal of difference in the geometry of the active channel was noted within each reach, as observed in the Rio Puerco.

Selected reaches were initially surveyed in 2000 and then re-surveyed in 2001. During the intervening period, a large flood occurred, which peaked at 326 cumecs on 23rd October 2000, at the Tucson gauge. Observations, both during this flood and during each survey, enabled the model of flood-scale change proposed in 1993 to be assessed and refinements made.

Pleistocene Reach

2000 Survey

The Santa Cruz River cuts through a Pleistocene sediment outcrop between roughly 800 metres south and 4.5 kilometres north of Pima Mine Road bridge (shown in Appendix 2, Figure A2.10). The morphology of this reach is significantly different from that of any other reach along either the Santa Cruz River or the other two arroyos studied in this project. The reason for this difference is the highly indurated valley fill sediments, which, as discussed in Chapter 5, have dramatically slowed both incision and lateral erosion. The high resistance of the sediments through this reach allows overhanging bank angles to be maintained along the arroyo walls. The weaker Holocene material which predominates in the reach upstream has been preferentially eroded. The trench width thus narrows from over 85 metres to below 30 metres in the space of 200 metres (see Appendix 2, Figure A2.11 and Appendix 3, Table A3.4). Along the Pleistocene reach itself, there is a gradual increase in width to approximately 40 metres. At the end of the

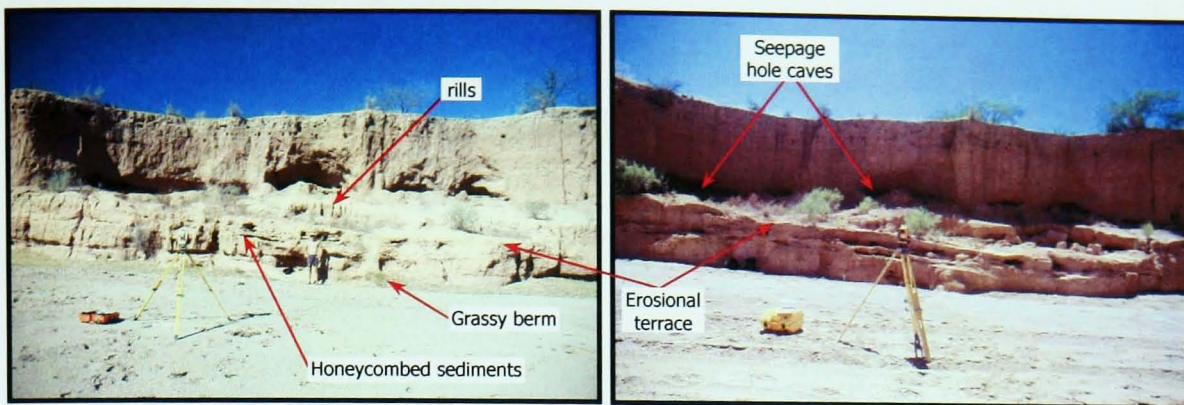


Figure 6.16 Erosional terrace, XS-3, North Pima Mine Road Sub-Reach, pre-and post-October 2000 flood.

Pleistocene outcrop, the width increases dramatically to approximately four times the width as Holocene sediments again predominate.

Distinct layering is exposed in the arroyo walls. Weaker layers have been preferentially eroded to form a characteristic bank morphology. Erosional terraces may be found on either side of the arroyo, above an extremely resistant calcified layer, which is longitudinally continuous (Figure 6.16). The sediment within this layer is calcified to such an extent that pseudokarst features, such as small stalactites, stalagmites and columns, have formed. Precipitated calcite nodules may also be found on the surface of this layer. Deep, horizontally extensive seepage holes have formed, giving the layer a honeycombed appearance. The seepage holes extended up to 1.3 metres into the bank but were a maximum of only 0.2 metres in height. The terrace surfaces are generally dissected by rills. Water draining into the arroyo from these rills forms flutes on the terrace slopes. Terraces tend to be found along the narrowest sections of this reach, especially the sub-reach south of Pima Mine Road (Appendix 2, Figure A2.12, XS-2 and XS-4). This is due to the indurated nature of the sediments which inhibits lateral erosion.

The resistant sediments within this reach also lend themselves to sustaining large seepage features without collapse. Above the highly indurated terrace layer, large seepage holes, which had occasionally enlarged to form sizeable caves, were observed (Figure 6.16; Appendix 2, Figure A2.12, XS-2 and XS-3). The largest cave surveyed extended over 3.5 metres into the bank and

had a sizeable failure block within it which had become detached from the cave roof.

The active channel within this reach was wide, shallow and was clearly defined by grassy depositional berms at the base of the arroyo walls (Figure 6.16). The flow pattern during the recession of the last flood could be observed, with a sequence of low alternate bars causing the active channel to switch from one side of the trench to the other. The low-flow planform pattern of the active channel itself was braided.

Evolution of the Pleistocene reach has been hindered by the erosion resistance of the sediments through which the arroyo is incising. Thus, widening due to lateral erosion is still occurring. Along the base of the arroyo walls, many post-flood failures were observed. Trees, some still clearly alive, overhung the arroyo edge, indicating the lateral instability of the contemporary arroyo, despite the resistance of the arroyo walls.

Along the east wall of the arroyo, extensive tributary arroyo systems extend back into the valley floor. One tributary arroyo surveyed was only separated from the main arroyo by a narrow wall of sediment (Appendix 2, Figure A2.12, XS-1). This wall had been undercut both by seepage and outer bank erosion from the tributary active channel. The tributary trenches have generally incised to elevations close to the base level of the main arroyo. Extension of the tributary network occurs by headward erosion of deep headcuts. Beyond the actual tributary headcut, in direct line with the tributary trench, collapsed voids or seepage holes may be found, indicating subsurface drainage connectivity. Confirming this, many seepage holes are connected to the tributary by pipes, even though they are separate at the surface. The lateral instability of the tributary arroyos appears to be greater than that observed along the main arroyo. This is due to the fact that these tributaries have not yet attained their maximum height and are still downcutting, with a series of knickpoints corresponding to sedimentary layers observed. Thus, these arroyos are at an earlier evolutionary stage, whereby erosion is still at a maximum since neither maximum bank heights

or widths have been achieved. The visual impact of trees overhanging the arroyo walls along the tributary arroyos is greater than along the main channel due to their narrower width. Thus, these trenches appear crowded by overhanging tree roots.

Morphological Change due to 2000 Flood

The large flood that occurred during October and November 2000 caused significant geomorphological change along this reach (shown in Appendix 2, Figures A2.11 and A2.12, and Appendix 3, Table A3.6). The greatest observable changes were erosion of the arroyo walls and aggradation of the arroyo bed. Prior to the flood, the 2000 surveys indicated a remarkable consistency in the arroyo depth: downstream of Pima Mine Road bridge, the five cross-sections all indicated a depth of 8.7 metres. After the flood, this consistency had been maintained, with 0.5 metres of bed aggradation occurring almost uniformly throughout the reach. Upstream of Pima Mine Road, the greatest change in any single cross-section was noted (Appendix 2, Figure A2.11, XS-1). The active channel had shifted laterally due to the deposition of a cobble point bar. The abrupt change in direction just downstream of this cross-section is thought to have been responsible for a loss in competence, thus causing the deposition of the larger sediment fractions. A large concrete block had also been deposited, indicating the high competence of the flood flow.

The morphology of the active channel had also changed significantly. Prior to the flood, this channel was generally narrow and flanked by grassy berms. However, general scour and subsequent deposition during the 2000 flood had removed these berms, causing widening of the active channel. Vegetation within the arroyo had been scoured or buried during the flood. However, rapid vegetation regrowth had occurred. Point bars were deposited along the wider downstream section of this reach, close to the change from Pleistocene to Holocene sediments. It was noted that these bars were composed of different sediment sizes. Generally the point bars were formed from finer sediments with a few cobbles lining the active channel.



Figure 6.17 Point bar armoured with cobbles close to widening of Pima Mine Road Sub-Reach, during 2000 flood.

However, just upstream of the widening at the end of the Pleistocene reach, the loss of competence had caused one point bar to become armoured with cobbles (Figure 6.17).

The repeat survey indicated that arroyo widening had occurred along the entire reach. Bank failure was responsible for width increases of between one and 2.5 metres of erosion. Where the cross-sections coincided with sections of the reach which had erosional terraces, erosion of these terraces, rather than the arroyo walls occurred. The resistant nature of the terrace sediments resulted in erosion occurring through direct scour, rather than block failure. Erosion was, therefore, less extensive along these terraced reaches, with width increases of generally less than one metre.

Lateral erosion, both in the main arroyo and in one of its large tributaries, had caused the thin wall of sediment separating the two to collapse during the 2000 flood (Figure 6.18; Appendix 2, Figure A2.12, XS-1). Subsequent floods may be large enough to capture the reach of the tributary system downstream of this breakthrough, which would cause significant widening at this point and, potentially, introduce a great deal of sediment into the system. However, this would require either a significant amount of degradation of the tributary bed or the occurrence of a superflood. Lateral, vertical and headwards enlargement of the tributary arroyos to the west of

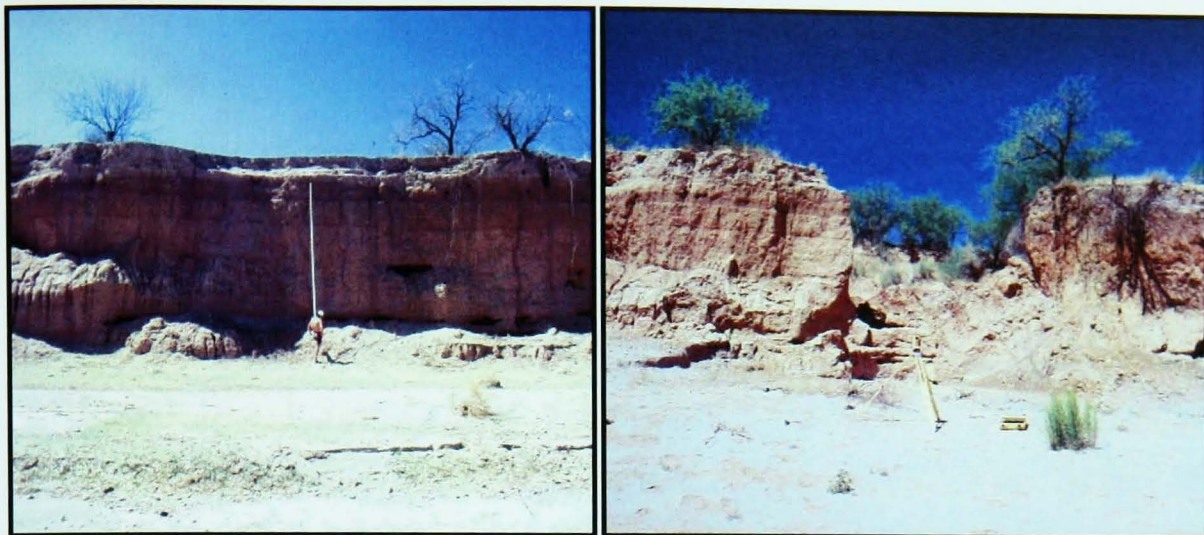


Figure 6.18 XS-1, North Pima Mine Road Sub-Reach, showing collapse of narrow wall of sediment separating tributary from main Santa Cruz River during 2000 flood.

the Santa Cruz River also occurred during the 2000 flood. Many post-flood failures were observed, occasionally blocking the entire arroyo. However, rather than blocking flood flows, these failure dams caused the active channel to be diverted, causing severe undercutting and failure of the arroyo walls. At the confluences between the tributary systems and the main arroyo, fresh deposits of parallel laminated, grey Holocene material were observed, easily visible against the much redder Pleistocene sediments.

Observations during post-flood surveying and in 1993 indicate that post-flood failures are more common along this reach than along reaches incised through Holocene sediments. It was also noted that the bank material along this reach is also less likely to remain intact during failure. It is, therefore, likely that the internal bonds within the Pleistocene arroyo wall sediments take longer to return to their highly cohesive dry state following a flood.

Observations during the falling limb confirmed the fact that infiltration of floodwaters into the arroyo walls and steady phases of the hydrograph were responsible for the creation of a notch along this reach. This observation indicates that, even though this was a large, prolonged flood, the arroyo walls did not become entirely saturated. Saturation of the sediments only occurred at the base, along the wetted perimeter of the channel, and at the top of the arroyo, where precipitation and surface runoff infiltrated into the bank.

Holocene Reach**2000 Survey**

The majority of the Santa Cruz River arroyo is incised into Holocene sediments. Four separate reaches were surveyed, with arroyo planform patterns ranging from almost straight to contorted meanders, each with similar morphological characteristics (shown in Appendix 2, Figure A2.10 and Appendix 3, Table A3.5). The active channel was wide and braided along the majority of the reaches studied. This channel was distinct, its width being determined by depositional features, such as berms, point bars and terraces, depending on the arroyo width and planform. At points where the active channel impinged against the arroyo walls, recent bank failures were observed, indicating continued arroyo widening.

As mentioned previously, the Holocene sediments are particularly vulnerable to runoff erosion, causing the formation of flutes along the walls of the arroyo through the entire reach. As with tributary systems along the Pleistocene reach, sink holes and pipes were found on the valley floor upstream of tributary gullies or arroyo headcuts, indicating the method of headward extension. Generally, the observed sink holes did not have an outlet, except where they were particularly close to an active tributary and were close to being amalgamated into the surface-water system. Exploitation of tension cracks by seepage erosion was observed along the outer banks of meander bends. Only occasionally had these cracks been eroded sufficiently to cause a pipe to form, with the outlet at the base of the arroyo wall.

The most sinuous reach, upstream of Martinez Hill, is atypical of the generally low-sinuosity arroyo (Appendix 2, Figure A2.15). However, as discussed in Chapter 5, the active channel in this reach has become less sinuous under the high-magnitude sequence of floods characteristic of the current flow regime. The Santa Cruz River is at its widest in this bedrock-affected reach, with arroyo widths reaching over 600 metres. However, there is an abandoned meander terrace over 150 metres wide that would

only be occupied by the largest floods. The braided active channel was far narrower than the arroyo itself and flowed along the inner edge of the arroyo meander bends. Semi-permanent bars and berms were observed to cause this braiding and channel narrowing. The outer bank of the meander bend is, therefore, only occupied and eroded during superfloods. However, actively eroding sink holes and tributary arroyos were numerous along both sides of this reach. A particularly large tributary and several large sink holes, one well over 10 metres in diameter, were observed close to the outer, right bank of the meander bend. Along this large tributary, the stabilising effect of vegetation was noted, with tree roots causing an arch to form over the tributary channel (Figure 6.19).

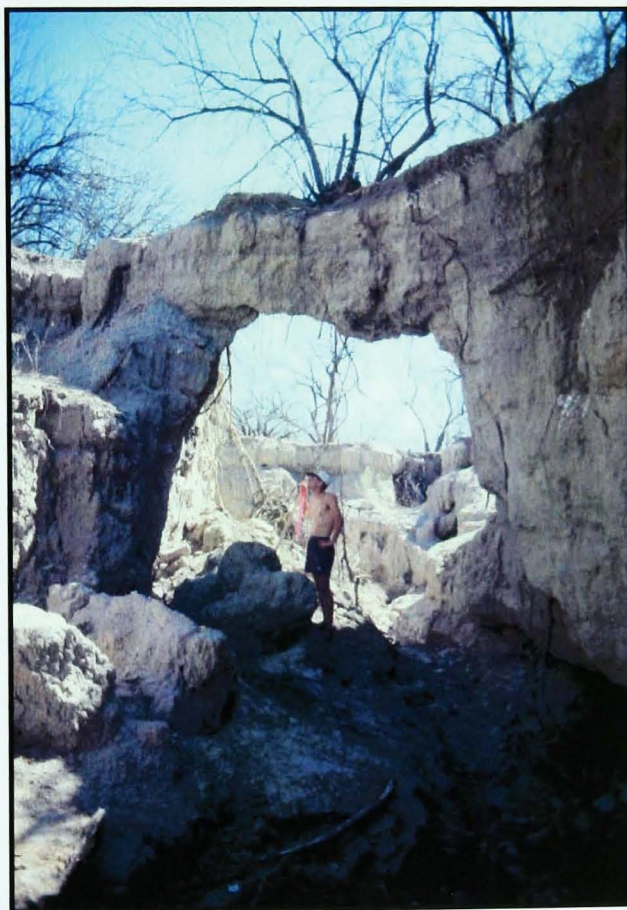


Figure 6.19 Arch formed due to tree roots binding sediments of upper layer, close to cross-section at Martinez Hill.

Two reaches were surveyed to represent bends with a large radius of curvature (Big Bend Reach) and a smaller radius of curvature (South of Straight Reach) (Appendix 2, Figure A2.13 and A2.14). With a maximum width of over 300 metres, the Big Bend Reach represented the widest alluvial reach of the Santa Cruz River, discounting the Martinez Hill section, which

had only attained its width due to the influence of a bedrock outcrop. This reach is the result of a series of smaller meanders which have coalesced as the active channel has become less sinuous, to form the large feature. This reach was the only reach to have developed a trapezoidal inner channel and aggraded, stabilised floodplain and point bar (Appendix 2, Figure A2.13, XS-4 and XS-5). This confirms the suggestion made in Chapter 5, that continued progression of arroyo evolution depends on the ability of arroyos to adjust laterally.

The smaller bends of South of Straight Reach were formed at the upstream end of the artificially straightened reach connecting the two original channels of the Santa Cruz River. The reach has attained an average width of approximately two-thirds the average of the Big Bend Reach. Although the point bar had aggraded significantly, the active channel had not yet formed a trapezoidal shape (Appendix 2, Figure A2.14). Recent arroyo wall failures were evidence that lateral erosion was still occurring, indicating that this reach had not yet attained a quasi-equilibrium morphology. The wall failures had caused the formation of a protective grassy berm at the base of the arroyo wall. Downstream migration of the meander bends, rather than cut-offs, had caused the formation of abandoned terraces and an elongated point bar along this reach (discussed in Chapter 5; Figure 5.19). Above one such terrace, where the arroyo wall remained vertical, exploitation of weaknesses by seepage and flow erosion had occurred. Large pipes were observed along the line of a former tension crack, with a fan of sediment eroded from these pipes extending from the exit at the base of the wall. The face of the arroyo wall at this point was also heavily fluted.

The point bar and inner terrace of the two sinuous reaches had aggraded as a series of splays were deposited during recent large floods. Along the South of Straight Reach, migration of the meandering active channel had exposed these parallel laminated flood deposits in the bars and terraces. A series of cobble-faced steps was observed along the outer edge of the point bars along both the Big Bend and South of Straight reaches, indicating the

different phases of deposition. The terrace and point bar surfaces had become vegetated, indicating the rapidity of vegetation invasion.

The fourth and final reach, close to Valencia Road was the least sinuous of those surveyed. This reach is located just downstream of the first major soil cement bank protection, at the Valencia Road bridge (Appendix 2, Figure A2.16) and slightly further upstream where the I19 crosses the arroyo close to Martinez Hill. As mentioned previously, this reach had been studied in 1991 and 1993 (Chapter 5; Ellis, 1993). The arroyo walls along this reach, with the exception of the point at which the active channel impinged against the arroyo walls, showed particularly well-developed flutes. This was due to the fact that, following the 1993 flood, a depositional berm had formed along the base of the arroyo wall as the active channel narrowed during subsequent smaller floods, thus protecting it from erosion. This berm was vegetated with grasses and trees, which had also become established since the 1993 flood. The arroyo walls were also being eroded by many tributary gullies and arroyos, causing a dissected appearance. Many sink holes were found along this reach, especially along the western margin, where these features were causing extension of the gully networks.

Within the arroyo of the Valencia Road Reach, just upstream from XS-7, an electricity pylon has had a marked effect on the geomorphology of the active channel (Figure 6.20; Appendix 2, Figure A2.16). Division of flow has caused a dramatic loss of both competence and sediment transport capacity. Consequently, a large bar has been deposited downstream of the pylon, with the bed of the chute channels on either side composed of the coarser fractions of sediment, including cobble-sized particles.

The downstream cross-sections along the Valencia Road reach were located in a sub-reach of the arroyo which was more sinuous. This reach had developed a morphology similar to that noted along the South of Straight reach, with aggraded, vegetated point bars and a clearly defined, broad, shallow active channel. Just downstream of XS-9, a tributary enters the main

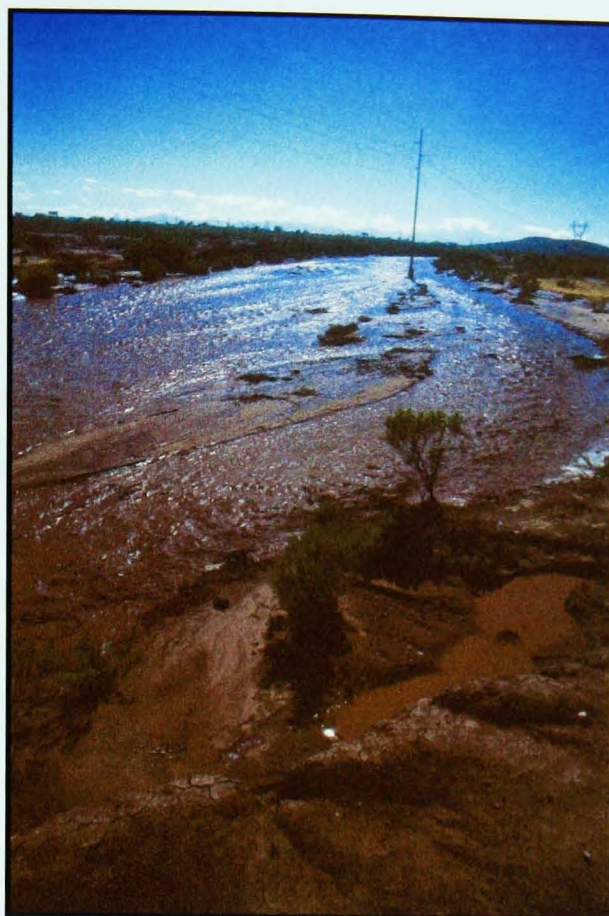


Figure 6.20 Braid bar deposited downstream of mid-stream pylon during 2000 flood, Valencia Road Sub-Reach.

arroyo, eroding this point bar. A gully had begun headcutting from this scoured section across the back of the point bar.

Morphological Change due to 2000 Flood

Along reaches incised into Holocene sediments, the greatest morphological change which occurred during the 2000 flood was due to the reworking of the sediments in the active channel within the wetted perimeter of the flow (shown in Appendix 2, Figures A2.11 to A2.16 and Appendix 3, Table A3.6). However, the morphological outcomes of this reworking were not consistent, in that some reaches aggraded and others eroded. Generally, prior to the flood, vegetation was relatively dense within the arroyo, especially on low, semi-permanent bars and berms. During the flood, the majority of the smaller vegetation within the wetted perimeter was removed. Vegetation that remained in place provided significant roughness, causing sediment to become trapped and creating small bars. During the post-flood survey, vegetation on bars and on valley floor was observed to be very lush due to abundant moisture available during the wet winter. Along

some reaches, morphological features were almost unrecognizable due to the density of vegetation, indicating the visual differences which may occur during just one wetter season.

At the Martinez Hill bedrock-affected reach, the active channel was significantly widened by the 2000 flood (Appendix 2, Figure A2.15). However, the channel bed had actually aggraded slightly during the switch from a deeper, narrower channel to a far wider, shallower channel. The low, semi-permanent bars flanking the active channel (noted during the previous survey) were eroded to allow this widening, uprooting the vegetation covering these bars. Erosion of inner banks of meander bends occurred due to thalweg shifting during the flood. The active channel remained predominantly braided in form, although the braid bars were no longer as distinct. Flood recession had caused various bank levels to be preserved on the bars, especially along the inner bank of the meander. Erosion of sink holes and tributary arroyos was also noted. In particular, the right bank tributary noted previously had headcut appreciably despite an extremely resistant caliche outcrop.

The two sinuous reaches, South of Straight and Big Bend, were the only two surveyed reaches in which the active channel had degraded slightly during the 2000 flood (Appendix 2, Figures A2.13 and A2.14). Along the Big Bend reach, since the active channel does not impinge against the arroyo wall at any point, very little morphological change had occurred outside the active channel. Along the South of Straight reach, however, erosion of the arroyo wall had occurred. The berm previously observed to be protecting the base of the bank had been removed. A basal wedge of failed material was observed downstream of the meander apex (Appendix 2, Figure A2.14, XS-3). Along both reaches, the active channel had become better defined, representing the low-flow stage of the 2000 flood.

Despite scour during the flood, net aggradation occurred along much of the Valencia Road Reach, especially along the straighter sub-reach and in particular downstream of the mid-channel pylon (Appendix 2, Figure

A2.16). Along the meandering sub-reach, however, a similar pattern of development was observed to that noted along the more sinuous reaches upstream, with widening and deepening of the active channel. During the flood, cantilever shear failures were observed along the outer bank of the meander. A basal wedge of failed material had accumulated, indicating a state of impeded removal, diverting the thalweg away from the cut bank and preventing further erosion. Post-flood beam and shear cantilever failures were observed.

During the 2000 flood, a notch had been eroded at same point on the right arroyo wall as before, although at a lower height (Figure 6.5; Appendix 2, Figure A2.16, XS-3). This again confirms the hypothesis that this feature is formed by seepage erosion during the falling stage of a flood, when the water level remains stable for some length of time. As expected, enlargement of other minor features such as flutes, sink holes and tributary gullies was also noted due to the high amount of runoff which also occurred.

San Simon River

General Observations

The large Fan and Barrier detention dams have caused significant upstream aggradation of the mainstem of the San Simon River, as discussed in Chapter 5. The morphological adjustment to the Barrier Dam has yet to progress far upstream. However, the Fan Dam has a major geomorphological effect, with a distinct morphological difference between the incised reaches observed downstream of the dam and those upstream of the aggraded reach above the dam (Appendix 2, Figures A2.17 to A2.23 and Appendix 3, Table A3.7). Downstream of the Fan Dam, the arroyo gradually increases in size, especially depth, reaching a maximum close to the Goat Well Sub-Reach. Arroyo morphology along this reach is remarkably consistent, apart from the increase in size. It is thought that this downstream increase occurs due to the increase in water and sediment discharges associated with tributary inputs during high-magnitude floods. However, it should be noted that no significant change in the morphology of



Figure 6.21 View upstream into Timber Draw emphasising the difference in bed elevation between the tributary and main channel of the San Simon River.

the San Simon River was observed downstream of the largest tributaries, Gold Gulch and Timber Draw.

The morphology of these major tributaries at the confluence with the main channel raises some important questions. The bed elevation of Timber Draw is significantly higher than that of the mainstem (Figure 6.21). The reason for this difference in elevation is unclear, since it would be logical for the tributary channel to adjust its gradient to match the level of the main arroyo. However, this is clearly not the case, since the aggraded bed of the tributary arroyo is composed entirely of unconsolidated sediments. Observations of

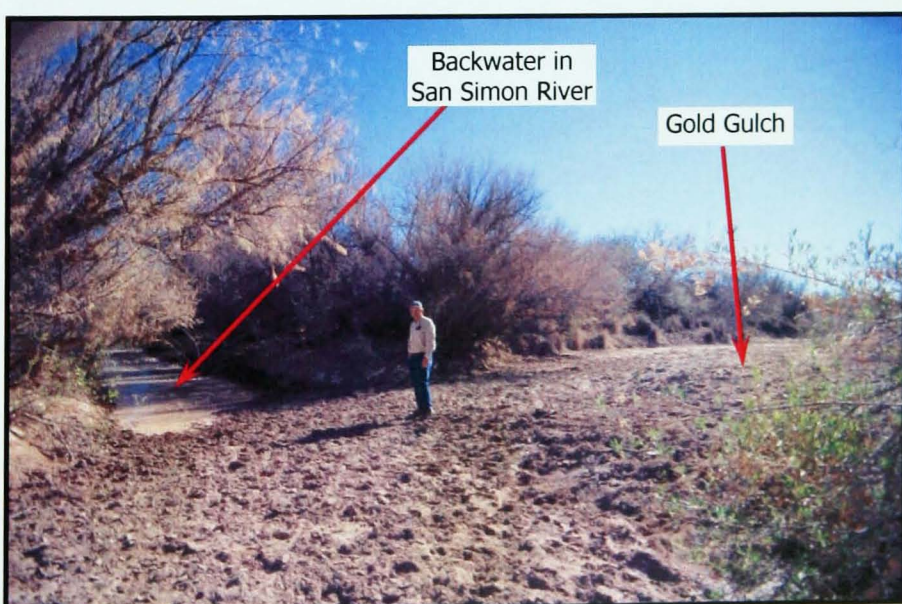


Figure 6.22 View upstream into Gold Gulch and San Simon River.

the confluence between Gold Gulch and the San Simon may provide an explanation for this problem. Upstream of this confluence, in the main arroyo, a backwater has formed, with a reverse gradient, indicating that the gradient is actually adjusted to the tributary, rather than the mainstem (Figure 6.22). It is, therefore, likely that, while large flows do not generally occur in the San Simon River itself, Gold Gulch may flow rather more frequently. The flow from Gold Gulch enters the main arroyo and erodes the sediments deposited by Timber Draw, creating the elevation difference.

Along this reach, it was noted that tamarisk had been cut down to provide makeshift sediment traps along mainstem, presumably by the BLM who are currently implementing a basin-wide monitoring project (Figure 6.23). Since these traps had been implemented, a small flood had occurred and observations indicated that sediment was being trapped successfully. However, it is not entirely clear why this modification has been carried out, since the active channel was not degrading along this reach.

Along the entire arroyo, there was a distinct difference between the size and appearance of the sediments of the active channel and the surrounding arroyo. The bed of the active channel was generally composed of coarse, pale grey sand, whereas the bed of the arroyo trench and its banks were formed in much finer, redder sediments. The bed sediments were also



Figure 6.23 Felled Tamarisk sediment traps in the main channel of the San Simon River, downstream of Gold Gulch.

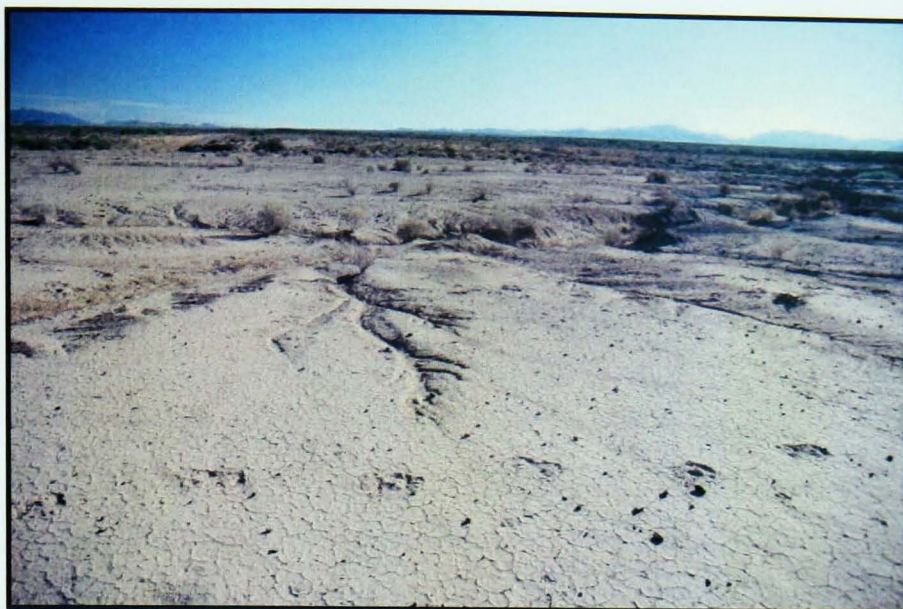


Figure 6.24 Headwards progression of tributary arroyo network due to sheetwash concentration into rills, then abrupt, deep headcut.

unconsolidated, compared with the bank sediments which were generally compacted.

The valley floor close to the San Simon River has been dissected by many networks of flow concentration features, ranging from small rills to large tributary arroyos in size. It was observed that these channels generally enlarge through headward erosion of an abrupt knickpoint, downstream from which the channel is generally a sizeable arroyo. Above this headcut, small rills concentrate sheetwash into the larger trench (Figure 6.24). In many places, however, these features appear relict. Weathering and desiccation have caused the surface sediments to become cracked and extremely brittle, indicating some time since active erosion.

Upstream Reach – coarse sediments

The San Simon Reach was the only section of the San Simon River to have a coarse bed, comprising coarse sand with significant quantity of gravel and small cobbles. As in all the surveyed reaches, the bed sediments along this reach were far coarser than the bank sediments. This reach was narrow, but widened as it entered a small meander bend (Appendix A2, Figure A2.18). The loss of competence due to this widening had caused the deposition of greater quantities of the coarser fractions of entrained sediment. The bed through the wide reach was highly indurated, with small headcuts and

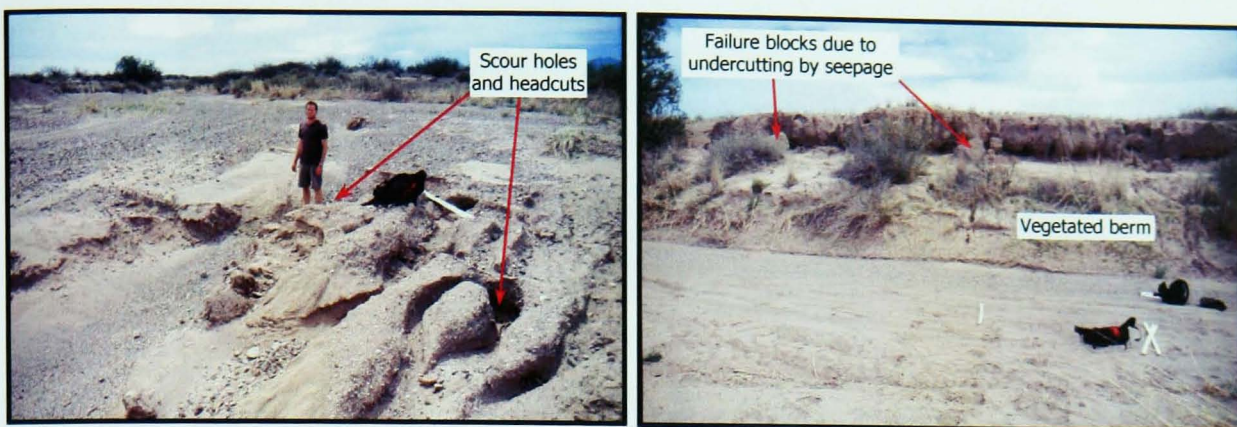


Figure 6.25 Morphological features of the San Simon Sub-Reach.

scour holes (Figure 6.25). Bulldozer marks indicated that sand and gravel mining was occurring along this reach. The removal of this material may be responsible for the headward erosion of knickpoints in the active channel and its tributaries.

The arroyo in this reach was shallow, with weathered walls which exhibited significant flute development, indicating the lack of lateral erosion. These flutes had also been enlarged by seepage. The walls were protected from fluvial erosion by a berm, which was densely vegetated with grasses and mature shrubs. Some failure blocks were, however, observed. These blocks had been undercut solely by seepage erosion (Figure 6.25).

Along the valley bottom, sheet wash erosion had left larger cobbles on small pedestals (Figure 6.26). Gully networks eroding headward from the main arroyo channel were also observed.



Figure 6.26 Sheetwash causing large blocks to become situated on pedestals, close to San Simon Sub-Reach.



Figure 6.27 Vegetated, stepped floodplain of Yellowhammer Sub-Reach.

Upstream Reach – fine sediments

The Yellowhammer reach, also upstream of the Fan Dam had the sandy bed observed along the majority of the arroyo, although some gravel was still present. This reach is low sinuosity and has a far more clearly defined active channel, with a very wide, trapezoidal channel (Appendix 2, Figure A2.19). An aggraded floodplain had formed along the entire reach and it was this which had resulted in the narrowing and sharpened definition of the active channel (Figure 6.27). Small steps along the front face of the floodplain were observed, presumably corresponding to different steady stages, possibly even during a single flood. The floodplain had been stabilised by dense tamarisk and other mature vegetation. The bed of this channel was observed to be cambered: sloping downwards from its centreline towards the banks (Figure 6.28). Another feature of the bed through this reach was the presence of several alternate bars, which resulted in steep downstream bar faces oblique across the entire channel. Several deep scour holes were also noted, seemingly at random locations.

Where the arroyo walls were isolated from the active channel by the floodplain, they were extremely weathered and dissected. However, where the active channel impinged the walls, some failures were observed, indicating that recent lateral erosion had occurred. The debris from the failures had accumulated at the base of the arroyo wall, forming a protective

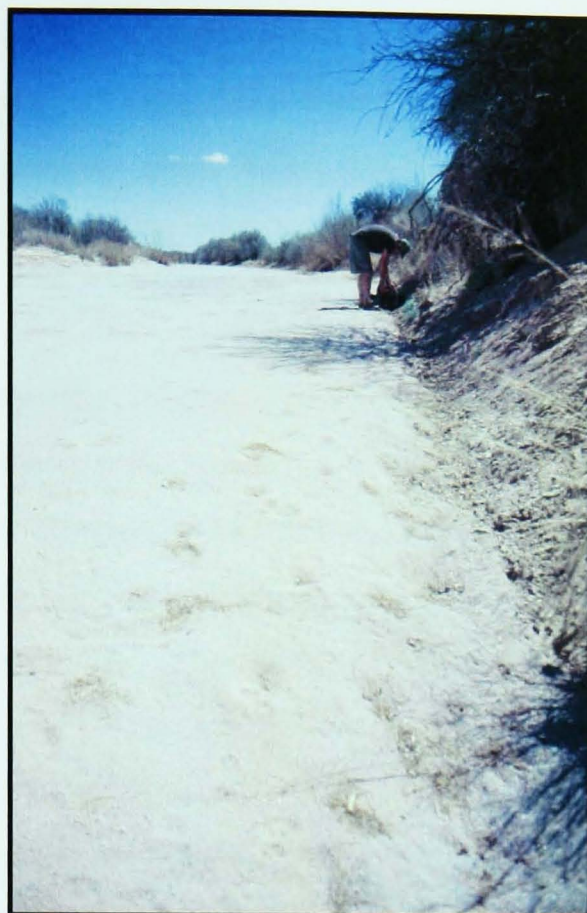


Figure 6.28 Bed cambering along Yellowhammer Sub-Reach, showing difference between bed and bank sediments of active channel.

basal wedge. At one cross-section, XS-4, tree roots had caused the upper sediments to become less erodible and the bank was overhanging. A seepage notch was observed along this reach at XS-2, most likely a relic of the 1983 flood (Appendix 2, Figure A2.19, XS-2 and XS-4).

The valley floor along the Yellowhammer reach was highly eroded, with gully networks radiating from the arroyo trench (Appendix 2, Figure A2.19, XS-2). Sheetwash had selectively eroded the fine sediments, causing the ridges between the gullies to be covered in a layer of gravel. Presumably the flow in the gullies was competent to transport any gravel within them, whereas the sheetwash on the inter-gully ridges was not. Aeolian deposits were observed on sparsely vegetated areas of the floodplain.

Lower Reach

The morphology of the arroyo downstream of the Fan Dam is typical of an arroyo in the later stages of evolution (discussed in Chapter 5). The active channel is trapezoidal and is bounded by an aggraded, densely vegetated

floodplain. The bed of the active channel is generally composed of coarse, unconsolidated sand, with the banks composed of redder, finer sediments. Tamarisk are particularly dense along the levees lining the active channel and also on the aggraded floodplain, making surveying particularly difficult.

As mentioned previously, there is a distinct downstream increase in the size of the arroyo, particularly the depth of the arroyo trench, due to increases in driving variables of flow and sediment discharge (Appendix 3, Table A3.7). However, the active channel becomes narrower and deeper with distance downstream (Figure 6.29). The sub-reach furthest upstream, Bailey Well, had the widest, shallowest active channel and smallest arroyo trench (Appendix 2, Figure A2.20). This reach was also the least sinuous. The arroyo walls along this reach were very low in both height and angle.



Figure 6.29 Trapezoidal active channel in a) Bailey Well Sub-Reach and b) Tanque Sub-Reach, Lower Reach.

Further downstream, cross-sections in the Tanque and Corral Sub-Reaches represent the morphological characteristics of large meander bends (Appendix 2, Figures A2.21 and A2.22). Both bends, particularly the Tanque bend, had become compressed due to bedrock outcrops just downstream. The active channel at Tanque bend had extended laterally into the floodplain, to create a tight bend, after which the bend had retreated, turning through nearly 90 degrees to form a cut-off across the former point bar (Appendix 2, Figure A2.21). The active channel through the Corral bend had also straightened, leaving an aggraded meander terrace. The arroyo

walls along this reach, while higher, were also heavily dissected and degraded, indicating the lack of active lateral erosion. As the active channel had straightened, it no longer impinged against the arroyo walls along the apices of meander bends. The reach averaged geometry of the active channel again indicates a downstream narrowing and deepening between the Tanque and Corral Sub-Reaches.

The Goat Well Sub-Reach, the furthest downstream of those surveyed, had distinctly different morphology to the other lower reaches, but was similar to the lower reaches of the Rio Puerco (Appendix 2, Figure A2.23). The arroyo walls have attained a height of 13 metres, which corresponds to their limiting (critical) height with respect to mass stability, and they are being actively eroded where the channel impinges. The arroyo walls appear to be highly unstable, with sediment flaking from them and an abundance of tension cracks (Figure 6.30). It is, therefore, likely that failures due to weathering, rather than oversteepening due to flow erosion, have caused significant volumes of sediment to accumulate. This failure debris has created a basal wedge at the toe of the arroyo wall, which prevents direct erosion by the active channel in most places. Where the arroyo walls are protected by the floodplain, they have degraded to such a degree that in many places they are no longer vertical.

The active channel is trapezoidal along some of this section, but along other sub-reaches, especially around the outer banks of meander bends, the channel has a wider, asymmetric planform (Figures 6.30 and 6.31). This is thought to be due to the high input of sediment from both tributaries and the actively eroding arroyo walls. Many large tributary arroyo networks enter the San Simon River along the Goat Well Sub-Reach (Appendix 2, Figure A2.23). These networks are still actively eroding, except where detention dams, such as the Goat Well dam across Slick Rock Wash, have prevented further erosion.

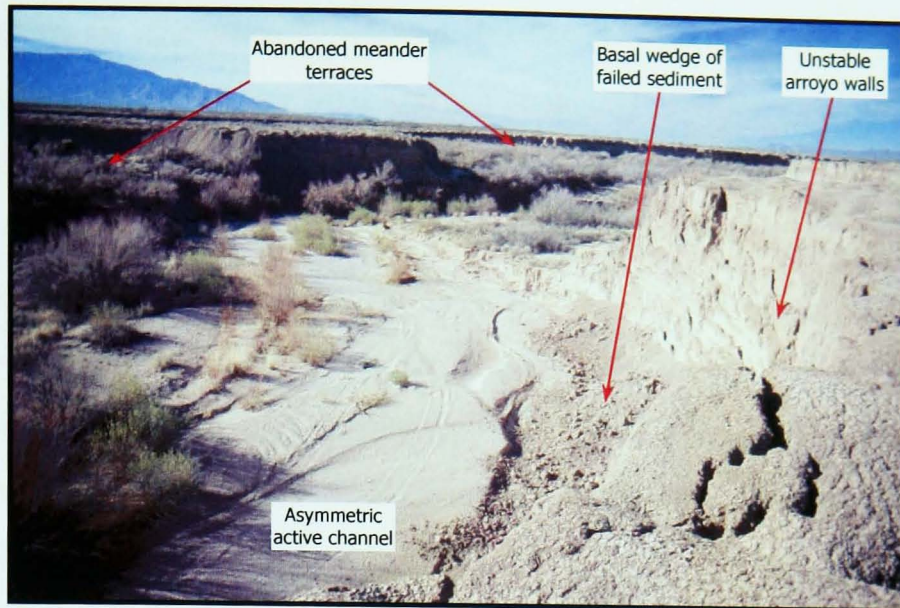


Figure 6.30 Morphological characteristics of Goat Well Sub-Reach, Lower Reach.



Figure 6.31 Trapezoidal active channel in Goat Well Sub-Reach, Lower Reach.

The active channel along the Goat Well Sub-Reach does not show a continuation of the downstream narrowing and deepening observed further upstream (Appendix 3, Table A3.7). This suggests that the size of the active channel along the Lower Reach of the San Simon River may, to some extent, represent a morphological adjustment to the localised controlling variables imposed on each sub-reach, rather than a reach-long trend. This again emphasises the discontinuous, event-driven nature of morphological development along arroyos.

6.3 COMPARISON OF MORPHOLOGY IN ARROYOS STUDIED

The contemporary morphology of arroyos has certain essential similarities, which enables generalisations to be made regarding the process-form interactions. During inter-flood periods, modification of the arroyo trench

occurs through comparable processes along all three arroyos studied. However, differences in the valley floor sediments has resulted in differences in the forms produced. In particular, the high levels of calcite cementation along the Santa Cruz River have led to pseudo-karst features, such as caves, seepage notches and holes. This difference has also affected the way in which gullies and tributary arroyos are propagated headwards. Along the Santa Cruz River, sink holes form above the headcut of a tributary arroyo or gully, which in time coalesce, extending the incised channel upstream. Along both the San Simon River and Rio Puerco sheetwash concentrates to form rills, which in turn flow into larger gullies, generally at an abrupt headcut. Thus the valley floor close to the arroyo walls is heavily dissected. Along the Rio Puerco, sink holes and piping networks were, however, also found above gully and tributary arroyo headcuts.

Large pipe networks were observed along the Rio Puerco. These differed in form from those found along the Santa Cruz River in the fact that these were true pipes, with both an inlet and an outlet. Similar features along the Santa Cruz River were either sink holes with no outlet or flutes which were surface features found along the arroyo walls, without the enclosed channel of true pipes. Seepage features were only observed in the Upper Reaches of the San Simon River.

Similar features along the different arroyos were formed by different processes. Terraces observed along the Pima Mine Road reach of the Santa Cruz River are erosional features; their height controlled entirely by the sedimentary layering exposed by the incising arroyo. However, terraces along the other arroyos and along the Holocene reaches of the Santa Cruz River were created due to the cut-off or retreat of active channel meander bends. These features are, therefore, mainly depositional.

Along the three arroyos studied, several geomorphologically distinct reaches were identified, which are thought to represent different stages in the progression of arroyo evolution. Observations and surveys of the contemporary arroyo have confirmed the suggestion proposed in Chapter 5,

that evolution has not progressed in a simple, headwards manner but is inter- and intra-reach-dependent, adjusting to localised differences in driving variables.

The Pleistocene reach along the Santa Cruz River, together with some very short sub-reaches of the Rio Puerco, still represents Stage 3 morphology (as defined in Chapter 2, Figures 2.4 and 2.5). The arroyo is still actively widening, with the active channel covering the base of the arroyo floor. The evolution of these reaches has been retarded by the high resistance of sediment or bedrock outcrops, which have slowed the rate of lateral erosion.

The middle three reaches along the Rio Puerco, the Holocene reaches of the Santa Cruz River and the upper reaches of the San Simon River have wide, shallow active channels, synonymous with Elliott's Stage 4 (Figure 2.5). The arroyo has widened sufficiently to allow the inner floodplain to begin to develop, although the active channel has not yet achieved a dynamically stable form. Appreciable differences in the geometry of the active channel, the maturity of the floodplain and the morphology of the arroyo occur between the reaches, indicating the different phases of morphological development within the evolutionary stage. The Middle Reach of the Rio Puerco represents an early Stage 4 morphology, whereas along the Santa Cruz River, the active channel of the widest arroyo sub-reaches is starting to develop a trapezoidal shape, indicating the most advanced evolutionary form. This morphological variability is likely to be in response to the different driving variables acting on each reach. During lower-magnitude events in these reaches, aggradation of the active channel occurs and sediment is stored within the arroyo trench in bars and berms. During higher-magnitude flow events, appreciable widening occurs (in unprotected reaches). However, the Santa Cruz River is the only arroyo studied in which sufficiently high-magnitude flow events still occur frequently enough to prevent significant system-wide aggradation and stabilisation.

The uppermost and lower reaches of the Rio Puerco and the lower reaches of the San Simon River have attained a late-stage form, with a stabilised inner

floodplain. However, distinct differences in the morphology were identified, whereby those reaches with a continually trapezoidal channel appear to represent a later stage of evolution than those in which sub-reaches with an asymmetric form are also present. In the lower reaches of the Rio Puerco, which still has sub-reaches which have an asymmetric form, a greater variability in the size of the active channel was noted, when compared with the San Simon River. It was noticeable that the reaches with an asymmetric form still present had a higher sediment input, from actively eroding tributaries and arroyo walls. This indicates a delicate balance between the stability of the arroyo form and the driving variables. Sufficient sediment must be supplied to a reach for floodplain aggradation and accretion to occur, but not so much that the sediment transport capacity is overloaded, causing the active channel to remain wider and shallower.

The trapezoidal channels were generally observed to have uniformly low-angled banks, without cut outer banks, even around the outer curve of meander bends. Thus, the flood events large enough to cause significant outer bank erosion must be larger than the bankfull events of these channels. Floodwaters go overbank, resulting in floodplain aggradation as the floodwaters are retarded by dense floodplain vegetation, rather than causing channel erosion. This minimises the geomorphological effect of large floods, maintaining the equilibrium channel dimensions. Thus, the recovery period along arroyo reaches which have developed the quasi-equilibrium channel form is far shorter than might be assumed (discussed in Chapter 2). This is, in part, due to the fact that semi-arid regions are often thought to have sparse vegetation (Wolman & Gerson, 1978; Hey, 1998). However, along the quasi-stable arroyo reaches, extremely dense stands of vegetation, especially tamarisk, occur.

Distinct differences between the geometry and dimensions of the trapezoidal channel along each of the quasi-stable reaches were also identified (Table 6.1). The embryonic trapezoidal channel of the Big Bend Sub-Reach of the Santa Cruz River has been included in Table 6.1 for comparative purposes.

In a perennial river, it would be likely that the difference in size was related to the difference in drainage basin area. However, given the poor longitudinal connectivity of arroyo systems (discussed in Chapter 4), this relationship cannot be inferred. Thus, other factors must be responsible for the observed variability in channel size and geometry.

As discussed in Chapters 2 and 5, stabilisation of the arroyo occurs, first by vertical aggradation of point bars and then lateral accretion of the newly developed floodplain. This pattern of development causes the active channel to narrow and deepen. This is the reason for the assumption that those reaches in which an asymmetric channel was no longer present represented a later stage of evolution. Contradicting this, Table 6.1 shows that, despite the fact that the active channel is larger on the Lower Rio Puerco, the width:depth ratio is lower than that on the Lower San Simon River, which would seem to suggest that this statement does not hold true. However, the size of bed and bank materials within the channel has a significant effect on the equilibrium geometry (Schumm, 1960).

River	Bankfull Width (m)	Bankfull Depth (m)	Bankfull W/D	Ideal W/D	Area (m)
Rio Puerco - Upper	9.7	1.6	6.2	7.4	10.4
- Lower	15.9	2.3	7.2	4.2	23.5
Santa Cruz River	72.1	2.9	24.7	23.5	139.9
San Simon River	14.7	1.4	10.5	12.0	15.6

Table 6.1 Comparison of bankfull geometry of trapezoidal channels.

It was noted in Chapter 4 that the percentage of clay and silt in the channel perimeter of the Rio Puerco was appreciably higher than that of the San Simon River, with values of 34.3 percent (Elliott, 1979) and 17.0 percent (Meyer, 1989) respectively. The Santa Cruz River had the lowest value of M for all three arroyos, with a value of 9.1 percent (Meyer, 1989). Equation 4.2 was used to calculate the ideal width:depth ratio for the average value of M

in each reach (Table 6.1). It is immediately obvious that the equilibrium form of the active channel of the Rio Puerco is substantially narrower and deeper than that of the San Simon River. Similarly, the Santa Cruz River is expected to develop a much wider, shallower channel than the other two arroyos studied. It is, therefore, likely that the differences in the channel geometry observed in Table 6.1 are due to a combination of stage of evolution and sediment size, whereby the active channel becomes narrower and deeper with time, within the constraints of the channel perimeter sediments.

It was noted in Chapter 4 that aggrading channels tend to have a higher width:depth ratio and degrading channels tend to have a lower width:depth ratio than that calculated using M (Schumm (1960)). However, while the ideal values of the width:depth ratio calculated from the average values of M were considered characteristic of generalised conditions within the arroyo, these values were not considered sufficiently representative to form any conclusions regarding the stability of the contemporary morphology of specific reaches.

Observations of the contemporary morphology of the arroyos studied have again emphasised the need to consider the specific control variables acting on geomorphologically distinct reaches within the system, rather than taking an holistic approach. Each reach evolves almost independently, adjusting to the external, driving influences. Reach-scale development is encouraged by the localised, longitudinally discontinuous nature of flow events.

6.4 FLOOD-SCALE ARROYO MODIFICATION MODEL

Although the processes of weathering and sub-aerial erosion which occur both between and during flow events do modify the arroyo morphology, their geomorphological effect is slight when compared with the effect of the flow events themselves. Arroyo morphology is, therefore, a product of the amalgamated effect of the sequence of flow events which have occurred since incision commenced. Field observations and photographic records provide a representation of this combined result. However, especially

during the earlier stages of evolution, prior to a more stable morphology being achieved, the snapshot views that fieldwork and observations of photographs afford may be misleading. Morphological change occurs during each flood, the amount dependent on the pattern, magnitude and sequence of flows. However, further understanding of the flood-scale behaviour of arroyo systems enables these short-term morphological fluctuations to be taken into account when attempting to determine a general long-term evolutionary trend.

The flood-scale model of arroyo evolution proposed by Ellis (1993) was based on observations of a Stage 4 reach of the Santa Cruz River (using the categories of Elliott's arroyo evolution model). Despite this, the essential concept - that floods of different magnitudes are responsible for correspondingly different morphological changes - has been found to apply equally to all three arroyo systems studied. Ellis' (1993) model was supported by the observations of the Santa Cruz River during the 2000 flood. During a flood, significant scour of bed sediments occurs initially, causing deepening and widening of the active channel to accommodate the increased discharge. However, narrowing occurs immediately, even during the falling limb, as sediments are re-deposited to form lateral berms and point bars. Subsequently, these bars are stabilised by rapid vegetation growth. During smaller flow events continued vertical and lateral aggradation of these bars occurs, causing narrowing of active channel. Further establishment of vegetation enables bar stabilisation to the point where all but largest flows are withheld. It can, therefore, be seen that even within an evolutionary stage, a significant variation in morphology may occur.

It was suggested, in Chapters 4 and 5, that the morphology of the arroyo is controlled by the flow regime, until a stabilised inner floodplain has formed, at which point the morphology affects the hydrograph to such an extent that the flow regime is altered. It is, therefore, vital to consider the evolutionary stage when determining the effect of floods of different magnitude. If the

reaches of contemporary arroyos are examined in the context of the current flow regime, the above model of morphological response to flooding can be seen to hold true for those reaches in which the morphology is still sufficiently adaptable to adjust somewhat to each and every flood. However, as aggradation and accretion build the inner floodplain, which is then further stabilised by vegetation, this adjustability is lost. At this point, the larger-magnitude flows, which had the greatest geomorphological effect on the arroyo morphology, no longer occur, since the peaks are attenuated by the increased in both floodplain area and roughness. A negative feedback mechanism is thus promoted, whereby flow velocities are reduced and sedimentation within the established vegetation is promoted. As the arroyo morphology evolves, individual floods, therefore, generate gradually lower amounts of geomorphological change.

CHAPTER 7

Effective Discharge

The previous chapters have examined the hydrologic regime and morphology of the study arroyos. To determine the degree to which the size and morphology of the active channels in arroyo systems are determined by the regime of flows which have been experienced, the effective discharge was calculated using available data from gauging stations and channel surveys and compared to the cross-sectional morphology of the active channels. As discussed in Chapter 2, theories of channel-forming flow have not been generally thought to be applicable to arroyo systems. The high flow variability, combined with long recovery periods associated with ephemeral rivers in semi-arid areas, have contributed to the belief that catastrophic events have greater morphological control than lower-magnitude, more frequent flow events (Schumm and Lichy, 1963; Wolman and Gerson, 1978; Hey, 1997). However, observations during this study have indicated that arroyo systems develop quasi-stable regime channels which are not morphologically affected by high-magnitude discharges.

Chapters 5 and 6, together with studies by other researchers, such as Nordin, 1961; Popp *et al.*, 1988; Parker, 1996; Elliott *et al.*, 1999; and Gellis and Elliott, 2001, have demonstrated the rapidity at which geomorphological change occurs within the arroyo trench. Even during single floods a large amount of scour and fill can occur, making underestimation of the actual bankfull flow likely. This morphological variability, combined with the longitudinal variability observed, affects both the magnitude and frequency of overbank flows and the efficiency of sediment transport (Popp *et al.*, 1988). This fact should be taken into consideration when examining the results of the bankfull and effective discharge calculations.

7.1 EFFECTIVE DISCHARGE CALCULATIONS

Methodology

The effective discharge at all available gauges was calculated using a computer program developed at Colorado State University by Chris Holmquist-Johnson and David Raff. This program follows the accepted

procedure for calculating the effective discharge, as outlined in Hey (1998), Thorne *et al.* (1998) and Soar and Thorne (2001). The methodology used is detailed in Appendix 1. These calculations require a flow frequency curve, which is combined with a sediment rating curve to produce a sediment load – discharge histogram, the peak of which denotes the effective discharge (Figure 2.1).

The first step in calculating the effective discharge was to construct the sediment rating curve for gauges with measured sediment load data. As shown in Chapter 4, it was determined that a double logarithmic scale provided the best correlation between the flow and sediment discharge data (Figures 4.12 and 4.13). This enabled a regression equation with the following form to be produced:

where Q_s = measured suspended sediment load (tonnes per day)

Q = water discharge (cumecs)

a = coefficient

b = exponent.

The values of the coefficient of determination (R^2), as noted in Chapter 4, indicate that there is a good correlation between the curves calculated and the actual discharge and sediment load relationship, with the exception of the data measured at the Arroyo Chico gauge. All relationships were found to be significant at the 99.99% level (also noted in Chapter 4). Table 7.1 shows a summary of the sediment rating curve variables for the gauges where sediment data was available.

Once these rating curves had been constructed, their equations were input into the effective discharge program, together with the raw discharge data. The program is set up to enable the user to vary the period of record for which the effective discharge is calculated. This is crucial in determining an accurate value or range of values of the effective discharge. The period of record must be sufficiently long to include the entire range of morphologically significant flows, but not so long that changes in flow or

Arroyo	Gauge	a	b	R ²
Instantaneous Measurements				
Rio Puerco	Bernardo	3846.7	1.3403	0.8842
Santa Cruz River	Tucson	149.63	1.5374	0.8145
Daily Average Data				
Rio Puerco	Bernardo	3932.9	1.4585	0.8363
	Above Arroyo Chico	2778.7	1.7105	0.9087
Arroyo Chico	Arroyo Chico	15113	0.462	0.3373
San Simon River	Solomon	4465.3	1.2174	0.9417

Table 7.1 Sediment rating curve variables (see Figure 4.12 and 4.13 for chart representation of these relationships). All relationships are significant at the 99.99% level.

sediment regime occur (Thorne *et al.*, 1998; Soar and Thorne, 2001). The regime analysis detailed in Chapter 4 indicated that all three arroyos had undergone significant changes in both flow and sediment discharge regimes over the period of record. The contemporary regime of the Santa Cruz River and San Simon River commenced in approximately 1960. However, as noted in Chapter 4, since this time, the non-stationarity in the flood frequency record for the Santa Cruz River indicates that even since this time, the runoff regime has continued to change. Along the Rio Puerco, the contemporary regime commenced in the mid-1970s, which is contemporaneous with the initial development of a quasi-equilibrium channel (discussed in Chapters 4 and 5).

Generally, calculations for perennial rivers are based on between 10 and 20 years' discharge data, in order to prevent regime changes affecting the result (Thorne *et al.*, 1998; Soar, 2001). However, if too few years are used for arroyos, the ephemeral nature of the flow regime causes sediment load peaks due to individual floods to assume excessive importance. Thus, it was felt that a longer timer period was justified. However, the sensitivity to the changing period of record was also investigated by using both longer and shorter periods of time for the effective discharge calculations.

The flashy nature of the discharge regime in arroyo systems presents a further difficulty when calculating the effective discharge. As discussed in Chapter 2, mean daily flow and sediment discharge records are likely to be unrepresentative of the actual flow events along these rivers (Hey, 1998; Soar, 2001). The sediment rating curve equations recorded in Table 7.1 indicate the difference caused by the difference in time-base. The availability of 15 minute data, as well as daily average data, at three of the gauges (Tucson and Continental, Santa Cruz River and Bernardo, Rio Puerco) enabled a comparison of the effective discharges calculated for each data type.

The second step necessary in calculating the effective discharge is the production of a flow-frequency histogram. The grouping and number of the discharge classes used in this histogram may influence the value of the discharge calculated (Hey, 1998; Thorne, *et al.*, 1998; Soar, 2001). If the class interval is too small, especially given the flashy regime of arroyos, the flow-frequency curve becomes too discontinuous to produce a continuous sediment load histogram. Soar (2001) suggests that the selected class interval should be small enough to represent accurately the frequency distribution but with no classes having a frequency of zero. However, if too few classes are used, the range of flows represented by each group becomes too large to be useful. When calculating the effective discharge for the gauges along the arroyos studied, it was impossible to find a class interval which gave enough detail but prevented some classes having zero frequency. After using several different class numbers, it was found that 25 classes gave the most continuous flow frequency distribution without losing vital detail, a result also found by Hey (1997).

Generally, during the calculation of effective discharge, if the peak sediment load falls within the first class, a logarithmic scale is advised for the flood frequency histogram (Hey, 1997). The logarithmic scale gives undue importance to the smaller values, which is useful for rivers with flashy regimes. However, studies by Soar (2001) and Holmquist-Johnson (2002)

have indicated that, while convenient, use of a logarithmic scale results in bias in the calculations resulting in overestimation of the effective discharge. Thus, even though the peak sediment load was found to be in the first class due to the flashy flow regime of the arroyos studied, an arithmetic scale was retained.

For the purposes of this study, peaks in the first discharge class were ignored and the effective discharge taken as being the next largest peak. This was justified for a number of reasons. The relationships between discharge and sediment discharge data were based on regression analysis, which, as can be seen in Chapter 4 (Figures, 4.12 and 4.13), has a tendency to over-predict in the lower range of values. Thus, the sediment transport rate calculated using the regression relationships also tends to overestimate the amount of sediment transported by low-magnitude events. The lowest-class peaks were also discarded due to the lack of morphological representation of low-magnitude flows within the arroyo trench. The low flow-stage of these small discharges only allows them to rework active channel bed sediments. Thus, in terms of arroyo morphology, these flows are geomorphologically ineffective.

The flow and sediment discharge data available for the three arroyos studied is summarised in Appendix 3. Unfortunately, due to their ephemeral nature, this data is neither continuous or of excellent quality. In many cases gauges were abandoned many years ago, or have not been continuously maintained. Fifteen minute discharge data, while available, is generally discontinuous due to the tendency of the gauges to become silted rapidly during flow events. This lack of continuous data may cause an inaccurate representation of the effective discharge since significant flows may not be represented or the flows used may not be representative of contemporary conditions. Other problems with data continuity and quality are noted in Appendix 3. However, despite these drawbacks, the data used for this study was the best available for the south-western arroyos and was sufficiently representative of the contemporary regime for the purposes of this project.

Rio Puerco Effective Discharge Results

Bernardo Gauge

The Bernardo gauge has the most continuous and complete record of both flow and sediment discharge of all the gauges used in this study (see Chapter 4). Both daily average and 15 minute discharge records are available, together with corresponding daily average and instantaneous sediment concentration records. The results of the effective discharge calculations for this station are illustrated in Figures 7.1 – 7.3 and are

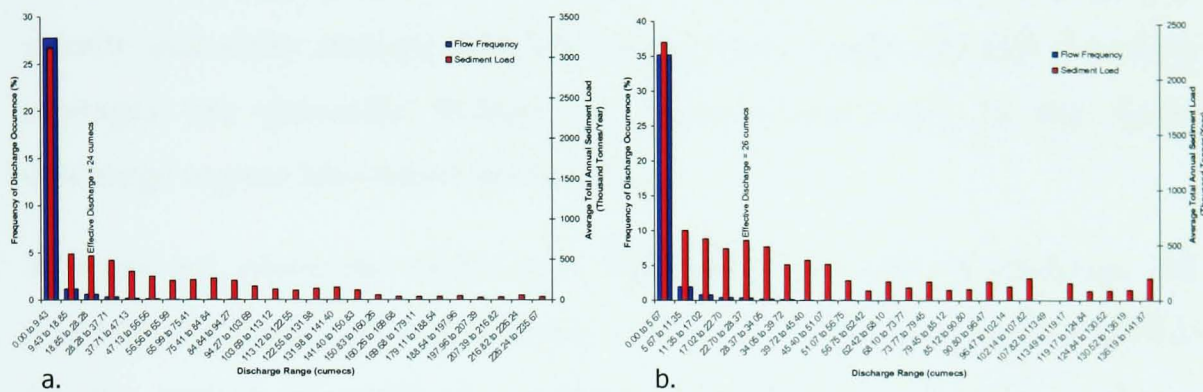


Figure 7.1 Effective discharge for Bernardo Gauge using a. 15 minute/instantaneous and b. Daily average flow and sediment discharge data, 1949 - 2000.

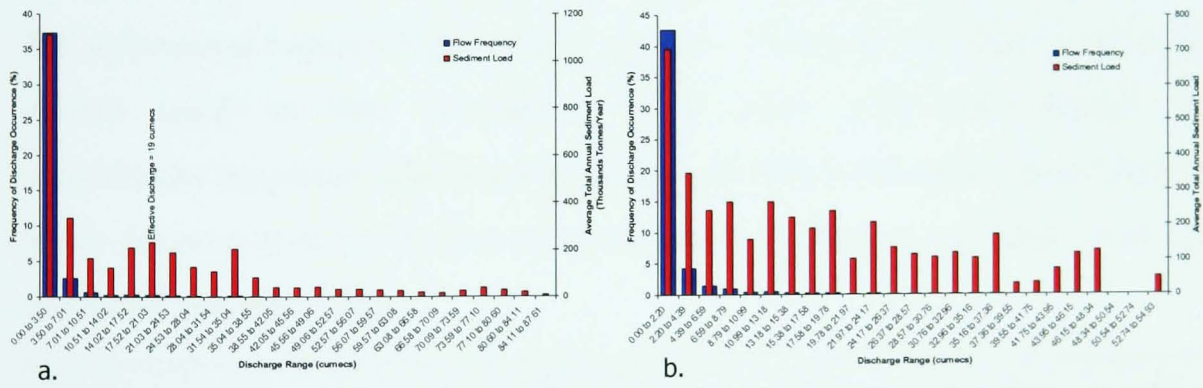


Figure 7.2 Effective discharge for Bernardo Gauge using a. 15 minute/instantaneous and b. Daily average flow and sediment discharge data, 1975 - 2000.

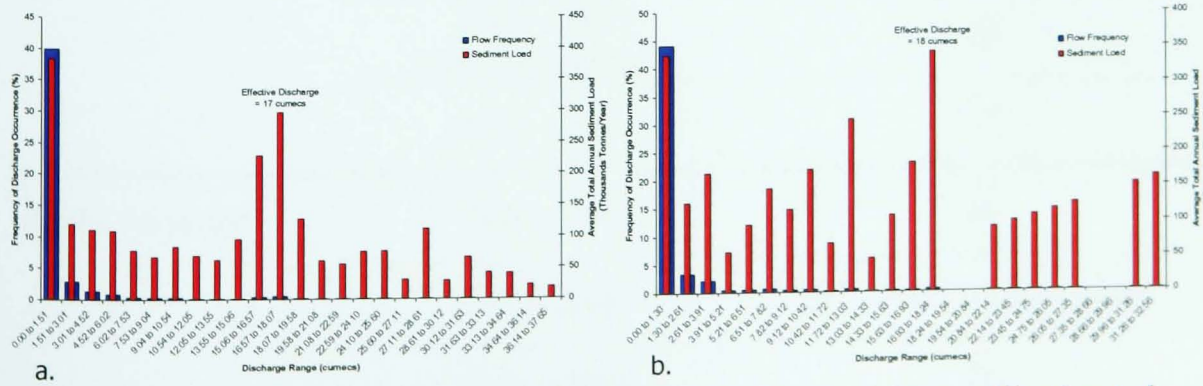


Figure 7.3 Effective discharge for Bernardo Gauge using a. 15 minute/instantaneous and b. Daily average flow and sediment discharge data, 1997 - 2000.

summarised in Table 7.2. These results indicate effective discharges that are considerably lower than the value of 40.1 cumecs obtained by Nash (1993), although this is likely to be an overestimate, as it was obtained using logarithmic class sizes.

The time periods chosen represent the entire period of record (1949 – 2000), the approximate period of the contemporary regime (1975 – 2000) and a very short, recent period (1997 – 2000). The results indicate that, if the peak in the first class is disregarded, the effective discharges calculated for both 15 minute and daily average data are very similar, despite the fact that daily averages are generally thought to be unrepresentative of the flashy discharge regime (discussed in Chapter 4).

As expected, given the decrease in both flow and sediment discharge, the effective discharge calculated for the current flow regime is lower than that for the period of record as a whole. Similarly, the effective discharge calculated for the most recent few years is lower still. As Figure 7.3 shows, this is the only chart which shows a distinct peak, which is consistent with the ephemeral nature of the arroyo regime. However, the short period of record used in this calculation is at odds with the concept of magnitude/frequency discussed in Chapter 2, where the most crucial factor is the frequency of occurrence of a particular discharge magnitude over an extended period of time.

Data Type	Period of Record Used	Effective Discharge (m ³ /s)
15 Minute	1949 – 2000	24
	1975 – 2000 (not continuous)	19
	1997 – 2000	17
Daily Average	1949 – 2000	26
	1975 – 2000	[12 - but no clear peak]
	1997 – 2000	18

Table 7.2 Summary of effective discharge calculations for Bernardo Gauge for different time periods and data types.

Rio Puerco Gauge

The data available for the Rio Puerco gauge consisted only of daily average data recorded between 1934 and 1976. This is believed to be problematic for calculating the contemporary effective discharge. As discussed in Chapter 5, the arroyo morphology has evolved significantly and changed dramatically since 1976. A trapezoidal inner channel, the morphology of which is thought to be controlled by a channel-forming discharge, has formed since this date. Since no sediment discharge data was recorded at this gauge, the regression equation for the nearest gauge, at Bernardo, was used. As Figure 7.4 and Figure 7.5 show, no clear effective discharge may be observed, even when the period of time used for the calculations is reduced to between 1960 and 1976. It is expected that, if the data between 1976 and the present day were available, a similar result to that noted at the Bernardo gauge would be observed, with an effective discharge defined by a peak in the sediment load yield histogram.

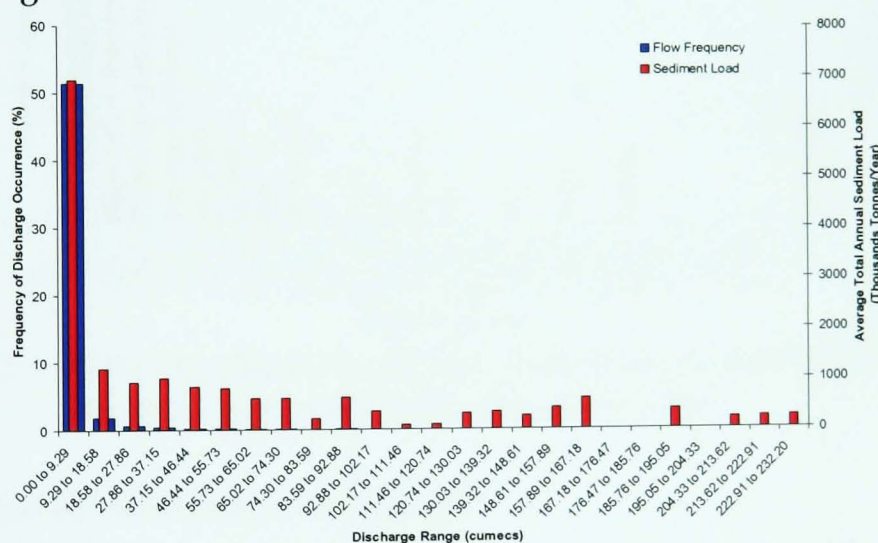


Figure 7.4 Effective discharge for Rio Puerco Gauge using daily average flow data, 1934 - 1976.

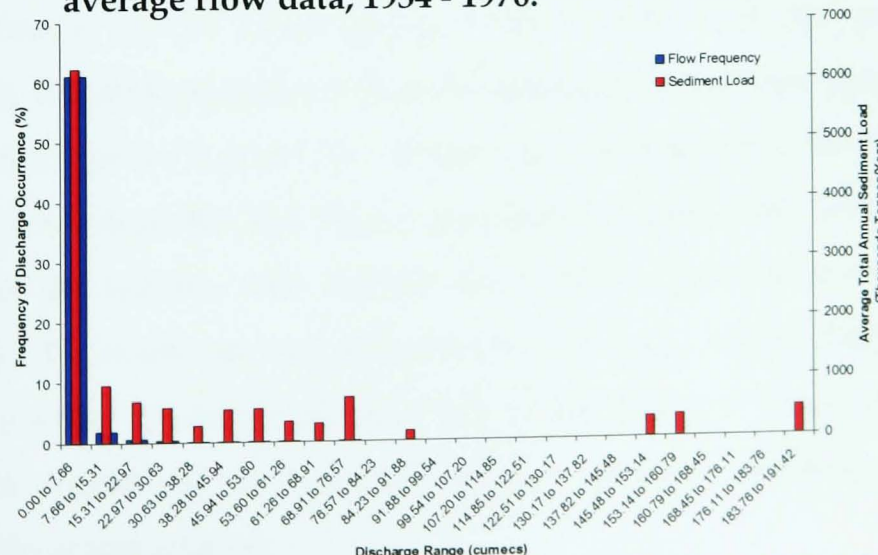


Figure 7.5 Effective discharge for Rio Puerco Gauge using daily average flow data, 1960 - 1976.

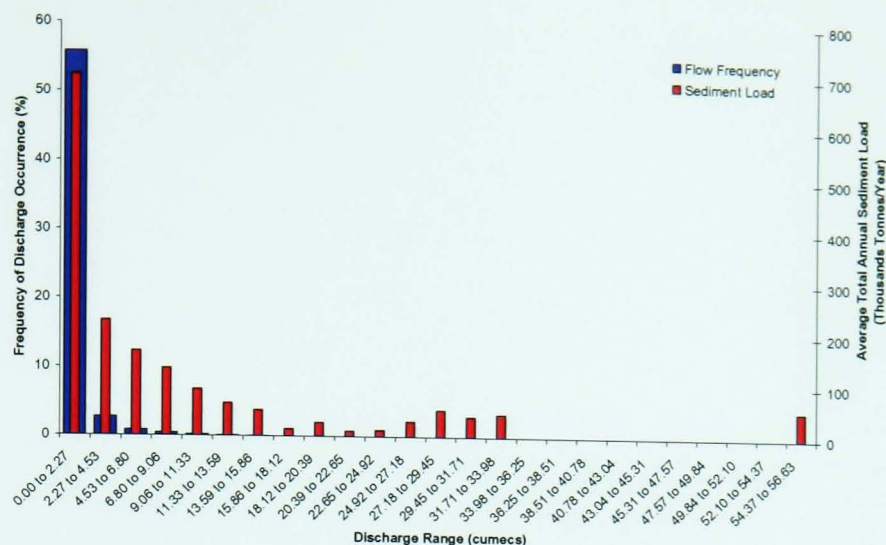


Figure 7.6 Effective discharge for Rio Puerco above Arroyo Chico Gauge using daily average flow data, 1951 - 2000.

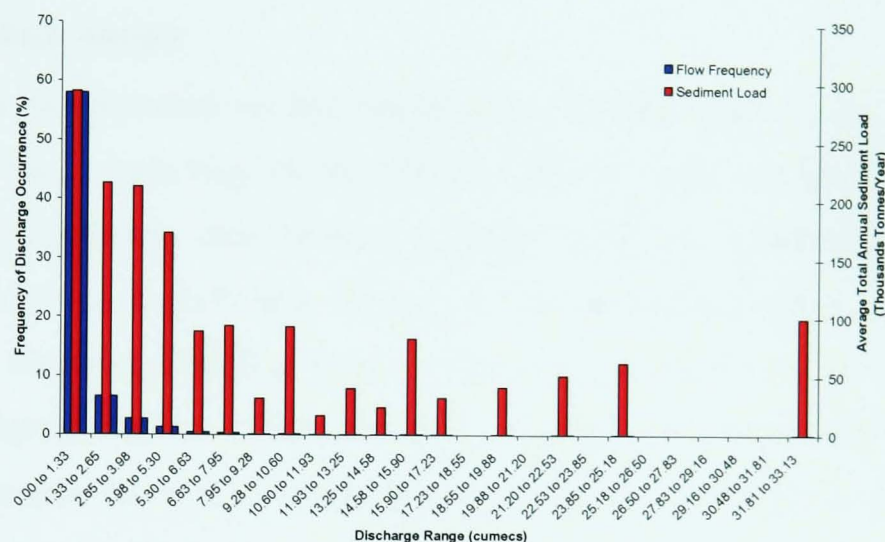


Figure 7.7 Effective discharge for Rio Puerco above Arroyo Chico Gauge using daily average flow data, 1990 - 2000.

Rio Puerco above Arroyo Chico Gauge

Daily average discharge and sediment discharge data is available for the Rio Puerco above Arroyo Chico gauge between 1951 and the present day. However, calculations indicate that no specific effective discharge occurs at this point (Figures 7.6 and 7.7). As discussed in Chapter 4, the flow regime along this reach of the Rio Puerco has behaved differently from the other gauges in the system, with annual flow totals increasing in recent years. Similarly, the reach has not attained the late-stage morphology observed along the lower reaches of the Rio Puerco (discussed in Chapters 5 and 6). Hence, it would not be expected that an effective discharge would be discernible at this station.

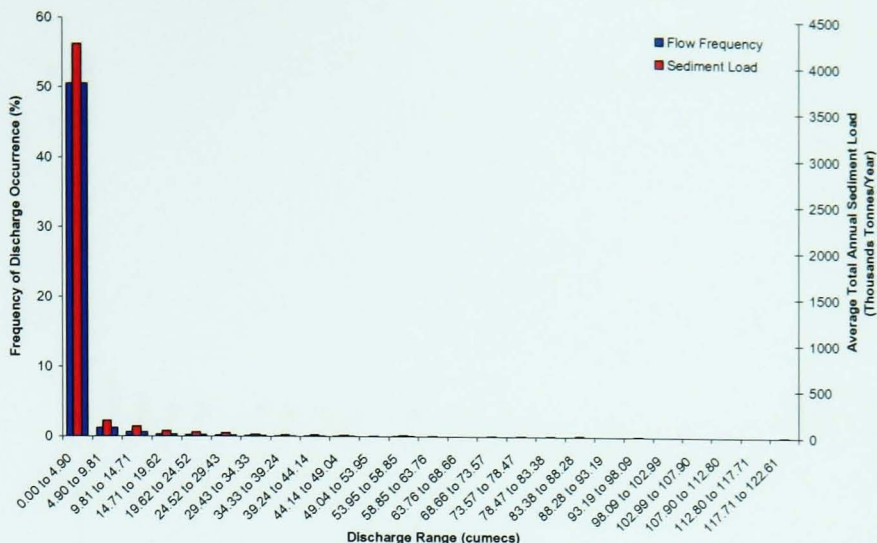


Figure 7.8 Effective discharge for Arroyo Chico Gauge using daily average flow data, 1943 - 1986.

Arroyo Chico Gauge

Although not situated on the mainstem of the Rio Puerco, the similarity between the morphology of the Arroyo Chico and the reaches of the main arroyo immediately downstream, together with the availability of daily average flow and sediment discharge data, prompted calculation of the effective discharge for this gauge. Flow and sediment discharge records were collected between 1943 and 1986. The flood frequency at this gauge was extremely skewed towards the lower values, resulting in a sediment load peak in the first class only. Figure 7.8 illustrates the entire period of record. Similar results for the period 1975 - 1986 were also calculated, again indicating the flashy nature of the flow regime and the early evolutionary stage of the arroyo morphology.

Santa Cruz River Effective Discharge Results

The Santa Cruz River has an appreciably different flow regime from the Rio Puerco, with records since 1960 showing an increase in the frequency of high-magnitude and super-floods (discussed in Chapter 4).

Tucson Gauge

Both 15 min and daily average discharge data are available for the Tucson Gauge. The daily average discharge data, in particular, has been recorded for a considerable period of time, dating back to 1905, although this record is

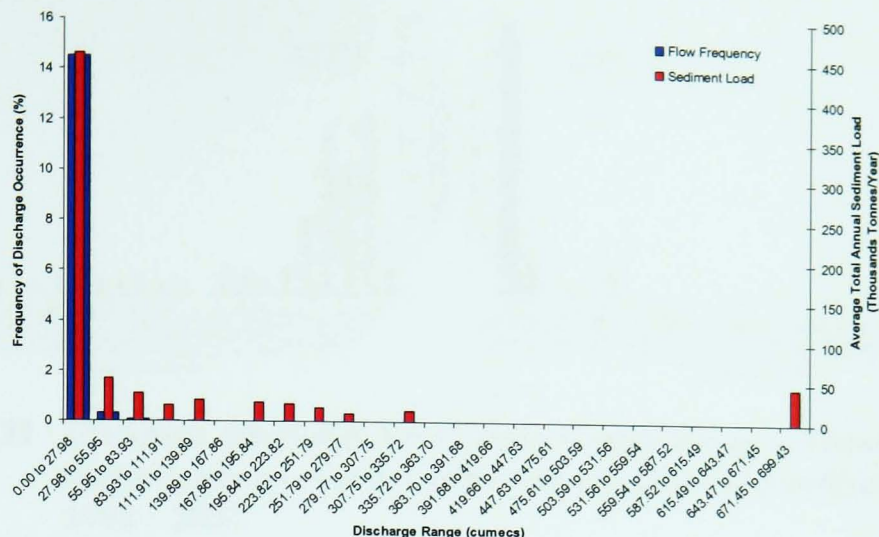


Figure 7.9 Effective discharge for Tucson Gauge using daily average flow data, 1905 – 2002.

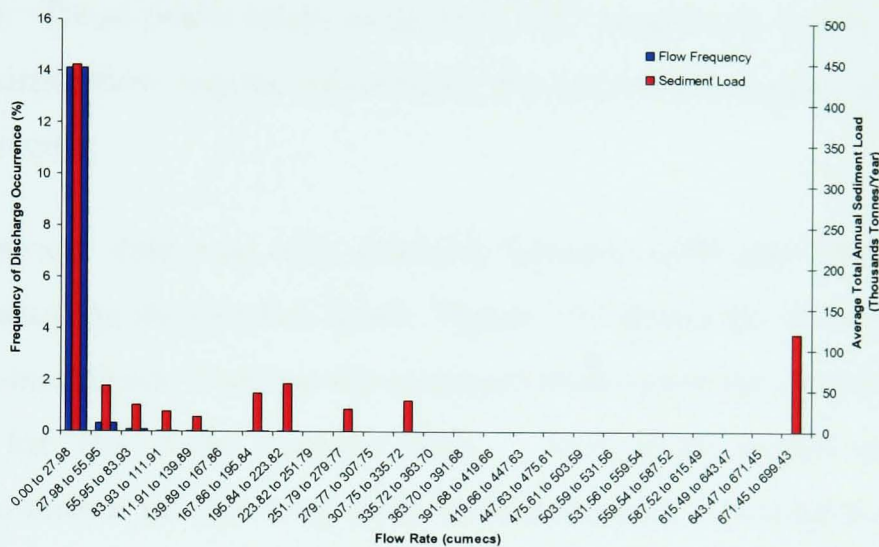


Figure 7.10 Effective discharge for Tucson Gauge using daily average flow data, 1960 – 2002.

by no means continuous. In particular, the flood of record, in 1983, and other high magnitude floods during the 1980s are missing from the flood series. The only sediment discharge data available was the instantaneous data reported by Roberts (1990), which was collected in 1988 and 1989.

The effective discharge calculations for this gauge do not indicate an identifiable effective discharge, with the largest peak occurring in the first class (Figures 7.9 and 7.10). A peak in the sediment load also occurs in the highest class. It is likely that, had the 1980s data been included in the flood series, this pattern of peaks in the first and last classes would have become more extreme. There is no real difference between the chart output for the entire period of record and only using the data for the current flow regime, between 1960 and 2002. The peaks of the sediment load occur within the

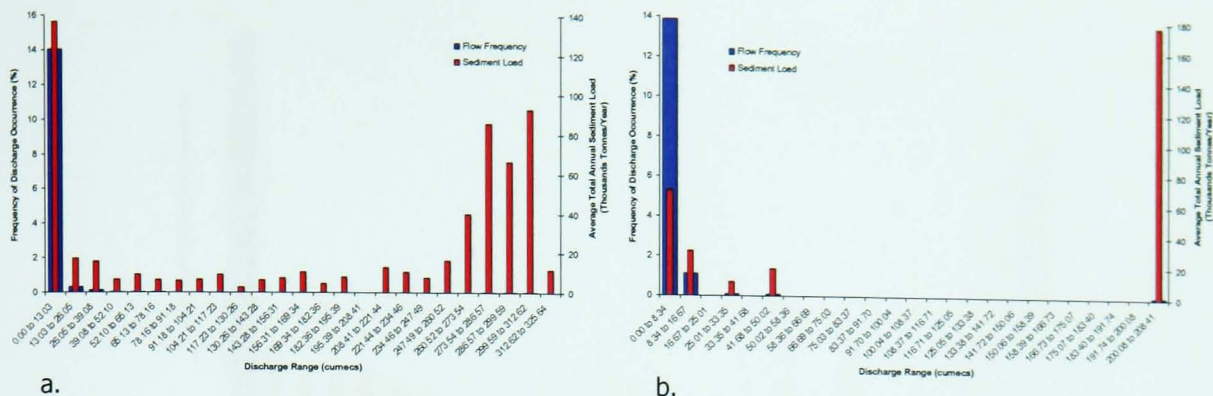


Figure 7.11 Effective discharge for Tucson Gauge using a. 15 minute/instantaneous and b. Daily average flow and sediment data, 1998 – 2000.

same discharge range in both Figure 7.9 and 7.10 but volumes are higher in the latter. These peaks relate to specific high-magnitude floods within the contemporary flow regime, illustrating the geomorphological effectiveness of these events.

Fifteen minute data was only available between 1998 and 2000, with this period including the October flood. Figure 7.11 shows the skewing effect of this high-magnitude flood on the sediment load curve, the effect being more marked for the daily average data. This short period of time is unrepresentative of the long-term flood-frequency conditions but again illustrates the geomorphological effectiveness of large floods on the Santa Cruz River arroyo system. Since the flood regime is still dominated by large-magnitude floods, these flows play a major role in controlling the movement of sediment and thus the evolving morphology of the arroyo trench.

Continental Gauge

Both daily average and 15 minute flow data is available for the Continental gauge, although the daily average data is discontinuous. However, the largest floods of record, in 1977, 1983 and 1993, are included, resulting in a more representative dataset than the Tucson gauge. Unfortunately, however, no sediment discharge data has been collected at this gauge. It was, therefore, decided that, given the similar geomorphology and close proximity of the Continental and Tucson gauges, the sediment rating curve

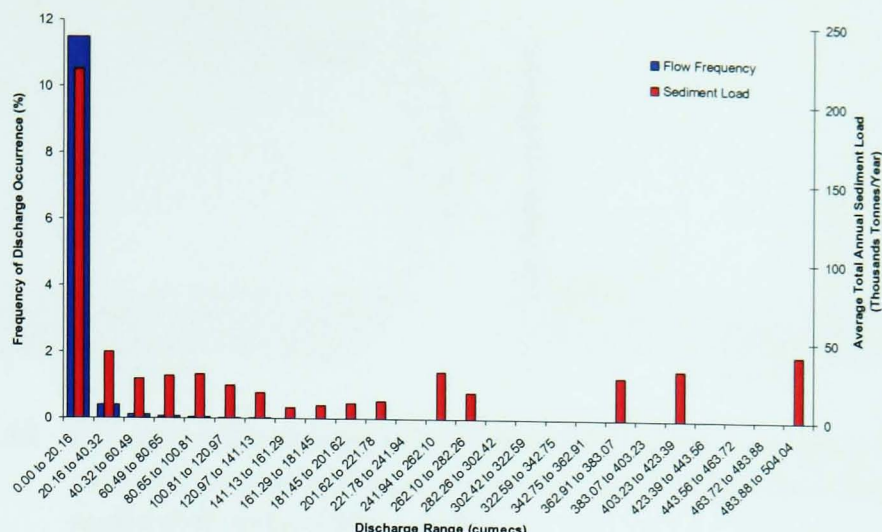


Figure 7.12 Effective discharge for Continental Gauge using daily average flow data, 1940 – 2002.

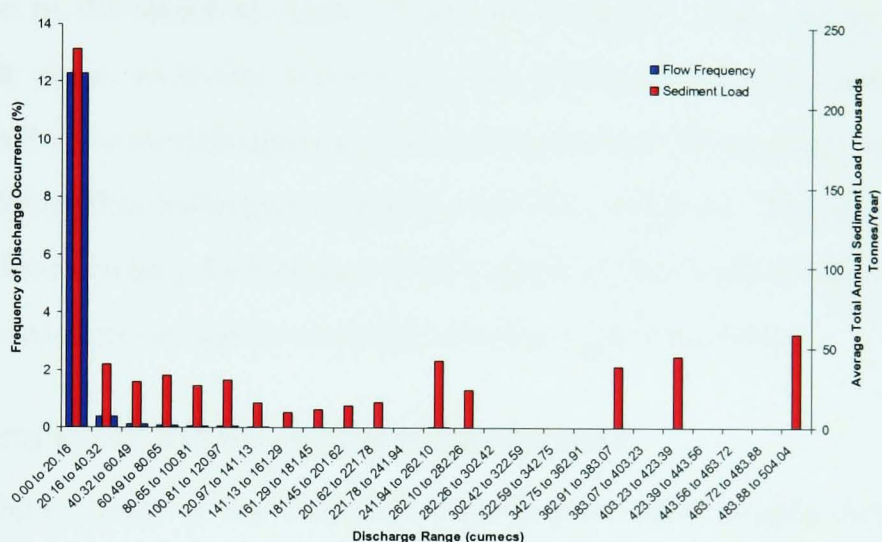
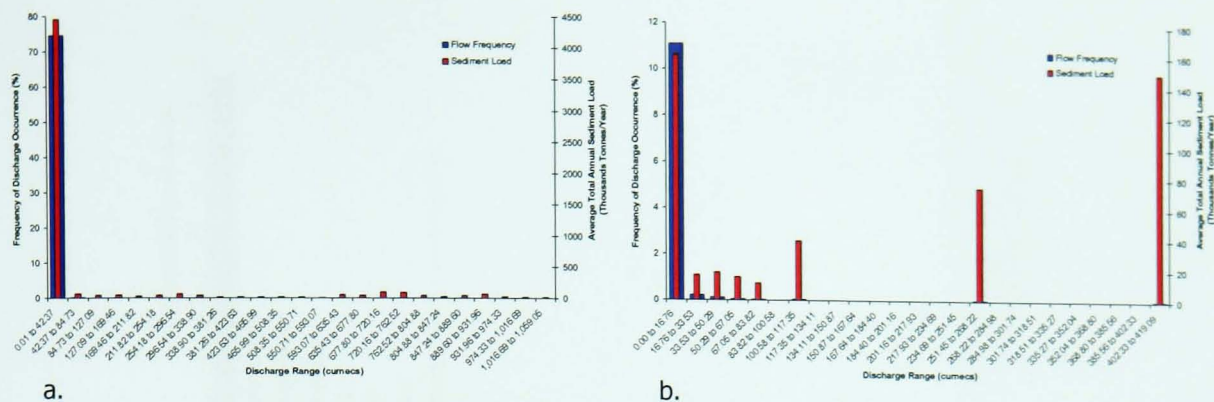


Figure 7.13 Effective discharge for Continental Gauge using daily average flow data, 1960 – 2002.

produced for the Tucson gauge would adequately describe the flow and sediment discharge relationship at the Continental gauge.

As Figures 7.12 and 7.13 show, there is very little difference in the pattern of the sediment load over the entire period of record and since 1960, when the contemporary regime commenced. This indicates the geomorphological importance of the high-magnitude flows which have occurred since 1960, which affect the entire flood frequency record. This is supported by the analysis of 15 minute and daily average data since 1987, where the sediment load peaks are in the highest discharge classes (see Figure 7.14).

It can, therefore, be seen that the sediment load peaks at the Santa Cruz River gauges inevitably coincided with specific high-magnitude floods,



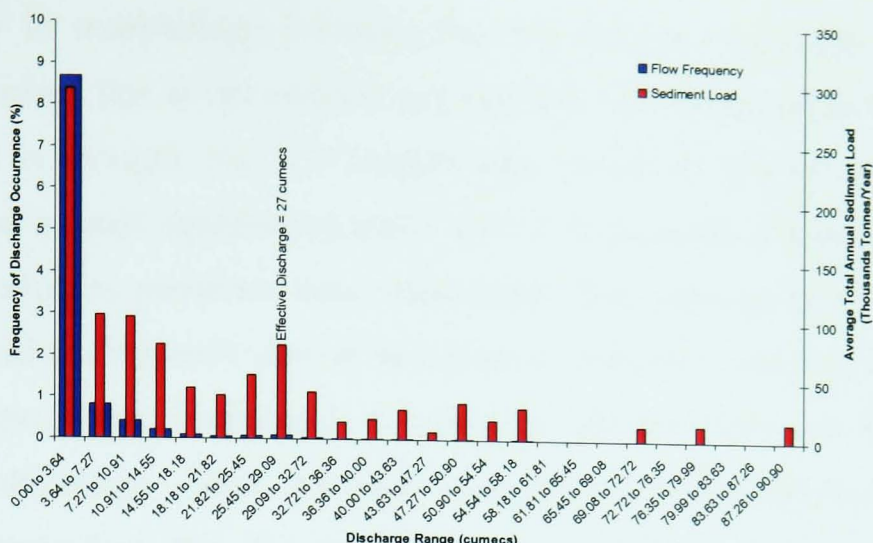


Figure 7.15 Effective discharge for Solomon and Barrier Dam Gauges combined, using daily average flow and sediment data, 1931 – 2000.

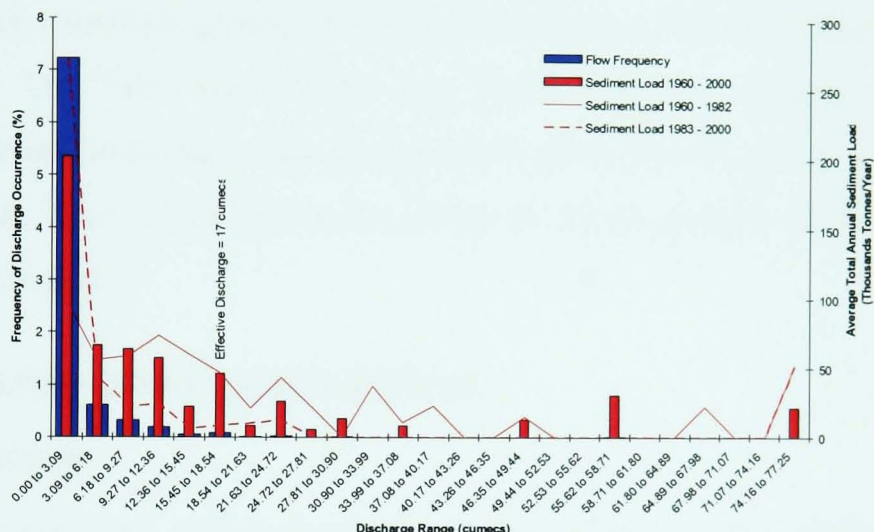


Figure 7.16 Effective discharge for Solomon and Barrier Dam Gauges combined using daily average flow and sediment data, 1960 – 2000.

a distinct and significant reduction in both the daily average and peak discharge data since the BLM began maintaining gauge records. However, examination of the sediment load curve in Figure 7.16 indicates an effective discharge of approximately 17 cumecs, if the peak in the first class is discarded. Given the possible under-calculation of flow discharges since 1983, it is entirely likely that this value is an under-estimation of the true effective discharge.

Conclusion

It is noticeable that the sediment load for the San Simon River has a similar pattern to that calculated for the Rio Puerco at Bernardo. Given the

similarity in morphology between the two arroyos, especially along the lower reaches, this is not entirely unexpected. As discussed in Chapters 5 and 6, it is thought that the morphology of arroyo reaches which have developed a quasi-equilibrium form, with a trapezoidal active channel and inner floodplain, promotes flow attenuation, thus altering the flow regime. This is further discussed later in this chapter. However, arroyos which have not achieved this compound morphology do not have an identifiable effective discharge. Thus, the Santa Cruz River and the Upper Rio Puerco system, including the Arroyo Chico, show distinct peaks in the first sediment load class. Along these reaches, the geomorphological effectiveness of these low flows is amplified by the method used, since their only effect, morphologically, is the reworking of sediments within the active channel. The Santa Cruz River also shows a peak sediment load in the highest class indicating the geomorphological effectiveness of the high-magnitude flows which still occur, although the importance of these flows is again amplified.

7.2 SLOPE-AREA CALCULATIONS

Methodology

The contemporary morphology of representative reaches along the three arroyos was discussed in detail in Chapter 6. From observations made in the field, in particular changes in bank gradient, sediment size and vegetation cover, the bankfull stage for the active channel at each cross section was identified (shown in Appendix 2). Along the reaches of the Santa Cruz River, repeat cross-sections were surveyed before and after the October 2000 flood. The position of the peak stage of this flood was noted on each cross-section to enable the stage-discharge relationship at each site to be determined. Once the bankfull stage had been chosen, the arroyo trench and channel geometry were calculated (summarised in Appendix 3).

Much variability was found between cross-sections, even within the same reach, both at the arroyo- and active channel-scales. As discussed in Chapter 6, this was mainly due to the tendency for both arroyo and channel

widths to increase at the apices of meander bends. Poor longitudinal flow connectivity, as discussed in Chapter 4, is also likely to have contributed to the geometrical variability. However, by using carefully selected geomorphological reaches and reach-averaged values, a more accurate representation of channel dimensions was achieved, since the influence of localised conditions was reduced.

Bankfull discharge was calculated using the equation:

where Q = discharge (cumecs)

A = Cross-sectional area of channel (m^2)

V = Velocity of flow (ms^{-1})

Manning's equation was used to calculate V:

where R = Hydraulic radius = $\frac{A}{P}$ (where P = wetted perimeter)

S = Slope of the energy grade line

n = Manning's flow resistant coefficient

Manning's resistant coefficient, n , was estimated, then checked against values used in previous research. Although the energy gradient should strictly be used for accurate calculation of " n ", bedslope may be used instead (Richards, 1982). Where possible both bedslope and water surface slope were used and the results compared.

Rio Puerco Slope-Area Results

The major drawback for the Rio Puerco survey data was that, although slope measurements were recorded during Elliott's 1970s survey, they were not during Gellis and Elliott's 1990s resurvey. Other usual sources of slope information, such as topographic maps, were even further out-of-date than the available cross-sections. Thus, where possible, more recent slope

measurements taken by other researchers were used. The 1970s slopes noted by Elliott (1979) and the estimated slopes were then used to create an upper and lower limit for the bankfull discharge. Nordin's slope measurements, made between July 10 and September 20 1961, indicate the extreme variability of the arroyo bedslope, with values between 0.00024 and 0.00148 being recorded over this short space of time. Thus, even if the slope is measured during a cross-section survey, it is not necessarily representative of conditions during a flow event. This variability creates further problems since the discharge calculations are most sensitive to small changes in the slope value. However, within the data constraints, a likely range for bankfull discharge at each cross-section was produced (see Appendix 3, Table A3.2).

The bankfull discharges calculated for the Rio Puerco were extremely variable, ranging between 9 cumecs and 111 cumecs. If just the cross-sections with well-defined trapezoidal active channels were observed, point values still varied widely, with a minimum of 26 cumecs and a maximum of 105 cumecs, reflecting the variability of the channel dimensions, in particular the slope. However, if the mean average was calculated using the lower and upper values at each trapezoidal cross-section, a much smaller range of between 46 cumecs and 52 cumecs resulted. The average values compare favourably with Popp *et al.*, (1988), who calculated a value of 51.1 cumecs close to the Rio Puerco gauge, although, again, a great deal of variability was reported.

Along the Upper Reach, above the Arroyo Chijuilla, a similar degree of variability was observed in the bankfull calculations. This reach had also developed a trapezoidal inner channel. The smaller dimensions of the channel along this reach resulted in a far lower average bankfull discharge than that calculated for the Lower Reach, with a value of 27 (shown in Appendix 3, Table A3.2).

To ensure that the discharge/area and discharge/velocity relationships calculated in this study were realistic representations of actual conditions, a

comparison was made to those actually measured in the field. The US Geological Survey records the values of the channel area and flow velocity to determine the stage/discharge relationship at each gauge. Figure 7.17 shows that the calculated values compared well to the values measured at the Bernardo Gauge.

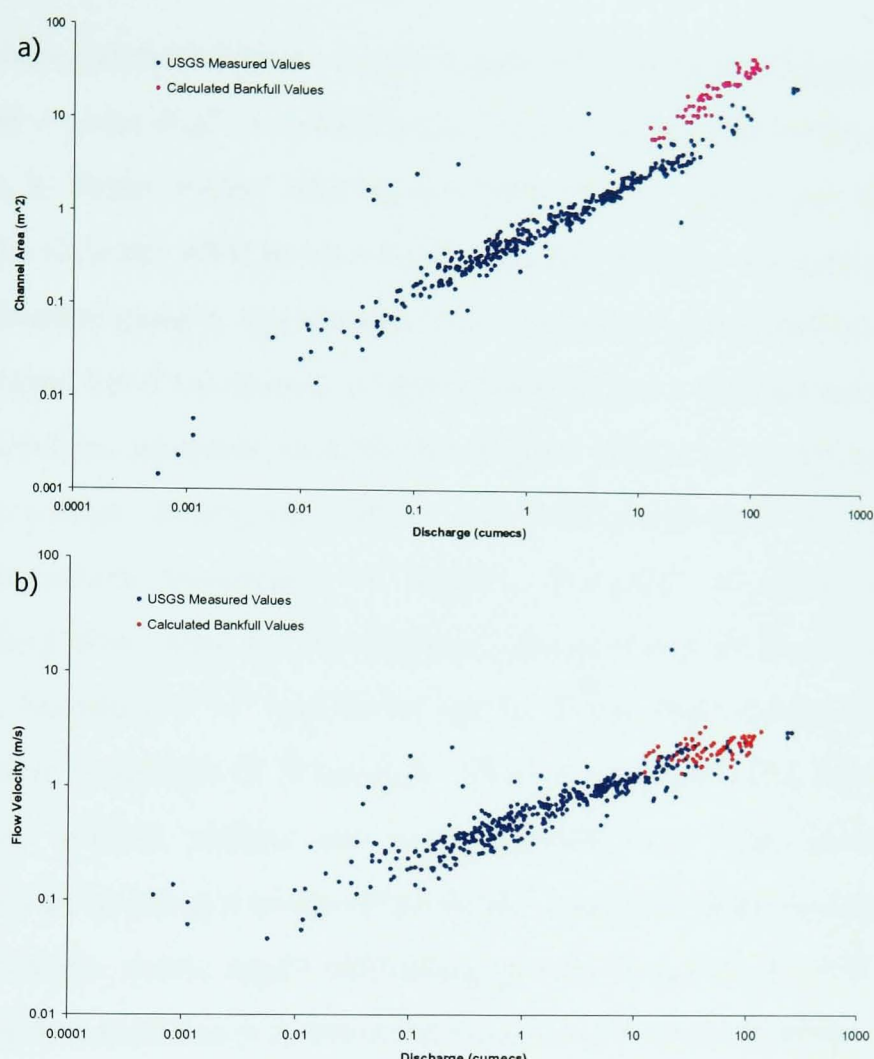


Figure 7.17 Comparison between actual values at the Bernardo Gauge and calculated bankfull values in the Lower Reach of the Rio Puerco, showing relationship between discharge and a) area and b) flow velocity.

Santa Cruz River Slope-Area Results

As discussed in Chapters 5 and 6, the Santa Cruz River has no easily identifiable bankfull stage along the majority of its active channel. The active channel, although generally visibly distinct, has generally poor morphological definition in comparison to the trapezoidal channels observed along the lower reaches of the Rio Puerco and San Simon River. Along the South of Straight and Big Bend reaches, however, the inner

floodplain had aggraded to an extent where a compound channel had begun to form and thus a bankfull level could be defined (discussed in Chapter 6). However, these reaches had not yet attained their equilibrium geometry and thus represent bankfull discharges which are considerably higher than would be found for a regime channel.

The variability in downstream channel geometry noted in Chapter 6 has also resulted in a great deal of variability in the calculated discharge values (see Appendix 3, Table A3.5). During the 2001 survey, the upper limit of the stage of the October 2000 flood was readily identifiable. At both the Tucson and Continental gauges, upstream and downstream of the surveyed reaches, the peak flood level fluctuated at approximately 300 cumecs for some hours. It was, therefore, assumed that the flood-peak discharge remained uniform along the arroyo during this flood and back-calculations were made to determine realistic Manning's "n" values. However, to obtain flood-level discharges of this value for the bankfull stages noted on the cross-sections surveyed, Manning's "n" had to be set far lower than is found in natural channels (see Appendix 3, Table 3.5). This suggests that the measured bed and water surface slopes are unrepresentative of the energy slope. Discharge values along a single cross-section also varied by several hundred cumecs in some cases, again indicating potential problems with applying techniques developed in perennial channels to ephemeral systems.

San Simon River Slope-Area Results

As discussed in Chapters 5 and 6, the contemporary channel of the San Simon River was distinctly trapezoidal along the lower reaches below the Fan Dam. The geometry of the channel upstream of this artificial grade control had been significantly affected and thus the bankfull stage, although distinct, was felt to be unrepresentative of a naturally evolved active channel.

The active channel of the lower reaches of the San Simon River shows far more consistency of geometry than observed along the Rio Puerco or Santa Cruz River (see Chapter 6 and Appendix 3). When averaged over the lower

reach, a bankfull discharge of 32 cumecs was calculated, with values ranging between 14 and 48 cumecs.

Conclusion

Bankfull discharges were calculated for the surveyed cross-sections for the three arroyos studied. There was a great deal of variability in these values, especially for the Santa Cruz River and to a lesser extent for the Rio Puerco, emphasising the need for the use of reach-averaged geometry to reduce the skewing effect of local influences. Meaningful results were only obtained for those reaches with trapezoidal active channels, where the bankfull level had a distinct morphological expression. In reaches without this quasi-equilibrium form, the channel was adjusted to the variability of flow, whereby the contemporary process-form relationship is not represented by a well-defined channel formed by a single identifiable discharge.

7.3 MORPHOLOGICAL REPRESENTATION OF EFFECTIVE AND BANKFULL DISCHARGES

In order to explore whether a morphological expression of the effective flow existed in late-stage evolving arroyo systems, a comparison was made between the calculated values of effective and bankfull discharge for the active channel.

Rio Puerco

An effective discharge was only identifiable at the Bernardo gauge on the Rio Puerco. The other gauges, either had incomplete data or no sediment load yield peak. The gauges with no recognizable effective discharge were those which had not evolved to the late-stage arroyo form. The cross-section closest to the Bernardo gauge was that surveyed at the Bernardo cableway (Appendix 2, Figure A2.9). However, as discussed in Chapter 5, the active channel at this point is degrading and thus this cross-section is unrepresentative of the flows experienced. However, if the next sub-reach upstream is observed, it can be seen that the bankfull discharge calculated has a reach average of between 28 and 30. This is slightly higher than the effective discharges noted in Table 7.2, which ranged between 17 and 26

cumecs. Thus, the results obtained indicate that the effective discharge is a high, in-bank flow. This finding concurs with other investigations of channel-forming flow in sand-bed rivers and rivers with flashy regimes (Thorne *et al.*, 1993; Biedenharn and Thorne, 1994; Hey, 1997; Soar and Thorne, 2001).

Although a representative bankfull discharge was calculated for Upper Reach 1, the closest gauge, Rio Puerco above Arroyo Chico, was situated below both the confluence with the Arroyo Chijuilla and the artificial Ventana sub-reach in an entirely different morphological reach. No effective discharge could be identified for this gauge and the active channel had not achieved the evolutionary stage of Upper Reach 1. Thus it was not possible to compare the bankfull discharge in the uppermost reach with a calculated effective discharge.

Santa Cruz River

No effective discharge could be identified at either gauge along the Santa Cruz River, indicating a channel in an intermediate stage of evolution, that is controlled by extreme events. However, the widest self-formed reaches have begun to create a trapezoidal inner channel. Along the Rio Puerco and San Simon River, a feedback effect was observed along reaches with a trapezoidal channel whereby the arroyo morphology evolved to the extent that flow attenuation and, therefore, modification of the flow and sediment regime occurred. The reaches of the Santa Cruz River where this morphology has begun to develop are short and the active channel has not achieved an equilibrium form. Thus, the arroyo morphology has not yet begun significantly to alter the flow and sediment regime. Since the arroyo has been prevented from expanding laterally to its maximum width, due the upstream outcropping of resistant sediments and the downstream implementation of artificial bank protection schemes, it seems unlikely that a trapezoidal channel will form along a significant proportion of the Santa Cruz River. Consequently both the arroyo and active channel will continue to be controlled by the flow variability, rather than an effective discharge.

San Simon River

Using the combined gauges of the San Simon River, an effective discharge of 17 cumecs was calculated for the contemporary flow regime, between 1960 and 2000. However, it is likely that this is an underestimate, given the noticeable reduction in recorded discharge since 1983. Therefore, the effective discharge for the entire period of record (1931 – 2000), 27 cumecs, may be more a representative value. The size of the active channel of the lower reaches of the San Simon River, although still highly variable, was less so than along the Rio Puerco or Santa Cruz River, giving an average bankfull discharge of 32 cumecs. The bankfull and effective discharge stages are thus very close, with bankfull stage being the higher of the two. The effective discharge is, therefore, again a high, in-bank flow, although the bankfull and effective discharges are much closer in value than observed on the Rio Puerco.

7.4 INTERPRETATION

As discussed in Chapter 2, effective discharge theories were developed for regime channels, defined as those which have no net change in Q capacity or morphology when averaged over a period of time (Hey, 1997). The channel or a river in regime can be changed dramatically during large floods provided lesser events restore the channel to its equilibrium state. Repeat cross-sections of Rio Puerco indicate that this restoration occurs along the majority of the active channel of its lower reaches. Although repeat cross-sections have not been surveyed along the lower reaches of the San Simon, the similarity of form and response to the Rio Puerco indicates that a quasi-equilibrium channel form is likely to have been attained along these reaches.

It was observed that the identification of an effective discharge along the three arroyos studied was linked to the morphology of the reach close to the gauge. Effective discharges were observed for those reaches which had developed a quasi-equilibrium form, with a trapezoidal active channel and inner floodplain. The morphology along these reaches is such that higher magnitude flows are subject to attenuation to such an extent that the

geomorphically effective catastrophic floods no longer occur. The channel morphology is, therefore, adjusted to lower-magnitude, more frequent flow events. However, this is not necessarily equivalent to the effective discharge. This study has found that, along these quasi-stable reaches, the bankfull discharge is of somewhat higher magnitude than the effective discharge, corroborating the results of Thorne *et al.* (1993), Biedenharn and Thorne (1994), Hey (1997) and Soar and Thorne (2001), who found this to be the case along rivers with fine-grained boundary sediments and flashy regimes.

The bankfull and effective discharges were found to correspond more closely on the lower San Simon River than the quasi-stable reaches of the Rio Puerco. As discussed in Chapter 6, the morphology of the lower San Simon River is thought to represent a later-stage form than that of the lower Rio Puerco. Therefore, it seems likely that the progressive narrowing and deepening of the arroyo channel represents adjustment to a quasi-equilibrium, regime form which is a morphological representation of the effective discharge.

Arroyo reaches which have not yet achieved this quasi-equilibrium form, such as those along the Santa Cruz River, Middle and Upper Reaches 2 and 3 of the Rio Puerco, behave differently in response to the variable flow regime. In Chapters 5 and 6, it was concluded that arroyo channels retained a highly adjustable form until the morphology had developed sufficiently to trigger a negative feedback mechanism, which then promoted stabilisation. In disequilibrium reaches, geomorphological change is event-driven, occurring through rapid adjustments to the magnitude and sequence of flooding, which results in an indeterminate form. Morphological representation of bankfull stage is, therefore, highly transient, dependent on the recently occurring flows. Similarly, gauges along these reaches did not exhibit an identifiable effective discharge, with peaks in the sediment load corresponding to the lowest discharge class and specific high-magnitude floods, especially catastrophic super-floods. Since the low flows only

interact with a small proportion of the channel perimeter, these flows cannot be geomorphologically effective no matter how frequently they occur. Catastrophic floods cause extremely large amounts of geomorphological change and, therefore, represent the most effective discharges. Magnitude-frequency concepts, therefore, have limited applicability in reaches which are morphologically controlled by high-magnitude, channel-deforming events.

CHAPTER 8

Discussion and Conclusions

8.1 DISCUSSION

8.1.1 Arroyo Evolution and Contemporary Morphology

The bulk of literature concerning arroyos has concentrated on the causal mechanisms of arroyo initiation. Along the three arroyos studied, downcutting commenced as a result of similar, but fundamentally different, processes, suggesting that thresholds intrinsic to each system were essentially responsible. The actual triggers of initiation were, therefore, simply mechanisms which caused the unincised channel to enter a degradational phase in systems which were nearing stability thresholds. The incision of the Santa Cruz River and San Simon River was initiated, in both cases, by a single large flood event, which exploited artificial irrigation and drainage concentration gullies. The Rio Puerco, however, became entrenched several decades prior to the arroyos studied in Arizona. By the time the first written reports of the condition of the channel were recorded in the mid-1800s, several discontinuous incised reaches existed. It is, therefore, concluded that entrenchment occurred in response to intrinsic geomorphic thresholds. Within the exposed valley-floor sediments in the arroyo walls, palaeoarroyos have been observed. Their presence provides evidence for many past episodes of cut and fill which are largely non-synchronous across the south-western USA. It is most likely that arroyo aggradation phases also occur in response to intrinsic geomorphic thresholds triggered by a variety of causal mechanisms.

The fact that the most recent phase of arroyo incision occurred within historic time has enabled a pattern of subsequent morphological evolution to be recognised. Of the three arroyos studied, the Rio Puerco has been subject to the least artificial change and was the basis for Elliott's (1999) arroyo evolution model. Therefore, a description of the evolution of the Rio Puerco should ideally serve to illustrate the natural pattern of development. However, it was discovered that the arroyo trench was divided into distinct geomorphological reaches which had not evolved at the same rate, due to

the different external, driving variables acting on each reach, despite the fact that Elliott's model indicated headwards progression of each morphological stage. Of the five reaches identified, only the uppermost and lower reaches have developed the quasi-equilibrium form typifying late-stage evolution. In these two reaches, the active channel has become trapezoidal in form, flanked by heavily vegetated levees, which effectively channelise the flow, preventing significant change in either geometry or position within the arroyo trench. Even within these reaches a certain amount of variability was observed. Around the outer banks of meander bends, sediment inputs from bank failures have caused the active channel to remain wide and shallow.

The active channel along the upper and lower reaches was highly sinuous along some sub-reaches, with hooked meanders developing. These meanders have developed within the constraints of both the flows controlling the active channel and former high-magnitude flows which created the arroyo trench. Thus, the radius of curvature of these meanders has become progressively tighter in response to the lower-magnitude flows occurring within the active channel, superimposed on an arroyo-scale wavelength. The active channel along other sub-reaches had retreated from the outer bank of the arroyo meander, cutting across the point bar to straighten its path.

The other three reaches have developed inner floodplains but still have active channels which are far broader and shallower than those observed in the upper and lower reaches. This was due to sediment supplied by large, actively eroding tributary systems: the Arroyo Chico and Arroyo Chijuilla, entering the main arroyo causing the transport capacity of flows to be exceeded. The other transitions between geomorphologically distinct reaches were induced by artificial and natural knickpoints. Several short sub-reaches within the upper Rio Puerco were bedrock controlled and were, therefore still actively widening.

The Santa Cruz River has been subject to the most artificial alteration of the three arroyos studied, due to the close proximity of the large city of Tucson.

The morphology of the Santa Cruz River only conforms to the definition of an arroyo stipulated in Chapter 1 along a short reach upstream of the metropolitan area. This reach has been effectively fixed by the bank protection lining the arroyo walls through Tucson. Soil cement has prevented width increases during flood events. A resistant outcrop of Pleistocene sediments at the upstream limit of the arroyo trench has had a similar effect. The primary mechanism of arroyo adjustment during high-magnitude floods is lateral erosion. Since this mechanism has been hindered, instability has persisted. Where the arroyo has been able to erode laterally without this restriction, a similar pattern of development to that observed along the Rio Puerco was observed. The inner floodplain has aggraded, causing the active channel to become much narrower, deeper and better-defined. Compared with other two arroyos studied, the Santa Cruz River is sparsely vegetated within the arroyo trench, as tamarisk have not been able to thrive. This is due to the fact that the flow regime of the Santa Cruz River is still dominated by high-magnitude flows, which occasionally inundate the entire arroyo floor.

The San Simon River has been artificially modified by sediment detention dams, which have been built across the main arroyo and many of the actively eroding tributaries. These dams have been highly successful in causing aggradation upstream from their location, effectively reversing the progression of evolution along these reaches. The arroyo system is, therefore, discontinuous along the San Simon River. The oldest detention dam, the Fan Dam, is the most significant feature affecting the morphology of the main arroyo. Upstream of this dam, the river is aggraded to the level of the pre-incision floodplain for over 20 kilometres, whereas below the structure, the arroyo is still incised. Along the lower reaches, the arroyo has, in the main, reached a quasi-equilibrium form. The active channel is trapezoidal and very consistent in size along the entire reach, despite the arroyo trench varying dramatically in size. As observed in the Rio Puerco, the channel of the San Simon River is flanked by dense tamarisk, effectively channelising it. The only sub-reach along the lower San Simon River which

shows significant variation is the Goat Well reach. The arroyo is deeper along this sub-reach, which has resulted in considerable bank instability where the active channel impinges against the arroyo wall. A basal wedge of failed sediment has, therefore, accumulated, locally overloading the transport capacity and resulting in an asymmetric channel planform. The lack of morphological variability along the San Simon River indicates that it is the most stable of the three arroyos studied, having attained a quasi-equilibrium form along much of the system.

8.1.2 General Conceptual Model of Arroyo Evolution

From the above observations it can, therefore, be seen that the morphological evolution of arroyo systems is by no means simple. Geomorphologically distinct reaches form in response to the specific inputs of flow and sediment to that particular reach. Consequently, each reach evolves at a different rate depending on these constraints. The arroyo morphology is also affected by external factors, such as artificial alteration of the channel or valley floor and bedrock outcropping, which may accelerate, slow, or even reverse the progression of evolution. Therefore, location-for-time substitution cannot be assumed in the arroyo systems studied.

The natural variability of systems has resulted in subtly, but distinctly, different morphologies in arroyo reaches which have reached the same stage of evolution, both along one arroyo and between different arroyos. This is partially due to the fact that the factors controlling morphological development, such as sediment size and propensity for vegetation recovery, also differ, especially between each system. There is also a misleading tendency for models of evolution to divide the morphological changes into distinct evolutionary stages. However, there is generally a continuum between the characteristic morphology of each stage, unless a threshold is involved. Thus, a reach in the early phase of a stage differs noticeably from a reach which has evolved further within the same stage.

The observations and cross-section surveys have led to the conclusion that refinements to the late-stage model are required for arroyo systems. A

feature of this late-stage arroyo morphology not identified by Elliott *et al.* (1999) was the presence of a deep, narrow trapezoidal active channel. This is in contrast to the active channel seen in Thorne's (1999) channel evolution model, which is asymmetric. In arroyos, the asymmetric channel form is observed at an earlier stage of evolution than the end-stage trapezoidal channel, which thus represents the new equilibrium form.

Arroyos are ephemeral, both in terms of the flow regime and morphologically. Adjustments are event-driven, temporally separate and heavily dependent on sequence, magnitude & frequency of flow events. Evolution of the arroyo system may be both hastened and retarded by this flow sequence, which assumes equal, if not more importance than the recovery time between events. Although the arroyo is subject to a small amount of weathering and erosion during the periods of no flow, this is far outweighed by the geomorphological change which occurs during flow events. This is in contrast to perennial streams, which are in a constant state of adjustment, assuming that the discharge exceeds the sediment transport threshold.

Within the constraints of the findings of this study (that arroyo evolution occurs within definable reaches according to the specific driving variables; has a late-stage quasi-equilibrium form and is event-driven), a conceptual model of arroyo evolution was developed (Figure 8.1). The initial evolutionary stages of the arroyos studied were found to fit the pattern of morphological change proposed in other incised channel and arroyo evolution models (Chapter 2; Elliott, 1979; Schumm *et al.*, 1984; Harvey and Watson, 1986; Simon and Hupp, 1991; Gellis, 1998; Elliott *et al.*, 1999; Thorne, 1999; Gellis and Elliott, 2001). Therefore, Stage 1 indicates the unincised, pre-modified channel and Stage 2, the incised arroyo prior to lateral expansion. The transition from a Stage 1 to a Stage 2 system was abrupt, generally due to the passage of a deep, aggressively eroding headcut working upstream through the system. Although some widening can occur in a Stage 2 arroyo, most lateral erosion does not occur until the critical bank

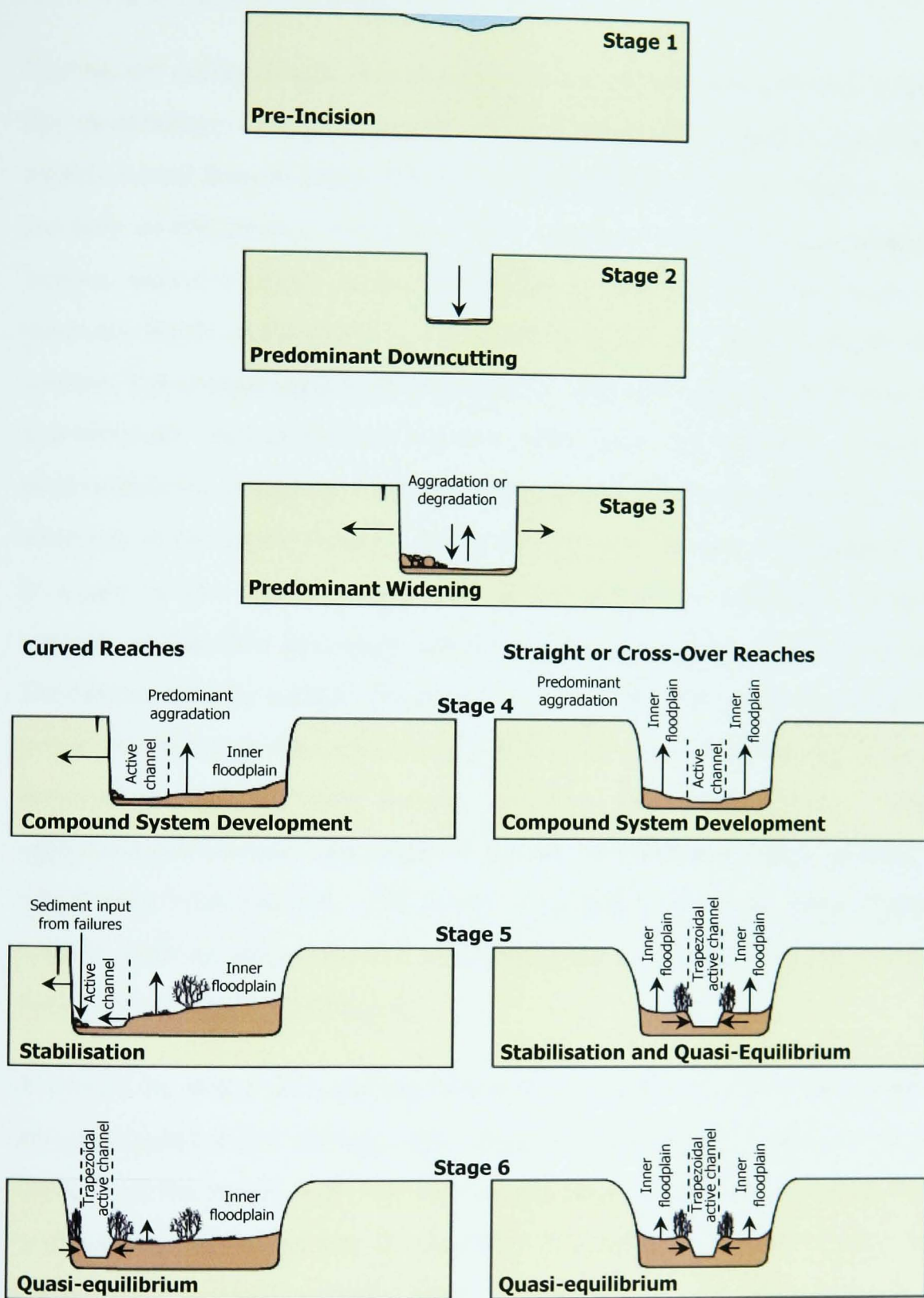


Figure 8.1 General conceptual model of arroyo evolution.

height threshold is reached. The transition to a Stage 3, predominantly widening arroyo, is, therefore, also abrupt.

During the earlier stages, the sinuosity of the arroyo trench does not affect the morphology to a great extent. Consequently, the width is too low to permit lateral bars to form, since even low-magnitude flows tend to cover the base of the arroyo. However, after widening predominates within the arroyo, lateral erosion occurs preferentially around the outer banks of meander bends, with point bars deposited opposite. In these wider sub-reaches, the morphological development is distinctly different to that in the low-sinuosity and cross-over reaches, which are still narrow. However, even within the straighter sections erosion tends to be asymmetric due to the sinuosity of the active channel. The gradual transition between Stages 3 and 4 occurs as the arroyo widens to a point where the sediment transport capacity of the flow is compromised, causing aggradation to predominate. Deposition initially occurs within the curved, wider sub-reaches but rapidly progresses through the entire reach. Berms and point bars are deposited or accumulate due to bank failure, building the arroyo floor. These aggradational features are stepped due to the different stage of flow at which they were created. The arroyo gradually evolves an inner channel system, with an active channel and floodplain, in response to the variable flow regime (Figure 8.1; Stage 4).

It should be noted that, during Stages 2 to 4, although there is a distinct morphological trend during each stage, the sequence of flows and the location of the reach, with respect to each flow, determines the short-term bed response of the arroyo. If a series of low-magnitude flows occurs, bed aggradation is likely to take place. By necessity, the large amount of sediment entering from the eroding bed and banks must progress through the arroyo system. Since floods rarely flow the entire length of the arroyo, sediment is deposited preferentially during the falling stage and in the downstream reaches of the flood, when the sediment transport capacity declines with discharge. Larger-magnitude flows, in contrast, cause net bed

degradation, with the highest discharges generally scouring much of the stored sediment. However, some re-deposition occurs even during these super-floods.

The sequence of flooding also affects the development of vegetation within the arroyo trench. A series of low-magnitude flows permits vegetation to become established on the depositional features. This provides an element of roughness, trapping further sediment. As the depositional features become more permanent in Stage 4, more mature vegetation is able to become established. Higher-magnitude flows tend to remove much of the vegetation within the channel, although the increased availability of moisture aids recovery after cessation of the flood. The recovery time after these events is also more rapid than previously thought since re-vegetation is assisted by the presence of fine sediments (Osterkamp and Costa, 1987; Kochel and Ritter, 1990).

As widening continues, a gradual transition to a more stable, Stage 5, morphology takes place (Figure 8.1). A negative feedback between the quantity and maturity of vegetation within the arroyo and the stability of the arroyo morphology takes place. As the arroyo becomes more stable in the latter phase of Stage 4, more mature vegetation is able to become established. This, in turn, increases the roughness of the floodplain, causing flow attenuation, and also binds the floodplain sediments as root networks are established. As development of the inner floodplain occurs, initially through vertical aggradation, followed by lateral accretion, the active channel gradually becomes narrower and deeper. Straighter sections of arroyos develop a quasi-equilibrium trapezoidal channel more rapidly than curved sub-reaches, which remain wider and shallower due to inputs of sediment where the channel impinges against arroyo walls.

As the morphological evolution progresses, floodplain aggradation and accretion continues. This results in a gradual narrowing and deepening of the active channel, which eventually becomes trapezoidal, even in the curved sub-reaches. This gradual progression eventually results in a quasi-

equilibrium, Stage 6, form being attained along the entire reach of an arroyo (Figure 8.1).

The observations of the contemporary arroyo, over a century after initiation, have enabled the previously proposed models of incised channel and arroyo evolution to be extended. It is highly likely that, as more time elapses, further morphological developments will result in the conceptual model presented above requiring equivalent adjustment. However, based on observations of the evolving and contemporary arroyos, there are two likely scenarios of future morphological change: the inner floodplain may continue to aggrade, maintaining the quasi-equilibrium channel dimensions; or incision may be renewed, initiating complex response within the system.

8.1.3 Channel-Forming Flow in Arroyos

A review of the literature regarding theories of channel-forming flows indicated that, in flashy, ephemeral channels, the concept of a single discharge to which the morphology was adjusted was redundant (Chapter 2). It was observed that rivers in which the peak discharge was much greater than the average discharge were unlikely to be adjusted to lower-magnitude, higher-frequency flows, due to the extremely erosive ability of the highest-magnitude super-floods (Baker, 1977; Hey, 1997). When combined with the premise that channels in semi-arid regions have long recovery times after high-magnitude events (Wolman and Miller, 1960; Baker, 1977; Wolman and Gerson, 1978; Graf, 1983a; Yu and Wolman, 1987; Kochel, 1988; Hey, 1997), this led to the conclusion that semi-arid ephemeral channels, including arroyos, would not be able to maintain an equilibrium form (Graf, 1988a). Observations made during this project, combined with those of other researchers, enabled this hypothesis to be examined. It was discovered that flow and sediment discharges had an interlinked relationship with the arroyo morphology, whereby differences in the stage of evolution affected the hydrologic regime and vice versa (Figure 8.2a. and b.). Thus, prior to deciding which stage each geomorphologically distinct reach of an arroyo system has attained, the flow and sediment discharge

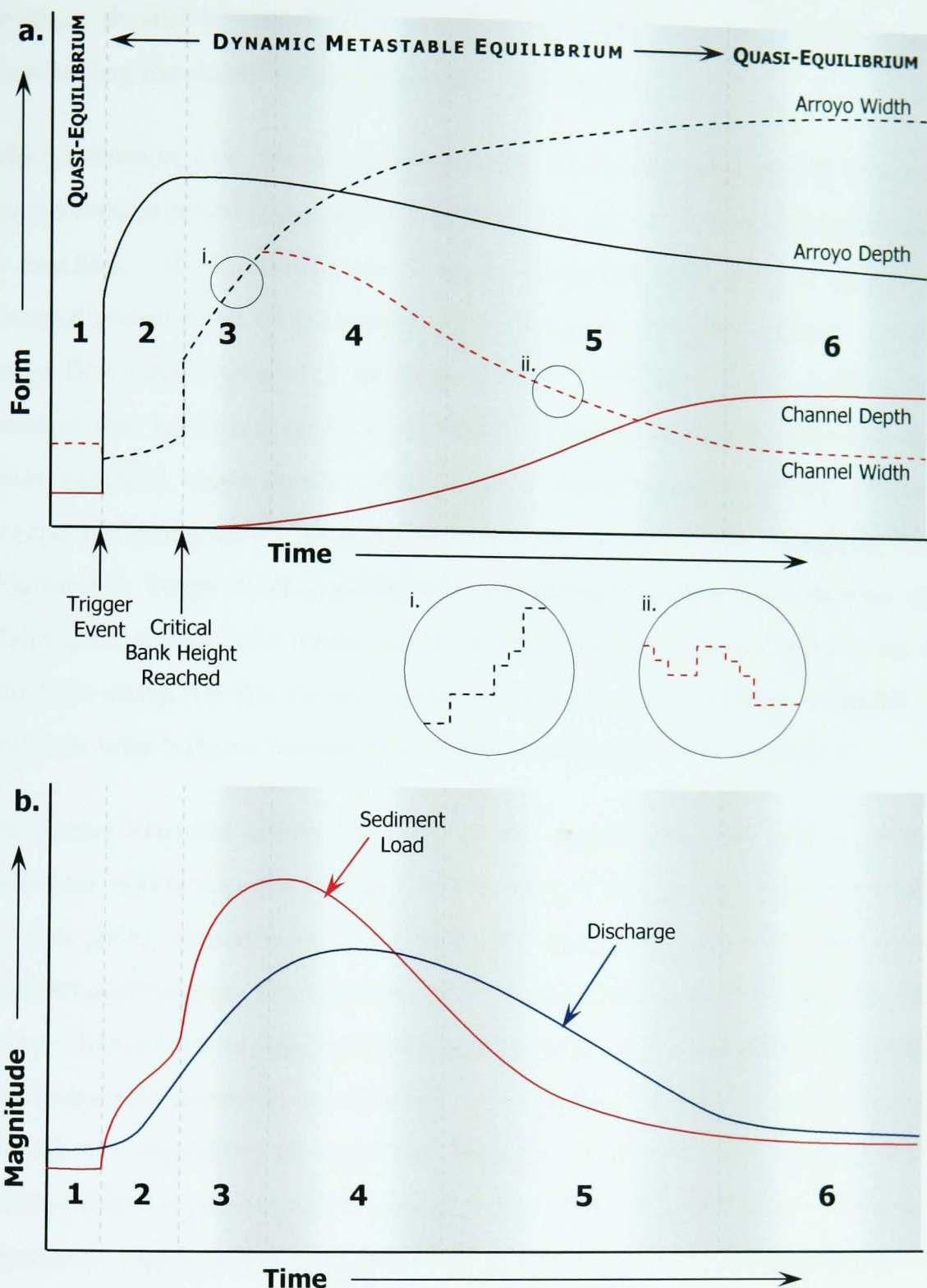


Figure 8.2 Simplified schematic representation of a) arroyo equilibrium and b) variation in flow and sediment discharge with time, in response to driving variables.

Figures 1 - 6 refer to stage of arroyo evolution illustrated in Figure 8.1, emphasising the continuum between stages 3 - 6. Insets i. and ii. illustrate the event-driven nature of form changes. i. applies only to the arroyo width, whereas ii. is equally applicable to the other variables.

regimes should be observed in combination with the morphology, rather than basing the classification on morphology alone.

After initiation, the arroyo predominantly downcuts (Figure 8.1; Stage 2) until a critical bank height specific to the local bank materials and conditions is reached. If observed over a short time-scale, the arroyo exhibits a disequilibrium form with respect to the flow and sediment regime. At this stage, flows are wall-to-wall and the low-flow channel is wide, shallow and braided due to high inputs of sediment. Once the critical bank height has been reached, mass bank failure causes predominantly lateral erosion, arroyo widening and a peak in sediment production and, therefore, load (Figure 8.1; Stage 3) (Figure 8.2b.). Contemporary reaches, such as the Pleistocene Santa Cruz River reach, or sub-reaches, such as those close to San Luis along the Rio Puerco, which are incised into resistant sediment or bedrock, which slows the rate of evolution, were classified as Stage 3.

The active channel covers the base of the trench until the arroyo attains sufficient width that the channel can no longer effectively erode the walls. At this point, lateral bars and berms are deposited, narrowing the active channel and forming an incipient inner floodplain (Figure 8.1; Stage 4). The active channel, therefore, increases in sinuosity as it meanders around the newly-formed depositional features. At this stage, the arroyo and channel should be regarded as separate features, with different process-form relationships depending on the magnitude of flow (Figure 8.2a.). The active channel is highly adjustable and change occurs during each flood: smaller floods rework low-flow channel sediments and larger-magnitude floods cause scour and refilling, generally resulting in net aggradation. The morphology of the channel is controlled by these extreme events and, therefore, a combination of both flow variability and channel-deforming events. The sequence of events is, therefore, crucial in determining the channel morphology. High-magnitude floods are geomorphologically effective and leave a lasting imprint. Observations from the surveyed cross-sections indicated that the Middle and Upper Reaches 2 and 3 of the Rio

Puerco, the majority of the Holocene reach of the Santa Cruz River and the Upper Reaches of the San Simon River are Stage 4 reaches.

In contrast to the declining magnitude of peak and average discharges in the lower Rio Puerco and San Simon River, peak and average flow magnitudes have exhibited an increasing trend in the Santa Cruz River, although widening and increased sediment storage within the arroyo trench is likely to have caused a decline in the sediment load. Short-term trends in the sediment balance were found to be adjusted to the dominant mechanism of flood-generation (Parker, 1996). Periods where floods were produced by predominantly monsoonal storms resulted in net aggradation, due to the dominance of short, localised flow events. The contemporary flow regime of the Santa Cruz River is, however, dominated by floods generated by frontal and tropical storms, which has resulted in increases in the channel cross-sectional area (Parker, 1996).

As widening continues, the capacity of the arroyo grows, enabling progressively larger floods to occur until maximum capacity is reached (Figure 8.2b.). At this point, the flood of record causes an intrinsic threshold to be crossed and aggradation then predominates. The incipient floodplain matures and grades, permitting permanent vegetation to become established, since inundation does not occur as frequently. This causes a feedback effect, whereby flood peaks are attenuated by the increase in floodplain vegetation roughness coefficients. This, in turn, leads to more deposition on the floodplain as attenuation increases, inevitably causing a decrease in peak flows and a continued decrease in sediment loads (Figure 8.2b). The vegetation is, therefore, able to become better established as stability is increased. This pattern of development causes the inner floodplain to aggrade initially vertically, then laterally, resulting in the active channel becoming narrower and deeper (Figure 8.1; Stage 5). Local influences, especially sediment inputs from bank failures, result in great deal of variability of channel form. However, the general trend is for the active channel to attain a trapezoidal form, flanked by densely vegetated levees.

The progression of morphological change to create the stable channel of Stage 5 alters the magnitude of flow and sediment discharges such that the hydraulic regime is no longer dominated by high-magnitude flows. Since the arroyo regime is flashy, smaller flows are still the most frequent but cause little geomorphological change. At this stage, an effective discharge can be identified, creating a small peak in the sediment load above the first discharge class. Cross-section surveys of the Rio Puerco have indicated that, at this stage, the channel is not adjusted to this flow. Bankfull discharge magnitudes are significantly larger than the effective discharge, indicating that morphology is still controlled to a large extent by variability of flow. However, this relationship indicates a negative feedback since the flow and sediment regimes are, to a large extent, controlled by the arroyo morphology.

The results of this study have indicated that the late-stage equilibrium form of the incised arroyo system is attained when the active channel becomes trapezoidal along the entire system. Aggradation continues to narrow and deepen the active channel, until an equilibrium geometry is reached. The width:depth ratio of this equilibrium form is dependent on the composition of the channel perimeter sediments. Channels with a high percentage of silt and clay tend to become narrower and deeper than channels composed of coarser sediment. Cross-sections surveyed along the San Simon River indicate that an equilibrium form is attained when the bankfull discharge is adjusted to the effective discharge. It is not until this morphology is achieved that the effective discharge becomes a truly channel-forming and maintaining flow.

It was mentioned previously that, when observed over a short time-scale, immediately following the incision-triggering event, the arroyo system appears to be in a state of disequilibrium. However, over the longer time-scale of subsequent evolution through the different stages of development, it is more accurate to describe the system as being in a state of dynamic metastable equilibrium (Figure 8.2a.). Progressive change is interrupted by

periods of abrupt change as intrinsic thresholds are crossed. Eventually, the system evolves to a quasi-equilibrium form. This pattern suggests that, when viewed over centuries, rather than decades, it is likely that arroyos are dynamic equilibrium systems, with intrinsic thresholds triggering new cycles of incision and re-filling.

8.2 CONCLUSIONS

The principal aim of this project was to derive a general explanation of the relationship between arroyo morphology, discharge variability and the antecedent sequence of events within the system. This relationship was investigated by examining the evolution and contemporary morphology of three arroyos: the Rio Puerco, the Santa Cruz River and the San Simon River, within the context of the discharge regime. One of the most important findings of this investigation was that arroyos, rather than evolving headwards as a coherent system, instead developed discrete geomorphological reaches, which evolved separately within the constraints of the external, driving variables.

Despite the fact that precipitation over the entire south-western USA has shown an increasing trend since the mid-20th Century, discharge trends in the three arroyos studied have generally not followed this pattern over the same time period. Although increasing peak and average discharges were recorded for the Santa Cruz River, the San Simon River experienced decreasing trends. The middle three reaches of the Rio Puerco saw an increasing discharge trend, similar to the Santa Cruz River, whereas the lower and upper reaches experienced a decreasing trend, similar to the San Simon River, emphasising the necessity to treat each reach separately. The conclusion drawn in this investigation was, therefore, that morphological differences between the reaches were responsible for this apparent inconsistency. The observations of arroyo evolution have emphasised the two-way interaction between discharge and morphology.

Within the context of the principal aim, the changing relationship between discharge and morphology was analysed, both spatially and temporally. If

observed at geologic timescales, arroyo systems are in a state of dynamic metastable equilibrium, with cycles of cut and fill triggered as intrinsic geomorphic thresholds were crossed. The latest phase of incision in the systems studied occurred during the mid- to late-19th Century due to a variety of destabilising mechanisms. Subsequent morphological change has enabled a general pattern of evolution to be identified within the geomorphological reaches, despite the indeterminate nature of the discharge events driving this modification. Morphological change is event-driven, with the amount of geomorphological change generally corresponding to the magnitude of the flow. It is these short-term changes which combine to produce the definable continuum of long-term evolution, which is only interrupted if an intrinsic geomorphic threshold is crossed. This continuum can be divided into stages, which each have a characteristic morphology.

Once the threshold of incision is surpassed, the arroyo predominantly degrades (Stage 2; Stage 1 representing pre-incision conditions) until the critical bank height threshold within each reach is attained. The reach then enters a phase of predominant widening (Stage 3). Reaches incised into bedrock or resistant sediment were the only sections of the arroyos studied in which this erosional, widening phase was still occurring. Eventually the trench becomes sufficiently wide that transport capacity of the flow is lost and sediment is deposited in the form of lateral bars and berms (Stage 4). The arroyo trench, however, continues to widen during high-magnitude flow events, enabling progressively larger discharges to occur, as observed along the Santa Cruz River and middle reaches of the Rio Puerco. These stages of evolution digress little from those proposed previously (summarised in Chapter 2). However, this investigation has emphasised the necessity of recognising that, where evolutionary stages are not separated by intrinsic thresholds, the division of morphological evolution into distinct stages is somewhat artificial, a point which is not clarified in previous channel evolution models.

The evidence uncovered during this investigation indicates that the flood of record occurs once the trench attains its maximum discharge capacity. The

large volume of sediment mobilised by this event is thought to trigger a predominantly aggradational phase and progression towards a stable, quasi-equilibrium form (Stage 5). Prior to this, channel adjustments are highly dependent on the sequence, magnitude and pattern of flows, with little geomorphological change occurring between the temporally separate events. Thus, even during phases of predominant degradation, a sequence of low-magnitude flows may cause the bed to aggrade. Similarly, the aggrading trend of a Stage 4 reach may be reversed by a super-flood.

As the quasi-stable channel form is attained, peak flows are attenuated, causing a perceptible change in the discharge regime. This provides an explanation for the declining discharge magnitudes observed in the San Simon River and reaches of the Rio Puerco. A negative feedback is triggered, whereby high-magnitude flows are suppressed, allowing mature vegetation to become established on the inner floodplain. This vegetation, in turn, encourages stabilisation as flows are further attenuated and sediment is trapped. Vertical aggradation and then lateral accretion of the inner floodplain occurs, causing the active channel to become narrower and deeper. The late-stage morphology proposed in the revised conceptual evolution model is, therefore, typified by a deep, narrow trapezoidal channel, flanked by heavily vegetated levees (Stage 6). The exact form and geometry of each reach is determined by the specific external, driving variables, combined with the sediment size within the channel boundary and vegetation density.

Although the morphology and discharge regime of the arroyo system are inextricably linked, this investigation has found that inputs of sediment to each reach are crucial in determining the rate of evolution. Sediment must be supplied in sufficient quantity that aggradation remains unhindered, but not so much that the sediment transport capacity is overloaded, causing the active channel to remain wide and shallow. Evolution of the middle reaches of the Rio Puerco has progressed slowly due to inputs of sediment from eroding tributaries. The Stage 5, quasi-stable reaches of the upper and lower

Rio Puerco differ from the Stage 6 reach of the lower San Simon River due to inputs of sediment from bank failures where the active channel impinges against the arroyo wall in curved reaches. These inputs prevent a trapezoidal channel form being attained along the entire reach.

The rate of evolution is also significantly affected by artificial adjustments to the arroyo trench. The findings of this research indicate that it is likely that the Santa Cruz River has been prevented from attaining a quasi-stable morphology due to the implementation of flood-control measures which prevent widening of the arroyo trench. In contrast to this, it is thought that the San Simon River has developed a quasi-equilibrium, Stage 6 form more rapidly due to the construction of sediment detention dams.

This project also set out to examine the applicability of channel-forming flow concepts to arroyo systems. This investigation discovered that the relationship between effective discharge and morphology was related to the stage of evolution of each reach. The flashy regime of arroyo systems caused magnitude/frequency concepts to be virtually meaningless. This research found that the effective discharge corresponded to individual high-magnitude events, indicating the dominance of rarely occurring destructive superfloods. The morphology of the arroyo is, therefore, event-driven and controlled by the flow variability and channel deforming flows. However, this investigation also found that, once the arroyo has attained a quasi-equilibrium form, with a trapezoidal inner channel, feedback occurs between morphology and flow/sediment regimes. The morphological adjustments affect the flow regime to such an extent that peak flows are attenuated, resulting in lower-magnitude flows becoming more frequent and, thus, assuming greater relative effectiveness. Initially, the bankfull flow of the active channel is significantly higher than the effective discharge, indicating that it is still adjusted to the flow variability. However, continued channel evolution in response to the change in flow regime results in a geometry adjusted to the effective discharge.

One of the most important findings of this investigation was that the arroyo trench and the active channel eventually evolve into a quasi-equilibrium form: the arroyo morphology controlled by flow variability during initial stages of evolution and the active channel controlled by a channel-forming flow developed during late-stage evolution. This illustrates the importance of treating arroyos essentially as valley systems, with the inner channel and floodplain behaving as a separate entity to the arroyo trench. A final conclusion of this research is, therefore, that dominant, channel-forming flow theories only apply in arroyo systems where the channel has attained a quasi-equilibrium form.

8.3 FUTURE RESEARCH AND MANAGEMENT ISSUES

It was observed that arroyo systems do not evolve in a system-wide, simple manner. Morphological change occurs within distinct geomorphological reaches, which adjust within the constraints of the external, driving variables. It is, therefore, critical to establish these parameters to understand fully the process-form interactions. It was determined that the most important controlling variables which need to be considered for each reach are as follows:

1. Discharge – magnitude, frequency, sequence, trends and longitudinal connectivity.
2. Sediment load – magnitude, trends, controls on variability.
3. Effective discharge – which is only definable in late-stage, quasi-equilibrium reaches.
4. Sediment size – percentage of silt and clay in the channel perimeter (M).
5. Cross-sectional surveys – in representative reaches to determine reach-averaged morphology and geometry of both arroyo and channel.
6. Slope – bed, water-surface and energy.
7. Artificial alterations and their effect on process-form interactions.
8. Stage of evolution, which strongly affects the short-term morphological adjustments of the reach.

Incised channels, including arroyos, cause concern in populated areas due to their propensity for lateral erosion, rapid geomorphological adjustment and downstream sedimentation during high-magnitude flood events. Harvey and Watson (1986) observed that, given enough time, disequilibrium incised channels will attain a new state of dynamic equilibrium. This study has established that a similar pattern of evolution occurs in arroyo systems, whereby quasi-equilibrium is re-established given the passage of time. Thus, the best management strategy for these systems is the “no-action” or “geomorphic alternative” (Harvey and Watson, 1986, p361). However, Harvey and Watson (1986) point out that this course is often economically impractical due to the destruction of land, infrastructure and buildings.

This research has highlighted some important issues for future management strategies in arroyo systems. By far the most significant is the detrimental effect of preventing lateral adjustments from occurring. It is hypothesised that arroyos naturally evolve to a relatively stable quasi-equilibrium morphology, with an aggrading system. Implementation of flood-protection schemes which fix the channel morphology within a stage of evolution ensure that high-magnitude floods and super-floods are not suppressed as the morphology evolves, creating a positive, rather than negative feedback. This emphasises the need for allowed adjustment in arroyo systems. Artificial adjustments to these systems need to be sympathetic to the nature of morphological change. However, this requires confidence in the proposed model of arroyo evolution. This study has demonstrated that event-scale adjustments within a reach are dependent on its stage of evolution. Reaches of an arroyo system which are classified as Stage 1 to Stage 4 show morphological change which is dependent on the timing and sequencing of events. During these stages, magnitude/frequency techniques have limited applicability. However, Stage 6 and, to some extent, Stage 5 reaches have developed a quasi-equilibrium morphology which suppresses high-magnitude floods. A negative feedback is, therefore, created, whereby the channel morphology is maintained by a definable

channel-forming flow. This late-stage morphology, therefore, represents the ideal for arroyo stabilisation schemes.

Event-scale and reach-scale change have not previously been included in generalised evolution models. However, this study has emphasised the necessity of recognising the event-driven nature of arroyo systems and the specific responses of geomorphological reaches within the system. There is, therefore, a need to rely less on statistical generalisation and more on a process-based, probabilistic approach to arroyo management.

References

- Anderson, M.G. and Calver, A. 1980. Channel Plan Changes Following Large Floods. In: Cullingford, R., Davidson, D. and Lewin, J. (Eds.), *Timescales in Geomorphology*, John Wiley & Sons, 43 - 52.
- Anderson, S.R. 1987. Cenozoic Stratigraphy and Geologic History of the Tucson Basin, Pima County, Arizona. US Geological Survey Water Resources Investigation Report, 87-4490.
- Anderson, T.W. 1972. Electrical-Analog Analysis of the Hydrologic System, Tucson Basin, SE Arizona. US Geological Survey Water-Supply Paper, 1939-C.
- Andrews, E.D. 1980. Effective and Bankfull Discharges of Streams in the Yampa River Basin, Colorado and Wyoming. *Journal of Hydrology*, **46**, 311 - 330.
- Andrews, E.D. 1982. Bank Stability and Channel Width Adjustment, East Fork River, Wyoming. *Water Resources Research*, **18** (4), 1184 - 1192.
- Antevs, E. 1952. Arroyo Cutting and Filling. *Journal of Geology*, **60**, 375 - 385.
- Bachman, G.O. and Menhart, H.H. 1978. New K-Ar dates and the Late Pliocene to Holocene Geomorphic History of the Central Rio Grande Region, New Mexico. *Geological Society of America Bulletin*, **89**, 283 - 292.
- Bailey, R.W. 1935. Epicycles of Erosion in the Valleys of the Colorado Plateau Province. *Journal of Geology*, **63** (4), 337 - 349.
- Baker, V. 1988. Flood Erosion. In: Baker, V.R., Kochel, R.C. and Patton, P.C. (Eds.), *Flood Geomorphology*, 81 - 95.
- Baker, V.R. 1977. Stream-Channel Response to Floods with Examples from Central Texas. *Geological Society of America Bulletin*, **88**, 1057 - 1071.
- Baker, V.R. 1984. Questions Raised by the Tucson Flood of 1983. *Arizona and Nevada Acad. of Sci.*, **14**, 211 - 219.
- Baker, V.R. and Costa, J.E. 1987. Flood Power. In: Mayer, L. and Nash, P. (Eds.), *Catastrophic Flooding*, Binghamton Symposia in Geomorphology.
- Baker, V.R. and Pickup, G. 1987. Flood Geomorphology of the Katherine Gorge, Northern Territory, Australia. *Geological Society of America Bulletin*, **98** (6), 635 - 646.

- Balling, R.C. and Wells, S.G. 1990. Historical Rainfall Patterns and Arroyo Activity within the Zuni River Drainage Basin, New Mexico. *Annals of the American Geographers*, **80** (4), 603 - 617.
- Bathurst, J.C., Thorne, C.R. and Hey, R.D. 1979. Secondary Flow and Shear Stress at River Bends. *Journal of the Hydraulics Division, Proceedings of the American Society of Civil Engineers*, **105** (HY10), 1277 - 1295.
- Begin, Z.B., Meyer, D.F. and Schumm, S.A. 1980. Sediment Production of Alluvial Channels in Response to Base Level Lowering. *Transactions of the ASAE*, 1183 - 1189.
- Bendix, J. 1992. Fluvial Adjustments on Varied Timescales in Bear Creek Arroyo, Utah, U.S.A. *Z. Geomorph. N.F.*, **36** (2), 141 - 163.
- Betancourt, J.L. 1987. The San Xavier Archaeological Project: Historic Channel Changes along the Santa Cruz River San Xavier Reach, Southern Arizona. *Southwest Cultural Series*, **1** (1), Section IIB.
- Betancourt, J.L. 1990. Tucson's Santa Cruz River and the Arroyo Legacy. Unpublished PhD thesis, University of Arizona, Tucson.
- Betancourt, J.L. and Turner, R.M. 1993. *Tucson's Santa Cruz River and the Arroyo Legacy*, University of Arizona Press, Tucson.
- Biedenharn, D.S. and Thorne, C.R. 1994. Magnitude-Frequency Analysis of Sediment Transport in the Lower Mississippi River. *Regulated Rivers: Research and Management*, **9**, 237 - 251.
- BLM. 1990. Restoration of the San Simon. Bureau of Land Management Report.
- Boyd, M., Eckstrom, D., Grijalva, R., Marsh, P. and Moore, E. 1993. January 1993 Floods, Pima County, Arizona. Pima County Department of Transportation and Flood Control District.
- Branson, F.A. and Janicki, A. 1986. Botanic and Hydrologic Changes on Rangelands of the Rio Puerco Basin, New Mexico. US Geological Survey Water-Resources Investigation Report, 86-4021.
- Brunsdon, D. and Thornes, J.B. 1979. Landscape Sensitivity and Change. *Transactions of the Institute of British Geographers New Series*, **4**, 463 - 484.
- Bryan, K. 1925. Date of Channel Trenching (Arroyo Cutting) in the Arid Southwest. *Science*, **62** (1607), 338 - 344.

- Bryan, K. 1928. Historic Evidence on Changes in the Channel of Rio Puerco, a Tributary of the Rio Grande in New Mexico. *Journal of Geology*, **XXXVI**, 265 - 282.
- Bryan, K. and Post, G.M. 1927. Erosion and Control of Silt on the Rio Puerco, New Mexico. Report to the Chief Engineer, Middle Rio Grande Conservancy District.
- Bull, W.B. 1964. History and Causes of Channel Trenching in Western Fresno County, California. *American Journal of Science*, **262**, 249 - 258.
- Bull, W.B. 1979. Threshold of Critical Power in Streams. *Geological Society of America Bulletin*, **90** (1), 453 - 464.
- Bull, W.B. 1997. Discontinuous Ephemeral Streams. *Geomorphology*, **19**, 227 - 276.
- Bull, W.B. and Scott, K.M. 1974. Impact of Mining Gravel from Urban Stream Beds in the SW USA. *Geology*, **2**, 171 - 174.
- Burkham, D.E. 1970. Depletion of Streamflow by Infiltration in the Main Channels of the Tucson Basin, SE. Arizona. US Geological Survey Water Supply Paper, 1939-B.
- Burkham, D.E. 1972. Channel Changes of the Gila River in Safford Valley, Arizona, 1948 - 1970. US Geological Survey Professional Paper, 655-G.
- Chang, H.H. 1979. Minimum Stream Power and River Channel Patterns. *Journal of Hydrology*, **41**, 303 - 327.
- Chorley, R.J., Schumm, S.A. and Sugden, D.E. 1984. *Geomorphology*, Methuen & Co. Ltd.
- Clarke, P.B. and Davies, S.M. 1988. The Application of Regime Theory to Wadi Channels in Desert Conditions, *International Conference on River Regime*, 67 - 82.
- Coleman, M., Gellis, A., Love, D. and Hadley, R. 2003. Channelization Effects on the Rio Puerco above La Ventana, New Mexico, http://climchange.cr.usgs.gov/rio_puerco/papers/channel.html.
- Constanz, J. and Thomas, C.L. 1996. The Use of Streambed Temperatures to Estimate the Depth, Duration and Rate of Percolation beneath Arroyos. *Water Resources Research*, **21** (12), 3597 - 3602.

- Constanz, J., Thomas, C.L. and Zellweger, G. 1994. Influence of Diurnal Variations in Stream Temperature on Streamflow Loss and Groundwater Recharge. *Water Resources Research*, **30** (12), 3253 - 3264.
- Cooke, R.U. and Reeves, R.W. 1976. *Arroyos and Environmental Change in the American Southwest*, Oxford University Press.
- Dahm, C.N. and Moore, D. 2003. <http://sevilleta.unm.edu/research/local/climate/enso/>.
- Davidson, E.S. 1973. Geohydrology and Water Resources of the Tucson Basin, Arizona. US Geological Survey Water Supply Paper, 1939-E.
- Dobyns, H.F. 1981. From Fire to Flood: Historic Human Destruction of the Sonoran Desert Riverine Oases. In: Bean, L.J. and Blackburn, T.C. (Eds.), Ballena Press Anthropological Papers.
- Dury, G.H. 1976. Discharge Prediction, Present and Former, From Channel Dimensions. *Journal of Hydrology*, **30**, 219 - 245.
- Edwards, T.K. and Glysson, G.D. 1999. Field Methods for Measurement of Fluvial Sediment. US Geological Survey Techniques of Water-Resources Investigations, C2.
- Elliott, J.G. 1979. Evolution of Large Arroyos, The Rio Puerco of New Mexico. Unpublished MSc thesis, Colorado State University, Fort Collins.
- Elliott, J.G., Gellis, A.C. and Aby, S.B. 1999. Evolution of Arroyos: Incised Channels of the Southwestern United States. In: Derby, S. and Simon, A. (Eds.), *Incised River Channels*, John Wiley & Sons, 153 - 185.
- Ellis, L.A. 1993. River Bank Erosion in Different Hydrologic Regimes. Unpublished MPhil thesis, University of Nottingham, Nottingham.
- Emmett, W.W. 1974. Channel Aggradation in Western United States as Indicated by Observations at Vigil Network Sites. *Z. Geomorph. N.F.*, **21**, 52 - 62.
- Frostick, L.E., Reid, I. and Layman, T. 1983. Changing Size Distribution of Suspended Sediment in Arid-Zone Flash Floods. In: Collinson, J.D. and Lewin, J. (Eds.), *Modern and Ancient Fluvial Systems*, Spec. Publs int. Ass. Sediment., 97 - 106.

- Gellis, A.C. 1998a. Characterisation and Evaluation of Channel and Hillslope Erosion in the Zuni Indian Reservation, New Mexico, 1992 - 95. US Geological Survey Water-Resources Investigations Report, 97-4281.
- Gellis, A.C. 1998b. History of Streamflow and Suspended-Sediment Collection in the Rio Puerco Basin, New Mexico. In: Harrison, L.B.J. (Ed.), *Soil, Water and Earthquakes around Socorro, New Mexico*, Rocky Mountain Cell, Friends of the Pleistocene Guidebook, 14.
- Gellis, A.C. and Elliott, J.G. 2001. Arroyo Changes in Selected Watersheds of New Mexico. In: Anthony, D.J., Harvey, M.D., Laronne, J.B. and Mossley, M.P. (Eds.), *Applying Geomorphology to Environmental Management*, Water Resources Publications, LCC, 225 - 240.
- Gellis, A.C., Hereford, R., Schumm, S.A. and Hayes, B.R. 1991. Channel Evolution and Hydrologic Variations in the Colorado River Basin: Factors Influencing Sediment and Salt Loads. *Journal of Hydrology*, **124**, 317 - 344.
- Gerson, R. 1977. Sediment Transport for Desert Watersheds in Erodible Materials. *Earth Surface Processes*, **2**, 343 - 361.
- Graf, J.B., Webb, R.H. and Hereford, R. 1991. Relation of Sediment Load and Flood-Plain Formation to Climatic Variability, Paria River Drainage Basin, Utah and Arizona. *Geological Society of America Bulletin*, **103**, 1405 - 1415.
- Graf, W.L. 1979a. Catastrophe Theory as a Model for Change in Fluvial Systems. In: Rhodes, D.D. and Williams, G.P. (Eds.), *Adjustments of the Fluvial System*, 13 - 32.
- Graf, W.L. 1979b. The Development of Montane Arroyos and Gullies. *Earth Surface Processes*, **4**, 1 - 14.
- Graf, W.L. 1983a. Flood-Related Change in an Arid-Region River. *Earth Surface Processes and Landforms*, **8**, 125 - 139.
- Graf, W.L. 1983b. The Arroyo Problem - Palaeohydrology and Palaeohydraulics in the Short Term. In: Gregory, K. (Ed.), *Background to Palaeohydrology*, Wiley.
- Graf, W.L. 1988a. Definition of Flood Plains along Arid-Region Rivers. In: Baker, V.R., Kochel, R.C. and Patton, P.D. (Eds.), *Flood Geomorphology*, Wiley, 231 - 242.

- Graf, W.L. 1988b. *Fluvial Processes in Dryland Rivers*, Springer-Verlag.
- Grissinger, E.H. 1982. Bank Erosion of Cohesive Sediments. In: Hey, R.C., Bathurst, J.C. and Thorne, C.R. (Eds.), *Gravel Bed Rivers*, Chichester, John Wiley & Sons, 273 - 287.
- Guber, A.L. 1988. Channel Changes of the San Xavier Reach of the Santa Cruz River, Tucson, Arizona, 1971 - 1988. Unpublished MA thesis, University of Arizona, Tucson.
- Gupta, A. 1983. High-Magnitude Floods and Stream Channel Response. In: Collinson, J.D. and Lewin, J. (Eds.), *Modern and Ancient Fluvial Systems*, Spec. Publs int Ass. Sediment., 219 - 227.
- Gupta, A. and Fox, H. 1974. Effects of High-Magnitude Floods on Channel Form: A Case Study in Maryland Piedmont. *Water Resources Research*, 10 (3), 499 - 509.
- Harvey, A.M. 1969. Channel Capacity and the Adjustment of Streams to Hydrologic Regime. *Journal of Hydrology*, 8, 82 - 98.
- Harvey, M.D. and Watson, C.C. 1986. Fluvial Processes and Morphological Thresholds in Incised Channel Restoration. *Water Resources Bulletin*, 22 (3), 359 - 368.
- Hastings, J.R. 1959. Vegetation Change and Arroyo Cutting in Southeastern Arizona. *Journal of Arizona Academy of Science*, 1 (3), 60 - 67.
- Hastings, J.R. and Turner, R.M. 1965. *The Changing Mile: An Ecological Study of Vegetation Change with Time in the Lower Mile of an Arid and Semi-Arid Region*, University of Arizona Press, Tucson.
- Haynes, C.V. and Huckell, B.B. 1986. Sedimentary Successions of the Prehistoric Santa Cruz River, Tucson, Arizona. Arizona Bureau of Mines and Geology Open-File Report.
- Heath, D.L. 1983. Flood and Recharge Relationships of the Lower Rio Puerco, New Mexico. *New Mexico Geological Society Guidebook*, 34th Field Conference (Socorro Region II).
- Heede, B.H. 1974. Stages of Development of Gullies in Western United States of America. *Z. Geomorph. N.F.*, 18 (3), 260 - 271.

- Hereford, R. 1984. Climate and Ephemeral-Stream Processes: Twentieth-Century Geomorphology and Alluvial Stratigraphy. *Geological Society of America Bulletin*, **95**, 645 - 668.
- Hereford, R. 1993. Entrenchment and Widening of the Upper San Pedro River, Arizona. Geological Society of America Special Paper, 282.
- Hey, R.D. 1997. Channel Response and Channel Forming Discharge: Literature Review and Interpretation. European Research Office of the US Army, R&D 6871-EN-01 First Interim Report.
- Hey, R.D. 1998. Channel Response and Channel Forming Discharge. European Research Office of the US Army, R&D6871-EN-01 Final Report.
- Hirschboek, K.K. 1985. Hydroclimatology of Flow Events in the Gila River Basin, Central and Southern Arizona. Unpublished PhD thesis, University of Arizona, Tucson.
- Hoffmann, J.P., Pool, D.R., Konieczki, A.D. and Carpenter, M.C. 1998. Causes of Sinks near Tucson, Arizona, USA. *Hydrogeology Journal*, **6**, 349 - 364.
- Holmquist-Johnson, C. 2002. Computational Methods for Determining Effective Discharge in the Yazoo River Basin, Mississippi. Unpublished MSc thesis, Colorado State University.
- Hooke, J.W. 1979. An Analysis of the Processes of River Bank Erosion. *Journal of Hydrology*, **42**, 39 - 62.
- House, P.K. and Hirschboek, K.K. 1995. Hydroclimatological and Palaeohydrological Context of Extreme Winter Flooding in Arizona, 1993. Arizona Geological Survey Open-File Report, 95-12.
- Jackson, G.W. 1989. Surficial Geologic Maps of the Northeastern, Southeastern and Southwestern Portions of the Tucson Metropolitan Area. Arizona Geological Survey Open-File Report, 89-2.
- Jobson, H.E. and Carey, W.P. 1989. Interaction of Fine Sediment with Alluvial Streambeds. *Water Resources Research*, **25** (1), 135 - 140.
- Jordan, G.L. and Maynard, M.L. 1970a. The San Simon Watershed: Historical Review. *Progressive Agriculture in Arizona*, **XXII** (4), 10 - 13.
- Katz, L.T. 1987. Steady State Infiltration Processes along the Santa Cruz and Rillito Rivers. Unpublished MSc thesis, University of Arizona, 119 pp.

- Katzer, K. and Schuster, J.H. 1984. The Quaternary Geology of the Tucson Basin, AZ and its Archaeological Implications. Unpublished MSc thesis, University of Arizona, Tucson.
- Kennedy, E.J. 1983. Computations of Continuous Records of Streamflow, Techniques of Water-Resources Investigations of the United States Geological Survey, Washington, United States Government Printing Office.
- Knighton, D. 1998. *Fluvial Forms and Processes, a New Perspective*, Arnold, London, 383 pp.
- Kochel, R.C. 1988. Geomorphic Impact of Large Floods: Review and New Perspectives on Magnitude and Frequency. In: Baker, V.R., Kochel, R.C. and Patton, P.C. (Eds.), *Flood Geomorphology*, John Wiley & Sons Ltd., 169 - 187.
- Kochel, R.C. and Ritter, D.F. 1990. Complex Geomorphic Response to Minor Climate Changes, San Diego County, CA. In: French, R.H. (Ed.), *Proceedings of the International Symposium on the Hydraulics and Hydrology of Arid Lands (H2AL)*, ASCE.
- Kondolf, G.M. and Curry, R.R. 1986. Channel Erosion Along the Carmel River, Monterey County, California. *Earth Surface Processes and Landforms*, **11**, 307 - 319.
- Lane, S.N. and Richards, K.S. 1997. Linking River Channel Form and Process: Time, Space and Causality Revisited. *Earth Surface Processes and Landforms*, **22**, 249 - 260.
- Larsen, C. and Herzog, M. 2000. Archaeological Site Locations within the Rio Puerco Drainage Basin, http://climchange.cr.usgs.gov/rio_puerco/archeo/.
- Lawler, D.M. 1992. Process Dominance in Bank Erosion Systems. In: Carling, P. and Petts, G. (Eds.), *Lowland Floodplain Rivers: Geomorphological Perspectives*, John Wiley & Sons Ltd, 117 - 143.
- Leighly, J. 1936. Meandering Arroyos of the Dry Southwest. *Geographical Review*, **26**, 270 - 282.
- Lekach, J. and Schick, A.P. 1982. Suspended Sediment in Desert Floods in Small Catchments. *Israel Journal of Earth Sciences*, **31**, pp 144-156.

- Leopold, L.B. 1951. Rainfall Frequency: An Aspect of Climatic Variation. *Transactions, American Geophysical Union*, **32** (2), 347 - 357.
- Leopold, L.B. 1976. Reversal of Erosion Cycle and Climate Change. *Quaternary Research*, **6**, 557 - 562.
- Leopold, L.B. 1992. The Sediment Size that Determines Channel Morphology. In: Billi, P., Hey, R.D., Thorne, C.R. and Tacconi, P. (Eds.), *Dynamics of Gravel Bed Rivers*, John Wiley & Sons Ltd., 297 - 311.
- Leopold, L.B. and Maddock, T. 1953. The Hydraulic Geometry of Stream Channels and Some Physiographic Implications. US Geological Survey Professional Paper, 252.
- Love, D.W. 1979. Quaternary Fluvial Adjustments in Chaco Canyon, New Mexico. In: Rhodes, D.D. and Williams, G.P. (Eds.), *Adjustments of the Fluvial System*, 277 - 308.
- Love, D.W. 1986. A Geological Perspective of Sediment Storage and Delivery along the Rio Puerco, Central New Mexico. In: Hadley, R.F. (Ed.), Albuquerque, New Mexico, IAHS.
- Love, D.W. 1992. Rapid Adjustment of the Rio Puerco to Meander Cutoff: Implications for Effective Geomorphic Processes, Crossing Thresholds and Timing of Events. *New Mexico Geological Society Guidebook*, 43rd Field Conference (San Juan IV), 399 - 406.
- Love, D.W. 1997. Implications for Models of Arroyo Entrenchment and Distribution of Archaeological Sites in the Middle Rio Puerco. In: Duran, M.S. and Kirkpatrick, D.T. (Eds.), *Layers of Time: Papers in Honour of Robert H Weber*, Archaeological Society of New Mexico, 69 - 84.
- Love, D.W. and Young, J.D. 1983. Progress Report on the Late Cenozoic Geologic Evolution of the Lower Rio Puerco, *34th Field Conference*, Socorro Region II, 277 - 284.
- Luzbetak, D.J., Jain, S.C. and Odgaard, A.J. 1988. Piping as a Mechanism for Bank Erosion along Rivers in Iowa. IIHR, 324.
- Macgilligan, F.J. 1992. Thresholds and the Spatial Variability of Flood Power During Extreme Floods. *Geomorphology*, **5**, 373 - 390.

- Malanson, G.P., Butler, D.R. and Georgakakos, K.P. 1992. Nonequilibrium Geomorphic Processes and Deterministic Chaos. *Geomorphology*, 5, 311 - 322.
- Mathis, M. 1983. San Simon Coordinated Resource Management Plan. Bureau of Land Management Report.
- McClure, B.C., Molitor, D. and Kreuper, D. 2000. Two Soil and Water Conservation Efforts in the State of Arizona, USA. BLM Draft Report.
- McKitterick, M.A. 1988. Surficial Geologic Maps of the Tucson Metropolitan Area. Arizona Geological Survey Open-File Report, 88-18.
- Melton, M.A. 1965. The Geomorphic and Palaeoclimatic Significance of Alluvial Deposits in Southern Arizona. *Journal of Geology*, 73, 1-38.
- Meyer, D.F. 1989. The Significance of Sediment Transport in Arroyo Development. U. S. Geological Survey Water-Supply Paper, 2349.
- Miller, S. 1987. The San Xavier Archaeological Project: Environmental Setting. *Southwest Cultural Series*, 1 (1), Section IIa.
- Molitor, D. 1997. Suspended Sediment Monitoring Project, San Simon Watershed, Southeast Arizona, 1983 to 1995. Bureau of Land Management, 573-070/29019 Region No. 8.
- Molnar, P. 2001. Precipitation and Erosion Dynamics in the Rio Puerco Basin. Unpublished PhD thesis, Colorado State University, Fort Collins.
- Moss, J.H. and Kochel, R.C. 1978. Unexpected Geomorphic Effects of the Hurricane Agnes Storm and Flood, Conestoga Drainage Basin, Southeastern Pennsylvania. *Journal of Geology*, 86 (1), 1 - 11.
- Nash, D.B. 1994. Effective Sediment-Transporting Discharge from Magnitude-Frequency Analysis. *The Journal of Geology*, 102 (1), pp 79-95.
- Newson, M. 1980. The Geomorphological Effectiveness of Floods - A Contribution Stimulated by Two Recent Events in Mid-Wales. *Earth Surface Processes*, 5, 1 - 16.
- Nordin, C.F. 1963a. A Preliminary Study of Sediment Transport Parameters, Rio Puerco, near Bernardo, New Mexico. US Geological Survey Professional Paper, 462-C.

- Nordin, C.F. 1963b. Observations on Sediment Transport and Channel Erosion - Rio Puerco near Bernardo, New Mexico, *ASCE Hydraulics Division Meeting*, University Park, Pennsylvania.
- Nouh, M. 1988. Regime Channels of an Extremely Arid Zone. In: White, W. (Ed.), *International Conference on River Regime*, John Wiley and Sons Ltd., 55 - 66.
- Olberg, C.R. and Schanck, F.R. 1913. Special Report on Irrigation and Flood Protection, Papago Indian Reservation. Department of the Interior Letter of Transmittal, Document No. 973.
- Osterkamp, W.R. and Costa, J.E. 1987. Changes Accompanying an Extraordinary Flood on a Sand-Bed Stream. In: Mayer, L. and Nash, D. (Eds.), *Catastrophic Flooding*, Binghamton Symposia in Geomorphology International Series, 201 - 224.
- Osterkamp, W.R. and Hedman, E.R. 1982. Perennial-Streamflow Characteristics Related to Channel Geometry and Sediment in Missouri River Basin. US Geological Survey Professional Paper, 1242.
- Parker, J.T.C. 1992. Channel Change on the Santa Cruz River, Pima County, Arizona, 1936 - 86. US Geological Survey Water Supply Paper, 2429.
- Parker, J.T.C. 1996. Geomorphology and Hydrology of the Santa Cruz River, Southeastern Arizona. Unpublished PhD thesis, University of Arizona, Tucson.
- Patton, P.C. and Schumm, S.A. 1975. Gully Erosion, Northwestern Colorado: A Threshold Phenomenon. *Geology*, 3, 88 - 90.
- Patton, P.C. and Schumm, S.A. 1981. Ephemeral-Stream Processes: Implications for Studies of Quaternary Valley Fill. *Quaternary Research*, 15, 24 - 43.
- Phillips, J.D. 1992a. Nonlinear Dynamical Systems in Geomorphology: Revolution or Evolution? *Geomorphology*, 5, 219 - 229.
- Phillips, J.D. 1992b. The End of Equilibrium? *Geomorphology*, 5, 195 - 201.
- Pickup, G. and Warner, R.F. 1976. Effects of Hydrologic Regime on Magnitude and Frequency of Dominant Discharge. *Journal of Hydrology*, 29, 51 - 75.

- Popp, C.J., Hawley, J.W., Love, D.W. and Dehn, M. 1988. Use of Radiometric (Cs-137, Pb-210), Geomorphic and Stratigraphic Techniques to Date Recent Oxbow Sediments in the Rio Puerco Drainage Grants Uranium Region, New Mexico. *Environ Geol Water Sci*, **11** (3), 253 - 269.
- Qi, P. and Zhao, Y. 1993. Characteristics of Sediment Transport and Channel Formation by Floods at Hyperconcentrations of Sediment in the Yellow River. *International Journal of Sediment Research*, **8** (1), 69 - 83.
- Bureau of Reclamation, 1996. Rio Puerco Sedimentation and Water Quality Study. US Department of the Interior Bureau of Reclamation Preliminary Findings Report.
- Reich, B.M. and Davis, D.R. 1987. Estimating the Regulatory Flood on a Degrading River. In: Singh, V.P. (Ed.), *Regional Flood Frequency Analysis*, D Reidel Publishing Company, 197 - 212.
- Renwick, W.H. 1992. Equilibrium, Disequilibrium and Nonequilibrium Landforms in the Landscape. *Geomorphology*, **5**, 265 - 276.
- Rich, J.L. 1911. Recent Stream Trenching in the Semi-arid Portion of Southwestern New Mexico, a Result of Removal of Vegetation Cover. *Am. Jour. Sci.*, **32** (190), 237 - 245.
- Richards, K.S. 1982. Form and Process in Alluvial Channels, Methuen, London, 361 pp.
- Roberts, R.A. 1990. Analysis of Sediment Transport in an Ephemeral Stream. Unpublished MSc thesis, University of Arizona, 145 pp.
- Roeske, R.H., Garrett, J.M. and Eychaner, J.H. 1989. Floods of October 1983 in Southeastern Arizona. US Geological Survey Water-Resources Investigation Report, 85-4225-C.
- Saarinen, T.F., Baker, V.R., Durrenberger, R. and Maddock, T. 1984. *The Tucson, Arizona, Flood of October 1983*, National Academy Press, Washington D.C., 112 pp.
- Schick, A.P. 1974. Formation and Obliteration of Desert Stream Terraces - A Conceptual Analysis. *Z. Geomorph. N.F.*, **21**, 88 - 105.
- Schumann, R.R. 1989. Morphology of Red Creek, Wyoming, an Arid-Region Anastomosing Channel System. *Earth Surface Processes and Landforms*, **14**, 277 - 288.

- Schumm, S.A. 1960. The Shape of Alluvial Channels in Relation to Sediment Type. US Geological Survey Professional Paper, 352-B, 30 pp.
- Schumm, S.A. 1973. Geomorphic Thresholds and Complex Response of Drainage Systems. In: Morisawa, M. (Ed.), *Fluvial Geomorphology*, Allen & Unwin, 299 - 310.
- Schumm, S.A. 1975. Episodic Erosion: A Modification of the Geomorphic Cycle. In: Melhorn, W.L. and Flemal, R.C. (Eds.), *Theories of Landform Development*, Binghamton, NY, State University of New York, 70 - 85.
- Schumm, S.A. 1979. Geomorphic Thresholds: the Concept and its Applications. *Transactions of the Institute of British Geographers New Series*, 4, 485 - 515.
- Schumm, S.A. and Hadley, R.F. 1957. Arroyos and the Semiarid Cycle of Erosion. *American Journal of Science*, 255, 161 - 174.
- Schumm, S.A., Harvey, M.D. and Watson, C.C. 1984. *Incised Channels: Morphology, Dynamics and Control*, Water Resources Publications, Littleton, Colorado, 200 pp.
- Schumm, S.A. and Khan, H.R. 1972. Experimental Study of Channel Patterns. *Geological Society of America Bulletin*, 83, 1755 - 1770.
- Schumm, S.A. and Lichy, R.W. 1963. Channel Widening and Flood Plain Construction Along Cimarron River in Southwestern Kansas. US Geological Survey Professional Paper, 352-D.
- Schumm, S.A., Mosley, M.P. and Weaver, W.E. 1987. *Experimental Fluvial Geomorphology*, Wiley, Chichester.
- Simon, A. 1992. Energy, Time and Channel Evolution in Catastrophically Disturbed Fluvial Systems. *Geomorphology*, 5, 324 - 372.
- Simon, A. and Hupp, C.R. 1991. Geomorphic and Vegetative Recovery Processes along Modified Stream Channels of West Tennessee. US Geological Survey Open-File Report, 91-502.
- Simons, Li and Associates, Inc. 1986. Santa Cruz River Management Plan Technical Report.
- Slavin, P.J. 1991. Geomorphic History of the Rio Puerco across the Jemez Lineament, Rio Grande Rift Boundary Zone, New Mexico. Unpublished MSc thesis, University of New Mexico, Albuquerque, 111 pp.

- Slezak-Pearthree, M. and Baker, V.R. 1987. Channel Change along the Rillito Creek System of SE. Arizona - 1941 through 1983. Implications for Flood Plain Management. *Arizona Bureau of Geology and Mineral Technology Geological Survey Branch* (Special Paper 6), 58 p.
- Soar, P.J. and Thorne, C.R. 2001. Channel Restoration Design for Meandering Rivers. US Army Corps of Engineers, Coastal and Hydraulics Laboratory, ERDC/CHL CR-01-1.
- Thomas, C.L., Stewart, A.E. and Constanza, J. 2000. Determination of Infiltration and Percolation Rates along a Reach of the Santa Fe River near La Bajada, New Mexico. US Geological Survey Water-Resources Investigation Report, 00-4141.
- Thorne, C.R. 1982. Processes and Mechanisms of Bank Erosion. In: Hey, R.D., Bathurst, J.C. and Thorne, C.R. (Eds.), *Gravel Bed Rivers*, John Wiley & Sons Ltd., 227 - 271.
- Thorne, C.R. 1990. Effects of Vegetation on Riverbank Erosion and Stability. In: Thornes, J.B. (Ed.), *Vegetation and Erosion*, John Wiley and Sons Ltd., 125 - 144.
- Thorne, C.R. 1999. Bank Processes and Channel Evolution in the Incised Rivers of North-Central Mississippi. In: Darby, S.E. and Simon, A. (Eds.), *Incised River Channels*, John Wiley & Sons Ltd., 97 - 121.
- Thorne, C.R. and Lewin, J. 1979. Bank Processes, Bed Material Movement and Planform Development in a Meandering River. In: Rhodes, D. and Williams, G. (Eds.), *Adjustments of the Fluvial System*, 117 - 137.
- Thorne, C.R. and Osman, A.M. 1988a. Riverbank Stability Analysis. II: Applications. *Journal of Hydraulic Engineering, ASCE*, **114** (2), 151 - 172.
- Thorne, C.R. and Osman, A.M. 1988b. The Influence of Bank Stability on Regime Geometry of Natural Channels. *Unknown*.
- Thorne, C.R., Russell, A.P.G. and Alam, M.K. 1993. Planform Pattern and Channel Evolution of the Brahmaputra River, Bangladesh. In: Best, J.L. and Bristow, C.S. (Eds.), *Braided Rivers*, Geological Society Special Publication, 257 - 276.
- Thorne, C.R., Soar, P.J., Hey, R.D. and Watson, C.C. 1998. Dominant Discharge Calculation: A Practical Guide. US Army Research,

- Development and Standardisation Group - UK Final Report, R&D8399-EN-01.
- Thorne, C.R. and Tovey, N.K. 1981. Stability of composite river banks. *Earth Surface Processes and Landforms*, **6**, 469 - 484.
- Thornes, J. 1980. Structural Instability and Ephemeral Channel Behaviour. *Z. Geomorph. N.F.*, **36**, 233 - 244.
- Tuan, Y.-F. 1966. New-Mexican Gullies: A Critical Review and Some Recent Observations. *Annals of the Association of American Geographers*, **56** (4), 573 - 597.
- Twidale, C.R. 1964. Erosion of an Alluvial Bank and Birdwood, South Australia. *Z. Geomorph. N.F.*, **2**, 189 - 211.
- Walling, D.E. and Webb, B.W. 1982. Sediment Availability and the Prediction of Storm-Period Yields. Exeter, IAHS Publ. No., 327 - 337.
- Waters, M.R. 1988. Holocene Alluvial Geology and Geoarchaeology of the San Xavier reach of the Santa Cruz River, Arizona. *Geological Society of America Bulletin*, **100**, 479-491.
- Webb, R.H. 1987. Occurrence and Geomorphic Effects of Streamflow and Debris Flow in Northern Arizona and Southern Utah. In: Mayer, L. and Nash, D. (Eds.), *Catastrophic Flooding*, Binghamton Symposia in Geomorphology International Series, 247 - 265.
- Webb, R.H. and Baker, V.R. 1987. Changes in Hydrologic Conditions Related to Large Floods on the Escalante River, South-Central Utah. In: Singh, V.P. (Ed.), *Proc. Int Symp on Flood Freq and Risk Analysis*, Regional Flood Frequency Analysis, D Reidel Publishing Company, 309 - 323.
- Webb, R.H. and Betancourt, J.L. 1992. Climatic Variability and Flood Frequency of the Santa Cruz River, Pima County, Arizona. US Geological Survey Water-Supply Paper, 2379.
- Whittow, J. 1984. *The Penguin Dictionary of Physical Geography*, Penguin Books, 591 pp.
- Widdison, J.G. 1959. Historical Geography of the Middle Rio Puerco Valley, New Mexico. *New Mexico Historical Review*, **34**, 248 - 284.
- Williams, G.P. 1978. Bank-Full Discharge of Rivers. *Water Resources Research*, **14** (6), 1141 - 1154.

- Wolman, M.G. 1959. Factors Influencing the Erosion of a Cohesive Bank. *American Journal of Science*, **257**, 204 - 216.
- Wolman, M.G. and Gerson, R. 1978. Relative Scales of Time and Effectiveness of Climate in Watershed Geomorphology. *Earth Surface Processes*, **3**, 189 - 208.
- Wolman, M.G. and Miller, J.P. 1960. Magnitude and Frequency of Forces in Geomorphic Processes. *Journal of Geology*, **68**, 54 - 74.
- Womack, W.R. and Schumm, S.A. 1977. Terraces of Douglas Creek, Northwestern Colorado: An Example of Episodic Erosion. *Geology*, **5**, 72 - 76.
- Yu, B. and Wolman, M.G. 1987. Some Dynamic Aspects of River Geometry. *Water Resources Research*, **23** (3), 501 - 509.

Appendix 1

Data Collection and Collation

APPENDIX 1

Data Collection and Collation

Data used in this thesis is summarised in Appendix 3.

A1.1 DAILY AVERAGE DISCHARGE DATA

All three rivers studied had long daily average discharge records collected from at least one gauge. Due to the ephemeral nature of the arroyos, discharge records. All records used were collected by the US Geological Survey and were generally described as being fair in quality by the researchers collecting them. The exception to this is at the Barrier Dam Gauge, which was installed and is maintained by the BLM (Bureau of Land Management) in Safford. This is the only gauge still running on the San Simon River and took the place of the Solomon Gauge in 1982. As with the US Geological Survey discharge data, records at the Barrier Dam Gauge are of fair quality. This study has combined the data from both the Solomon and Barrier Dam gauges for the purposes of calculating variables such as annual totals and effective discharge for the San Simon River, since this is the most comprehensive dataset. However, differences were noted between the methods of collection and processing used by the two agencies. This resulted in dramatically lower discharges being recorded since 1982, which cannot entirely be attributed to the change in flow regime.

A1.2 15 MINUTE DISCHARGE DATA

15 minute discharge data was not readily available for any of the three rivers studied over the entire period of record. However, it was possible to obtain this data for the Rio Puerco due to the availability of the original stripcharts. Although it would theoretically have been possible to obtain stripcharts for other time-periods and gauges, it was decided that, due to the time-consuming nature of the work required to extract the data, it was best to concentrate on the 1949 to 1984 period at the Bernardo gauge, close to the mouth of the Rio Puerco, during which time comprehensive sediment concentration data had been collected. After 1984, the stripcharts for subsequent years could not be found and thus a large break in data exists

until 1993, when the US Geological Survey began storing 15 minute discharge records. Attempts were made to obtain stripcharts for other Rio Puerco gauges, however, it was discovered that the boxes that they had been stored in had been incorrectly labelled and were, hence, unavailable.

Method of Converting Stripchart Trace to Discharge Values

1. An Altek Digitiser was used to digitise the stripchart trace, with software developed by the US Geological Survey specifically for the purpose of converting the trace to actual gauge heights.
2. A portion of the stripchart was taped to the digitising tablet, ensuring that no creases remained.
3. The bottom two and top right corners of the graph were digitised and a scale entered into the computer. Midnight was entered as 240000, not 000000. The gauge height scale was multiplied by 100, so that 3.0 was entered as 300.
4. All changes in gradient or direction were digitised, noting the following:
 - a. If the trace indicated that the discharge had been fluctuating greatly, due to the presence of waves and dune or anti-dune bedforms (which commonly occurred during spring and high-magnitude runoff events), the centre-line of the trace was digitised.
 - b. If the gauge had become silted up or isolated due to shifts in the position of the active channel, this fact was noted and the trace was not digitised.
 - c. Occasionally, peak discharges caused the trace to go above the top of the graph. In this case, the trace reversed, drawing a trough instead of a peak. The digitising program had been created to cope with this, so that it automatically calculated the true gauge height, not the trough drawn on the stripchart.
 - d. Care must be taken to note changes in scale and gaps in the record (which may appear continuous at first glance), often due to folds in the original during blue-lining.
5. Once the trace for one section had been digitised, it was checked immediately for errors. Often the peak values had been written onto the

chart by hand and these could be used to determine whether the digitising was accurate.

6. After the entire trace for the year had been digitised entirely and gauge heights obtained, the US Geological Survey software was used to convert these values into discharge values. The first stage required the relevant rating curve to be associated with the correct time-period of usage. The software required the stage-discharge relationship to be entered and this record was saved under a specific code. A separate spreadsheet was then used to enter the start and end dates of usage. Rating curves could be used for more than one period of time. It was noted that, during the 1950s and 1960s many rating curve changes were used. However, the same rating curve has now been in use since 1978.
7. Once the rating curves had been allocated, the gauge adjustments and pen corrections were entered. Gauge shift adjustments indicated the changing bed level during floods. This is extremely important in arroyo systems since large amounts of scour typically occur during the rising limb of floods, with sediment being re-deposited during the falling limb, often with little or no change in net bed level. Pen corrections indicated errors in the recording device. Records of these adjustments were often faint and sometimes missed off altogether. Sometimes even when the correct shifts were entered, the daily average would be incorrect.
8. Initially, the discharge at each change in gradient and direction was calculated. This enabled the discharge every 15 minutes to be extrapolated, again using US Geological Survey software. The daily average was calculated for the data and this was checked against the published daily average values. Days which were more than five percent different were checked for errors. If, after corrections had been made, the two values were still significantly different and there were no obvious errors in the recorded daily average value, the 15 minute data was deleted.

The stripcharts and associated sediment discharge records were generally in poor condition and were of poor quality due ephemeral nature of the Rio

Puerco, which caused the gauge to be highly prone to silting. The poor condition of the stripcharts was due to the fact that in many cases the original chart had been stored in a separate place, with a blue-line copy only in with the sediment data. This copy was often faint and written comments hard to read. During the earlier decades, records were generally more accurate and the gauge was better maintained. Once computers became more widely used, much data was no longer stored, since computer storage space was non-existent or extremely limited. Often useful explanatory comments, such as gauge shifts and pen corrections, were no longer written down and thus much detail has been lost from the 1970s and 1980s records.

Despite the problems encountered, however, after the data had been processed for the purposes of this project, it was found to compare favourably to the published daily average data, except where this data was obviously erroneous. There were days when the published discharge was obviously far higher or lower than was recorded on the stripchart. For example, on the 3rd to 5th of April and 3rd to 4th of September 1961, these days had been recorded as having no flow on the stripchart (marked with "NF" as well as having no trace). However, flow was recorded in the published daily average record.

The above method of calculating discharge from stripchart records is standard for the US Geological Survey. This method, including the calculation of rating curves, shift adjustments and pen corrections is explained in detail in Kennedy (1983). The obvious difficulty in using the method outlined above to create discharge values every 15 minutes was that the calculations had already been carried out by experienced US Geological Survey personnel, who may not have documented calculations in their entirety. Thus a certain amount of back-calculation was necessary to complete the analysis. If there was any doubt as to the accuracy of the 15 minute discharge data, it was discarded. It should be kept in mind that the daily average discharge records for the Rio Puerco are noted as being of fair or poor quality in the vast majority of cases. However, since this is the only

data available, the nature of the records was taken into account when the data was being used for analysis.

A1.3 SEDIMENT DISCHARGE DATA

The majority of arroyo systems have very few sediment discharge measurements due to their flashy discharge regime. The three rivers studied were chosen specifically for the fact that at least some sediment records had been collected. The Rio Puerco at Bernardo had by far the most data, with over 5000 instantaneous sediment concentration measurements between 1949 and the present. The sediment samples were collected using a depth-integrated sampler (Edwards and Glysson, 1999). The sediment concentration was then calculated using the ratio between the weight of sediment to the weight of the water/sediment sample (Porterfield, 1972). Some errors in the original sediment calculations were noted and corrected. It was also noted that prior to 1968, sediment concentrations were recorded in parts per million. These were converted to the standard modern measurement of mg/l using the US Geological Survey conversion factor noted in Porterfield, 1972, p43. This was vital due to the extremely high concentrations measured. The concentration measurements were converted to a sediment load using the following equation (Porterfield, 1972):

$$Q_s = Q_w \times C_s \times k \quad \dots \dots \dots \quad A1.1$$

where Q_s = sediment load (tonnes/day)

Q_w = water discharge (cumecs)

C_s = concentration of suspended sediment (Mg/l)

k = coefficient, which is calculated using equation A1.2, assuming the use of metric units, where the weight of 1 m³ of water is 1 tonne and the time interval is 24 hours or 86400 seconds.

$$k = \frac{86400 \times 1 \text{ tonne/m}^3}{1,000,000} = 0.0864 \quad \dots \dots \dots \quad A1.2$$

Thus

$$Q_s = Q_w \times C_s \times 0.0864 \quad \dots \dots \dots \quad A1.3$$

Along the Rio Puerco, instantaneous sediment discharge data was also collected by the US Geological Survey at the Rio Puerco above Arroyo Chico gauge and at the Arroyo Chico gauge itself. However, since the only discharge data available for these gauges was daily average values, the corresponding daily average sediment loads, recorded by the US Geological Survey, were used.

A small amount of daily average sediment load data was recorded for the San Simon River at Solomon during the 1950s. Data was also collected by the Bureau of Land Management (BLM) at the Barrier Dam Gauge since 1984, although only monthly averages were recorded. Sediment concentration data was also collected at Bailey Well, Fan Dam and Yellowhammer sites. However, the corresponding discharge data was not recorded, thus rendering the data inadequate for the purposes of this project.

Measurements of sediment discharge from the Santa Cruz River were taken by Roberts (1990) close to the Tucson gauge. Several events during 1988 and 1989 were sampled and the instantaneous sediment concentration and equivalent discharge were recorded. The sediment concentrations were converted to sediment loads using the method outlined above.

The sediment data was collected along all three arroyo systems using the techniques outlined above, which are standard US Geological Survey methods.

Nordin (1963) noted that the sediment transported along the Rio Puerco showed nearly uniform concentration dispersion, thus enabling representative samples to be taken from anywhere within the flow. The same dispersal was also noted along the Santa Cruz River (Roberts, 1990). Thus the sediment discharge measurements collated for this project are assumed to represent accurately the volumes and concentrations of sediment transported.

A1.4 EFFECTIVE DISCHARGE CALCULATION

The effective discharge was calculated using a computer program developed by David Raff and Chris Holmquist-Johnson at Colorado State University (CSU). The method used may be found in Holmquist-Johnson (2002), which is similar to, and partially based on, the methodology of Thorne *et al.*, (1998) and Soar and Thorne (2001). There are several stages to determining the effective discharge:

Step 1 - Calculating the Flow Frequency Curve

The discharge range over the period of record was calculated by subtracting the minimum discharge from the maximum. This enabled a class interval to be determined, by dividing this range into the required number of classes. If too many classes are used, the curve produced is not continuous, with too many zero values. If too few classes are used, empirical information is lost. In this study the best representation of the data was achieved by using 25 classes. The frequency with which discharges falling into each class was then determined by examining the flows over the period of record. This frequency is simplified if expressed as a percentage occurrence (Soar and Thorne, 2001).

Step 2 – Calculating the Sediment Rating Curve

The measured suspended sediment load was used. The discharge was plotted against the sediment load. A power best-fit regression line was then fitted to this data, of the form (repeated from equation 7.1):

where Q_s = measured suspended sediment load (tonnes per day)

Q = water discharge (cumecs)

a = coefficient

b = exponent.

The values of a and b for each dataset are summarised in Chapter 7.

Step 3 – Construction of a Sediment Load Histogram

The sediment load histogram was constructed using discharges equal to the arithmetic mean of each class of the flow frequency curve. For each discharge, the equivalent sediment load was found from the sediment rating curve. This was then multiplied by the percentage frequency of occurrence of that discharge class to give the total daily sediment load (tonnes per day), averaged over the period of record.

Step 4 – Finding Effective Discharge

The effective discharge is equivalent to the peak of the sediment load histogram. In flashy, ephemeral streams, such as arroyos, the peak inevitably occurs in the first class, due to the predominance of low flows. However, this value should be disregarded, since there is no morphological representation of this discharge. Instead, the next largest peak should be used.

Method of Calculating Effective Discharge

The CSU computer program used in this project to calculate the effective discharge required several datasets to be input. Firstly, the discharge data was entered into a file, together with the corresponding stage, if available, date and time. Figure A1.1 shows the other data required to run the program. The period of record could be chosen, together with the number of classes. The values of a and b calculated in step 2 were also entered into the input form. These inputs enabled the flow frequency curve and the sediment load histogram to be calculated automatically. The program output was in the form of both a summary table and the graphs used in Chapter 7. The only major change subsequently made to this output was that the values of the total daily sediment load (tonnes per day), used in the sediment load histogram, were multiplied out to give a more meaningful value of total annual sediment load, averaged over the period of record (tonnes per year, or just tonnes, since the value is an annual total): in other words the average total annual sediment load.

Effective Discharge Input

Units
 English Units Metric Units

Flow Data Selection
Enter Range of Years to Calculate Effective Discharge:
 All Years
 Specify Years [] to []

Sediment Transport Information

$$Q_s = aQ^b$$

QsQ1
 Enable a = [] b = []
From Qmin = [] to Qmax = []

QsQ2
 Enable a = [] b = []
From Qmin = [] to Qmax = []

QsQ3
 Enable a = [] b = []
From Qmin = [] to Qmax = []

Bin Information

Arithmetic Bins

<input type="checkbox"/> Variation 1	Number of Bins	[]
<input type="checkbox"/> Variation 2	Number of Bins	[]
<input type="checkbox"/> Variation 3	Number of Bins	[]
<input type="checkbox"/> Variation 4	Number of Bins	[]
<input type="checkbox"/> Variation 5	Number of Bins	[]

Logarithmic Bins

<input type="checkbox"/> Variation 1	Number of Bins	[]
<input type="checkbox"/> Variation 2	Number of Bins	[]
<input type="checkbox"/> Variation 3	Number of Bins	[]
<input type="checkbox"/> Variation 4	Number of Bins	[]
<input type="checkbox"/> Variation 5	Number of Bins	[]

Buttons: Cancel, Continue >>

Figure A1.1 Input form for CSU effective discharge program.

A1.5 CROSS-SECTION SURVEYS

As discussed in Chapter 1, the reaches surveyed along the Santa Cruz and San Simon Rivers were chosen after field reconnaissance and inspection of aerial photographs. This ensured that morphologically distinct reaches were defined. Cross-sections were then surveyed along sub-reaches which were representative of the morphology of the different reaches. The location of each cross-section and the cross-sections themselves are shown in Appendix 2.

The exact position of each cross-section was initially chosen by marking the approximate position of the survey line on the relevant aerial photograph. Once in the field, the cross-section was located using features which were identifiable, both on the aerial photograph and on the ground, such as large trees and gullies. When the line of the cross-section had been pinpointed, the end points were marked with rebar and the exact location recorded using a Global Positioning System (GPS). When marking the cross-sections, it was ensured that the rebar was placed far enough back from the edge of

the arroyo trench, on the unincised valley floor to prevent their being eroded out in the near future.

The surveying was carried out using a total station placed on an adjustable tripod. This was placed on the line of the cross-section at a point where the entire arroyo and its features could be seen. A bearing to the rebar on each bank was taken. The surveying was then carried out using a reflective prism. The points recorded were carefully chosen in order to reflect accurately the morphology of the arroyo and were aligned with the initial bearing in order to ensure that a straight cross-section was obtained. As a general rule, every change in slope was recorded, together with changes in vegetation and sediment. The bankfull stage was determined by observing the slope changes and, in particular, the lower limit of permanent vegetation. Above the arroyo trench, the valley floor was surveyed up to the point at which it became level, in order to document tributary rills, gullies and arroyos.

The arroyo walls were surveyed by placing the prism on a pole, which could be extended over 9 metres (30 feet), so that it could be raised to the appropriate height up the wall. Care was taken when surveying these walls, especially when close to the top edge, due to the instability of the wall sediments, especially in areas where the walls were overhanging or had visible tension cracks behind them. An extendible pole was also used to survey areas which had particularly dense vegetation, which reduced both accessibility and visibility.

In order to determine the relative position of each cross-section, with respect to the other cross-sections along the same reach, back-sights were taken to known points on the previous cross section. This also enabled the bed- and water-surface slope to be calculated. The lack of monumented altitudes close to the surveyed reaches prevented their relative positions within the arroyo system to be calculated.

Cross-sections along the Rio Puerco were surveyed by John Elliott, during the 1970s, and John Elliott and Allen Gellis, during the 1990s. Similar survey techniques to those used in this study, described above, were employed. The cross-sections were monumented using rebar, the positions of which were recorded using a GPS. The surveying was carried out using a total station and prism, recording points along as straight a cross-section as possible. The major difference between the surveys was that Elliott's cross-sections were individual surveys, rather than the reaches surveyed on the other two arroyos.

Appendix 2

Location of Cross-Sections

APPENDIX 2

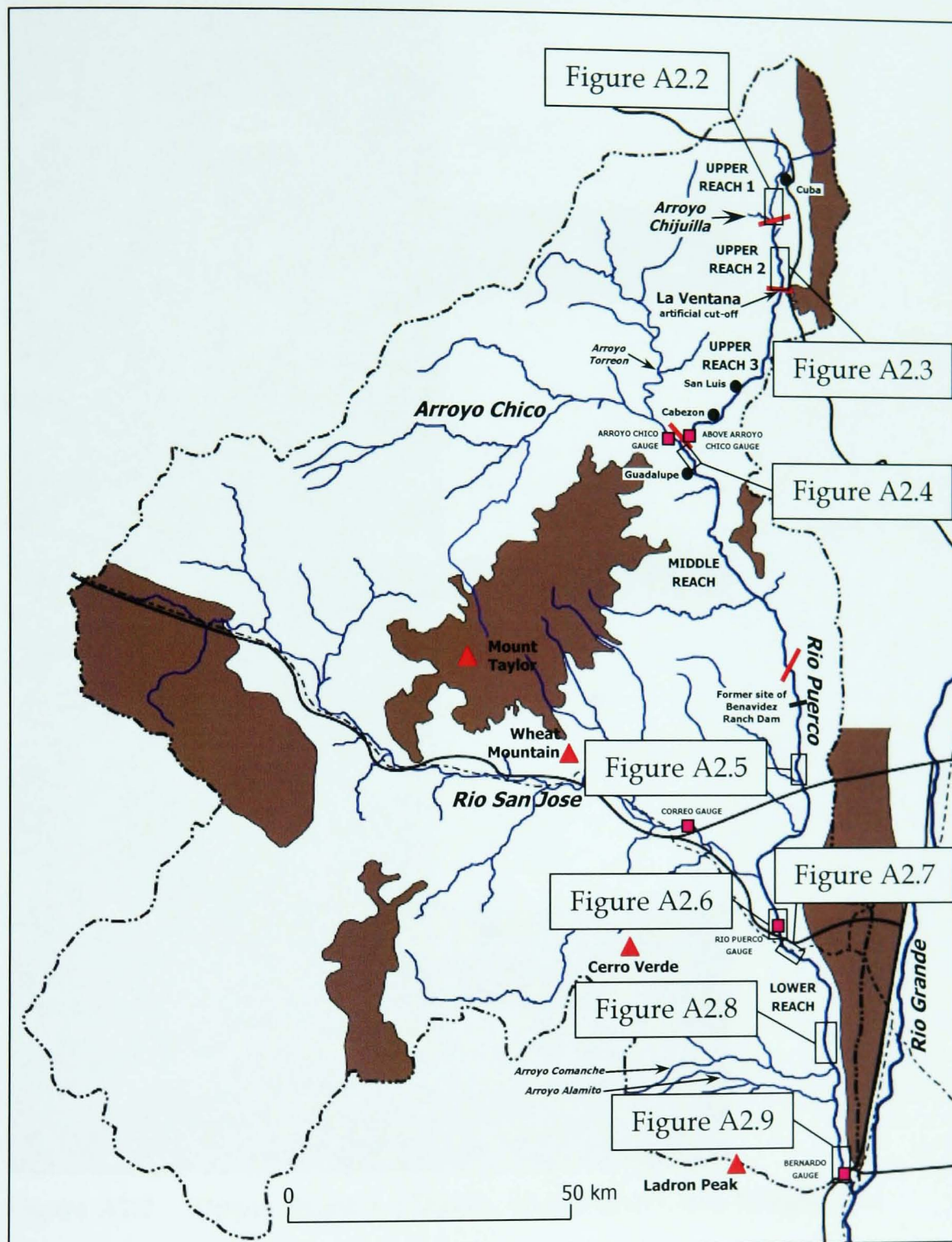
Location of Cross-Sections

Figure A2.1 Location of Rio Puerco cross-sections.

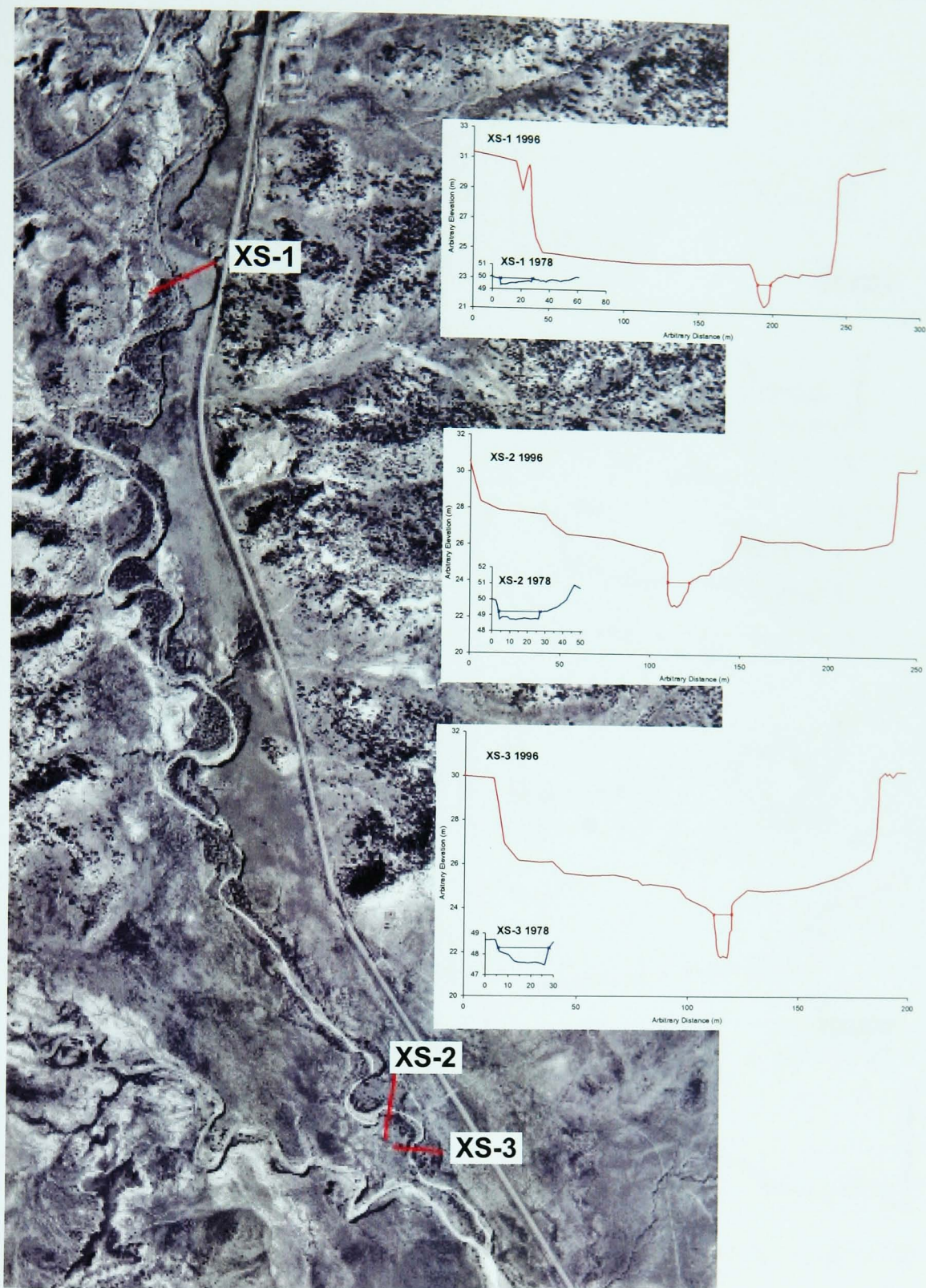


Figure A2.2 Upper Reach 1, Elliott's XS-1, 2 and 3, Rio Puerco.

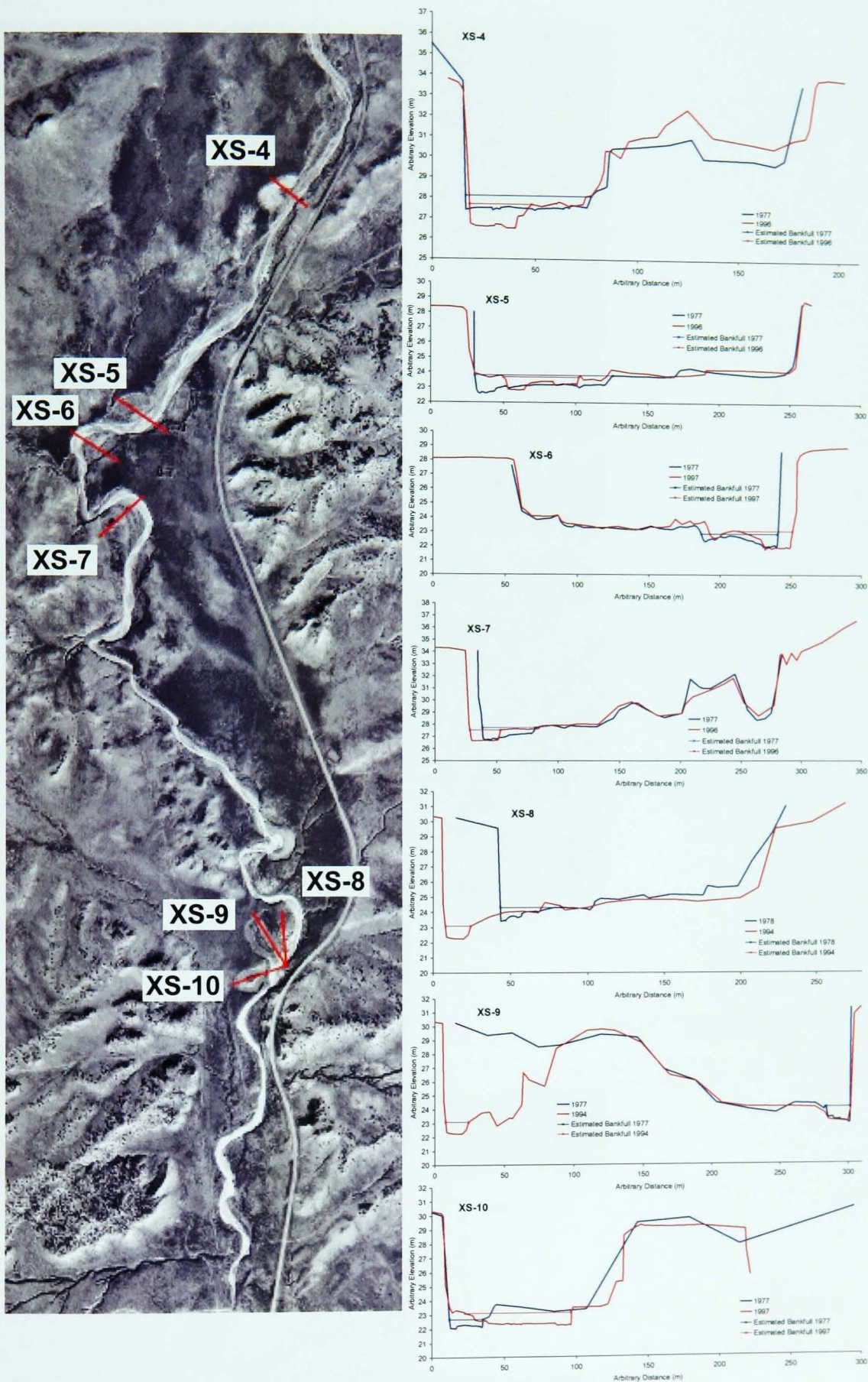


Figure A2.3 Upper Reach 2, Elliott's XS-4 to 10, Rio Puerco.

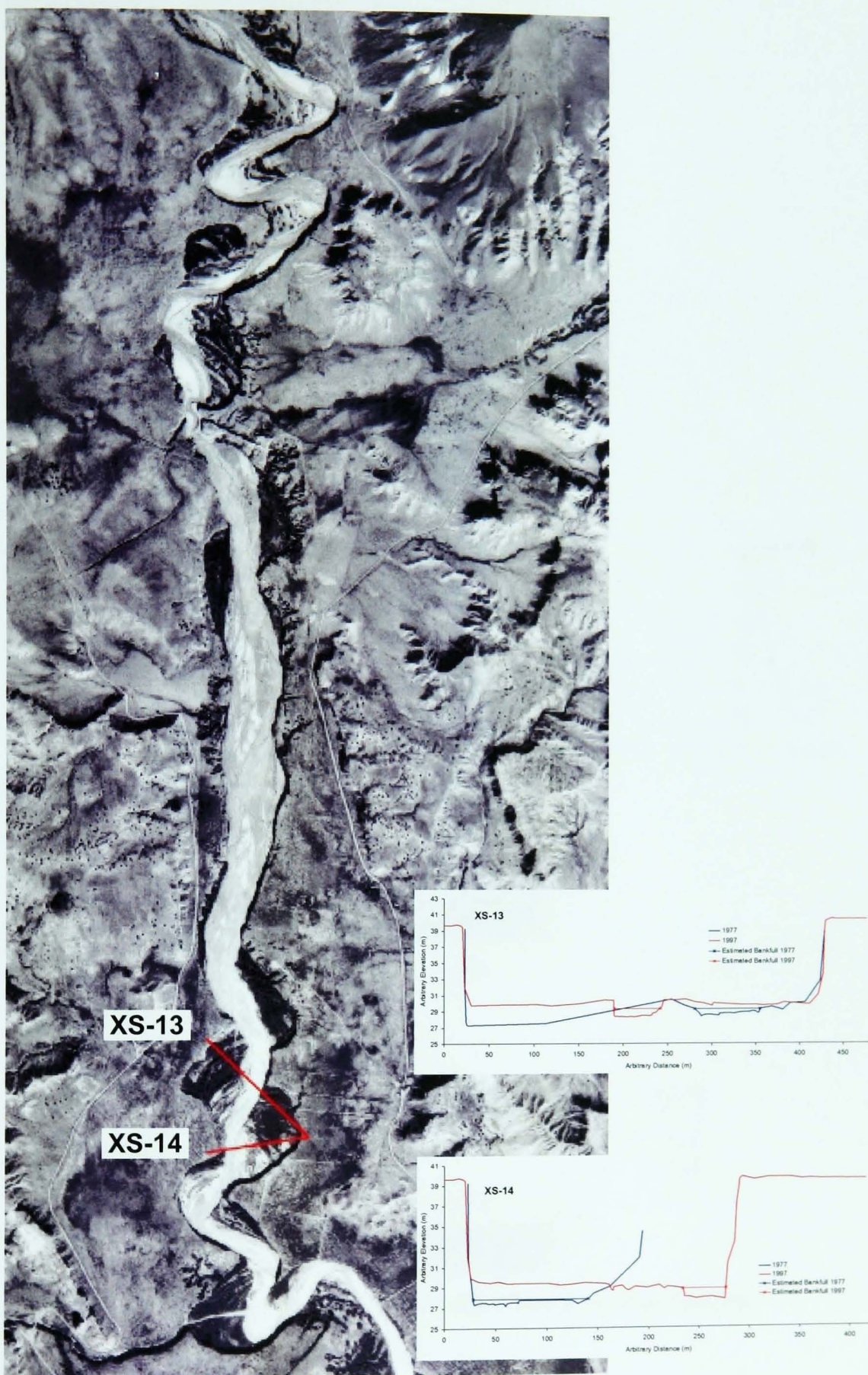


Figure A2.4 Middle Reach, Elliott's XS-13 and 14, Rio Puerco.

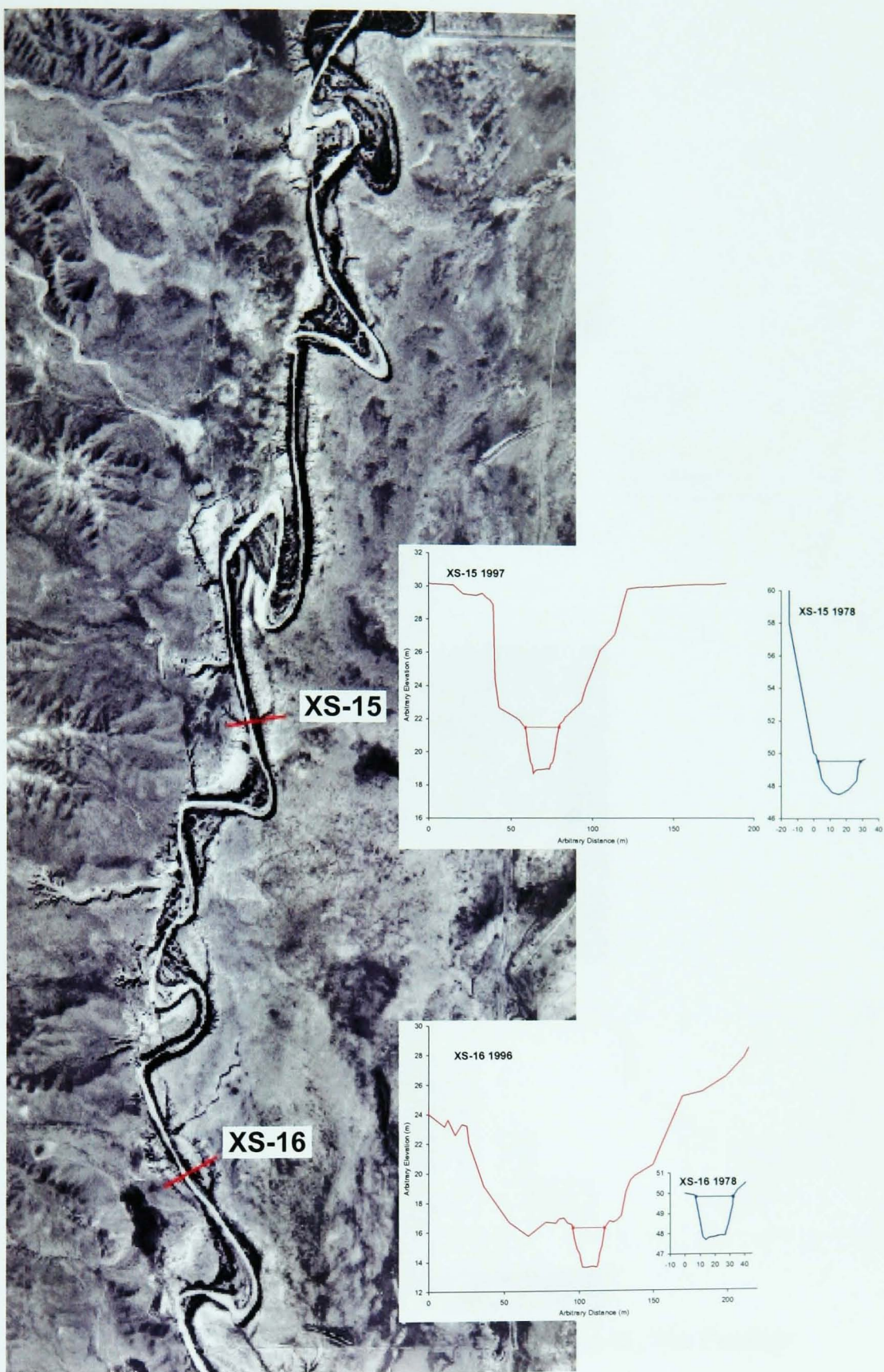


Figure A2.5 Lower Reach, Elliott's XS-15 and 16, Rio Puerco.

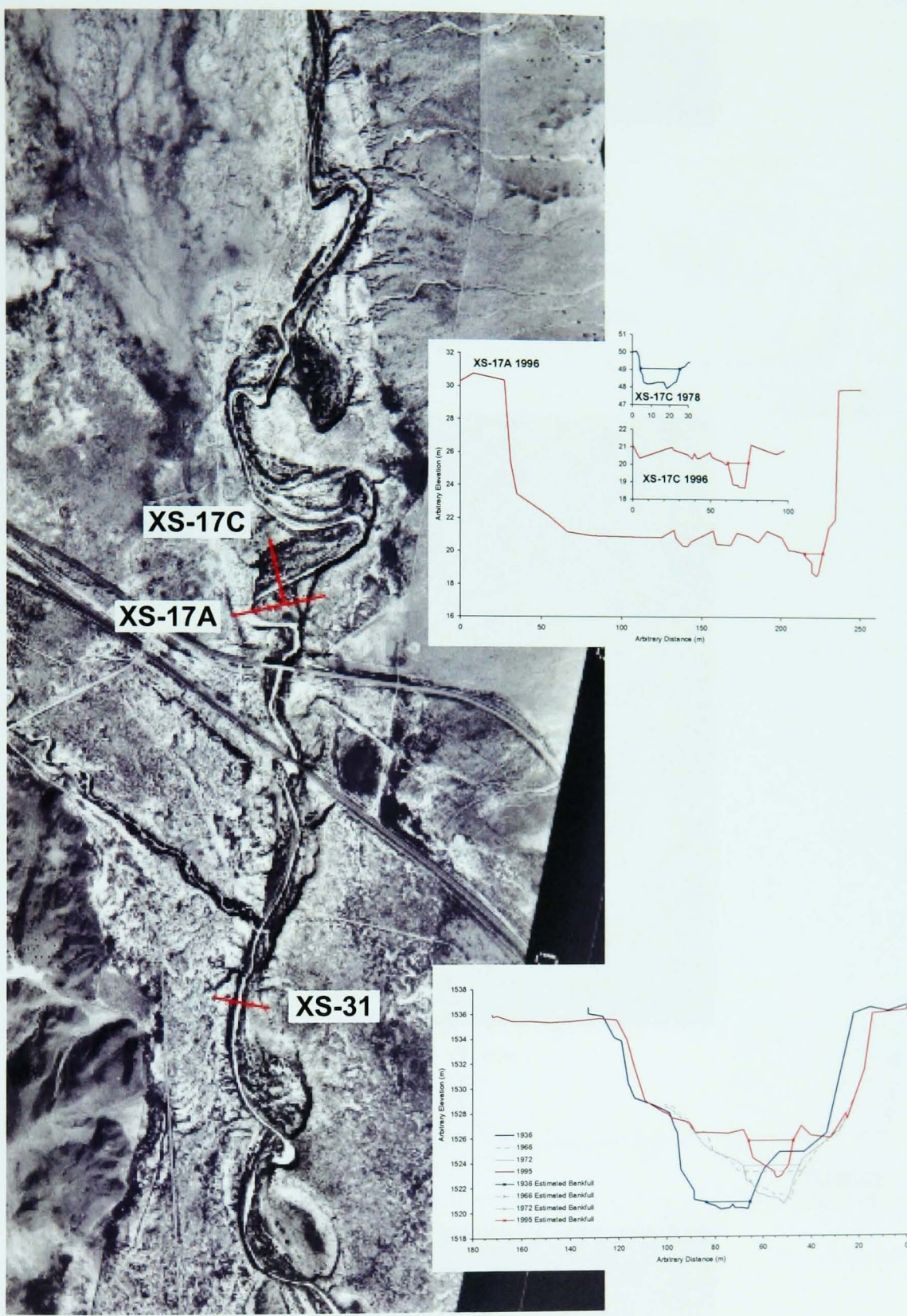


Figure A2.6 Lower Reach, Elliott's XS-17 and 31, Rio Puerco.

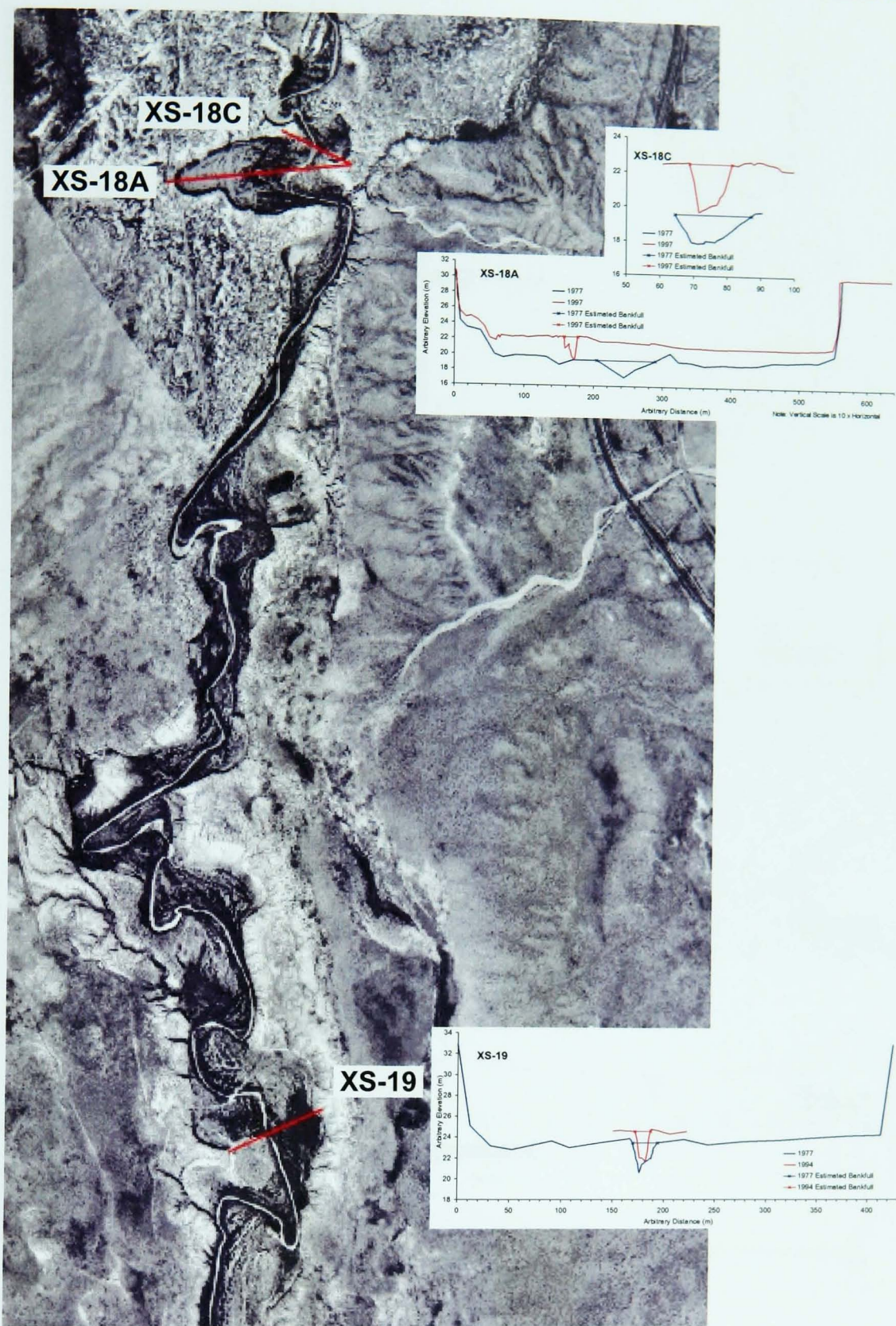


Figure A2.7 Lower Reach, Elliott's XS-18 and 19, Rio Puerco.

Appendix 2 – Location of Cross-Sections

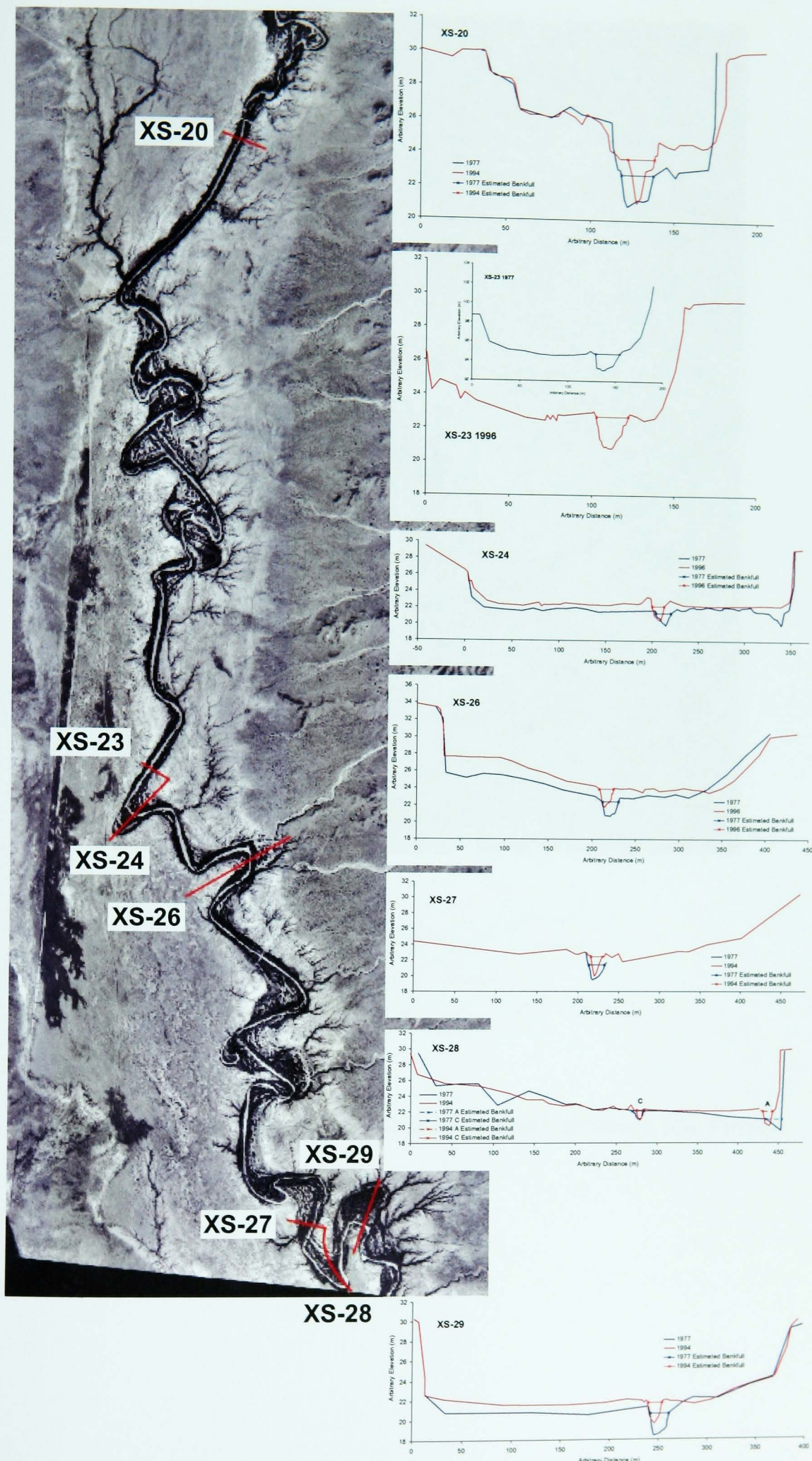


Figure A2.8 Lower Reach, Elliott's XS-20 to 29, Rio Puerco.

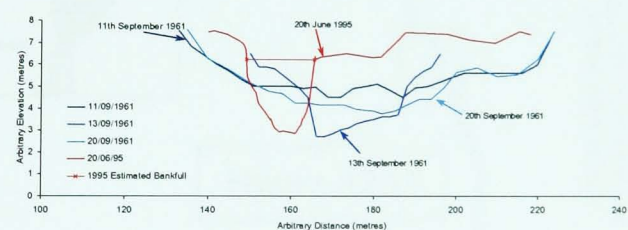
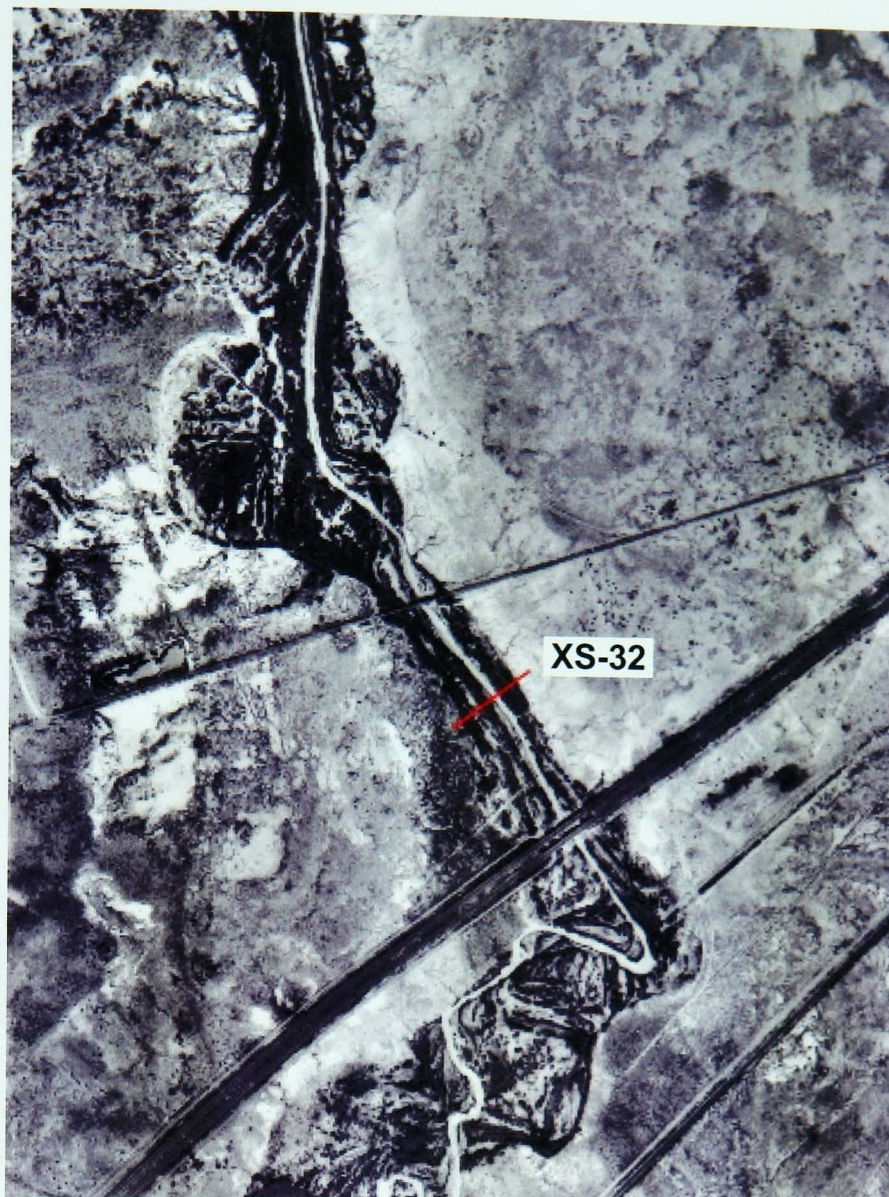


Figure A2.9 Lower Reach, XS-32 at Bernardo Cableway, Rio Puerco.

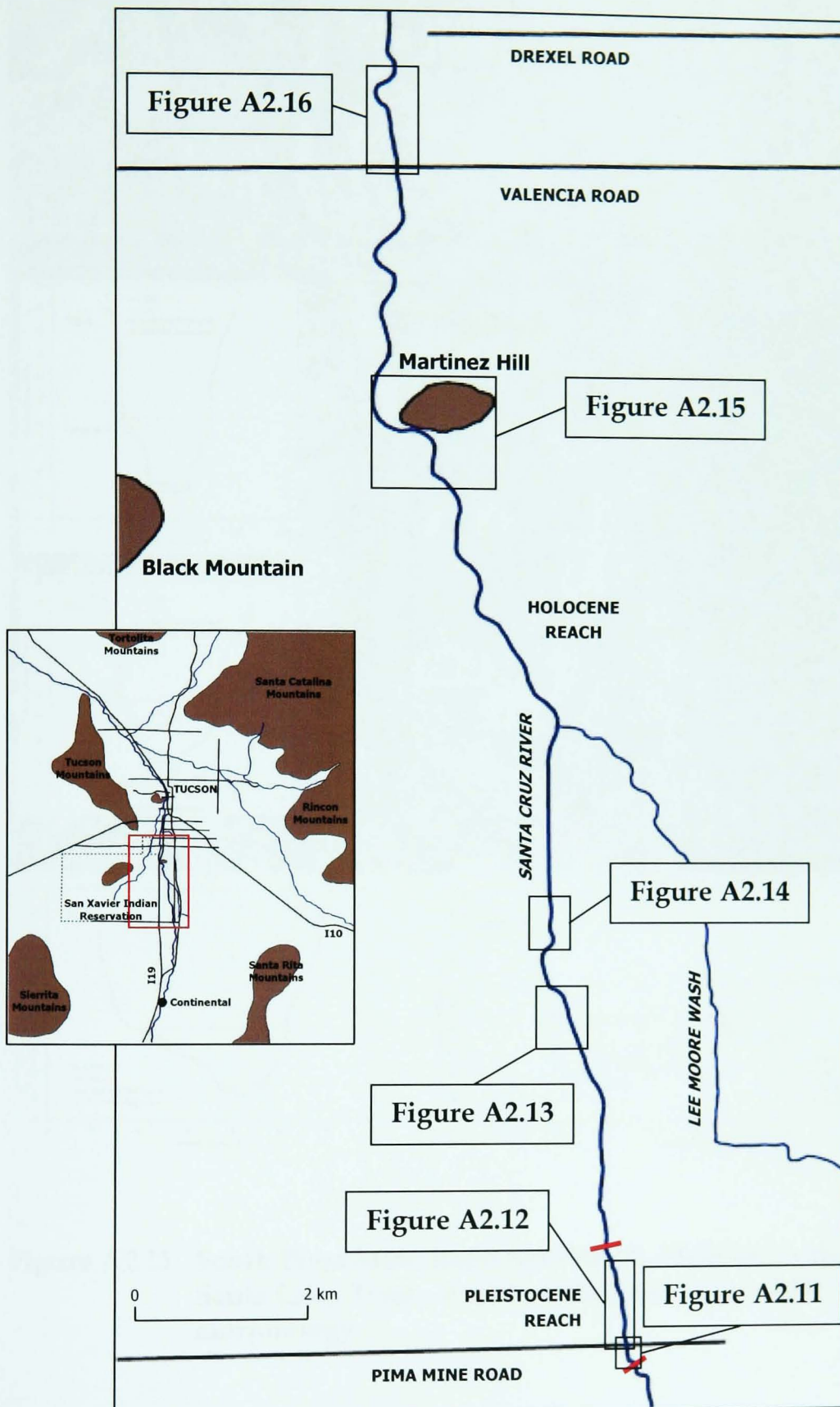


Figure A2.10 Location of Santa Cruz River cross-sections, inset shows location of larger map.

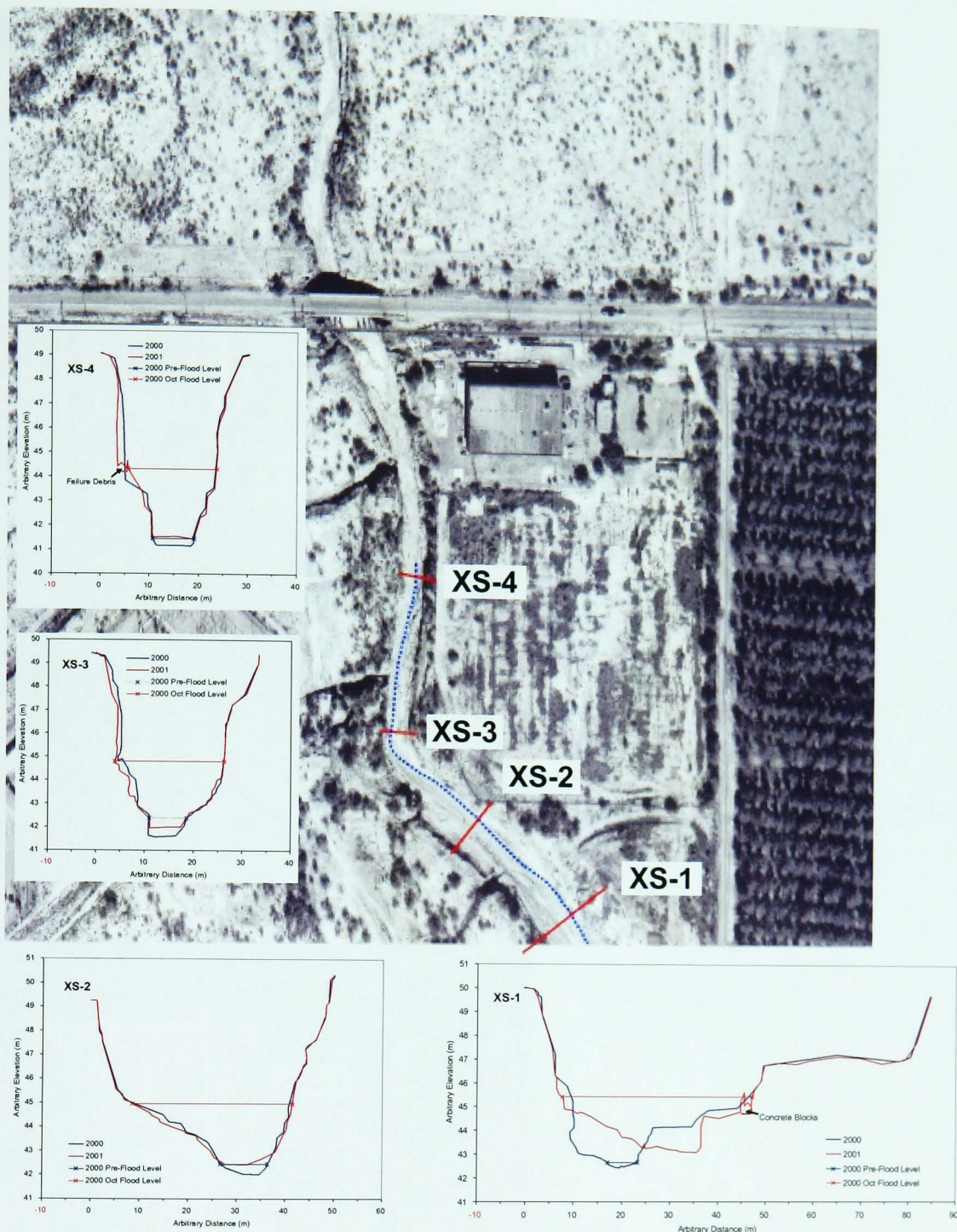


Figure A2.11 South Pima Mine Road Sub-Reach, Pleistocene Reach, Santa Cruz River. Aerial photograph shows 2001 morphology.

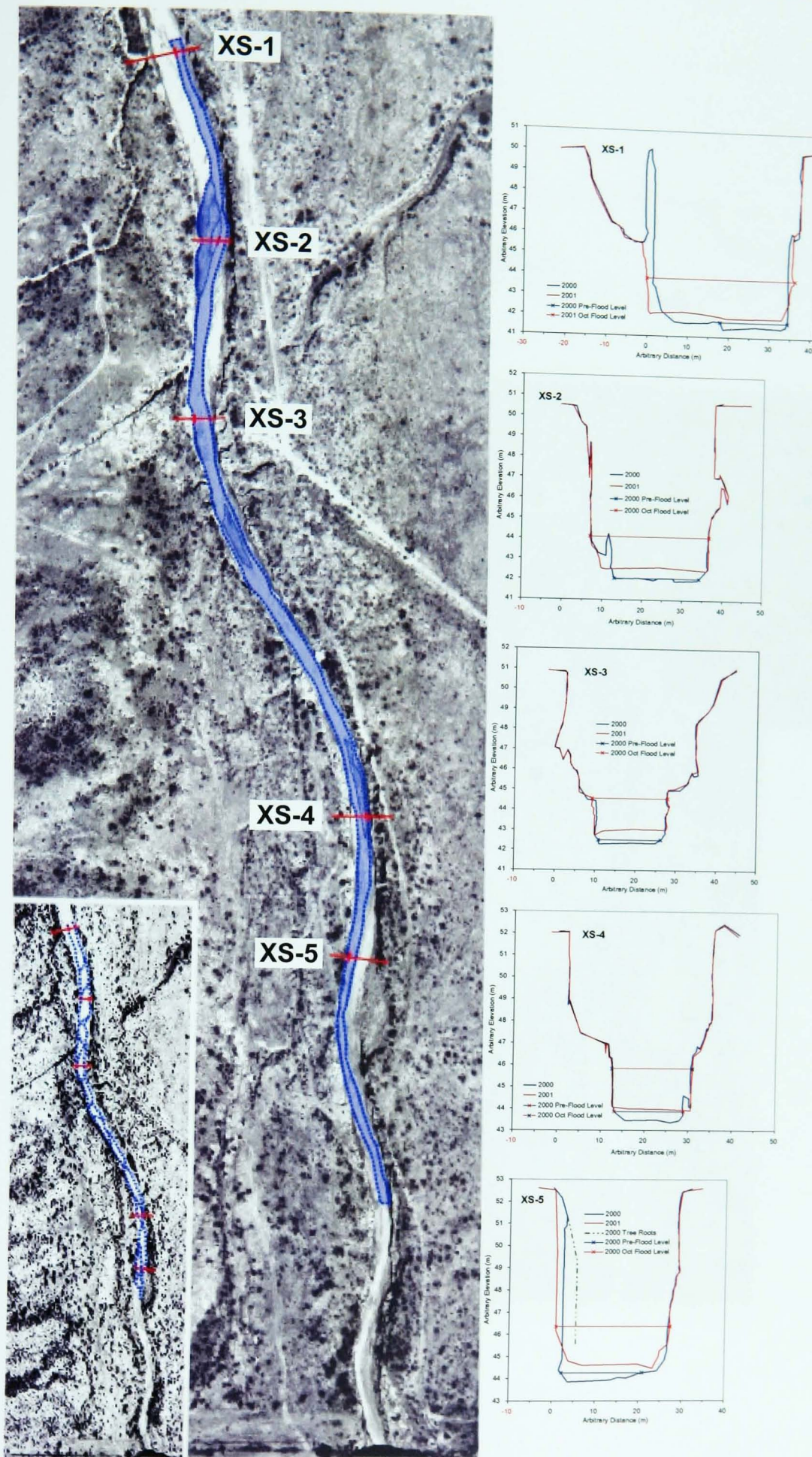


Figure A2.12 North Pima Mine Road Sub-Reach, Pleistocene Reach, Santa Cruz River. Aerial photograph shows 2001 morphology, inset shows pre-flood morphology.

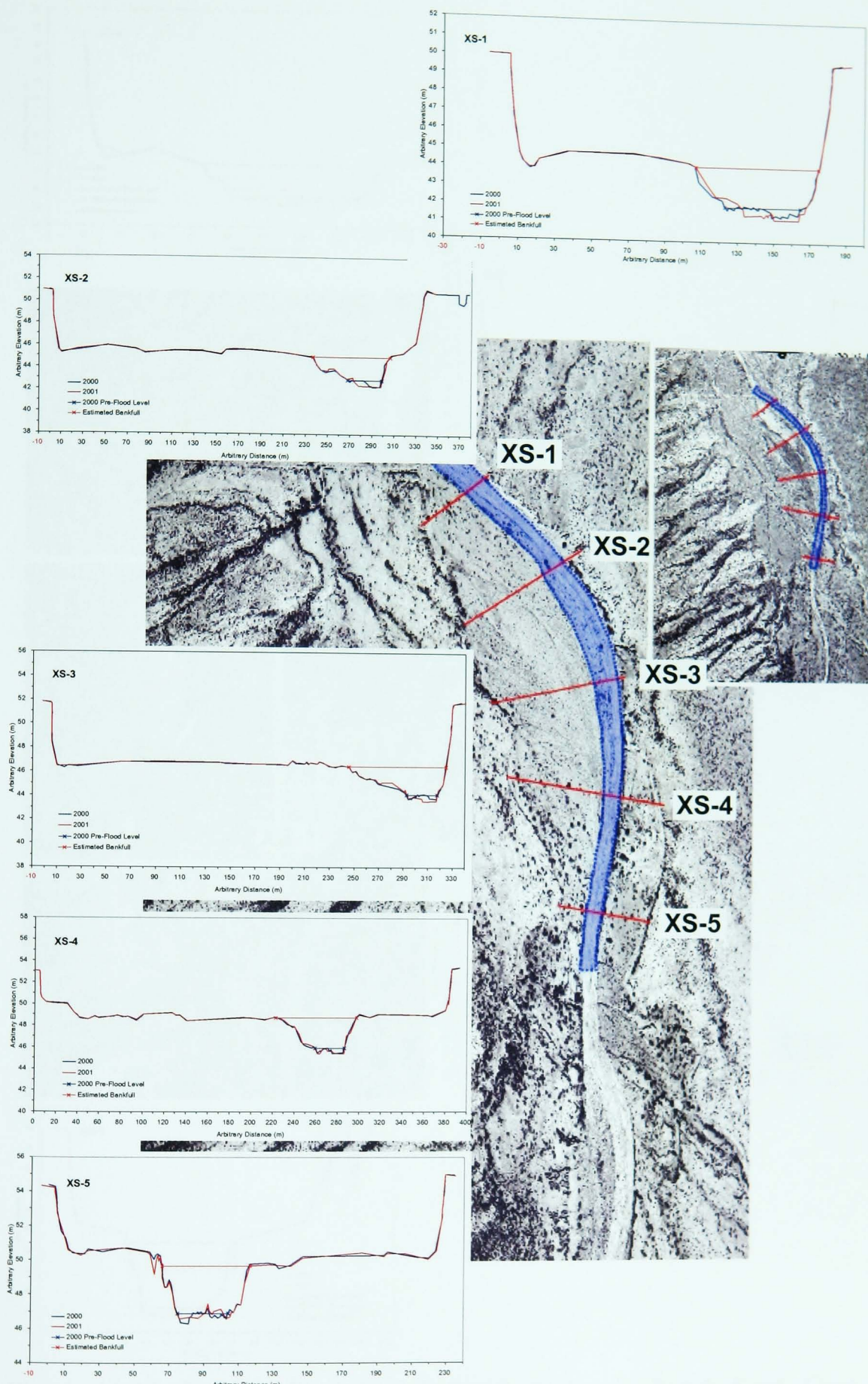


Figure A2.13 Big Bend Sub-Reach, Holocene Reach, Santa Cruz River. Aerial photograph shows 2001 morphology, inset shows pre-flood morphology.

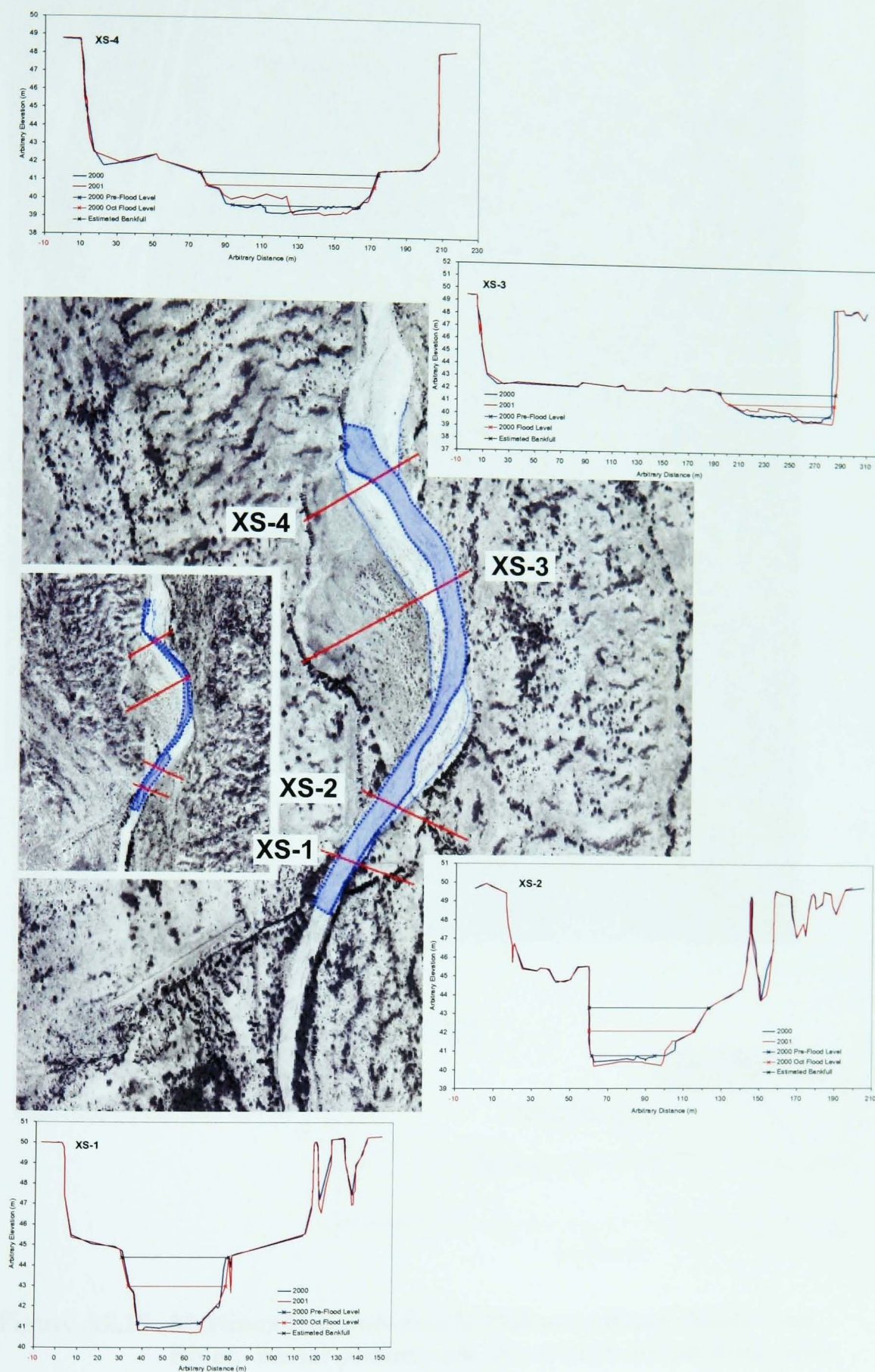


Figure A2.14 South of Straight Sub-Reach, Holocene Reach, Santa Cruz River. Aerial photograph shows 2001 morphology, inset shows pre-flood morphology.

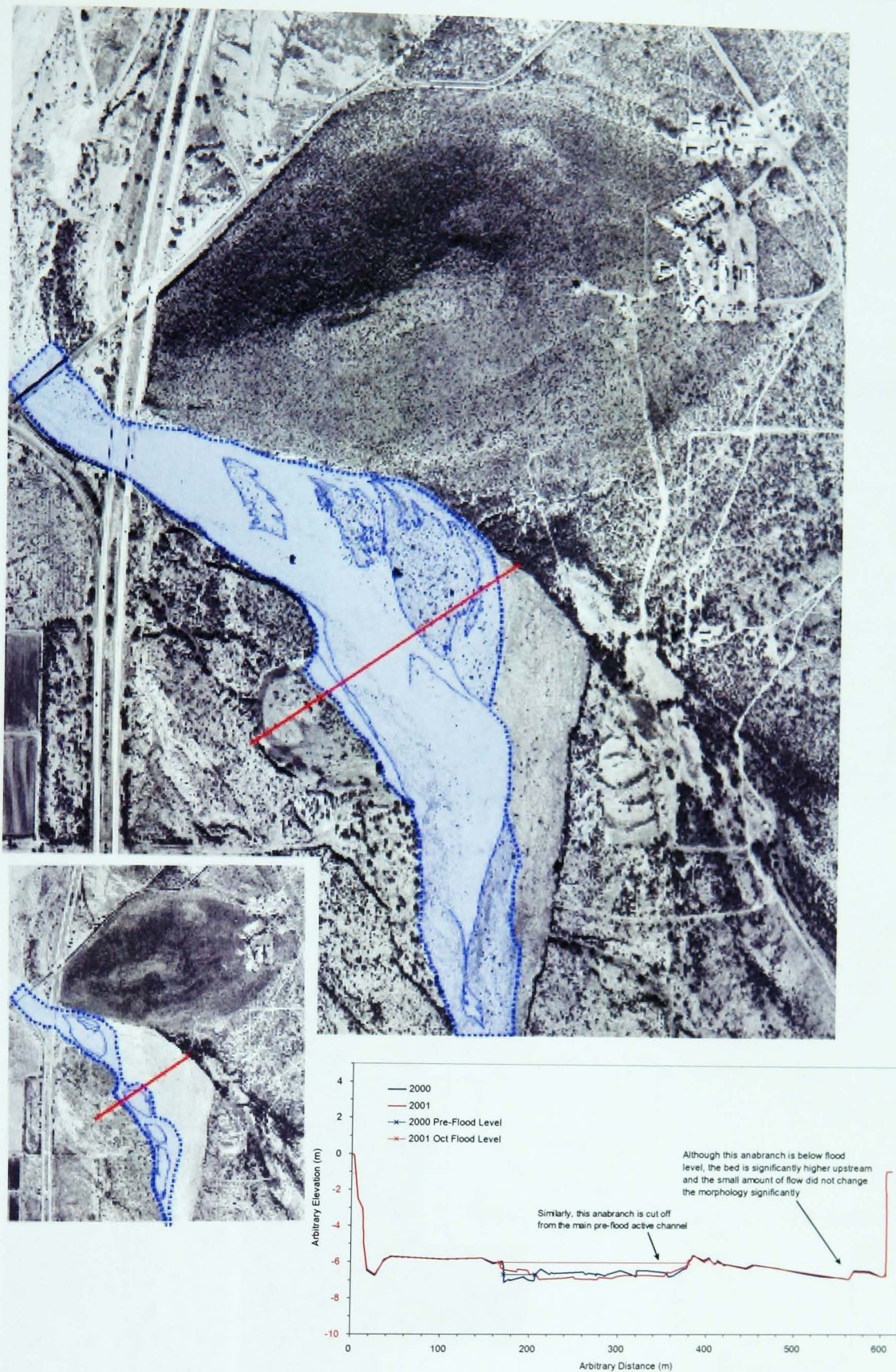


Figure A2.15 Martinez Hill Sub-Reach, Holocene Reach, Santa Cruz River. Aerial photograph shows 2001 morphology, inset shows pre-flood morphology.

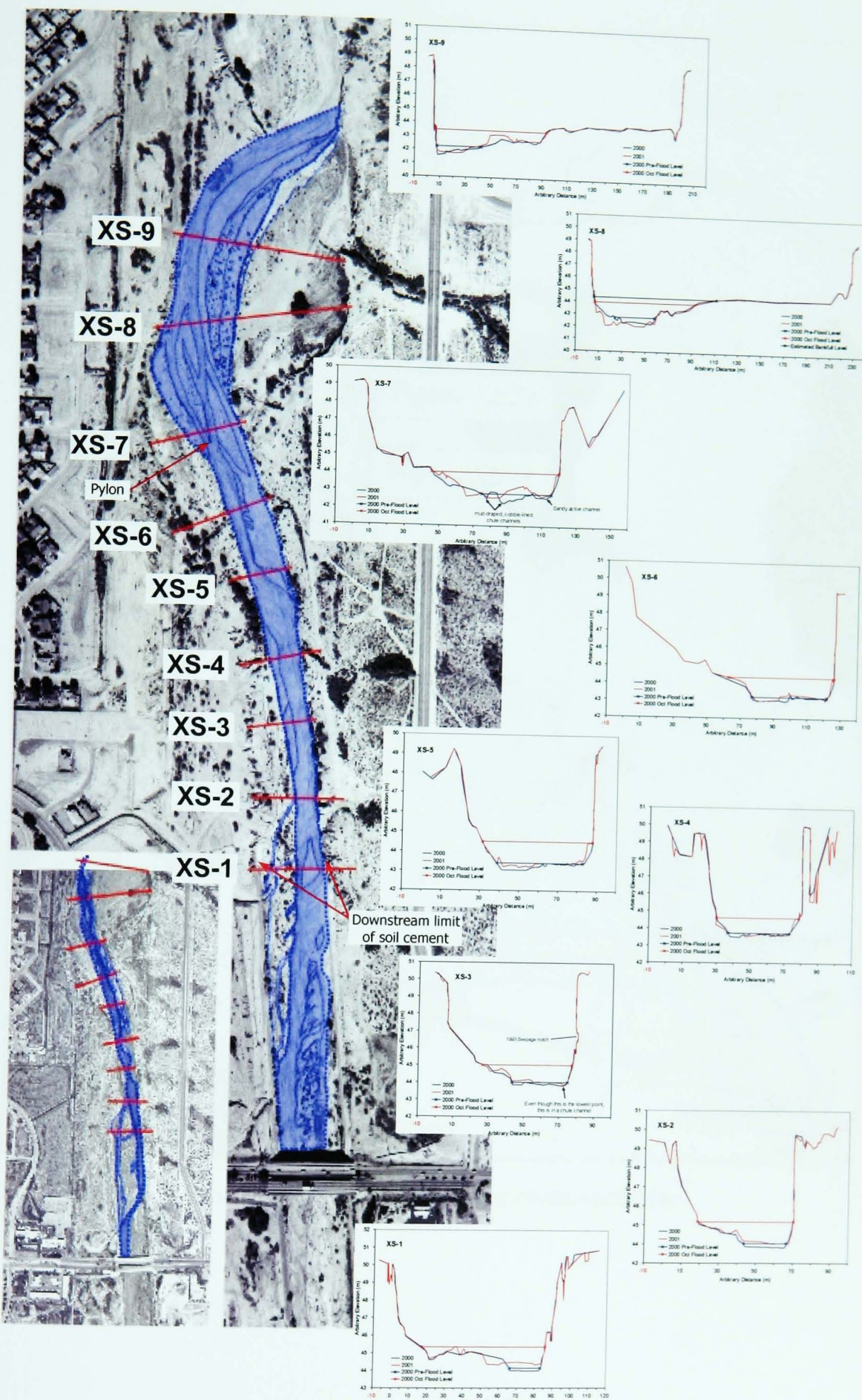


Figure A2.16 Valencia Road Sub-Reach, Holocene Reach, Santa Cruz River. Aerial photograph shows 2001 morphology, inset shows pre-flood morphology.

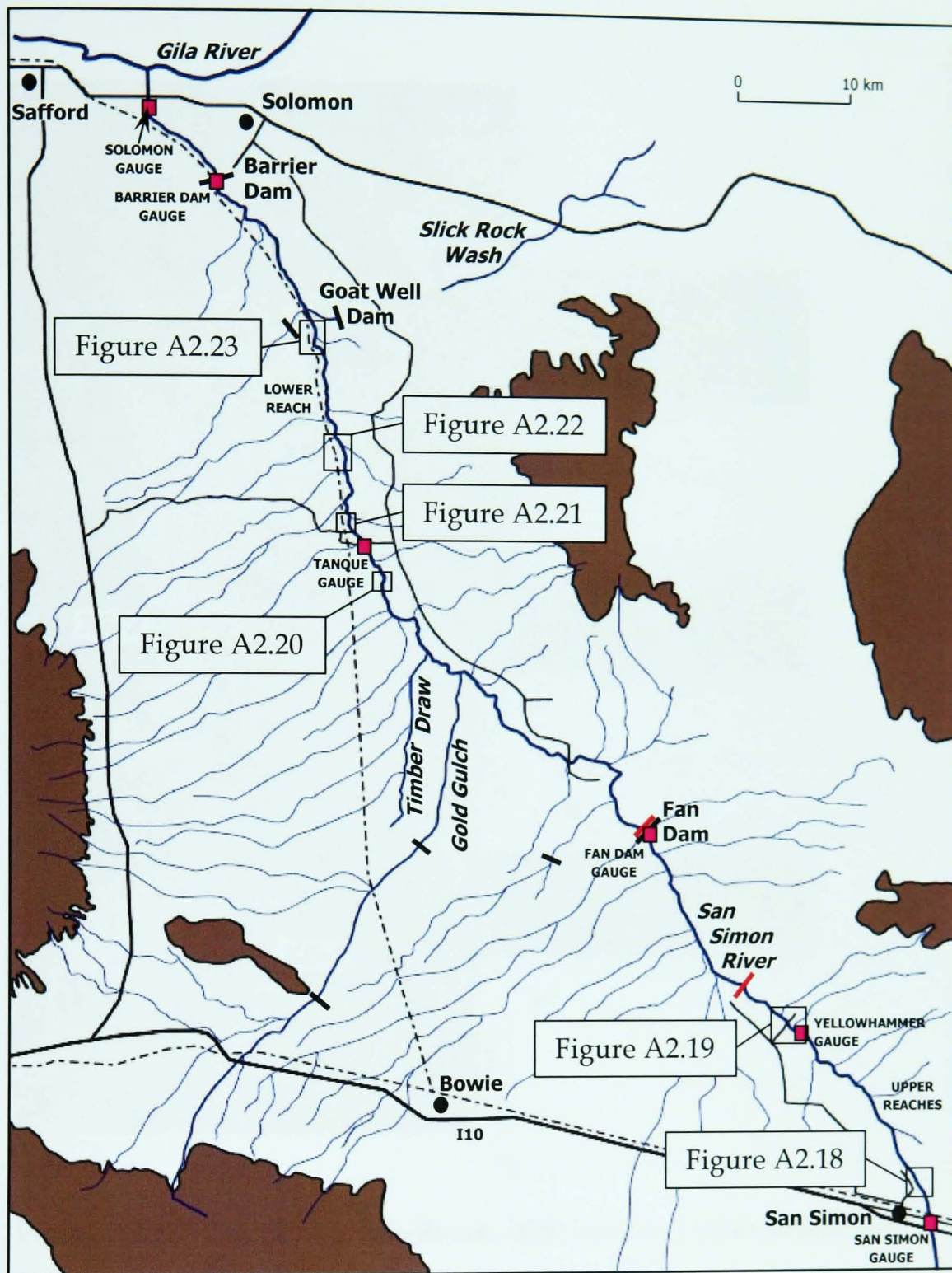


Figure A2.17 Location of San Simon River cross-sections.

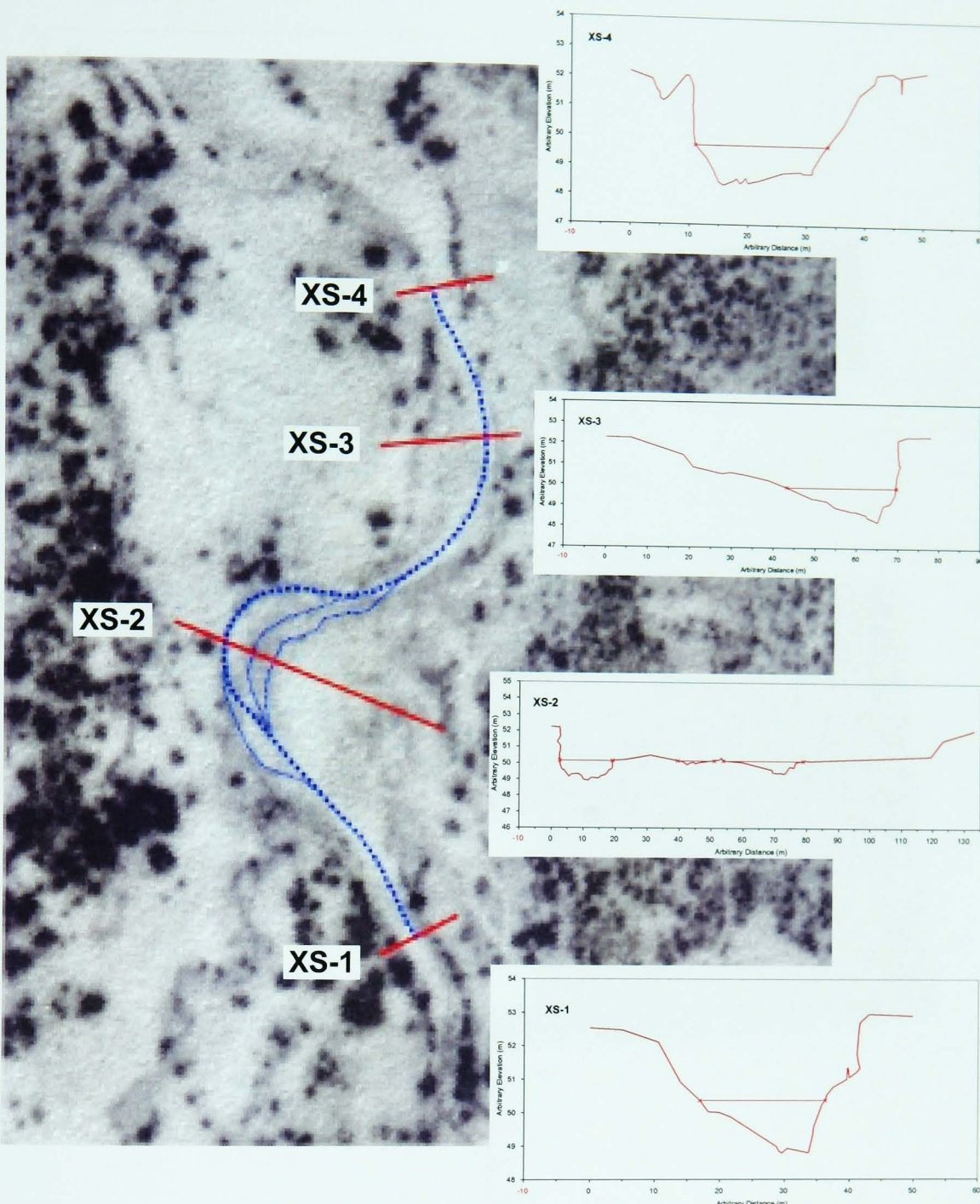


Figure A2.18 San Simon Sub-Reach, 2000 Survey, Upper Reach, San Simon River.

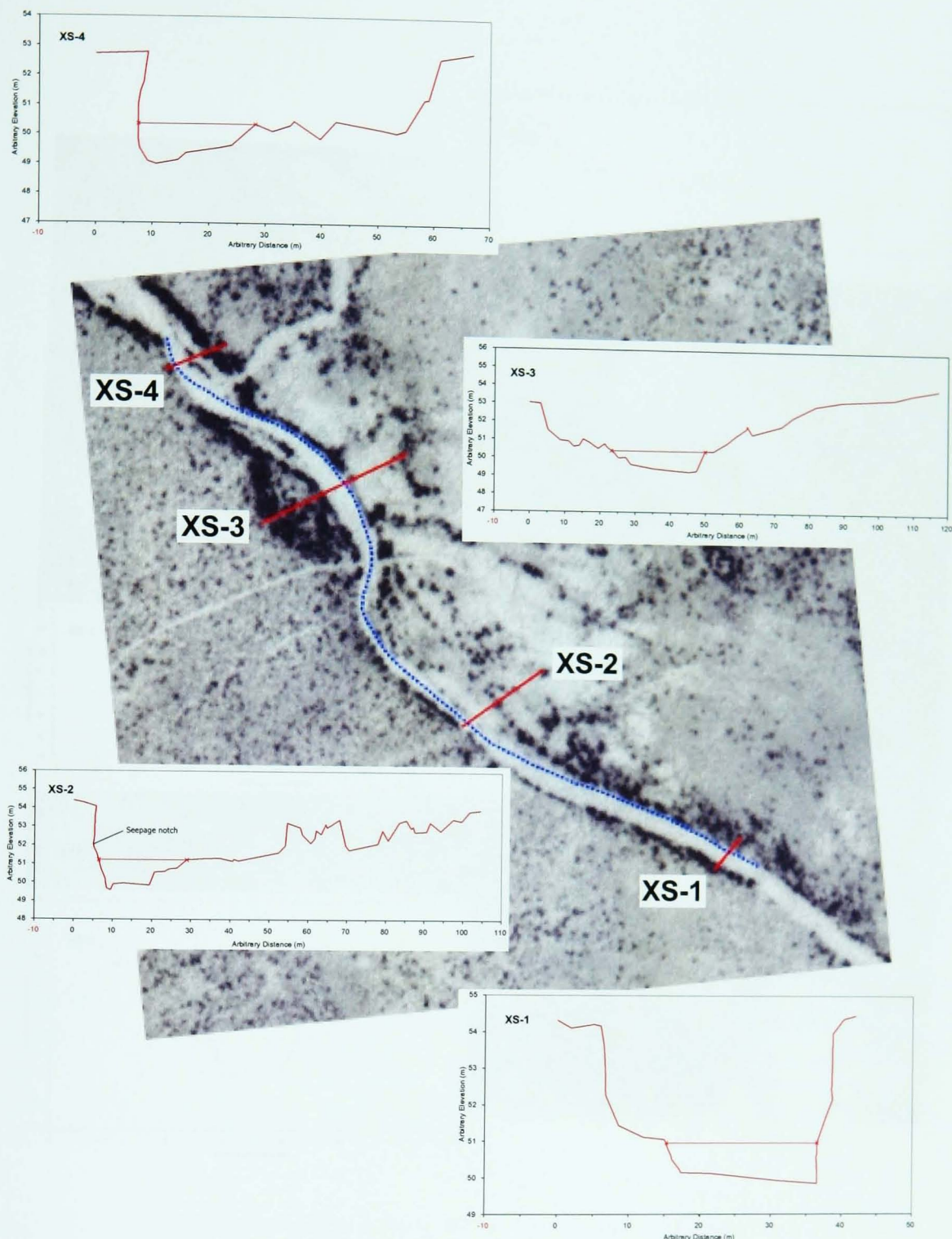


Figure A2.19 Yellowhammer Sub-Reach, XS-1 and 2, 2000 Survey; XS 3 and 4, 2001 Survey, Upper Reach, San Simon River.

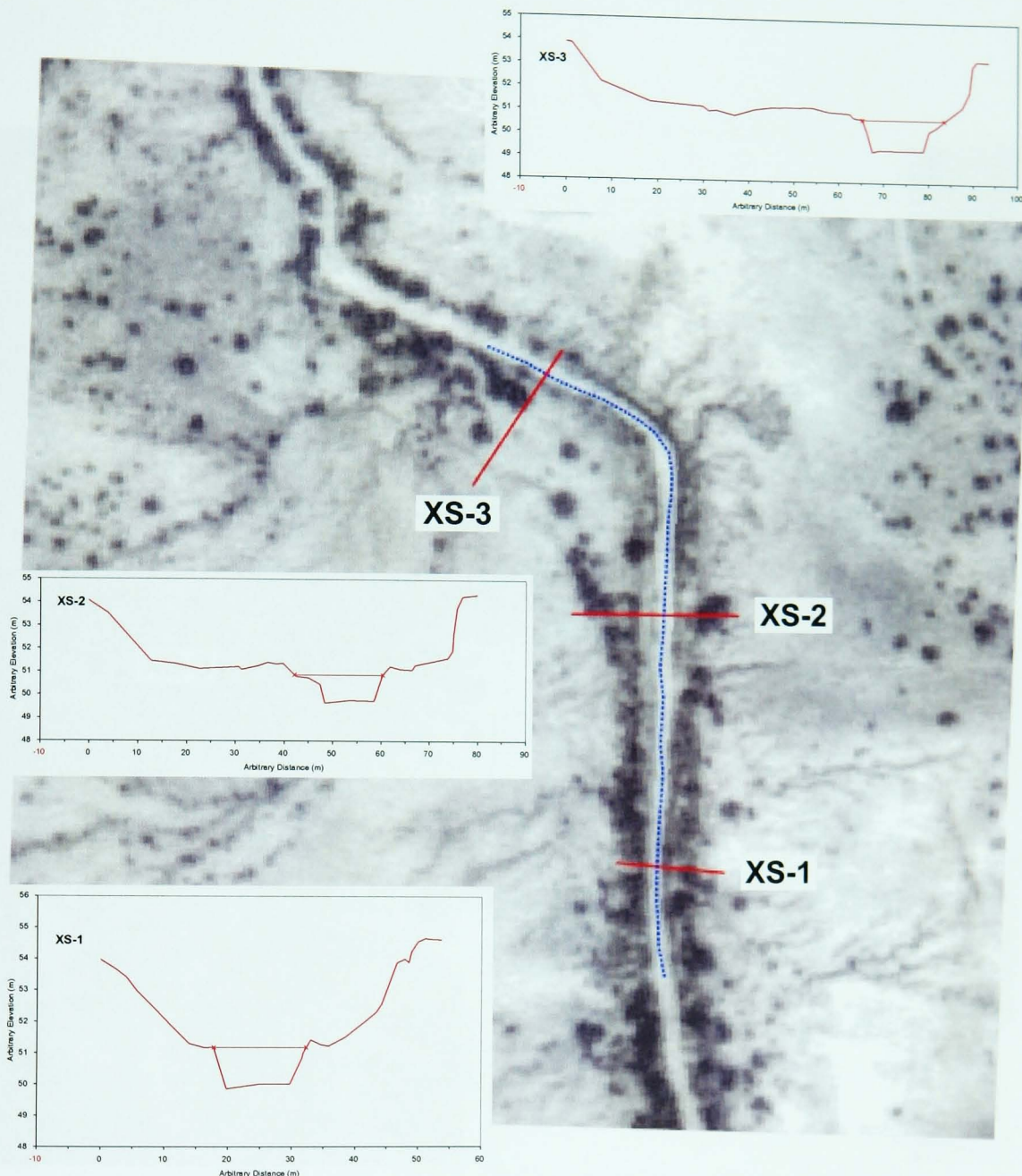


Figure A2.20 Bailey Well Sub-Reach, 2001 Survey, Lower Reach, San Simon River.

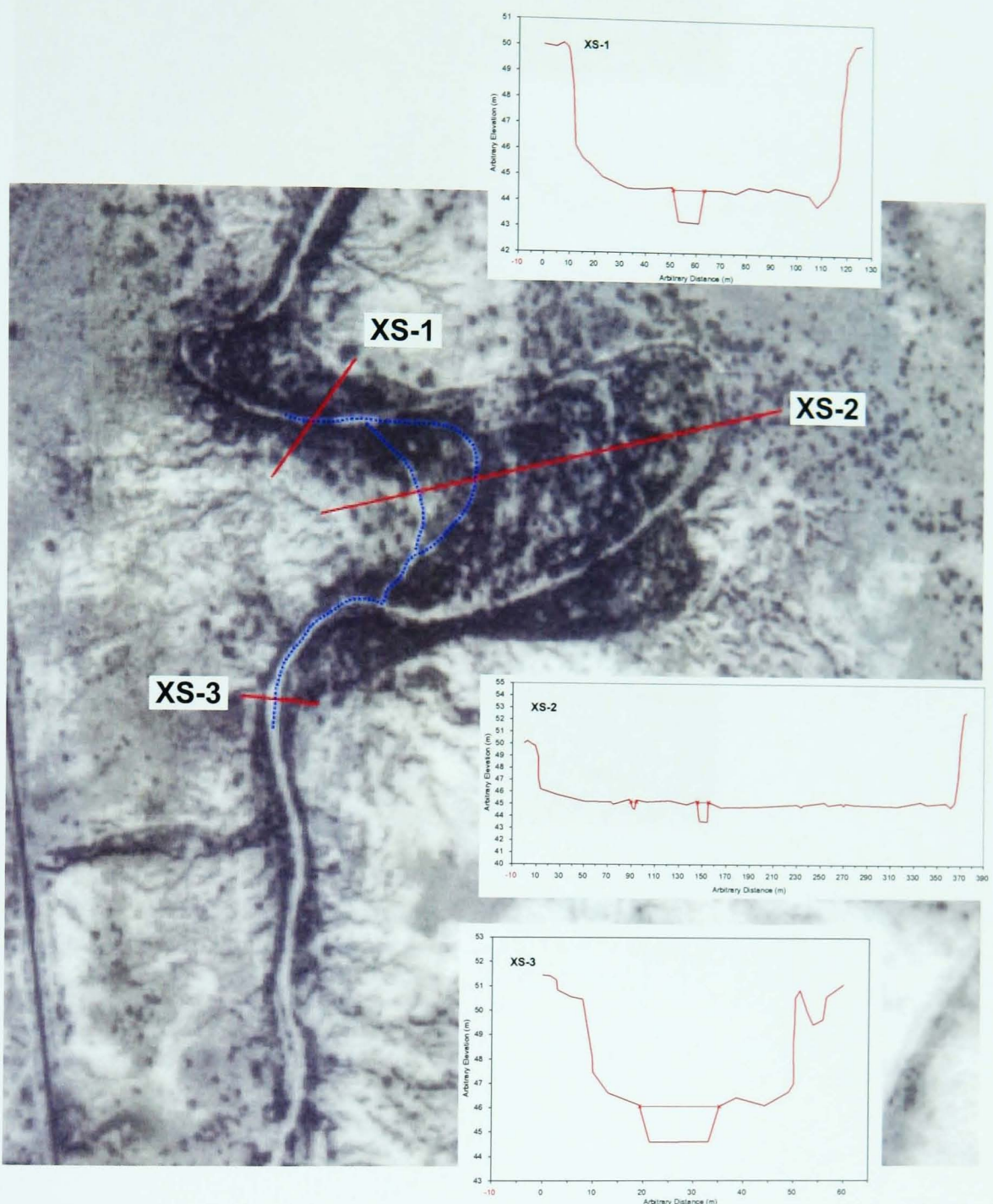


Figure A2.21 Tanque Sub-Reach, 2001 survey, Lower Reach, San Simon River.

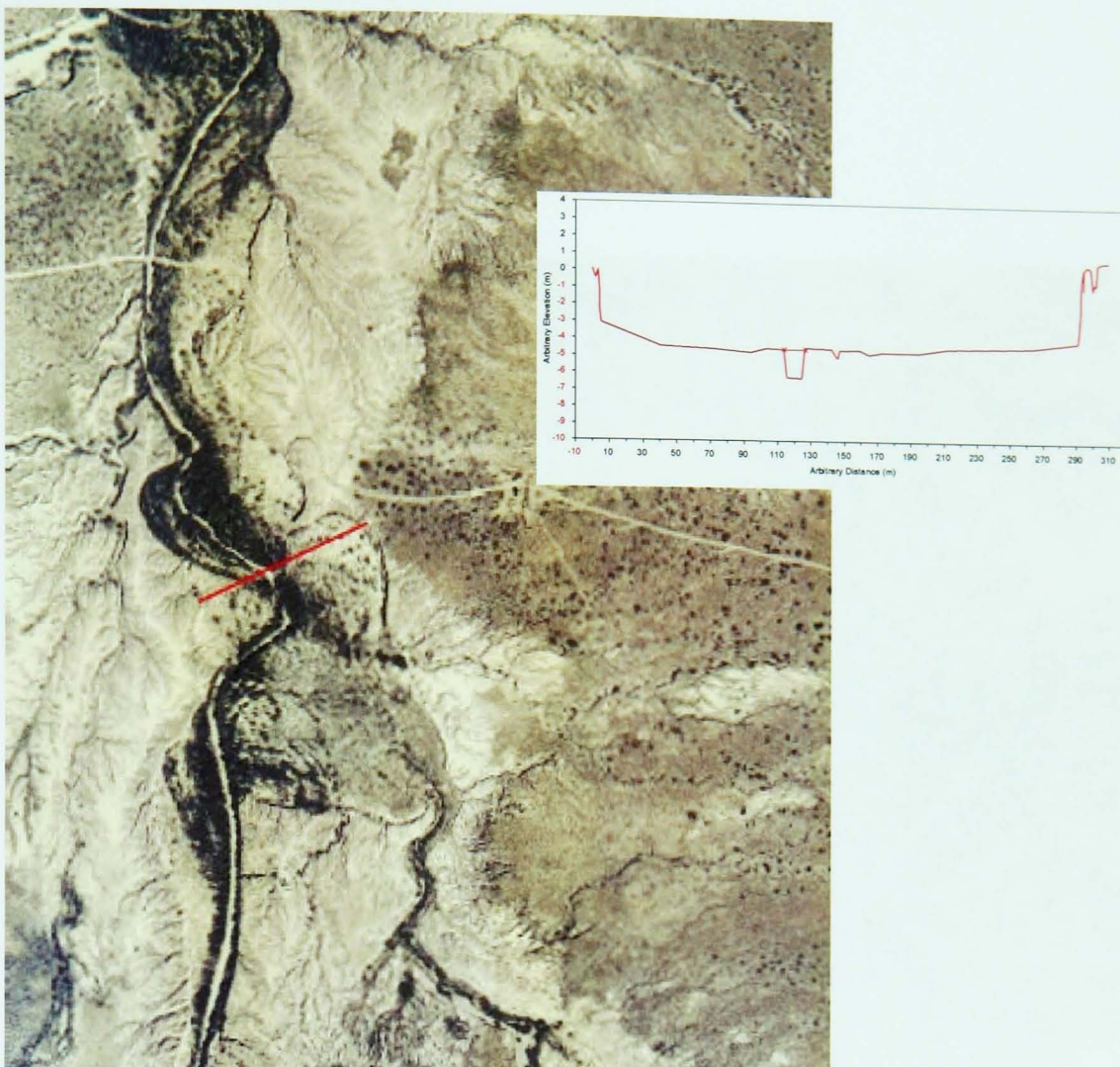


Figure A2.22 Corral Sub-Reach, Lower Reach, 2001 survey, San Simon River.

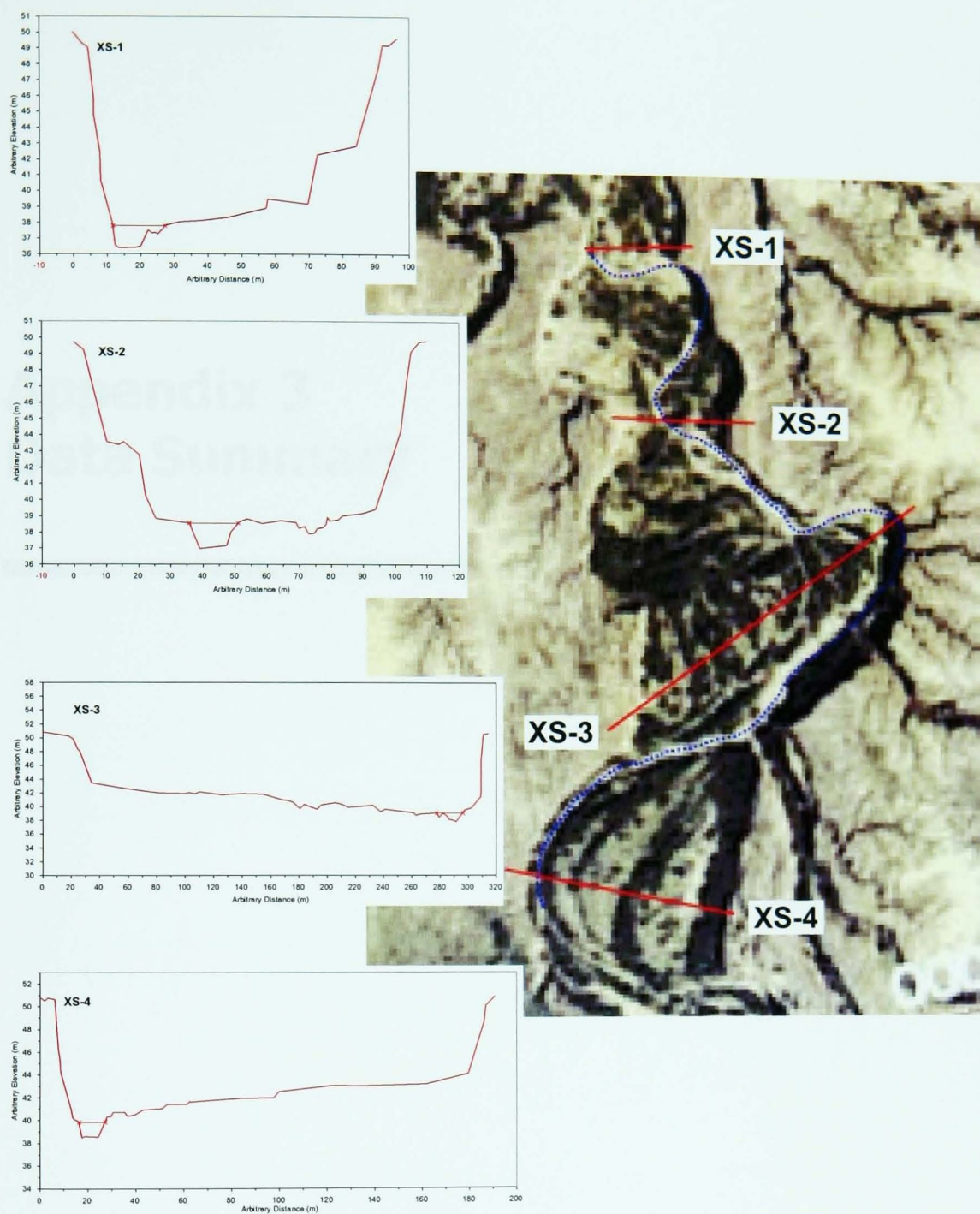


Figure A2.23 Goat Well Sub-Reach, 2001 survey, Lower Reach, San Simon River.

Appendix 3

Data Summary

Data Summary

$$* R = \text{Hydraulic Radius} = \frac{W \cdot D}{(2D + W)}$$

Table A3.1 1970s cross-section geometry, Rio Puerco.

River	Reach	XS	XS-Area (m ³)	Wetted Perimeter (m)	R*	Width (W) (m)	Mean Depth (D) (m)	W/D	Bankfull Depth (Dbf) (m)	W/Dbf	Bed Slope	Arroyo Width (m)	Arroyo Depth (m)	Arroyo W/D	Manning's "n"	Bankfull velocity (m ³ /s)	Bankfull Discharge (cumecs)
Rio Puerco 1970s	Last	1	7.3	23.1	0.3	22.7	0.3	70.3	0.6	40.6	0.0034				0.002	12.31	90.1
	Forbidden	2	9.8	23.9	0.4	23.6	0.4	56.6	1.7	13.7	0.0036				0.002	15.07	148.2
	Forbidden	3	12.9	22.5	0.6	22.3	0.6	38.6	0.8	26.7	0.0044				0.002	20.78	268.1
	reach	10.0	23.2	0.4	22.9	0.4	55.2	1.0	27.0	0.0038					0.002	16.04	160.7
Marion Butte E R P		4	35.2	61.8	0.6	61.1	0.6	105.9	0.7	85.2	0.0045	167.1	6.4	26.0	0.002	20.96	738.9
		5	68.2	95.6	0.7	95.2	0.7	132.8	1.6	61.3	0.0029	229.0	6.1	37.8	0.002	19.55	1333.8
		6	24.4	54.8	0.4	54.1	0.5	120.3	0.9	57.0	0.0034	189.0	7.0	26.9	0.002	15.44	376.0
		7	9.4	18.6	0.5	18.6	0.5	36.5	1.1	17.6	0.0028	249.5	7.4	33.8	0.002	15.29	144.3
	Horsefly	8	14.3	40.6	0.4	39.7	0.4	110.4	0.9	43.2	0.0056	188.2	7.8	24.0	0.002	16.94	241.6
		9	9.9	12.4	0.8	17.8	0.6	31.9	1.8	9.7	0.0024	156.5	8.4	18.6	0.002	19.18	190.0
		10	10.8	23.6	0.5	23.1	0.5	49.3	0.7	35.6	0.0033	135.2	8.4	16.1	0.002	15.53	168.2
	reach	24.6	43.9	0.5	44.2	0.5	83.9	1.1	44.2	0.0036	187.8	7.4	26.2	0.002	18.18	447.5	
	Guadalupe	13	39.1	74.5	0.5	74.1	0.5	140.4	2.0	37.2	0.0014	405.5	13.3	30.6	0.002	11.06	432.7
		14	30.3	112.9	0.3	112.6	0.3	418.8	0.7	156.1	0.0024	170.7	12.6	13.5	0.002	9.26	280.4
Canoncito Mesita Negra Isleta Bryan/Hadley Hidden Lady Hidden Lady Sand Butte Huning Bridge Angular Powerline County Line	reach	34.7	93.7	0.4	93.4	0.4	279.6	1.4	96.6	0.0019	288.1	12.9	22.1	0.002	10.69	371.0	
	15	39.4	27.3	1.4	26.6	1.5	18.0	2.1	12.9	0.0013					0.002	23.02	906.9
	Mesita Negra	16	40.9	26.1	1.6	25.2	1.6	15.5	2.2	11.6	0.0017				0.002	27.85	1139.3
	Isleta	17C	16.9	21.9	0.8	21.4	0.8	27.2	1.4	15.4	0.0012				0.002	14.57	245.8
	Bryan/Hadley	31	47.2	25.0	1.9	17.9	2.6	6.8	3.1	5.8	0.0015				0.002	29.56	1395.7
	Hidden Lady	18A	87.0	85.6	1.0	85.5	1.0	84.0	1.7	50.4	0.0022	560.9	13.4	41.8	0.002	23.70	2062.3
	Hidden Lady	18C													0.002		
	Sand Butte	19	34.7	25.8	1.3	24.5	1.4	17.2	2.9	8.4	0.0008	425.0	12.3	34.4	0.002	17.24	598.9
	Huning Bridge	20	27.0	20.2	1.3	19.3	1.4	13.8	1.9	10.0	0.0006	137.2	9.3	14.7	0.002	14.85	400.3
	Angular	23	31.2	26.5	1.2	25.6	1.2	21.0	1.7	14.8	0.0012				0.002	19.32	602.9
		24	14.0	17.1	0.8	16.6	0.8	19.8	1.6	10.7	0.0022	351.0	9.5	37.0	0.002	20.59	288.9
	Powerline	26	23.7	19.5	1.2	18.8	1.3	14.9	1.7	11.0	0.0018	375.5	13.1	28.6	0.002	24.16	572.5
	County Line	27	25.3	20.5	1.2	19.7	1.3	15.4	2.0	10.1	0.0012				0.002	19.97	506.2
		28A	14.1	20.0	0.7	19.0	0.7	25.7	1.5	12.9	0.0012				0.002	13.72	193.5
		28C	8.9	14.1	0.6	13.8	0.6	21.4	1.0	13.3	0.0030	448.1	10.4	43.0	0.002	20.09	178.5
		29	33.2	20.8	1.6	19.7	1.7	11.7	2.3	8.7	0.0012	372.2	11.9	31.3	0.002	23.68	786.2
	meander	20.9	20.0	1.0	19.3	1.1	19.6	1.6	12.1	0.0016	386.7	11.2	35.0	0.002	20.42	427.1	
	cross-over	37.8	24.9	1.5	22.7	1.7	14.2	2.4	9.7	0.0012	137.2	10.8	24.6	0.002	22.67	857.8	
	reach	31.7	26.4	1.2	25.3	1.3	22.3	1.9	14.0	0.0015	381.4	11.4	33.0	0.002	21.88	693.2	

Table A3.2
1990s cross-section geometry, Rio Puerco.

River	Reach	XS	XS-Area (m ³)	Wetted Perimeter (m)	R	Width (m)	Mean Depth (m)	W/D	Bankfull Depth (m)	W/D _{bf}	Bed Slope	Water Surface Slope	Arroyo Width (m)	Arroyo Depth (m)	Arroyo W/D	Manning's "n"	Bankfull velocity ₁ (m ² /s)	Bankfull Q ₁ * (cumecs)	Bankfull velocity ₂ (m ² /s)	Bankfull Q ₂ [†] (cumecs)
Rio Puerco 1990s	Last	1	6.6	9.9	0.7	8.9	0.7	11.9	1.5	5.8	0.0034	0.0030	206.2	9.9	20.9	0.022	1.91	12.6	2.03	13.5
	Forbidden	2	12.3	13.0	0.9	12.1	1.0	11.9	1.4	8.8	0.0036	0.0030	238.4	7.9	30.2	0.022	2.39	29.4	2.62	32.2
	Forbidden	3	12.4	10.2	1.2	8.2	1.5	5.4	2.0	4.1	0.0044	0.0035	173.6	8.6	20.2	0.022	3.06	38.0	3.43	42.7
	reach	10.4	11.0	0.9	9.7	1.1	9.7	1.6	6.2	0.0038	0.0032	206.1	8.8	23.8	0.022	2.46	25.7	2.69	28.1	
Marion Butte E R P	4	27.3	31.0	0.9	30.1	0.9	33.2	1.2	25.2	0.0045	0.0040	173.6	7.3	23.7	0.022	2.64	72.0	2.80	76.4	
	5	25.8	52.7	0.5	52.4	0.5	106.1	0.9	60.5	0.0029	0.0030	234.2	5.8	40.2	0.022	1.55	40.0	1.52	39.4	
	6	28.3	38.3	0.7	37.8	0.7	50.4	1.3	28.8	0.0034	0.0030	198.8	7.2	27.6	0.022	2.03	57.6	2.17	61.3	
	7	20.3	26.2	0.8	25.7	0.8	36.5	0.9	29.0	0.0028	0.0030	257.6	7.4	34.7	0.022	2.88	94.3	2.79	91.1	
	Horsefly	8	12.0	16.8	0.7	16.4	0.7	22.4	0.9	19.3	0.0056	0.0030	217.3	9.0	24.2	0.022	1.98	23.7	2.71	32.4
	9	12.0	17.0	0.7	16.6	0.7	22.9	0.9	19.5	0.0024	0.0030	298.9	9.1	32.9	0.022	1.98	23.8	1.77	21.3	
	10	51.4	74.3	0.7	73.5	0.7	105.1	0.9	81.2	0.0033	0.0030	126.4	8.2	15.4	0.022	1.95	100.1	2.04	105.0	
	reach	25.3	36.6	0.7	36.0	0.7	51.4	1.0	37.6	0.0036	0.0031	215.2	7.7	28.4	0.022	2.16	58.5	2.30	62.3	
	Guadalupe	13	46.3	52.9	0.9	52.0	0.9	58.5	1.1	47.2	0.0014	0.0033	411.0	12.3	33.4	0.022	2.39	110.6	1.56	72.1
	14	37.4	44.0	0.9	43.2	0.9	49.9	1.1	40.5	0.0024	0.0033	269.5	12.1	22.3	0.022	2.34	87.6	2.00	74.7	
Canoncito Mesita Negra Isleta 17C Bryan/Hadley Hidden Lady Hidden Lady Sand Butte Huning Bridge Angular 24 Powerline County Line 28A 28C 29 Bernardo cableway	reach	41.8	48.4	0.9	47.6	0.9	54.2	1.1	43.8	0.0019	0.0033	340.2	12.2	27.9	0.022	2.37	99.0	1.80	75.1	
	15	41.3	22.1	1.9	20.7	2.0	10.3	2.8	7.3	0.0013	0.0011	82.0	11.3	7.2	0.020	2.51	103.8	2.73	112.8	
	Mesita Negra	16	43.0	22.8	1.9	21.4	2.0	10.6	2.7	7.9	0.0017	0.0011	174.2	14.9	11.7	0.020	2.53	108.8	3.15	135.3
	Isleta	17A	8.9	12.4	0.7	11.6	0.8	15.2	1.4	8.3	0.0012	0.0021	209.7	11.6	18.0	0.020	1.83	16.3	1.38	12.3
	17C	14.3	14.2	1.0	14.3	1.1	13.5	1.4	10.0	0.0012	0.0021				0.020	2.30	32.9	1.74	24.9	
	Bryan/Hadley	31	36.7	20.4	1.8	18.8	2.0	9.6	3.0	6.3	0.0015	0.0013	106.7	13.2	8.1	0.020	2.67	98.0	2.87	105.3
	Hidden Lady	18A	26.6	21.1	1.3	18.8	1.4	13.3	2.9	6.4	0.0022	0.0013	557.3	11.2	49.7	0.020	2.10	56.0	2.74	72.9
	Hidden Lady	18C	23.3	14.4	1.6	12.6	1.8	6.8	2.8	4.5					0.020					
	Sand Butte	19	27.5	16.7	1.7	14.9	1.8	8.1	2.9	5.2	0.0008	0.0013				0.020	2.52	69.3	1.98	54.4
	Huning Bridge	20	19.6	17.3	1.1	16.0	1.2	13.0	2.7	6.0	0.0006	0.0010	143.1	9.1	15.7	0.020	1.72	33.9	1.34	26.2
	Angular	23	24.6	20.3	1.2	19.4	1.3	15.2	1.9	10.2	0.0012	0.0010	155.0	8.8	17.7	0.020	1.80	44.3	1.97	48.5
Bernardo cableway	24	15.1	14.1	1.1	13.3	1.1	11.7	1.5	9.0	0.0022	0.0018	349.5	8.9	39.4	0.020	2.22	33.4	2.45	37.0	
	Powerline	26	20.5	17.4	1.2	16.4	1.2	13.2	2.2	7.5	0.0018	0.0020	374.8	12.1	31.0	0.020	2.49	51.1	2.36	48.4
	County Line	27	18.3	15.2	1.2	14.1	1.3	10.9	2.5	5.7	0.0012	0.0010				0.020	1.79	32.9	1.97	36.0
	28A	15.5	13.4	1.2	12.4	1.3	9.9	1.9	6.7	0.0012	0.0010				0.020	1.75	27.1	1.91	29.6	
	28C	7.0	9.1	0.8	8.5	0.8	10.4	1.4	6.3	0.0030	0.0025	457.4	9.8	46.8	0.020	2.10	14.7	2.30	16.1	
	29	20.9	19.0	1.1	14.6	1.4	10.1	2.1	6.8	0.0012	0.0010	379.7	10.7	35.5	0.020	1.69	35.4	1.85	38.8	
	meander	19.3	16.4	1.2	14.8	1.3	11.8	2.1	7.2	0.0015	0.0014	337.7	10.5	31.9	0.020	2.87	116.6	2.87	116.6	
	cross-over	34.8	19.7	1.7	18.0	1.9	9.7	2.9	6.3	0.0012	0.0012	126.5	12.1	10.7	0.020	2.47	85.9	2.49	86.7	
Bernardo cableway	reach	22.7	16.9	1.3	15.5	1.4	11.4	2.3	7.1	0.0015	0.0014	271.8	11.1	25.5	0.020	2.25	51.1	2.28	51.9	

* Calculated using water surface slope

† Calculated using bed slope

Table A3.3 Difference between 1970s and 1990s geometry, Rio Puerco.

River	Reach	XS	XS-Area (m ³)	Wetted Perimeter (m)	R	Width (m)	Mean Depth (m)	W/D	Bankfull Depth (m)	W/Dbf	Arroyo Width (m)	Arroyo Depth (m)	Arroyo W/D
Rio Puerco	Last	1	-0.7	-13.2	0.4	-13.8	0.4	-58.4	1.0	-34.7			
	Forbidden	2	2.4	-10.9	0.5	-11.5	0.6	-44.7	-0.4	-4.9			
	Forbidden	3	-0.5	-12.3	0.6	-14.1	0.9	-33.2	1.2	-22.6			
	reach		0.4	-12.2	0.5	-13.1	0.7	-45.4	0.6	-20.7			
	Marion Butte	4	-8.0	-30.8	0.3	-31.0	0.3	-72.7	0.5	-60.0	6.5	0.9	-2.3
	E R P	5	-42.4	-43.0	-0.2	-42.8	-0.2	-26.7	-0.7	-0.8	5.2	-0.2	2.4
		6	3.9	-16.5	0.3	-16.4	0.3	-69.9	0.4	-28.2	9.8	0.2	0.7
	Horsefly	7	10.9	7.6	0.3	7.1	0.3	-4.2	-0.2	11.4	8.1	0.0	0.9
		8	-2.3	-23.7	0.4	-23.3	0.4	-87.9	-0.1	-23.9	29.0	1.2	0.1
		9	2.1	4.6	-0.1	-1.2	0.2	-9.0	-1.0	9.8	142.3	0.7	14.3
		10	40.6	50.7	0.2	50.4	0.2	55.8	0.3	45.6	-8.8	-0.2	-0.7
	reach		0.7	-7.3	0.2	-8.2	0.2	-30.7	-0.1	-6.6	27.5	0.4	2.2
	Guadalupe	13	7.2	-21.6	0.4	-22.1	0.4	-81.9	-0.9	10.0	5.5	-1.0	2.9
		14	7.1	-69.0	0.6	-69.4	0.6	-368.9	0.3	-115.6	98.8	-0.5	8.8
	reach		7.1	-45.3	0.5	-45.7	0.5	-225.4	-0.3	-52.8	52.1	-0.8	5.8
	Canoncito	15	1.9	-5.2	0.4	-5.9	0.5	-7.6	0.8	-5.6			
	Mesita Negra	16	2.1	-3.3	0.3	-3.8	0.4	-4.9	0.5	-3.7			
	Isleta	17C	-8.0	-9.4	-0.1	-9.8	-0.0	-11.9	-0.0	-7.0			
	Bryan/Hadley	31	-10.5	-4.6	-0.1	0.9	-0.7	2.8	-0.1	0.5			
	Hidden Lady	18A	-60.4	-64.5	0.2	-66.7	0.4	-70.8	1.2	-44.0	-3.6	-2.2	7.9
	Sand Butte	19	-7.2	-9.1	0.3	-9.5	0.4	-9.1	-0.0	-3.3			
	Huning Bridge	20	-7.3	-2.9	-0.2	-3.3	-0.2	-0.8	0.7	-4.0	5.9	-0.2	1.0
	Angular	23	-6.6	-6.2	0.0	-6.2	0.1	-5.7	0.2	-4.7			
		25	1.0	-3.0	0.2	-3.4	0.3	-8.1	-0.1	-1.7	-1.5	-0.6	2.4
	Powerline	26	-3.2	-2.1	-0.0	-2.4	-0.0	-1.8	0.5	-3.5	-0.7	-1.0	2.4
	County Line	27	-7.0	-5.3	-0.0	-5.6	0.0	-4.4	0.5	-4.4			
		28A	1.4	-6.6	0.5	-6.6	0.5	-15.8	0.4	-6.2			
		28C	-1.9	-5.0	0.1	-5.3	0.2	-11.0	0.3	-6.9			
		29	-12.3	-1.8	-0.5	-5.1	-0.2	-1.6	-0.1	-1.9	7.5	-1.2	4.3
	meander		-1.6	-3.7	0.1	-4.5	0.2	-7.8	0.5	-4.9	-49.0	-0.7	-3.1
	cross-over		-3.1	-5.2	0.2	-4.6	0.2	-4.5	0.5	-3.5	-10.7	1.3	-13.9
	reach		-9.0	-9.6	0.1	-9.8	0.1	-10.9	0.3	-6.9	-109.6	-0.4	-7.4

Table A3.4 Geometry of Pleistocene Reaches, Santa Cruz River.

River	Reach	XS	XS-Area (m ³)	Wetted Perimeter (m)	R	Width (m)	Mean Depth (m)	W/D	Bankfull Depth (m)	W/Dbf	Bed Slope	Water Surface Slope	Arroyo Width (m)	Arroyo Depth (m)	Arroyo W/D	Manning's "n"	Bankfull velocity ₁ (m ² /s)	Bankfull Q ₁ (cumecs)	Bankfull velocity ₂ (m ² /s)	Bankfull Q ₂ (cumecs)
Santa Cruz Pleistocene	South Pima Mine Road 2000	1	0.9	6.4	0.1	6.2	0.1	42.2	0.2	27.3	0.0040	0.0021	84.4	7.6	11.2	0.032	0.39	0.4	0.54	0.5
		2	2.9	9.9	0.3	9.8	0.3	32.5	0.4	22.7	0.0041	0.0014	47.7	7.2	6.6	0.028	0.59	1.7	1.02	3.0
		3	5.5	8.7	0.6	7.7	0.7	10.8	0.8	9.5	0.0039	0.0043	30.3	7.8	3.9	0.028	1.72	9.4	1.64	9.0
		4	2.3	8.7	0.3	8.4	0.3	30.7	0.3	27.3	0.0036	0.0079	26.0	7.8	3.3	0.028	1.31	3.0	0.89	2.1
		reach	2.9	8.4	0.3	8.0	0.4	29.1	0.4	21.7	0.0039	0.0049	28.1	7.8	3.6	0.029	1.17	3.4	1.04	3.0
	Oct 2000 Flood Level	1	58.4	42.9	1.4	40.2	1.5	27.7	2.4	16.5	0.0061	0.0052	85.0	6.9	12.3	0.032	2.76	161.4	3.00	175.0
		2	50.4	33.9	1.5	32.9	1.5	21.5	2.5	12.9	0.0052	0.0034	47.8	6.8	7.0	0.028	2.69	135.9	3.37	169.9
		3	41.1	22.2	1.9	22.5	1.8	12.3	2.8	7.9	0.0043	0.0028	31.8	7.4	4.3	0.028	2.84	116.7	3.55	146.2
		4	36.0	19.9	1.8	18.0	2.0	9.0	2.9	6.3	0.0043	0.0040	27.1	7.5	3.6	0.028	3.37	121.5	3.49	125.6
		reach	46.5	29.7	1.6	28.4	1.7	17.6	2.7	10.9	0.0037	0.0036	29.4	7.5	3.9	0.029	2.87	133.5	2.90	134.7
North Pima Mine Road	2000	5	5.3	18.8	0.3	18.7	0.3	65.7	0.4	46.4	0.0041	0.0032	26.6	8.7	3.0	0.028	0.88	4.7	0.99	5.3
		4	6.0	15.9	0.4	15.8	0.4	41.6	0.5	30.9	0.0037	0.0037	33.3	8.7	3.8	0.028	1.13	6.8	1.13	6.8
		3	2.6	15.6	0.2	15.4	0.2	89.7	0.2	69.8	0.0029	0.0037	32.1	8.7	3.7	0.028	0.66	1.8	0.59	1.6
		2	1.4	26.6	0.1	21.1	0.1	318.4	0.1	158.8	0.0031	0.0027	30.6	8.7	3.5	0.028	0.26	0.4	0.28	0.4
		1	4.2	16.6	0.3	16.5	0.3	65.2	0.4	44.9	0.0037	0.0022	36.8	8.7	4.2	0.028	0.66	2.7	0.86	3.6
	Oct 2000 Flood Level	reach	3.9	18.7	0.2	17.5	0.2	157.8	0.3	91.1	0.0033	0.0034	31.9	8.7	3.7	0.028	0.77	3.0	0.77	3.0
		5	40.5	27.5	1.5	26.4	1.5	17.2	1.9	13.9	0.0044	0.0030	28.8	8.1	3.5	0.028	2.52	102.2	3.06	123.8
		4	36.5	21.8	1.7	18.4	2.0	9.3	2.1	8.9	0.0040	0.0036	33.3	8.2	4.1	0.028	3.03	110.3	3.17	115.8
		3	29.2	22.5	1.3	18.7	1.6	11.9	1.9	10.1	0.0028	0.0038	32.4	8.2	3.9	0.028	2.61	76.4	2.24	65.6
		2	44.1	31.8	1.4	29.7	1.5	20.0	1.7	17.9	0.0027	0.0025	30.6	8.2	3.8	0.028	2.24	98.8	2.32	102.2
		1	61.9	38.4	1.6	36.2	1.7	21.2	1.9	18.9	0.0035	0.0018	39.3	8.2	4.8	0.028	2.08	129.0	2.89	179.0
		reach	42.4	28.4	1.5	25.9	1.7	12.8	1.9	11.0	0.0034	0.0034	32.9	8.2	4.0	0.028	2.70	114.5	2.71	115.1

Table A3.5
Geometry of Holocene Reaches of Santa Cruz River, 2000 and 2001.

River	Reach	XS	XS-Area (m ³)	Wetted Perimeter (m)	R	Width (m)	Mean Depth (m)	W/D	Bankfull Depth (m)	W/Dbf	Bed Slope	Water Surface Slope	Arroyo Width (m)	Arroyo Depth (m)	Arroyo W/D	Manning's "n"	Bankfull velocity, (m ² /s)	Bankfull Q ₁ (cumecs)	Bankfull velocity ₂ , (m ² /s)	Bankfull Q ₂ (cumecs)	
Santa Cruz Holocene	Big Bend	5	5.4	22.7	0.2	29.3	0.2	157.7	0.6	48.0	0.0018	0.0020	225.2	8.4	26.9	0.032	0.54	3.0	0.51	2.8	
		2000	4	8.0	27.6	0.3	27.3	0.3	93.4	0.5	55.3	0.0039	0.0042	381.1	7.7	49.4	0.032	0.89	7.1	0.85	6.8
		3	4.5	19.6	0.2	25.0	0.2	140.5	0.4	65.5	0.0053	0.0051	324.0	8.0	40.6	0.030	0.89	4.0	0.90	4.0	
		2	7.6	19.9	0.4	30.7	0.2	124.5	0.6	49.8	0.0033	0.0037	333.9	8.6	39.0	0.030	1.06	8.0	1.00	7.6	
		1	7.3	34.9	0.2	41.6	0.2	238.5	0.2	264.9	0.0020	0.0036	176.3	8.1	21.8	0.030	0.70	5.1	0.52	3.8	
	Bankfull	reach	6.5	24.9	0.3	30.8	0.2	149.2	0.5	108.9	0.0034	0.0037	288.1	8.1	35.5	0.031	0.82	5.4	0.78	5.1	
		5	120.9	52.7	2.3	50.8	2.4	21.3	3.1	16.5	0.0025	0.0020	225.5	8.1	27.9	0.032	2.40	290.2	2.71	327.6	
		4	147.7	76.3	1.9	75.1	2.0	38.2	3.3	22.5	0.0045	0.0051	381.3	7.8	49.1	0.032	3.46	510.8	3.27	483.4	
		3	133.4	80.2	1.7	79.2	1.7	47.0	2.9	27.4	0.0052	0.0064	324.0	8.2	39.6	0.030	3.73	497.6	3.37	449.8	
		2	121.1	70.6	1.7	69.8	1.7	40.2	2.7	26.2	0.0038	0.0039	334.5	8.6	39.1	0.030	2.98	360.9	2.95	357.0	
		1	137.2	68.6	2.0	67.7	2.0	33.4	2.8	24.0	0.0039	0.0033	176.9	8.6	20.6	0.030	3.04	416.8	3.29	451.0	
		reach	132.0	69.7	2.0	68.5	2.0	35.5	3.0	22.1	0.0039	0.0041	288.4	8.2	35.3	0.031	3.22	425.1	3.14	415.0	
South of Straight	2000	1	4.0	28.5	0.1	28.2	0.1	200.3	0.3	82.6	0.0031	0.0032	115.0	9.3	12.4	0.012	1.27	5.0	1.25	5.0	
		2	6.7	33.4	0.2	33.2	0.4	91.0	0.3	101.6	0.0027	0.0026	139.0	9.4	14.9	0.022	0.79	5.3	0.81	5.5	
		3	12.1	56.0	0.2	61.3	0.2	341.9	0.5	130.1	0.0022	0.0021	279.3	9.8	28.6	0.038	0.44	5.3	0.45	5.6	
		4	11.0	60.2	0.2	69.8	0.2	443.5	0.4	162.3	0.0022	0.0024	197.7	9.2	21.4	0.035	0.45	5.0	0.43	4.7	
		reach	8.4	44.5	0.2	48.1	0.2	269.1	0.4	119.2	0.0024	0.0023	182.8	9.4	19.3	0.027	0.58	4.9	0.60	5.1	
	Oct 2000 Flood Level	1	78.8	45.9	1.7	44.9	1.8	25.5	2.3	19.7	0.0039	0.0067	115.0	9.4	12.2	0.030	3.90	307.6	2.99	236.1	
		2	75.9	56.8	1.3	55.5	1.4	40.6	1.9	29.0	0.0029	0.0049	139.3	9.6	14.5	0.021	4.06	308.1	3.14	237.9	
		3	63.9	83.7	0.8	82.9	0.8	107.6	1.5	56.1	0.0018	0.0022	281.8	9.9	28.4	0.008	4.87	311.2	4.49	287.1	
		4	87.4	93.0	0.9	92.6	0.9	98.1	1.6	58.3	0.0017	0.0011	198.2	9.3	21.3	0.009	3.59	313.5	4.44	388.2	
		reach	76.5	69.8	1.2	69.0	1.2	68.0	1.8	40.8	0.0023	0.0033	183.6	9.6	19.2	0.017	3.81	291.6	3.16	242.1	
Martinez Hill	2000	1	145.1	51.2	2.8	49.2	2.9	16.7	3.7	13.3	0.0039	0.0080				0.030	5.96	864.7	4.18	606.9	
		2	148.8	66.0	2.3	63.3	2.4	26.9	3.1	20.1	0.0029	0.0061				0.021	6.37	948.5	4.44	661.1	
	2001	3	144.0	92.7	1.6	91.5	1.6	58.1	2.4	38.3	0.0018	0.0032				0.008	9.54	1374.9	7.21	1039.0	
		4	153.1	99.2	1.5	98.7	1.6	63.6	2.3	43.4	0.0017	0.0023				0.009	7.17	1097.2	6.18	946.2	
		reach	147.8	77.3	2.0	75.7	2.1	41.3	2.9	28.8	0.0023	0.0044				0.017	6.30	931.0	4.54	671.5	
		9.0	36.0	0.3	35.4	0.3	139.0	0.4	82.6			603.3	7.1	84.7							
		149.0	213.1	0.7	213.0	0.7	304.5	0.9	227.8			603.3	6.9	86.9							
Valencia	2000	1	2.6	17.4	0.1	17.3	0.1	116.8	0.2	108.3	0.0013	0.0008	90.2	6.9	13.1	0.026	0.29	0.8	0.39	1.0	
		2	4.3	23.3	0.2	23.2	0.2	124.5	0.2	104.2	0.0007	0.0005	64.2	6.0	10.7	0.030	0.24	1.0	0.29	1.3	
		3	3.7	31.6	0.1	31.6	0.1	270.9	0.2	147.5	0.0019	0.0018	73.5	6.7	10.9	0.032	0.31	1.2	0.33	1.2	
		4	2.7	24.3	0.1	36.5	0.1	498.5	0.2	148.5	0.0039	0.0032	58.6	6.4	9.1	0.035	0.37	1.0	0.41	1.1	
		5	7.9	43.4	0.2	43.3	0.2	238.7	0.4	119.7	0.0041	0.0031	69.0	6.4	10.7	0.038	0.47	3.7	0.54	4.3	
		6	5.5	38.6	0.1	6.6	0.8	8.0	0.3	24.9	0.0009	0.0020	122.8	6.4	19.2	0.030	0.41	2.2	0.28	1.5	
		7	7.5	34.0	0.2	33.8	0.2	153.1	0.5	62.7	0.0051	0.0030	113.1	6.9	16.5	0.035	0.57	4.3	0.74	5.5	
		8	12.2	34.7	0.4	34.3	0.4	96.6	0.5	63.1	0.0007	0.0007	226.1	6.9	33.0	0.028	0.47	5.7	0.48	5.8	
		9	11.2	35.1	0.3	34.7	0.3	107.3	0.7	52.4	0.0053	0.0043	196.1	7.1	27.7	0.035	0.88	9.8	0.97	10.9	
		reach	6.4	31.4	0.2	29.1	0.3	179.4	0.4	92.4	0.0027	0.0022	112.6	6.6	16.8	0.032	0.49	3.1	0.55	3.5	
2001	2001	1	41.5	51.5	0.8	67.6	0.6	110.0	1.0	66.6	0.0026	0.0014	90.3	6.5	13.8	0.008	4.04	167.6	5.47	227.0	
		2	38.3	52.2	0.7	51.7	0.7	69.9	1.1	45.2	0.0021	0.0015	64.7	5.8	11.2	0.008	3.95	151.5	4.70	179.9	
		3	37.5	51.5	0.7	51.1	0.7	69.7	1.2	44.4	0.0028	0.0033	73.7	6.7	11.0	0.008	5.77	216.1	5.38	201.5	
		4	40.9	49.9	0.8	48.8	0.8	58.3	1.1	45.4	0.0037	0.0030	58.0	6.4	9.1	0.008	5.98	244.5	6.63	270.8	
		5	55.7	57.3	1.0	56.7	1.0	57.6	1.3	43.1	0.0034	0.0011	68.8	6.3	10.9	0.008	4.11	228.9	7.17	399.3	
		6	58.2	63.9	0.9	63.4	0.9	69.0	1.4	46.3	0.0022	0.0016	122.8	6.4	19.3	0.008	4.65	270.4	5.46	317.9	
		7	68.4	74.8	0.9	74.2	0.9	80.4	1.5	51.1	0.0027	0.0021	113.0	6.6	17.2	0.010	4.29	293.7	4.86	332.6	
		8	105.1	87.1	1.2	86.5	1.2	71.2	1.9	45.4	0.0044	0.0009	226.1	7.0	32.1	0.012	2.89	303.9	6.24	655.5	
		9	82.2	43.4	1.9	86.7	0.9	91.5	1.7	51.1	0.0025	0.0044	196.8	6.9	28.4	0.028	3.61	296.5	2.74	225.5	
		reach	58.6	59.1	1.0	65.2	0.9	75.3	1.3	48.7	0.0029	0.0022	112.7	6.5	17.0	0.011	4.26	249.9	4.97	291.5	

Table A3.6
**Difference in geometry of Santa Cruz River cross-sections
due to October 2000 flood.**

Reach	XS	XS-Area (m ³)	Wetted Perimeter (m)	R	Width (m)	Mean Depth (m)	W/D	Bankfull Depth (m)	W/Dbf	S	s	Arroyo Width (m)	Arroyo Depth (m)	Arroyo W/D
South Pima Mine Road	1	57.5	36.6	1.2	34.0	1.3	-14.5	2.2	-10.8	0.0021	0.0031	0.6	-0.7	1.1
	2	47.5	24.0	1.2	23.1	1.2	-11.0	2.1	-9.7	0.0012	0.0020	0.1	-0.4	0.4
	3	35.7	13.5	1.2	14.8	1.1	1.5	2.0	-1.6	0.0004	-0.0015	1.5	-0.4	0.4
	4	33.7	11.2	1.5	9.6	1.7	-21.7	2.6	-21.1	0.0007	-0.0039	1.0	-0.3	0.3
	reach	43.6	21.3	1.3	20.4	1.3	-11.4	2.2	-10.8	0.0011	-0.0001	0.8	-0.4	0.6
North Pima Mine Road 2000	5	57.8	21.8	1.4	19.8	1.5	-43.9	1.6	-26.0	-0.0002	-0.0004	2.6	-0.5	0.6
	4	42.7	5.2	1.3	8.6	1.4	-298.4	1.5	-140.9	-0.0004	-0.0001	0.0	-0.5	0.2
	3	26.6	7.0	1.1	3.3	1.4	-77.8	1.6	-59.7	-0.0001	0.0001	0.2	-0.4	0.2
	2	30.4	5.9	1.3	2.6	1.6	-32.2	1.6	-22.0	0.0003	-0.0000	0.0	-0.6	0.3
	1	35.1	8.7	1.2	7.7	1.2	-48.5	1.5	-32.4	0.0003	-0.0002	2.2	-0.6	0.5
Big Bend 2000	5	130.0	33.7	1.8	26.1	1.9	-205.2	2.7	-240.9	0.0019	-0.0003	0.6	0.5	-1.2
	4	113.5	50.7	1.3	39.1	1.5	-84.3	2.0	-23.6	0.0006	0.0002	0.6	0.0	0.1
	3	128.9	60.6	1.4	54.2	1.5	-93.5	2.5	-38.1	-0.0001	0.0012	0.0	0.2	-1.0
	2	139.7	48.7	1.6	47.8	1.7	-55.2	2.8	-32.8	0.0006	0.0008	0.1	0.0	-0.3
	1	115.4	30.0	2.1	21.5	2.2	-136.3	2.5	-31.5	0.0007	-0.0001	0.4	-0.3	1.1
South of Straight 2000	5	74.9	17.5	1.6	16.7	1.6	-174.7	1.9	-63.0	0.0008	0.0034	0.0	0.1	-0.2
	2	69.2	23.4	1.1	22.3	1.0	-50.4	1.6	-72.6	0.0002	0.0024	0.3	0.3	-0.4
	3	51.8	27.7	0.5	21.6	0.6	-234.3	1.0	-74.0	-0.0004	0.0000	2.5	0.2	-0.2
	4	76.4	32.8	0.8	22.8	0.8	-345.3	1.2	-104.0	-0.0004	-0.0013	0.5	0.1	-0.1
	reach	68.1	25.3	1.0	20.9	1.0	-201.2	1.4	-78.4	0.0000	0.0011	0.8	0.2	-0.2
Martinez Hill	2000	140.0	177.2	0.4	177.6	0.4	165.6	0.5	145.2	-	-	0.0	-0.2	2.2
Valencia	1	38.9	34.0	0.7	50.2	0.5	-6.8	0.9	-41.7	0.0013	0.0006	0.2	-0.3	0.7
	2	34.0	28.9	0.5	28.5	0.6	-54.6	0.9	-59.0	0.0014	0.0010	0.5	-0.2	0.5
	3	33.8	19.8	0.6	19.5	0.6	-201.1	0.9	-103.2	0.0009	0.0015	0.2	-0.1	0.1
	4	38.2	25.6	0.7	12.3	0.8	-440.2	0.8	-103.1	-0.0003	-0.0002	-0.6	-0.0	-0.0
	5	47.9	13.9	0.8	13.3	0.8	-181.1	1.0	-76.6	-0.0007	-0.0019	-0.2	-0.1	0.2
	6	52.7	25.3	0.8	56.8	0.1	61.0	1.1	21.4	0.0012	-0.0004	0.0	-0.0	0.0
	7	61.0	40.8	0.7	40.3	0.7	-72.7	0.9	-11.6	-0.0024	-0.0009	-0.1	-0.3	0.7
	8	92.9	52.5	0.9	52.2	0.9	-25.5	1.4	-17.7	0.0036	0.0002	0.0	0.2	-0.8
	9	70.9	8.3	1.6	52.0	0.6	-15.8	1.0	-1.3	-0.0028	0.0001	0.6	-0.2	0.7
	reach	52.2	27.7	0.8	36.1	0.6	-104.1	1.0	-43.6	0.0003	-0.0000	0.1	-0.1	0.2

Table A3.7 Geometry of San Simon cross-sections, 2000 or 2001.

River	Reach	XS	XS-Area (m ³)	Wetted Perimeter (m)	R	Width (m)	Mean Depth (m)	W/D	Bank-full Depth (m)	W/Dbf	Bed Slope	Water Surface Slope	Arroyo Width (m)	Arroyo Depth (m)	Arroyo W/D	Manning's "n"	Bankfull velocity ₁ (m ² /s)	Bankfull Q ₁ (cumecs)	Bankfull velocity ₂ (m ² /s)	Bankfull Q ₂ (cumecs)	
San Simon	San Simon	1	17.3	20.0	0.9	19.4	0.9	21.7	1.6	12.3	-0.0007	0.0010	31.1	4.2	7.5	0.030	0.94	16.3	-	-	
		2000	2	24.2	54.4	0.4	53.3	0.5	117.5	1.2	43.4	0.0012	0.0011	120.3	3.3	36.8	0.028	0.69	16.7	0.73	17.7
			3	21.7	27.0	0.8	26.4	0.8	32.1	1.7	16.0	0.0011	0.0017	64.1	4.1	15.7	0.031	1.15	25.0	0.91	19.8
			4	20.6	23.2	0.9	22.6	0.9	24.7	1.4	16.7	-0.0011	0.0022	31.3	3.9	8.1	0.030	1.44	29.8	-	-
			reach	20.9	31.1	0.8	30.4	0.8	49.0	1.5	22.1	0.0009	0.0013	61.7	3.8	16.0	0.030	1.00	20.9	0.81	17.0
Yellowhammer		1	17.3	24.3	0.7	21.2	0.8	26.0	1.1	18.9	0.0033	0.0052	32.0	4.6	6.9	0.028	2.05	35.4	1.63	28.2	
		2000	2	8.3	14.3	0.6	13.6	0.6	22.3	1.0	14.1	0.0033	0.0052	48.9	4.5	10.9	0.028	1.79	14.9	1.43	11.9
			upper reach	12.8	19.3	0.6	17.4	0.7	24.2	1.0	16.5	0.0033	0.0052	40.5	4.6	8.9	0.028	1.92	24.6	1.53	19.6
		2001	3	22.3	27.0	0.8	26.7	0.8	32.0	1.1	23.5	0.0026	0.0005	78.8	3.7	21.2	0.028	0.72	16.0	1.60	35.5
		2001	4	18.5	21.8	0.8	20.7	0.9	23.1	1.3	15.3	0.0026	0.0005	51.8	3.8	13.6	0.028	0.73	13.6	1.62	30.0
			lower reach	20.4	24.4	0.8	23.7	0.9	27.5	1.2	19.4	0.0026	0.0005	65.3	3.8	17.4	0.028	0.71	14.4	1.62	32.9
			reach	16.6	21.9	0.7	20.5	0.8	25.8	1.1	17.9	0.0030	0.0029	52.9	4.2	13.1			1.57	26.3	
Bailey Well		1	14.8	15.2	1.0	14.6	1.0	14.3	1.3	11.1	0.0016	0.0022	47.0	4.8	9.8	0.025	1.82	27.0	1.56	23.05	
		2001	2	14.4	18.9	0.8	18.2	0.8	23.2	1.2	14.8	0.0022	0.0017	71.7	4.7	15.2	0.025	1.37	19.7	1.55	22.21
			3	18.6	19.0	1.0	18.3	1.0	18.1	1.4	13.1	0.0027	0.0012	88.7	4.5	19.5	0.025	1.38	25.6	2.06	38.20
			reach	15.9	17.7	0.9	17.0	0.9	18.5	1.3	13.0	0.0021	0.0017	69.1	4.7	14.8	0.025	1.56	24.9	1.71	27.1
Tanque		1	12.9	13.0	1.0	12.3	1.0	11.8	1.3	9.5	0.0019	0.0037	109.6	7.1	15.5	0.028	2.16	27.7	1.56	20.1	
		2001	2	15.0	16.0	0.9	14.1	1.1	13.2	1.6	8.6	0.0027	0.0033	360.7	9.2	39.1	0.028	1.96	29.4	1.78	26.6
			3	20.0	16.7	1.2	15.8	1.3	12.5	1.5	10.8	0.0035	0.0029	42.3	6.9	6.2	0.028	2.18	43.5	2.38	47.6
			reach	15.9	15.3	1.0	14.1	1.1	12.5	1.5	9.6	0.0029	0.0032	170.9	7.7	22.2	0.028	2.08	33.2	1.97	31.5
Corral		1	17.9	14.2	1.3	12.9	1.4	9.3	1.7	7.5	0.0016	0.0029	288.6	7.1	40.6	0.028	2.24	40.1	1.66	29.8	
Goat Well		4	11.8	11.9	1.0	11.0	1.1	10.2	1.4	7.8	0.0016	0.0019	180.6	12.3	14.6	0.025	1.75	20.6	1.60	18.8	
		2001	3	11.6	22.2	0.5	18.8	0.6	30.5	1.3	14.9	0.0026	0.0021	289.3	13.0	22.3	0.025	1.18	13.7	1.31	15.2
			2	16.7	15.9	1.1	15.2	1.1	13.8	1.6	9.7	0.0029	0.0026	101.9	12.9	7.9	0.025	2.09	35.1	2.22	37.2
			1	17.5	16.7	1.0	10.5	1.7	6.4	1.4	7.6	0.0022	0.0029	87.5	13.6	6.4	0.025	2.22	38.8	1.95	34.1
			reach	14.4	16.7	0.9	13.9	1.1	15.2	1.4	10.0	0.0023	0.0024	164.8	13.0	12.8	0.025	1.82	26.2	1.80	25.9

Flow Data

River	Gauge	Type	Dates		Comments
			From	To	
Santa Cruz	Tucson	Daily Mean Average	01/10/1905	31/12/1913	USGS Data
			01/10/1914	30/09/1981	
			08/07/1986	28/08/1986	
			20/10/1988		Partial duration series until 1995
			07/07/1990		
			15/07/1990		
			24/07/1990		
			24/08/1992	25/08/1992	
			08/01/1993	09/01/1993	
			11/01/1993	13/01/1993	
Continental	15 Minute	Daily Mean Average	18/01/1993	22/01/1993	
			01/10/1995	19/09/2002	
			24/07/1998	26/09/2000	
		Daily Mean Average	01/05/1940	30/09/1946	
			01/10/1951	30/09/1984	
			01/10/1991	07/05/2002	
			01/10/1987	30/09/2000	
San Simon	Fan Dam	Daily Mean Average	01/11/1955	30/06/1959	USGS Data
San Simon	Solomon	Daily Mean Average	01/08/1919	30/09/1925	
			01/06/1931	31/10/1933	
			01/05/1935	30/06/1941	
		Daily Peaks			Sporadic Dates between 1923 and 1941
		Daily Mean Average	01/06/1931	30/09/1932	
			01/05/1935	30/09/1982	
		Daily Peaks			Sporadic Dates between 1931 and 1983
		Daily Mean Average	02/07/1957	30/06/1959	
		Daily Peaks			Sporadic Dates between 1982 and 1985
		Daily Mean Average	01/10/1982	31/12/2000	BLM Data
Rio Puerco	Barrier Dam	Daily Peaks			Sporadic dates over period of record until 28/08/91
		Daily Mean Average	01/11/1939	30/09/2000	
		15 Minute	01/10/1948	30/09/1951	Digitised from original stripcharts
			01/10/1952	30/09/1965	
			01/10/1966	19/09/1984	Data from 1970 onwards poor due to silting gauge
			16/11/1991	30/09/2000	USGS Data
		Daily Mean Average	01/03/1964	31/12/1976	
		Daily Mean Average	01/10/1951	30/09/2000	
		Daily Mean Average	01/10/1943	30/09/1986	
		Daily Mean Average	01/04/1943	30/09/1994	
Sediment Data					
River	Gauge	Type	Dates		Comments
			From	To	
Santa Cruz	Tucson	Instantaneous	19/07/1988	06/10/1989	Corresponding Q also recorded
		Continental			
San Simon	Fan Dam				
		San Simon			
		Solomon	Daily Mean Average	09/07/1957	26/08/1957
		Tanque			
		Barrier Dam			
		Daily Mean Average	01/10/1955	30/01/2000	
		Instantaneous	01/10/1948	30/09/2000	Corresponding Q also recorded
		Daily Mean Average	10/01/1994	30/09/1999	
		Daily Mean Average	04/10/1955	31/10/1955	
			01/03/1956	31/03/1956	
Arroyo Chico	At Rio Puerco				
		Abv Arroyo Chico	Daily Mean Average	01/06/1956	30/06/1956
		Daily Mean Average	01/10/1978	30/09/1986	
		Daily Mean Average	01/04/1943	30/09/1994	
		Daily Mean Average			
Precipitation Data					
Location	Type	Dates		Comments	
		From	To		
San Simon	Monthly Mean	Jan 1881	Apr 1998		
University of Arizona	Monthly Mean	May 1867	Apr 1998		
Rio Puerco Data	Annual Totals	1890	2000	From Molnár (2001)	

Table A3.8 Summary of flow, sediment and discharge data.